Section 13

Distillation

J. D. Seader, Ph.D., *Professor of Chemical Engineering, University of Utah, Salt Lake City, Utah; Fellow, American Institute of Chemical Engineers; Member, American Chemical Society; Member, American Society for Engineering Education. (Section Editor°)*

Jeffrey J. Siirola, Ph.D., *Research Fellow, Eastman Chemical Company; Member, National Academy of Engineering; Fellow, American Institute of Chemical Engineers, American Chemical Society, American Association for Artificial Intelligence, American Society for Engineering Education. (Enhanced Distillation)*

Scott D. Barnicki, Ph.D., *Senior Research Chemical Engineer, Eastman Chemical Company. (Enhanced Distillation)*

° Certain portions of this section draw heavily on the work of Buford D. Smith, editor of this section in the fifth edition.

ENHANCED DISTILLATION

PETROLEUM AND COMPLEX-MIXTURE DISTILLATION

BATCH DISTILLATION

DYNAMIC DISTILLATION

PACKED COLUMNS

Nomenclature and Units

Symbol	Definition	SI units	U.S. customary units
A	Absorption factor		
A	Area	m^2	ft^2
C	Number of chemical species		
D	Distillate flow rate	(kg·mol)/s	(lb·mol)/h
E	Deviation from set point		
E	Residual of heat-transfer expression	kW	Btu/h
E	Residual of phase equilibrium expression	(kg·mol)/s	(lb·mol)/h
F	Feed flow rate	(kg·mol)/s	(lb·mol)/h
F	Vector of stage functions		
G	Interlink flow rate	(kg·mol)/s	(lb·mol)/h
G	Volume holdup of liquid	m^3	ft^3
H	Residual of energy balance	kW	Btu/h
H	Height of a transfer unit	m	ft
H	Enthalpy	J/(kg·mol)	Btu/(lb·mol)
K	Vapor-liquid equilibrium ratio (K value)		
K_C	Controller gain		
K_D	Chemical equilibrium constant for dimerization		
K_d	Liquid-liquid distribution ratio		
L	Liquid flow rate	(kg·mol)/s	(lb·mol)/h
M	Residual of component material balance	(kg·mol)/s	(lb·mol)/h
M	Liquid holdup	kg·mol	lb·mol
N	Number of transfer units		
N	Number of equilibrium stages		
N_c	Number of relationships		
N_i	Number of design variables		
N_m	Minimum number of equilibrium stages		
N_p	Number of phases		
N_r	Number of repetition variables		
N_o	Number of variables		
N	Rate of mass transfer	(kg·mol)/s	(lb·mol)/h
P	Pressure	Pa	psia
P	Residual of pressure-drop expression	Pa	psia
P^{sat}	Vapor pressure	Pa	psia
Q	Heat-transfer rate	kW	Btu/h
Q_c	Condenser duty	kW	Btu/h
Q_r	Reboiler duty	kW	Btu/h
Q	Residual of phase-equilibrium expression		
R	External-reflux ratio		
R_m	Minimum-reflux ratio		
S	Residual of mole-fraction sum		
S	Sidestream flow rate	(kg·mol)/s	(lb·mol)/h
S	Stripping factor		
S	Vapor-sidestream ratio		
T	Temperature	K	°R
U	Liquid-sidestream rate	(kg·mol)/s	(lb·mol)/h
V	Vapor flow rate	(kg·mol)/s	(lb·mol)/h
W	Vapor-sidestream rate	(kg·mol)/s	(lb·mol)/h
X	Vector of stage variables		
a	Activity		
b	Component flow rate in bottoms	(kg·mol)/s	(lb·mol)/h
d	Component flow rate in distillate	(kg·mol)/s	(lb·mol)/h
e	Rate of heat transfer	kW	Btu/h
f	Fraction of feed leaving in bottoms		
f	Fugacity	Pa	psia
f	Function in homotopy expression		
g	Function in homotopy expression		
g	Residual of energy balance	kW	Btu/h
h	Height	m	ft
h	Homotopy function		
ℓ	Component flow rate in liquid	(kg·mol)/s	(lb·mol)/h
p	Pressure	kPa	psia
q	Measure of thermal condition of feed		
q_c	Condenser duty	kW	Btu/h
q_r	Reboiler duty	kW	Btu/h
r	Sidestream ratio		
s	Liquid-sidestream ratio		
t	Homotopy parameter		
t	Time	s	h
v	Component flow rate in vapor	(kg·mol)/s	(lb·mol)/h
w	Weight fraction		
x	Mole fraction in liquid		
y	Mole fraction in vapor		
z	Mole fraction in feed		

Greek symbols

α	Relative volatility		
γ	Activity coefficient		
ε	Convergence criterion		
ξ	Scale factor		
η	Murphree-stage efficiency		
θ	Time for distillation	s	h
Θ	Parameter in Underwood equations		
Θ	Holland theta factor		
λ	Eigenvalue		
τ	Sum of squares of residuals		
τ	Feedback-reset time	s	h
Φ	Fugacity coefficient of pure component		
ϕ	Entrainment or occlusion ratio		
$\hat{\Phi}$	Fugacity coefficient in mixture		
Φ_A	Fraction of a component in feed vapor that is not absorbed		
Φ_S	Fraction of a component in entering liquid that is not stripped		
Ψ	Factor in Gilliland correlation		

General References: Billet, *Distillation Engineering,* Chemical Publishing, New York, 1979. Fair and Bolles, "Modern Design of Distillation Columns," *Chem. Eng.,* **75**(9), 156 (Apr. 22, 1968). Fredenslund, Gmehling, and Rasmussen, *Vapor-Liquid Equilibria Using UNIFAC, a Group Contribution Method,* Elsevier, Amsterdam, 1977. Friday and Smith, "An Analysis of the Equilibrium Stage Separation Problem—Formulation and Convergence," *Am. Inst. Chem. Eng. J.,* **10,** 698 (1964). Hengstebeck, *Distillation—Principles and Design Procedures,* Reinhold, New York, 1961. Henley and Seader, *Equilibrium-Stage Separation Operations in Chemical Engineering,* Wiley, New York, 1981. Hoffman, *Azeotropic and Extractive Distillation,* Wiley, New York, 1964. Holland, *Fundamentals and Modeling of Separation Processes,* Prentice-Hall, Englewood Cliffs, N.J., 1975. Holland, *Fundamentals of Multicomponent Distillation,* McGraw-Hill, New York, 1981. King, *Separation Processes,* 2d ed., McGraw-Hill, New York, 1980. Kister, *Distillation Design,* McGraw-Hill, New York, 1992. Kister, *Distillation Operation,* McGraw-Hill, New York, 1990. Robinson and Gilliland, *Elements of Fractional Distillation,* 4th ed., McGraw-Hill, New York, 1950. Rousseau, ed., *Handbook of Separation Process Technology,* Wiley-Interscience, New York, 1987. Seader, *The B.C. (Before Computers) and A.D. of Equilibrium-Stage Operations,* Chem. Eng. Educ., Vol. **14**(2), (Spring 1985). Seader, *Chem. Eng. Progress,* **85**(10), 41 (1989). Smith, *Design of Equilibrium Stage Processes,* McGraw-Hill, New York, 1963. Treybal, *Mass Transfer Operations,* 3d ed., McGraw-Hill, New York, 1980. *Ullmann's Encyclopedia of Industrial Chemistry,* Vol. **B3,** VCH, Weinheim, 1988. Van Winkle, *Distillation,* McGraw-Hill, New York, 1967.

CONTINUOUS-DISTILLATION OPERATIONS

GENERAL PRINCIPLES

Separation operations achieve their objective by the creation of two or more coexisting zones which differ in temperature, pressure, composition, and/or phase state. Each molecular species in the mixture to be separated reacts in a unique way to differing environments offered by these zones. Consequently, as the system moves toward equilibrium, each species establishes a different concentration in each zone, and this results in a separation between the species.

The separation operation called *distillation* utilizes vapor and liquid phases at essentially the same temperature and pressure for the coexisting zones. Various kinds of devices such as *random* or *structured packings* and *plates* or *trays* are used to bring the two phases into intimate contact. Trays are stacked one above the other and enclosed in a cylindrical shell to form a *column.* Packings are also generally contained in a cylindrical shell between hold-down and support plates. A typical tray-type distillation column plus major external accessories is shown schematically in Fig. 13-1.

The *feed* material, which is to be separated into fractions, is introduced at one or more points along the column shell. Because of the difference in gravity between vapor and liquid phases, liquid runs down the column, cascading from tray to tray, while vapor flows up the column, contacting liquid at each tray.

Liquid reaching the bottom of the column is partially vaporized in a heated *reboiler* to provide *boil-up,* which is sent back up the column. The remainder of the bottom liquid is withdrawn as *bottoms,* or bottom product. Vapor reaching the top of the column is cooled and condensed to liquid in the *overhead condenser.* Part of this liquid is returned to the column as *reflux* to provide liquid overflow. The remainder of the overhead stream is withdrawn as *distillate,* or overhead product. In some cases only part of the vapor is condensed so that a vapor distillate can be withdrawn.

This overall flow pattern in a distillation column provides countercurrent contacting of vapor and liquid streams on all the trays through the column. Vapor and liquid phases on a given tray approach thermal, pressure, and composition equilibriums to an extent dependent upon the efficiency of the contacting tray.

The *lighter* (lower-boiling) components tend to concentrate in the vapor phase, while the *heavier* (higher-boiling) components tend toward the liquid phase. The result is a vapor phase that becomes richer in light components as it passes up the column and a liquid phase that becomes richer in heavy components as it cascades downward. The overall separation achieved between the distillate and the bottoms depends primarily on the *relative volatilities* of the components, the number of contacting trays, and the ratio of the liquid-phase flow rate to the vapor-phase flow rate.

If the feed is introduced at one point along the column shell, the column is divided into an upper section, which is often called the *rectifying* section, and a lower section, which is often referred to as the *stripping* section. These terms become rather indefinite in *multiple-feed* columns and in columns from which a liquid or vapor *sidestream* is withdrawn somewhere along the column length in addition to the two end-product streams.

EQUILIBRIUM-STAGE CONCEPT

Until recently, energy and mass-transfer processes in an actual distillation column were considered too complicated to be readily modeled in any direct way. This difficulty was circumvented by the *equilibrium-stage model,* developed by Sorel in 1893, in which vapor and liquid streams leaving an equilibrium stage are in complete equilibrium with each other and thermodynamic relations can be used to determine the temperature of and relate the concentrations in the equilibrium streams at a given pressure. A hypothetical column composed of equilibrium stages (instead of actual contact trays) is designed to accomplish the separation specified for the actual column. The number of hypothetical equilibrium stages required is then converted to a number of actual trays by means of *tray efficiencies,* which describe the extent to which the performance of an actual contact tray duplicates the performance of an equilibrium stage. Alternatively and preferably, tray inefficiencies can be accounted for by using rate-based models that are described below.

Use of the equilibrium-stage concept separates the design of a distillation column into three major steps: (1) Thermodynamic data and methods needed to predict equilibrium-phase compositions are assembled. (2) The number of equilibrium stages required to accomplish a specified separation, or the separation that will be accomplished in a given number of equilibrium stages, is calculated. (3) The number of equilibrium stages is converted to an equivalent number of actual contact trays or height of packing, and the column diameter is determined. Much of the third step is eliminated if a rate-based model is used. This section deals primarily with the second step. Section 14 covers the third step. Sections 3 and 4 cover the first step, but a summary of methods and some useful data are included in this section.

COMPLEX DISTILLATION OPERATIONS

All separation operations require energy input in the form of heat or work. In the conventional distillation operation, as typified in Fig. 13-1, energy required to separate the species is added in the form of heat to the reboiler at the bottom of the column, where the temperature is highest. Also, heat is removed from a condenser at the top of the column, where the temperature is lowest. This frequently results

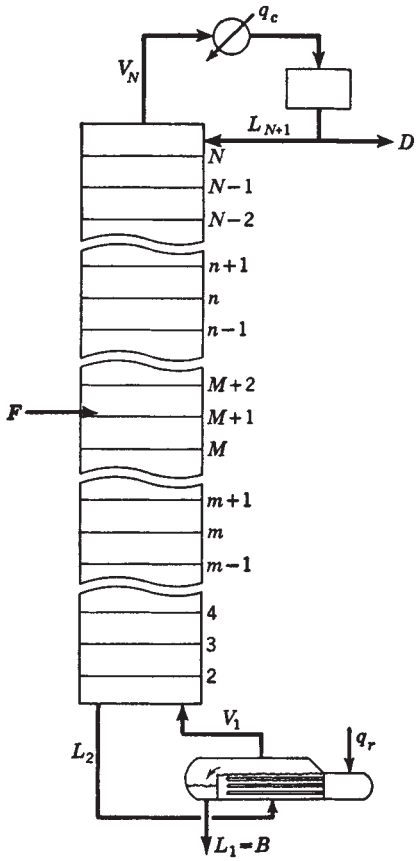

FIG. 13-1 Schematic diagram and nomenclature for a simple distillation column with one feed, a total overhead condenser, and a partial reboiler.

in a large energy-input requirement and low overall thermodynamic efficiency, when the heat removed in the condenser is wasted. Complex distillation operations that offer higher thermodynamic efficiency and lower energy-input requirements have been under intense investigation. In some cases, all or a portion of the energy input is as work.

Complex distillation operations may utilize single columns, as shown in Fig. 13-2 and discussed by Petterson and Wells [*Chem. Eng.*, **84**(20), 78 (Sept. 26, 1977)], Null [*Chem. Eng. Prog.*, **72**(7), 58 (1976)], and Brannon and Marple [*Am. Inst. Chem. Eng. Symp. Ser. 76,* **192**, 10 (1980)], or two or more columns that are thermally linked as shown in Figs. 13-3 and 13-6 and discussed by Petterson and Wells (op. cit.) and Mah, Nicholas, and Wodnik [*Am. Inst. Chem. Eng. J.*, **23,** 651 (1977)].

In Fig. 13-2*a,* which is particularly useful when a large temperature difference exists between the ends of the column, interreboilers add heat at lower temperatures and/or intercondensers remove heat at higher temperatures. As shown in Fig. 13-2*b,* these intermediate heat exchangers may be coupled with a heat pump that takes energy from the intercondenser and uses shaft work to elevate this energy to a temperature high enough to transfer it to the interreboiler.

Particularly when the temperature difference between the ends of the column is not large, any of the three heat-pump systems in Fig. 13-2*c, d,* and *e* that involve thermal coupling of the overhead condenser and bottoms reboiler might be considered to eliminate external heat transfer almost entirely, substituting shaft work as the prime energy input for achieving the separation. More complex arrangements are considered by Björn, Grén, and Ström [*Chem. Eng. Process.*, **29,** 185 (1991)]. Alternatively, the well-known multiple-column or split-tower arrangement of Fig. 13-3*a,* which corresponds somewhat to the energy-saving concept employed in multieffect evaporation, might be used. The feed is split more or less equally among columns that operate in parallel, but at different pressures, in a cascade that decreases from left to right. With proper selection of column-operating pressure, this permits the overhead vapor from the higher-pressure column to be condensed in the reboiler of the lower-pressure column. External heat-transfer media are needed only for the reboiler of the first effect and the condenser of the last effect. Thus, for N effects, utility requirements are of the order $1/N$ of those for a conventional single-effect column. Wankat [*Ind. Eng. Chem. Res.*, **32,** 894 (1993)] develops a large number of more complex multieffect schemes, some of which show significant reductions in energy requirements.

In another alternative, shown in Fig. 13-3*b,* the rectifying section may be operated at a pressure sufficiently higher than that of the stripping section such that heat can be transferred between any desired pairs of stages of the two sections. This technique, described by Mah et al. (op. cit.) and referred to as SRV (secondary reflux and vaporization) distillation, can result in a significant reduction in utility requirements for the overhead condenser and bottoms reboiler.

When multicomponent mixtures are to be separated into three or more products, sequences of simple distillation columns of the type shown in Fig. 13-1 are commonly used. For example, if a ternary mixture is to be separated into three relatively pure products, either of the two sequences in Fig. 13-4 can be used. In the direct sequence, shown in Fig. 13-4*a,* all products but the heaviest are removed one by one as distillates. The reverse is true for the indirect sequence, shown in Fig. 13-4*b.* The number of possible sequences of simple distillation columns increases rapidly with the number of products. Thus, although only the 2 sequences shown in Fig. 13-4 are possible for a mixture separated into 3 products, 14 different sequences, one of which is shown in Fig. 13-5, can be synthesized when 5 products are to be obtained.

As shown in a study by Tedder and Rudd [*Am. Inst. Chem. Eng. J.*, **24,** 303 (1978)], conventional sequences like those of Fig. 13-4 may not always be the optimal choice, particularly when species of intermediate volatility are present in large amounts in the feed or need not be recovered at high purity. Of particular interest are thermally coupled systems. For example, in Fig. 13-6*a,* an impure-vapor sidestream is withdrawn from the first column and purified in a side-cut rectifier, the bottoms of which is returned to the first column. The thermally coupled system in Fig. 13-6*b,* discussed by Stupin and Lockhart [*Chem. Eng. Prog.*, **68**(10), 71 (1972)] and referred to as Petlyuk towers, is particularly useful for reducing energy requirements when the initial feed contains close-boiling species. Shown for a ternary feed, the first column in Fig. 13-6*b* is a prefractionator, which sends essentially all of the light component and heavy component to the distillate and bottoms respectively, but permits the component of intermediate volatility to be split between the distillate and bottoms. Products from the prefractionator are sent to appropriate feed trays in the second column, where all three products are produced, the middle product being taken off as a sidestream. Only the second column is provided with condenser and reboiler; reflux and boil-up for the prefractionator are obtained from the second column. This concept is readily extended to separations that produce more than three products. Procedures for the optimal design of thermally coupled systems are presented by Triantafyllou and Smith [*Trans. I. Chem. E.*, **70,** Part A, 118 (1992)]. A scheme for combining thermal coupling with heat pumps is developed by Agrawal and Yee [*Ind. Eng. Chem. Res.*, **33,** 2717 (1994)].

RELATED SEPARATION OPERATIONS

The simple and complex distillation operations just described all have two things in common: (1) both rectifying and stripping sections are provided so that a separation can be achieved between two components that are adjacent in volatility; and (2) the separation is effected only by the addition and removal of energy and not by the addition of any mass separating agent (MSA) such as in liquid-liquid extraction.

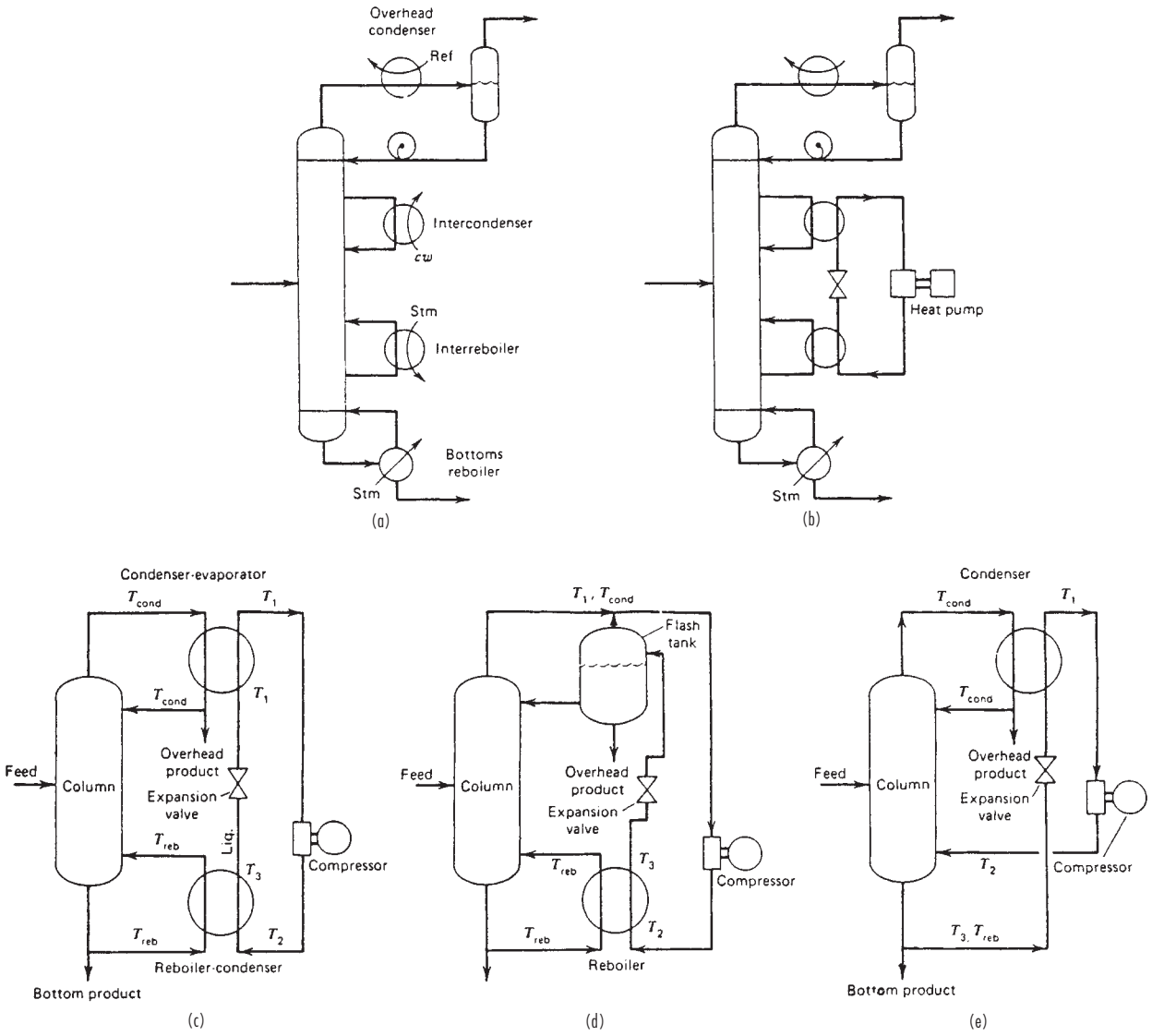

FIG. 13-2 Complex distillation operations with single columns. (*a*) Use of intermediate heat exchangers. (*b*) Coupling of intermediate heat exchangers with heat pump. (*c*) Heat pump with external refrigerant. (*d*) Heat pump with vapor compression. (*e*) Heat pump with bottoms flashing.

Sometimes, alternative single- or multiple-stage vapor-liquid separation operations, of the types shown in Fig. 13-7, may be more suitable than distillation for the specified task.

A single-stage flash, as shown in Fig. 13-7*a*, may be appropriate if (1) the relative volatility between the two components to be separated is very large; (2) the recovery of only one component, without regard to the separation of the other components, in one of the two product streams is to be achieved; or (3) only a partial separation is to be made. A common example is the separation of light gases such as hydrogen and methane from aromatics. The desired temperature and pressure of a flash may be established by the use of heat exchangers, a valve, a compressor, and/or a pump upstream of the vessel used to separate the product vapor and liquid phases. Depending on the original condition of the feed, it may be partially condensed or partially vaporized in a so-called flash operation.

If the recovery of only one component is required rather than a sharp separation between two components of adjacent volatility, absorption or stripping in a single section of stages may be sufficient. If the feed is vapor at separation conditions, absorption is used either with a liquid MSA absorbent of relatively low volatility as in Fig. 13-7*b* or with reflux produced by an overhead partial condenser as in Fig. 13-7*c*. The choice usually depends on the ease of partially condensing the overhead vapor or of recovering and recycling the absorbent. If the feed is liquid at separation conditions, stripping is used, either with an externally supplied vapor stripping agent of relatively high volatility as shown in Fig. 13-7*d* or with boil-up produced by a partial reboiler as in Fig. 13-7*c*. The choice depends on the ease of partially reboiling the bottoms or of recovering and recycling the stripping agent.

If a relatively sharp separation is required between two components of adjacent volatility, but either an undesirably low temperature is required to produce reflux at the column-operating pressure or an undesirably high temperature is required to produce boil-up, then refluxed stripping as shown in Fig. 13-7*g* or reboiled absorption

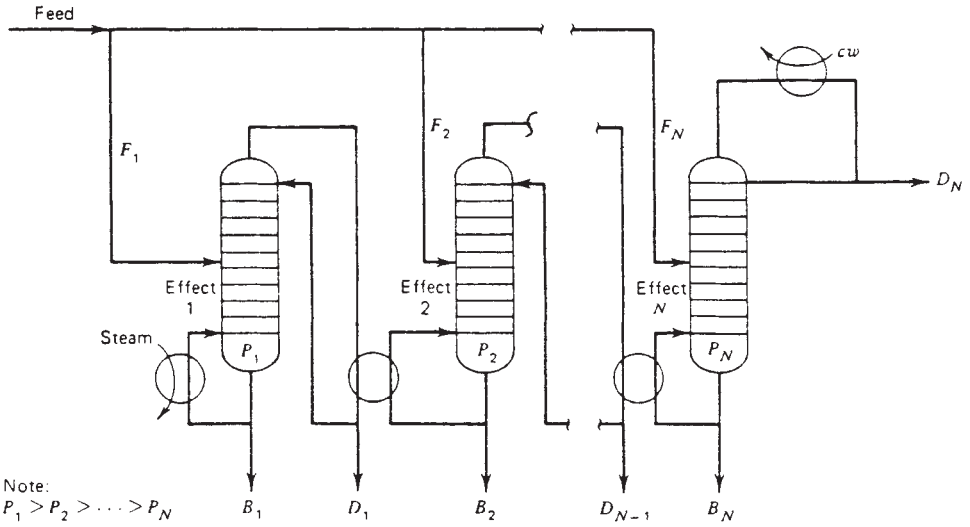

(a)

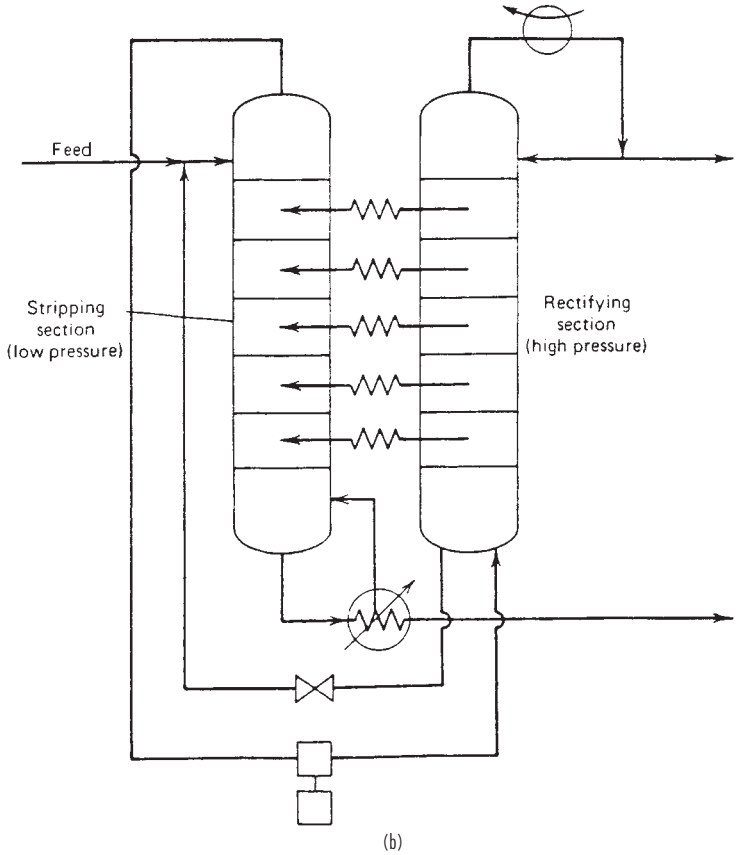

(b)

FIG. 13-3 Complex distillation operations with two or more columns. (*a*) Multieffect distillation. (*b*) SRV distillation.

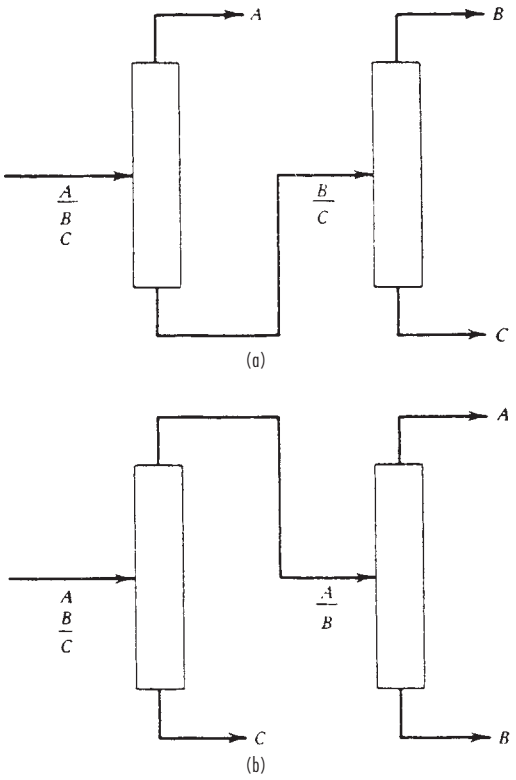

FIG. 13-4 Distillation sequences for the separation of three components. (*a*) Direct sequence. (*b*) Indirect sequence.

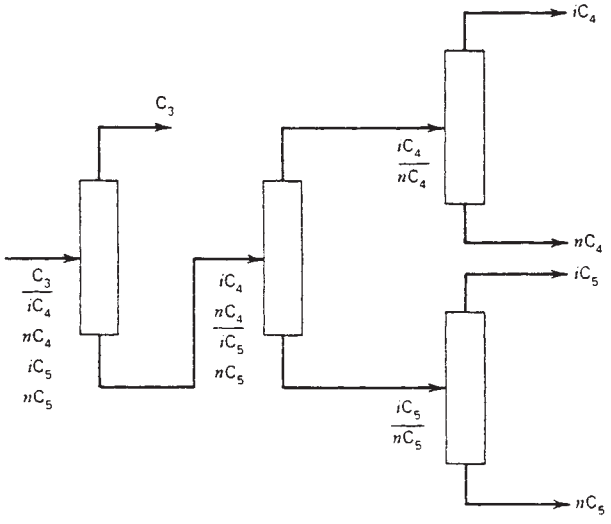

FIG. 13-5 One of 14 different sequences for the separation of a 5-component mixture by simple distillation.

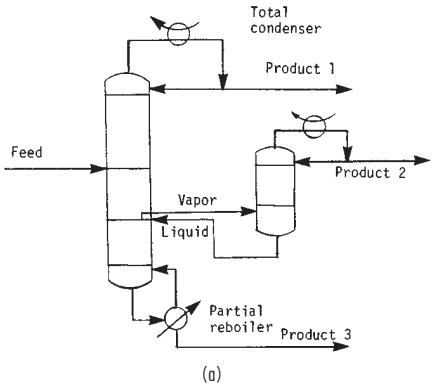

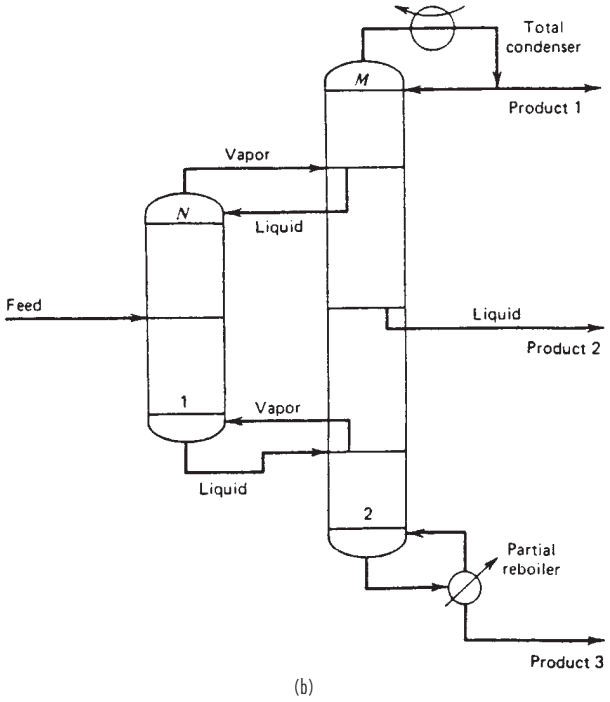

FIG. 13-6 Thermally coupled systems for separation into three products. (*a*) Fractionator with vapor sidestream and side-cut rectifier. (*b*) Petlyuk towers.

as shown in Fig. 13-7*f* may be used. In either case, the choice of MSA follows the same consideration given for simple absorption and stripping.

When the volatility difference between the two components to be separated is so small that a very large number of stages would be required, then extractive distillation, as shown in Fig. 13-7*h*, should be considered. Here, an MSA is selected that increases the volatility difference sufficiently to reduce the stage requirement to a reasonable number. Usually, the MSA is a polar compound of low volatility that leaves in the bottoms, from which it is recovered and recycled. It is introduced in an appreciable amount near the top stage of the column so as to affect the volatility difference over most of the stages. Some reflux to the top stage is utilized to minimize the MSA content in the distillate. An alternative to extractive distillation is azeotropic distillation, which is shown in Fig. 13-7*i* in just one of its many modes. In a common mode, an MSA that forms a heterogeneous minimum-

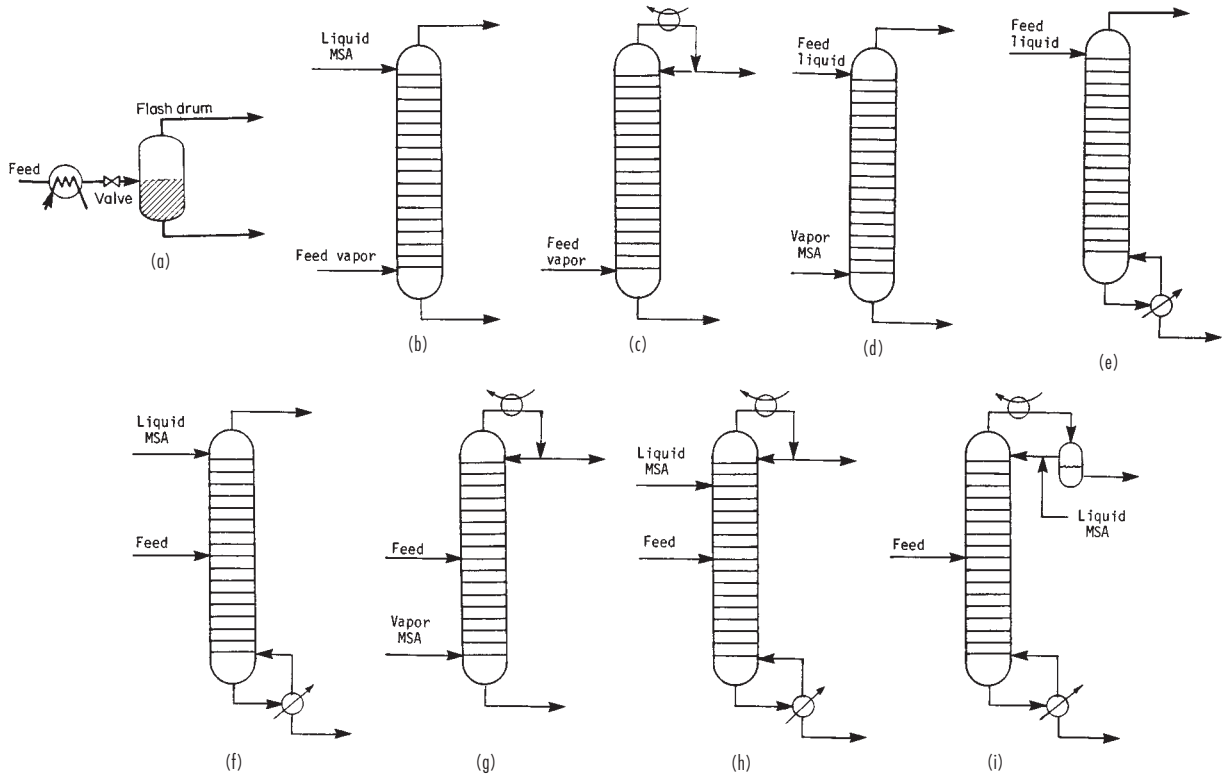

FIG. 13-7 Separation operations related to distillation. (*a*) Flush vaporization or partial condensation. (*b*) Absorption. (*c*) Rectifier. (*d*) Stripping. (*e*) Reboiled stripping. (*f*) Reboiled absorption. (*g*) Refluxed stripping. (*h*) Extractive distillation. (*i*) Azeotropic distillation.

boiling azeotrope with one or more components of the feed is utilized. The azeotrope is taken overhead, and the MSA-rich phase is decanted and returned to the top of the column as reflux.

Numerous other multistaged configurations are possible. One important variation of a stripper, shown in Fig. 13-7*d*, is a refluxed stripper, in which an overhead condenser is added. Such a configuration is sometimes used to steam-strip sour water containing NH_3, H_2O, phenol, and HCN.

All the separation operations shown in Fig. 13-7, as well as the simple and complex distillation operations described earlier, are referred to here as distillation-type separations because they have much in common with respect to calculations of (1) thermodynamic properties, (2) vapor-liquid equilibrium stages, and (3) column sizing. In fact, as will be evident from the remaining treatment of this section, the trend is toward single generalized digital-computer-program packages that compute many or all distillation-type separation operations.

This section also includes a treatment of distillation-type separations from a rate-based point of view that utilizes principles of mass transfer and heat transfer. Section 14 also presents details of that subject as applied to absorption and stripping.

SYNTHESIS OF MULTICOMPONENT SEPARATION SYSTEMS

The sequencing of distillation columns and other types of equipment for the separation of multicomponent mixtures has received much attention in recent years. Although one separator of complex design can sometimes be devised to produce more than two products, more often a sequence of two-product separators is preferable. Often, the sequence includes simple distillation columns. A summary of sequencing methods, prior to 1977, that can lead to optimal or near-optimal designs, is given by Henley and Seader [op. cit.]. More recent methods for distillation-column sequencing are reviewed by Modi and Westerberg [*Ind. Eng. Chem. Res.*, **31,** 839 (1992)], who also present a more generally applicable method based on a marginal price that is the change in price of a separation operation when the separation is carried out in the absence of nonkey components. The synthesis of sequences that consider a wide range of separation operations in a knowledge-based approach is given by Barnicki and Fair for liquid mixtures [*Ind. Eng. Chem. Res.*, **29,** 421 (1990)] and for gas/vapor mixtures [*Ind. Eng. Chem. Res.*, **31,** 1679 (1992)]. A knowledge-based method is also given by Sheppard, Beltramini, and Motard [*Chem. Eng. Comm.*, **106** (1991)] for the synthesis of distillation sequences that involve nonsharp separations where nonkey components distribute. The problem-decomposition approach of Wahnschafft, Le Rudulier, and Westerberg [*Ind. Eng. Chem. Res.*, **32,** 1121 (1993)] is directed to the synthesis of complex separation sequences that involve nonsharp splits and recycle, including azeotropic distillation. The method is applied using a computer-aided separation process designer called *SPLIT*. An expert system, called *EXSEP*, for the synthesis of solvent-based separation trains is presented by Brunet and Liu [*Ind. Eng. Chem. Res.*, **32,** 315 (1993)]. The use of ternary-composition diagrams and residue-curve maps, of the type made popular by Doherty and coworkers, is reviewed and evaluated for application to the synthesis of complex separation sequences by Fien and Liu [*Ind. Eng. Chem. Res.*, **33,** 2506 (1994)].

THERMODYNAMIC DATA

INTRODUCTION

Reliable thermodynamic data are essential for the accurate design or analysis of distillation columns. Failure of equipment to perform at specified levels is often attributable, at least in part, to the lack of such data.

This subsection summarizes and presents examples of phase equilibrium data currently available to the designer. The thermodynamic concepts utilized are presented in the subsection "Thermodynamics" of Sec. 4.

PHASE EQUILIBRIUM DATA

For a binary mixture, pressure and temperature fix the equilibrium vapor and liquid compositions. Thus, experimental data are frequently presented in the form of tables of vapor mole fraction y and liquid mole fraction x for one constituent over a range of temperature T for a fixed pressure P or over a range of pressure for a fixed temperature. A compilation of such data, mainly at a pressure of 101.3 kPa (1 atm, 1.013 bar), for binary systems (mainly nonideal) is given in Table 13-1. More extensive presentations and bibliographies of such data may be found in Hala, Wichterle, Polak, and Boublik [*Vapour-Liquid Equilibrium Data at Normal Pressures,* Pergamon, Oxford (1968)]; Hirata, Ohe, and Nagahama [*Computer Aided Data Book of Vapor-Liquid Equilibria,* Elsevier, Amsterdam (1975)]; Wichterle, Linek, and Hala [*Vapor-Liquid Equilibrium Data Bibliography,* Elsevier, Amsterdam, 1973, Supplement I, 1976, Supplement II, (1979)]; Oe [*Vapor-Liquid Equilibrium Data,* Elsevier, Amsterdam (1989)]; Oe [*Vapor-Liquid Equilibrium Data at High Pressure,* Elsevier, Amsterdam (1990)]; Walas [*Phase Equilibria in Chemical Engineering,* Butterworth, Boston (1985)]; and, particularly, Gmehling and Onken [*Vapor-Liquid Equilibrium Data Collection,* DECHEMA Chemistry Data ser., vol. **1** (parts 1–10), (Frankfort, 1977)].

For application to distillation (a nearly isobaric process), as shown in Figs. 13-8 to 13-13, binary-mixture data are frequently plotted, for a fixed pressure, as y versus x, with a line of 45° slope included for reference, and as T versus y and x. In most binary systems, one of the components is more volatile than the other over the entire composition range. This is the case in Figs. 13-8 and 13-9 for the benzene-toluene system at pressures of both 101.3 and 202.6 kPa (1 and 2 atm), where benzene is more volatile than toluene.

For some binary systems, one of the components is more volatile over only a part of the composition range. Two systems of this type, ethyl acetate–ethanol and chloroform-acetone, are shown in Figs. 13-10 to 13-12. Figure 13-10 shows that for two binary systems chloroform is less volatile than acetone below a concentration of 66 mole percent chloroform and that ethyl acetate is less volatile than ethanol below a concentration of 53 mole percent ethyl acetate. Above these concentrations, volatility is reversed. Such mixtures are known as azeotropic mixtures, and the composition in which the reversal occurs, which is the composition in which vapor and liquid compositions are equal, is the azeotropic composition, or azeotrope. The azeotropic liquid may be homogeneous or heterogeneous (two immiscible liquid phases). Many of the binary mixtures of Table 13-1 form homogeneous azeotropes. Non-azeotrope-forming mixtures such as benzene and toluene in Figs. 13-8 and 13-9 can be separated by simple distillation into two essentially pure products. By contrast, simple distillation of azeotropic mixtures will at best yield the azeotrope and one essentially pure species. The distillate and bottoms products obtained depend upon the feed composition and whether a minimum-boiling azeotrope is formed as with the ethyl acetate–ethanol mixture in Fig. 13-11 or a maximum-boiling azeotrope is formed as with the chloroform-acetone mixture in Fig. 13-12. For example, if a mixture of 30 mole percent chloroform and 70 mole percent acetone is fed to a simple distillation column, such as that shown in Fig. 13-1, operating at 101.3 kPa (1 atm), the distillate could approach pure acetone and the bottoms could approach the azeotrope.

An example of heterogeneous-azeotrope formation is shown in Fig. 13-13 for the water–normal butanol system at 101.3 kPa. At liquid compositions between 0 and 3 mole percent butanol and between 40 and 100 mole percent butanol, the liquid phase is homogeneous. Phase splitting into two separate liquid phases (one with 3 mole percent butanol and the other with 40 mole percent butanol) occurs for any overall liquid composition between 3 and 40 mole percent butanol. A minimum-boiling heterogeneous azeotrope occurs at 92°C (198°F) when the vapor composition and the overall composition of the two liquid phases are 75 mole percent butanol.

For mixtures containing more than two species, an additional degree of freedom is available for each additional component. Thus, for a four-component system, the equilibrium vapor and liquid compositions are only fixed if the pressure, temperature, and mole fractions of two components are set. Representation of multicomponent vapor-liquid equilibrium data in tabular or graphical form of the type shown earlier for binary systems is either difficult or impossible. Instead, such data, as well as binary-system data, are commonly represented in terms of K values (vapor-liquid equilibrium ratios), which are defined by

$$K_i = y_i/x_i \tag{13-1}$$

and are correlated empirically or theoretically in terms of temperature, pressure, and phase compositions in the form of tables, graphs, and equations. K values are widely used in multicomponent-distillation calculations, and the ratio of the K values of two species, called the relative volatility,

$$\alpha_{ij} = K_i/K_j \tag{13-2}$$

is a convenient index of the relative ease or difficulty of separating components i and j by distillation. Rarely is distillation used on a large scale if the relative volatility is less than 1.05, with i more volatile than j.

GRAPHICAL *K*-VALUE CORRELATIONS

As discussed in Sec. 4, the K value of a species is a complex function of temperature, pressure, and equilibrium vapor- and liquid-phase compositions. However, for mixtures of compounds of similar molecular structure and size, the K value depends mainly on temperature and pressure. For example, several major graphical K-value correlations are available for light-hydrocarbon systems. The easiest to use are the DePriester charts [*Chem. Eng. Prog. Symp. Ser.* 7, **49,** 1 (1953)], which cover 12 hydrocarbons (methane, ethylene, ethane, propylene, propane, isobutane, isobutylene, *n*-butane, isopentane, *n*-pentane, *n*-hexane, and *n*-heptane). These charts are a simplification of the Kellogg charts [*Liquid-Vapor Equilibria in Mixtures of Light Hydrocarbons, MWK Equilibrium Constants, Polyco Data,* (1950)] and include additional experimental data. The Kellogg charts, and hence the DePriester charts, are based primarily on the Benedict-Webb-Rubin equation of state [*Chem. Eng. Prog.,* **47,** 419 (1951); **47,** 449 (1951)], which can represent both the liquid and the vapor phases and can predict K values quite accurately when the equation constants are available for the components in question.

A trial-and-error procedure is required with any K-value correlation that takes into account the effect of composition. One cannot calculate K values until phase compositions are known, and those cannot be known until the K values are available to calculate them. For K as a function of T and P only, the DePriester charts provide good starting values for the iteration. These nomographs are shown in Fig. 13-14*a* and *b*. SI versions of these charts have been developed by Dadyburjor [*Chem. Eng. Prog.,* **74**(4), 85 (1978)].

The Kellogg and DePriester charts and their subsequent extensions and generalizations use the molar average boiling points of the liquid and vapor phases to represent the composition effect. An alternative measure of composition is the convergence pressure of the system, which is defined as that pressure at which the K values for all the components in an isothermal mixture converge to unity. It is analogous to the critical point for a pure component in the sense that the two

TABLE 13-1 Constant-Pressure Liquid-Vapor Equilibrium Data for Selected Binary Systems

Component		Temperature, °C	Mole fraction *A* in		Total pressure, kPa	Reference
A	*B*		Liquid	Vapor		
Acetone	Chloroform	62.50	0.0817	0.0500	101.3	1
		62.82	0.1390	0.1000		
		63.83	0.2338	0.2000		
		64.30	0.3162	0.3000		
		64.37	0.3535	0.3500		
		64.35	0.3888	0.4000		
		64.02	0.4582	0.5000		
		63.33	0.5299	0.6000		
		62.23	0.6106	0.7000		
		60.72	0.7078	0.8000		
		58.71	0.8302	0.9000		
		57.48	0.9075	0.9500		
Acetone	Methanol	64.65	0.0	0.0	101.3	2
		61.78	0.091	0.177		
		59.60	0.190	0.312		
		58.14	0.288	0.412		
		56.96	0.401	0.505		
		56.22	0.501	0.578		
		55.78	0.579	0.631		
		55.41	0.687	0.707		
		55.29	0.756	0.760		
		55.37	0.840	0.829		
		55.54	0.895	0.880		
		55.92	0.954	0.946		
		56.21	1.000	1.000		
Acetone	Water	74.80	0.0500	0.6381	101.3	3
		68.53	0.1000	0.7301		
		65.26	0.1500	0.7716		
		63.59	0.2000	0.7916		
		61.87	0.3000	0.8124		
		60.75	0.4000	0.8269		
		59.95	0.5000	0.8387		
		59.12	0.6000	0.8532		
		58.29	0.7000	0.8712		
		57.49	0.8000	0.8950		
		56.68	0.9000	0.9335		
		56.30	0.9500	0.9627		
Carbon tetrachloride	Benzene	80.0	0.0	0.0	101.3	4
		79.3	0.1364	0.1582		
		78.8	0.2157	0.2415		
		78.6	0.2573	0.2880		
		78.5	0.2944	0.3215		
		78.2	0.3634	0.3915		
		78.0	0.4057	0.4350		
		77.6	0.5269	0.5480		
		77.4	0.6202	0.6380		
		77.1	0.7223	0.7330		
Chloroform	Methanol	63.0	0.040	0.102	101.3	5
		60.9	0.095	0.215		
		59.3	0.146	0.304		
		57.8	0.196	0.378		
		55.9	0.287	0.472		
		54.7	0.383	0.540		
		54.0	0.459	0.580		
		53.7	0.557	0.619		
		53.5	0.636	0.646		
		53.5	0.667	0.655		
		53.7	0.753	0.684		
		54.4	0.855	0.730		
		55.2	0.904	0.768		
		56.3	0.937	0.812		
		57.9	0.970	0.875		
Ethanol	Benzene	76.1	0.027	0.137	101.3	6
		72.7	0.063	0.248		
		70.8	0.100	0.307		
		69.2	0.167	0.360		
		68.4	0.245	0.390		
		68.0	0.341	0.422		
		67.9	0.450	0.447		
		68.0	0.578	0.478		
		68.7	0.680	0.528		
		69.5	0.766	0.566		

TABLE 13-1 Constant-Pressure Liquid-Vapor Equilibrium Data for Selected Binary Systems (*Continued*)

Component		Temperature, °C	Mole fraction *A* in		Total pressure, kPa	Reference
A	*B*		Liquid	Vapor		
		70.4	0.820	0.615		
		72.7	0.905	0.725		
		76.9	0.984	0.937		
Ethanol	Water	95.5	0.0190	0.1700	101.3	7
		89.0	0.0721	0.3891		
		86.7	0.0966	0.4375		
		85.3	0.1238	0.4704		
		84.1	0.1661	0.5089		
		82.7	0.2337	0.5445		
		82.3	0.2608	0.5580		
		81.5	0.3273	0.5826		
		80.7	0.3965	0.6122		
		79.8	0.5079	0.6564		
		79.7	0.5198	0.6599		
		79.3	0.5732	0.6841		
		78.74	0.6763	0.7385		
		78.41	0.7472	0.7815		
		78.15	0.8943	0.8943		
Ethyl acetate	Ethanol	78.3	0.0	0.0	101.3	8
		76.6	0.050	0.102		
		75.5	0.100	0.187		
		73.9	0.200	0.305		
		72.8	0.300	0.389		
		72.1	0.400	0.457		
		71.8	0.500	0.516		
		71.8	0.540	0.540		
		71.9	0.600	0.576		
		72.2	0.700	0.644		
		73.0	0.800	0.726		
		74.7	0.900	0.837		
		76.0	0.950	0.914		
		77.1	1.000	1.000		
Ethylene glycol	Water	69.5	0.0	0.0	30.4	9
		76.1	0.23	0.002		
		78.9	0.31	0.003		
		83.1	0.40	0.010		
		89.6	0.54	0.020		
		103.1	0.73	0.06		
		118.4	0.85	0.13		
		128.0	0.90	0.22		
		134.7	0.93	0.30		
		145.0	0.97	0.47		
		160.7	1.00	1.00		
n-Hexane	Ethanol	78.30	0.0	0.0	101.3	10
		76.00	0.0100	0.0950		
		73.20	0.0200	0.1930		
		67.40	0.0600	0.3650		
		65.90	0.0800	0.4200		
		61.80	0.1520	0.5320		
		59.40	0.2450	0.6050		
		58.70	0.3330	0.6300		
		58.35	0.4520	0.6400		
		58.10	0.5880	0.6500		
		58.00	0.6700	0.6600		
		58.25	0.7250	0.6700		
		58.45	0.7650	0.6750		
		59.15	0.8980	0.7100		
		60.20	0.9550	0.7450		
		63.50	0.9900	0.8400		
		66.70	0.9940	0.9350		
		68.70	1.0000	1.0000		
Methanol	Benzene	70.67	0.026	0.267	101.3	11
		66.44	0.050	0.371		
		62.87	0.088	0.457		
		60.20	0.164	0.526		
		58.64	0.333	0.559		
		58.02	0.549	0.595		
		58.10	0.699	0.633		
		58.47	0.782	0.665		
		59.90	0.898	0.760		
		62.71	0.973	0.907		

TABLE 13-1 Constant-Pressure Liquid-Vapor Equilibrium Data for Selected Binary Systems (*Continued*)

Component		Temperature, °C	Mole fraction *A* in		Total pressure, kPa	Reference
A	*B*		Liquid	Vapor		
Methanol	Ethyl acetate	76.10	0.0125	0.0475	101.3	12
		74.15	0.0320	0.1330		
		71.24	0.0800	0.2475		
		67.75	0.1550	0.3650		
		65.60	0.2510	0.4550		
		64.10	0.3465	0.5205		
		64.00	0.4020	0.5560		
		63.25	0.4975	0.5970		
		62.97	0.5610	0.6380		
		62.50	0.5890	0.6560		
		62.65	0.6220	0.6670		
		62.50	0.6960	0.7000		
		62.35	0.7650	0.7420		
		62.60	0.8250	0.7890		
		62.80	0.8550	0.8070		
		63.21	0.9160	0.8600		
		63.90	0.9550	0.9290		
Methanol	Water	100.0	0.0	0.0	101.3	13
		96.4	0.020	0.134		
		93.5	0.040	0.230		
		91.2	0.060	0.304		
		89.3	0.080	0.365		
		87.7	0.100	0.418		
		84.4	0.150	0.517		
		81.7	0.200	0.579		
		78.0	0.300	0.665		
		75.3	0.400	0.729		
		73.1	0.500	0.779		
		71.2	0.600	0.825		
		69.3	0.700	0.870		
		67.5	0.800	0.915		
		66.0	0.900	0.958		
		65.0	0.950	0.979		
		64.5	1.000	1.000		
Methyl acetate	Methanol	57.80	0.173	0.342	101.3	14
		55.50	0.321	0.477		
		55.04	0.380	0.516		
		53.88	0.595	0.629		
		53.82	0.643	0.657		
		53.90	0.710	0.691		
		54.50	0.849	0.783		
		56.86	1.000	1.000		
1-Propanol	Water	100.00	0.0	0.0	101.3	15
		98.59	0.0030	0.0544		
		95.09	0.0123	0.1790		
		91.05	0.0322	0.3040		
		88.96	0.0697	0.3650		
		88.26	0.1390	0.3840		
		87.96	0.2310	0.3970		
		87.79	0.3110	0.4060		
		87.66	0.4120	0.4280		
		87.83	0.5450	0.4650		
		89.34	0.7300	0.5670		
		92.30	0.8780	0.7210		
		97.18	1.0000	1.0000		
2-Propanol	Water	100.00	0.0	0.0	101.3	16
		97.57	0.0045	0.0815		
		96.20	0.0069	0.1405		
		93.66	0.0127	0.2185		
		87.84	0.0357	0.3692		
		84.28	0.0678	0.4647		
		82.84	0.1330	0.5036		
		82.52	0.1651	0.5153		
		81.52	0.3204	0.5456		
		81.45	0.3336	0.5489		
		81.19	0.3752	0.5615		
		80.77	0.4720	0.5860		
		80.73	0.4756	0.5886		
		80.58	0.5197	0.6033		
		80.52	0.5945	0.6330		
		80.46	0.7880	0.7546		
		80.55	0.8020	0.7680		

TABLE 13-1 Constant-Pressure Liquid-Vapor Equilibrium Data for Selected Binary Systems (*Continued*)

Component A	Component B	Temperature, °C	Mole fraction A in Liquid	Mole fraction A in Vapor	Total pressure, kPa	Reference
		81.32	0.9303	0.9010		
		81.85	0.9660	0.9525		
		82.39	1.0000	1.0000		
Tetrahydrofuran	Water	73.00	0.0200	0.6523	101.3	17
		66.50	0.0400	0.7381		
		65.58	0.0600	0.7516		
		64.94	0.1000	0.7587		
		64.32	0.2000	0.7625		
		64.27	0.3000	0.7635		
		64.23	0.4000	0.7643		
		64.16	0.5000	0.7658		
		63.94	0.6000	0.7720		
		63.70	0.7000	0.7831		
		63.54	0.8000	0.8085		
		63.53	0.8200	0.8180		
		63.57	0.8400	0.8260		
		63.64	0.8600	0.8368		
		63.87	0.9000	0.8660		
		64.29	0.9400	0.9070		
		65.07	0.9800	0.9625		
		65.39	0.9900	0.9805		
Water	Acetic acid	118.3	0.0	0.0	101.3	18
		110.6	0.1881	0.3063		
		107.8	0.3084	0.4467		
		105.2	0.4498	0.5973		
		104.3	0.5195	0.6580		
		103.5	0.5824	0.7112		
		102.8	0.6750	0.7797		
		102.1	0.7261	0.8239		
		101.5	0.7951	0.8671		
		100.8	0.8556	0.9042		
		100.8	0.8787	0.9186		
		100.5	0.9134	0.9409		
		100.2	0.9578	0.9708		
		100.0	1.0000	1.0000		
Water	1-Butanol	117.6	0.0	0.0	101.3	19
		111.4	0.049	0.245		
		106.7	0.100	0.397		
		102.0	0.161	0.520		
		101.0	0.173	0.534		
		98.5	0.232	0.605		
		96.7	0.288	0.654		
		95.2	0.358	0.693		
		93.6	0.487	0.739		
		93.1	0.551	0.751		
		93.0	0.580	0.752		
		92.9	0.628	0.758		
		92.9	0.927	0.758		
		93.2	0.986	0.760		
		95.2	0.993	0.832		
		96.8	0.996	0.883		
		100.0	1.000	1.000		
Water	Formic acid	102.30	0.0405	0.0245	101.3	20
		104.60	0.1550	0.1020		
		105.90	0.2180	0.1620		
		107.10	0.3210	0.2790		
		107.60	0.4090	0.4020		
		107.60	0.4110	0.4050		
		107.60	0.4640	0.4820		
		107.10	0.5220	0.5670		
		106.00	0.6320	0.7180		
		104.20	0.7400	0.8360		
		102.90	0.8290	0.9070		
		101.80	0.9000	0.9510		
		100.00	1.0000	1.0000		
Water	Glycerol	278.8	0.0275	0.9315	101.3	21
		247.0	0.0467	0.9473		
		224.0	0.0690	0.9563		
		219.2	0.0767	0.9743		
		210.0	0.0901	0.9783		
		202.5	0.1031	0.9724		
		196.5	0.1159	0.9839		

TABLE 13-1 Constant-Pressure Liquid-Vapor Equilibrium Data for Selected Binary Systems (*Concluded*)

Component		Temperature, °C	Mole fraction *A* in		Total pressure, kPa	Reference
A	*B*		Liquid	Vapor		
		175.2	0.1756	0.9899		
		149.3	0.3004	0.9964		
		137.2	0.3847	0.9976		
		136.8	0.3895	0.9878		
		131.8	0.4358	0.9976		
		121.5	0.5633	0.9984		
		112.8	0.7068	0.9993		
		111.3	0.7386	0.9994		
		106.3	0.8442	0.9996		
		100.0	1.0000	1.0000		

NOTE: To convert degrees Celsius to degrees Fahrenheit, °C = (°F − 32)/1.8. To convert kilopascals to pounds-force per square inch, multiply by 0.145.

[1] Kojima, Kato, Sunaga, and Hashimoto, *Kagaku Kogaku,* **32,** 337 (1968).
[2] Marinichev and Susarev, *Zh. Prtkl. Khtm.,* **38,** 378 (1965).
[3] Kojima, Tochigi, Seki, and Watase, *Kagaku Kogaku,* **32,** 149 (1968).
[4] *International Critical Tables,* McGraw-Hill, New York, 1928.
[5] Nagata, *J. Chem. Eng. Data,* **7,** 367 (1962).
[6] Ellis and Clark, *Chem. Age India,* **12,** 377 (1961).
[7] Carey and Lewis, *Ind. Eng. Chem.,* **24,** 882 (1932).
[8] Chu, Getty, Brennecke, and Paul, *Distillation Equilibrium Data,* New York, 1950.
[9] Trimble and Potts, *Ind. Eng. Chem.,* **27,** 66 (1935).
[10] Sinor and Weber, *J. Chem. Eng. Data,* **5,** 243 (1960).
[11] Hudson and Van Winkle, *J. Chem. Eng. Data,* **14,** 310 (1969).
[12] Murti and Van Winkle, *Chem. Eng. Data Ser.,* **3,** 72 (1958).
[13] Dunlop, M.S. thesis, Brooklyn Polytechnic Institute, 1948.
[14] Dobroserdov and Bagrov, *Zh. Prtkl. Kthm. (Leningrad),* **40,** 875 (1967).
[15] Smirnova, *Vestn. Leningr. Univ. Fiz. Khim.,* 81 (1959).
[16] Kojima, Ochi, and Nakazawa, *Int. Chem. Eng.,* **9,** 342 (1964).
[17] Shnitko and Kogan, *J. Appl. Chem.,* **41,** 1236 (1968).
[18] Brusset, Kaiser, and Hoequel, *Chim. Ind., Gente Chim.* **99,** 207 (1968).
[19] Boublik, *Collect. Czech. Chem. Commun.,* **25,** 285 (1960).
[20] Ito and Yoshida, *J. Chem. Eng. Data,* **8,** 315 (1963).
[21] Chen and Thompson, *J. Chem. Eng. Data,* **15,** 471 (1970).

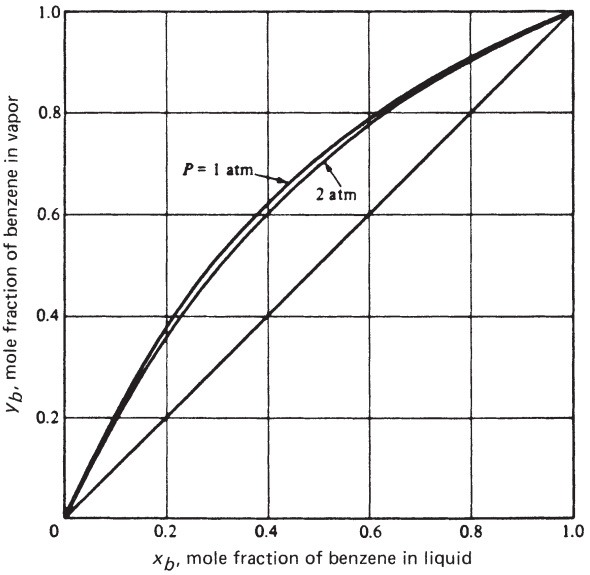

FIG. 13-8 Isobaric *y-x* curves for benzene-toluene. (*Brian,* Staged Cascades in Chemical Processing, *Prentice-Hall, Englewood Cliffs, NJ, 1972.*)

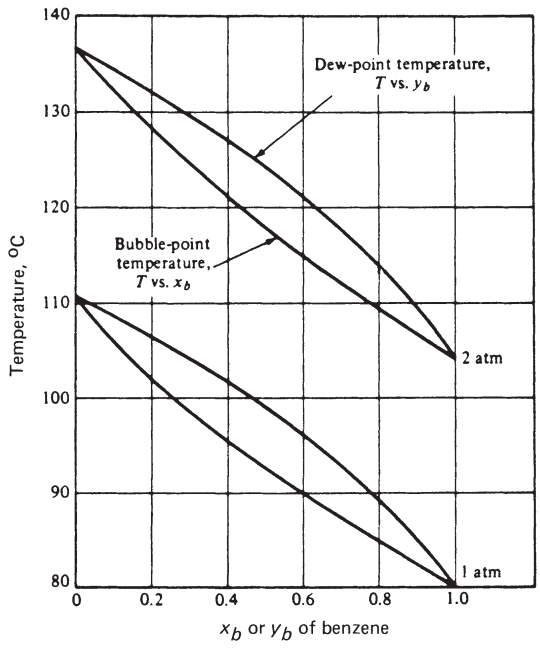

FIG. 13-9 Isobaric vapor-liquid equilibrium data for benzene-toluence. (*Brian,* Staged Cascades in Chemical Processing, *Prentice-Hall, Englewood Cliffs, NJ, 1972.*)

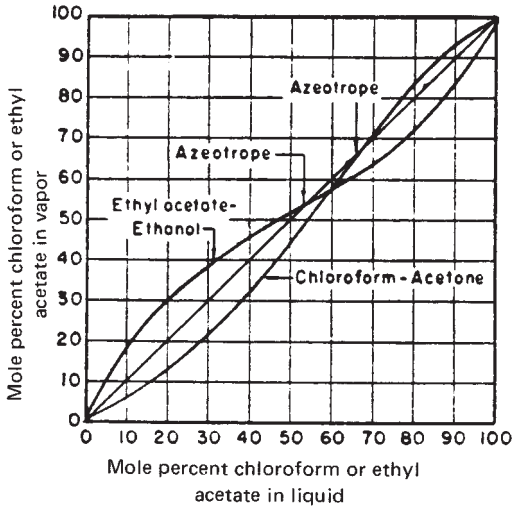

FIG. 13-10 Vapor-liquid equilibriums for the ethyl acetate–ethanol and chloroform-acetone systems at 101.3 kPa (1 atm).

phases become indistinguishable. The behavior of a complex mixture of hydrocarbons for a convergence pressure of 34.5 MPa (5000 psia) is illustrated in Fig. 13-15.

Two major graphical correlations based on convergence pressure as the third parameter (besides temperature and pressure) are the charts published by the Gas Processors Association (GPA, *Engineering Data Book,* 9th ed., Tulsa, 1981) and the charts of the American Petroleum Institute (API, *Technical Data Book—Petroleum Refining,* New York, 1966) based on the procedures from Hadden and Grayson [*Hydrocarbon Process., Pet. Refiner,* **40**(9), 207 (1961)]. The former uses the method proposed by Hadden [*Chem. Eng. Prog. Symp. Ser. 7,* **49,** 53 (1953)] for the prediction of convergence pressure as a function of composition. The basis for Hadden's method is illustrated in Fig. 13-16, where it is shown that the critical loci for various mixtures of methane-propane-pentane fall within the area circumscribed by the three binary loci. (This behavior is not always typical of more nonideal systems.) The critical loci for the ternary mixtures vary linearly, at constant temperature, with weight percent propane on a methane-free basis. The essential point is that critical loci for mixtures are independent of the concentration of the lightest component in a mixture. This permits representation of a multicomponent mixture as a pseudo binary. The light component in this pseudo binary is the lightest species present (to a reasonable extent) in the multicomponent mixture. The heavy component is a pseudo substance whose critical temperature is an average of all other components in the multicomponent

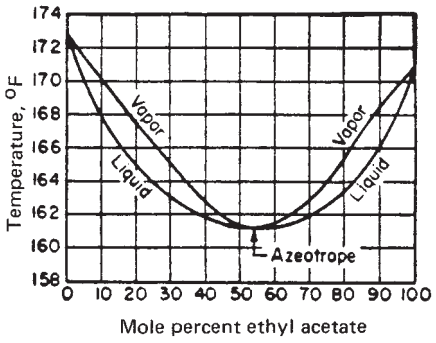

FIG. 13-11 Liquid boiling points and vapor condensation temperatures for minimum-boiling azeotrope mixtures of ethyl acetate and ethanol at 101.3 kPa (1 atm) total pressure.

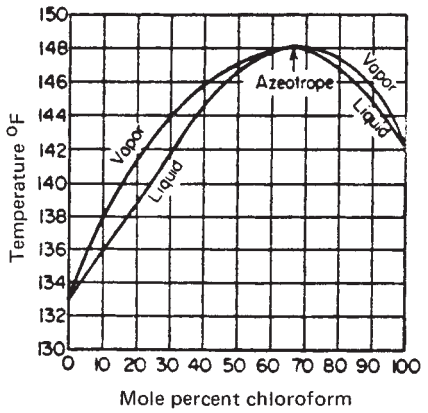

FIG. 13-12 Liquid boiling points and vapor condensation temperatures for maximum-boiling azeotrope mixtures of chloroform and acetone at 101.3 kPa (1 atm) total pressure.

mixture. This pseudocritical point can then be located on a *P-T* diagram containing the critical points for all compounds covered by the charts, and a critical locus can be drawn for the pseudo binary by interpolation between various real binary curves. Convergence pressure for the mixture at the desired temperature is read from the assumed loci at the desired system temperature. This method is illustrated in the left half of Fig. 13-17 for the methane-propane-pentane ternary. Associated *K* values for pentane at 104°C (220°F) are shown to the right as a function of mixture composition (or convergence pressure).

The GPA convergence-pressure charts are primarily for alkane and alkene systems but do include charts for nitrogen, carbon dioxide, and hydrogen sulfide. The charts may not be valid when appreciable amounts of naphthenes or aromatics are present; the API charts use special procedures for such cases. Useful extensions of the convergence-pressure concept to more varied mixtures include the nomographs of Winn [*Chem. Eng. Prog. Symp. Ser. 2,* **48,** 121 (1952)], Hadden and Grayson (op. cit.), and Cajander, Hipkin, and Lenoir [*J. Chem. Eng. Data,* **5,** 251 (1960)].

ANALYTICAL *K*-VALUE CORRELATIONS

The widespread availability and utilization of digital computers for distillation calculations have given impetus to the development of analytical expressions for *K* values. McWilliams [*Chem. Eng.,* **80**(25), 138 (1973)] presents a regression equation and accompanying regression coefficients that represent the DePriester charts of Fig. 13-14. Regression equations and coefficients for various versions of the GPA convergence-pressure charts are available from the GPA.

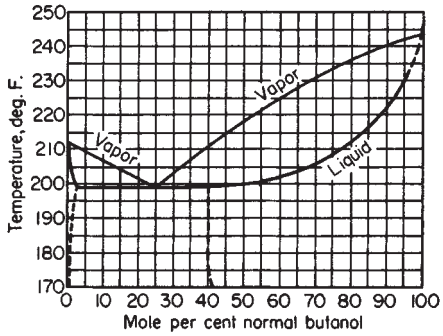

FIG. 13-13 Vapor-liquid equilibrium data for an *n*-butanol–water system at 101.3 kPa (1 atm); phase splitting and heterogeneous-azeotrope formation.

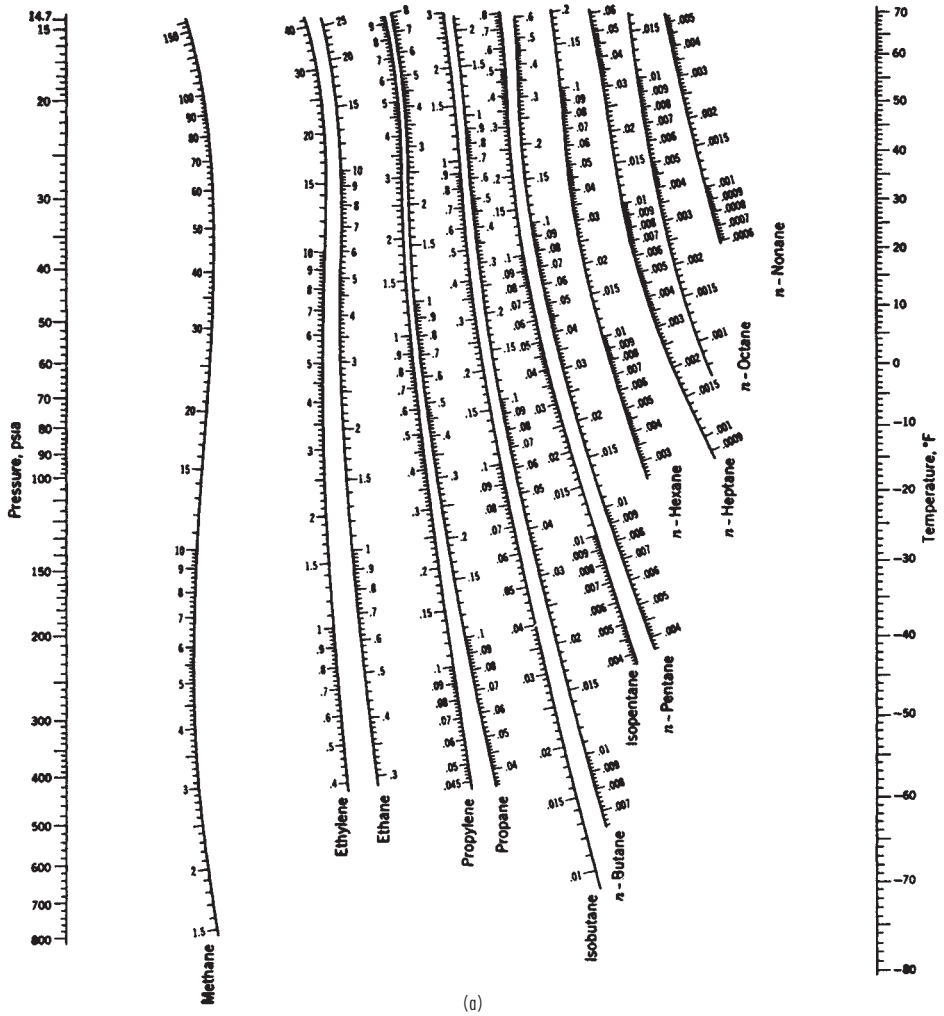

FIG. 13-14 *K* values ($K = y/x$) in light-hydrocarbon systems. (*a*) Low-temperature range. [*DePriester,* Chem. Eng. Prog. Symp. Sec. 7, ***49,*** *1 (1953).*]

Preferred analytical correlations are less empirical in nature and most often are theoretically based on one of two exact thermodynamic formulations, as derived in Sec. 4. When a single pressure-volume-temperature (*PVT*) equation of state is applicable to both vapor and liquid phases, the formulation used is

$$K_i = \hat{\Phi}_i^L / \hat{\Phi}_i^V \tag{13-3}$$

where the mixture fugacity coefficients $\hat{\Phi}_i^L$ for the liquid and $\hat{\Phi}_i^V$ for the vapor are derived by classical thermodynamics from the *PVT* expression. Consistent equations for enthalpy can similarly be derived.

Until recently, equations of state that have been successfully applied to Eq. (13-3) have been restricted to mixtures of nonpolar compounds, namely, hydrocarbons and light gases. These equations include those of Benedict-Webb-Rubin (BWR), Soave (SRK) [*Chem. Eng. Sci.,* **27,** 1197 (1972)], who extended the remarkable Redlich-Kwong equation, and Peng-Robinson (PR) [*Ind. Eng. Chem. Fundam.,* **15,** 59 (1976)]. The SRK and PR equations belong to a family of so-called cubic equations of state. The Starling extension of the BWR equation (*Fluid Thermodynamic Properties for Light Petroleum Systems,* Gulf, Houston, 1973) predicts *K* values and enthalpies of the normal paraffins up through *n*-octane, as well as isobutane, isopentane, ethylene, propylene, nitrogen, carbon dioxide, and hydrogen sulfide, including the cryogenic region. Computer programs for *K* values derived from the SRK, PR and other equations of state are widely available in all computer-aided process design and simulation programs. The ability of the SRK correlation to predict *K* values even when the pressure approaches the convergence pressure is shown for a multicomponent system in Fig. 13-18. Similar results are achieved with the PR correlation. The Wong-Sandler mixing rules for cubic equations of state now permit such equations to be extended to mixtures of organic chemicals, as shown in a reformulated version by Orbey and Sandler [*AIChE J.,* **41,** 683 (1995)].

An alternative *K*-value formulation that has received wide application to mixtures containing polar and/or nonpolar compounds is

$$K_i = \gamma_i^L \Phi_i^L / \hat{\Phi}_i^V \tag{13-4}$$

where different equations of state may be used to predict the pure-component liquid fugacity coefficient Φ_i^L and the vapor-mixture fugacity coefficient, and any one of a number of mixture free-energy models may be used to obtain the liquid activity coefficient γ_i^L. At low to moderate pressures, accurate prediction of the latter is crucial to the application of Eq. (13-4).

When either Eq. (13-3) or Eq. (13-4) can be applied, the former is generally preferred because it involves only a single equation of state

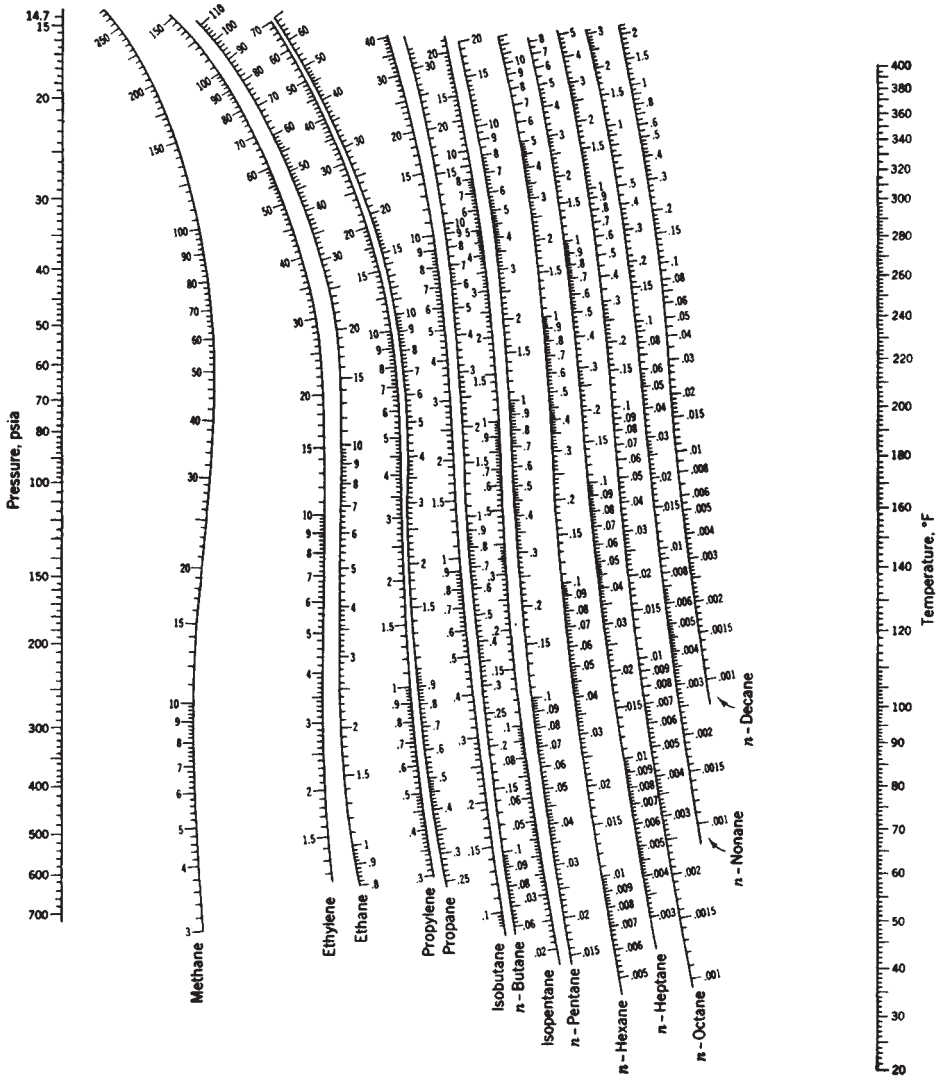

(b)

FIG. 13-14 (*Continued*) *K* values ($K = y/x$) in light-hydrocarbon systems. (*b*) High-temperature range. [*DePriester,* Chem. Eng. Prog. Symp. Sec. 7, ***49,*** *1 (1953).*]

applicable to both phases and thus would seem to offer greater consistency. In addition, the quantity Φ_i^L in Eq. (13-4) is hypothetical for any components that are supercritical. In that case, a modification of Eq. (13-4) that uses Henry's law is sometimes applied.

For mixtures of hydrocarbons and light gases, Chao and Seader (CS) [*AIChE,* **7,** 598 (1961)] applied Eq. (13-4) by using an empirical expression for Φ_i^L based on the generalized corresponding-states *PVT* correlation of Pitzer et al., the Redlich-Kwong equation of state for $\hat{\Phi}_i^V$, and the regular solution theory of Scatchard and Hildebrand for γ_i^L. The predictive ability of the last-named theory is exhibited in Fig. 13-19 for the heptane-toluene system at 101.3 kPa (1 atm). Five pure-component constants for each species (T_c, P_c, ω, δ, and v^L) are required to use the CS method, which when applied within the restrictions discussed by Lenoir and Koppany [*Hydrocarbon Process.,* **46**(11), 249 (1967)] gives good results. Revised coefficients of Grayson and Streed (GS) (Pap. 20-P07, Sixth World Pet. Conf., Frankfurt, June, 1963) for the Φ_i^L expression permit application of the CS correlation to higher temperatures and pressures and give improved predictions for hydrogen. Jin, Greenkorn, and Chao [*AIChE J,* **41,** 1602 (1995)] present a revised correlation for the standard-state liquid fugacity of hydrogen, applicable from 200 to 730 *K.*

For mixtures containing polar substances, more complex predictive equations for γ_i^L that involve binary-interaction parameters for each pair of components in the mixture are required for use in Eq. (13-4), as discussed in Sec. 4. Six popular expressions are the Margules, van Laar, Wilson, NRTL, UNIFAC, and UNIQUAC equations. Extensive listings of binary-interaction parameters for use in all but the UNIFAC equation are given by Gmehling and Onken (op. cit.). They obtained the parameters for binary systems at 101.3 kPa (1 atm) from best fits of the experimental *T-y-x* equilibrium data by setting Φ_i^V and Φ_i^L to their ideal-gas, ideal-solution limits of 1.0 and P^{sat}/P respectively, with the vapor pressure P^{sat} given by a three-constant Antoine equation, whose values they tabulate. Table 13-2 lists their parameters for some of the binary systems included in

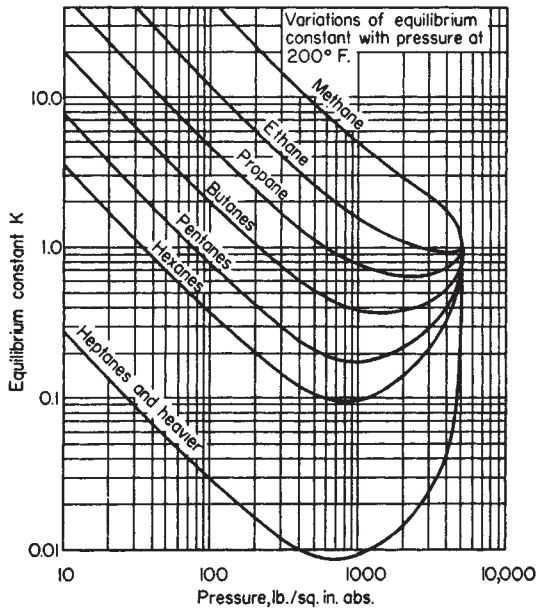

FIG. 13-15 Typical variation of K values with total pressure at constant temperature for a complex mixture. Light hydrocarbons in admixture with crude oil. [*Katz and Hachmuth,* Ind. Eng. Chem., **29,** *1072 (1937).*]

Table 13-1, based on the binary-system activity-coefficient-equation forms given in Table 13-3. Consistent Antoine vapor-pressure constants and liquid molar volumes are listed in Table 13-4. The Wilson equation is particularly useful for systems that are highly nonideal but do not undergo phase splitting, as exemplified by the ethanol-hexane system, whose activity coefficients are shown in Fig. 13-20. For systems such as this, in which activity coefficients in dilute regions may

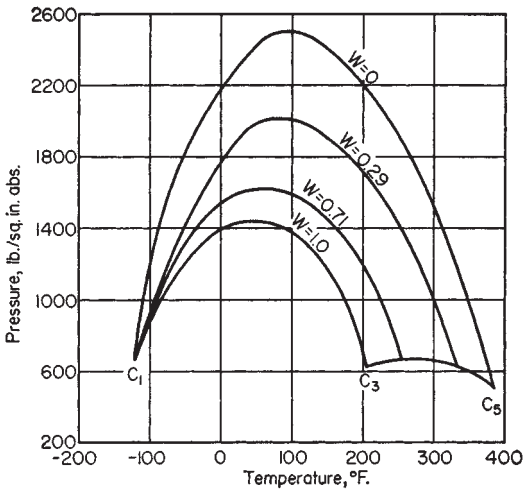

FIG. 13-16 Critical loci for a methane-propane-pentane system according to Hadden. [Chem. Eng. Prog. Symp. Sec. 7, **49,** *53 (1953).*] Parameter W is weight fraction propane on a methane-free basis.

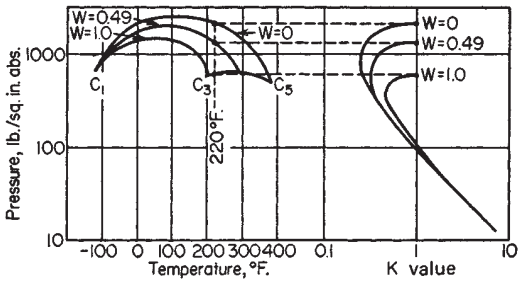

FIG. 13-17 Effect of mixture composition upon K value for n-pentane at 104°C (220°F). K values are shown for various values of W, weight fraction propane on a methane-free basis for the methane-propane-pentane system. [*Hadden,* Chem. Eng. Prog. Symp. Sec. 7, **49,** *58 (1953).*]

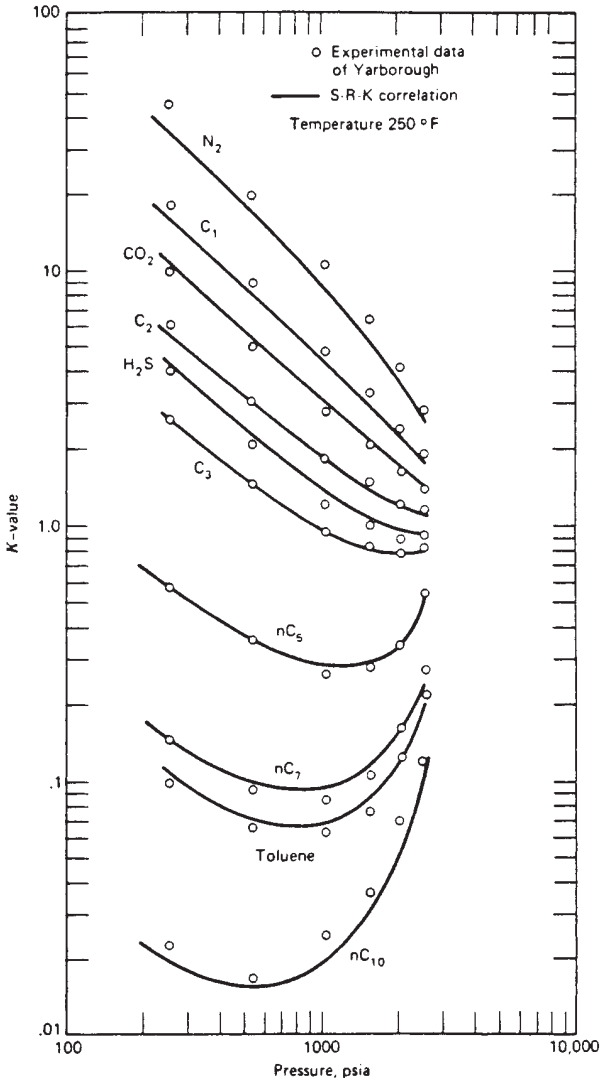

FIG. 13-18 Comparison of experimental K-value data and SRK correlation. [*Henley and Seader,* Equilibrium-Stage Separation Operations in Chemical Engineering, *Wiley, New York, 1981; data of Yarborough,* J. Chem. Eng. Data, ***17,*** *129 (1972).*]

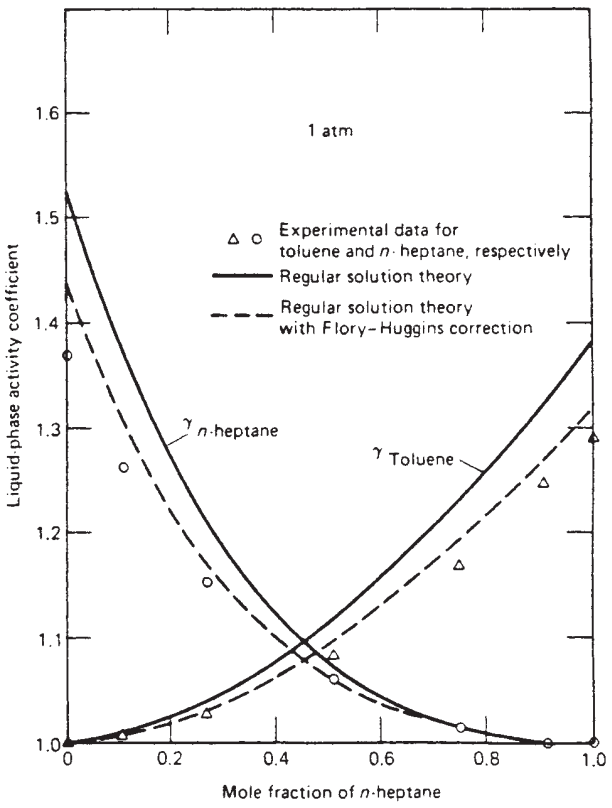

FIG. 13-19 Liquid-phase activity coefficients for an *n*-heptane-toluene system at 101.3 kPa (1 atm). [*Henley and Seader,* Equilibrium-Stage Separation Operations in Chemical Engineering, *Wiley, New York, 1981; data of Yerazunis et al.,* Am. Inst. Chem. Eng. J., ***10,*** *660 (1964).*]

exceed values of approximately 7.5, the van Laar equation erroneously predicts phase splitting.

Tables 13-1, 13-2, and 13-4 include data on formic acid and acetic acid, two substances that tend to dimerize in the vapor phase according to the chemical-equilibrium expression

$$K_D = P_D/P_M^2 = 10^{A+B/T} \tag{13-5}$$

where K_D is the chemical-equilibrium constant for dimerization, P_D and P_M are partial pressures of dimer and monomer respectively in torr, and T is in K. Values of A and B for the first four normal aliphatic acids are:

	A	B
Formic acid	–10.743	3083
Acetic acid	–10.421	3166
n-Propionic acid	–10.843	3316
n-Butyric acid	–10.100	3040

As shown by Marek and Standart [*Collect. Czech. Chem. Commun.,* **19,** 1074 (1954)], it is preferable to correlate and utilize liquid-phase activity coefficients for the dimerizing component by considering separately the partial pressures of the monomer and dimer. For example, for a binary system of components 1 and 2, when only compound 1 dimerizes in the vapor phase, the following equations apply if an ideal gas is assumed:

$$P_1 = P_D + P_M \tag{13-6}$$

$$y_1 = (P_M + 2P_D)/P \tag{13-7}$$

These equations when combined with Eq. (13-5) lead to the following equations for liquid-phase activity coefficients in terms of measurable quantities:

$$\gamma_1 = \frac{Py_1}{P_1^{sat}x_1}\left\{\frac{1+(1+4K_DP_1^{sat})^{0.5}}{1+[1+4K_DPy_1(2-y_1)]^{0.5}}\right\} \tag{13-8}$$

$$\gamma_2 = \frac{Py_1}{P_2^{sat}x_2}\left(\frac{2\{1-y_1+[1+4K_DPy_1(2-y_1)]^{0.5}\}}{(2-y_1)\{1+[1+4K_DPy_1(2-y_1)]^{0.5}\}}\right) \tag{13-9}$$

Detailed procedures, including computer programs for evaluating binary-interaction parameters from experimental data and then utiliz-

TABLE 13-2 Binary-Interaction Parameters*

System	Margules		van Laar		Wilson (cal/mol)	
	$\overline{A}_{12}$	$\overline{A}_{21}$	A_{12}	A_{21}	$(\lambda_{12}-\lambda_{11})$	$(\lambda_{21}-\lambda_{22})$
Acetone (1), chloroform (2)	–0.8404	–0.5610	–0.8643	–0.5899	116.1171	–506.8519
Acetone (1), methanol (2)	0.6184	0.5788	0.6184	0.5797	–114.4047	545.2942
Acetone (1), water (2)	2.0400	1.5461	2.1041	1.5555	344.3346	1482.2133
Carbon tetrachloride (1), benzene (2)	0.0948	0.0922	0.0951	0.0911	7.0459	59.6233
Chloroform (1), methanol (2)	0.8320	1.7365	0.9356	1.8860	–361.7944	1694.0241
Ethanol (1), benzene (2)	1.8362	1.4717	1.8570	1.4785	1264.4318	266.6118
Ethanol (1), water (2)	1.6022	0.7947	1.6798	0.9227	325.0757	953.2792
Ethyl acetate (1), ethanol (2)	0.8557	0.7476	0.8552	0.7526	58.8869	570.0439
n-Hexane (1), ethanol (2)	1.9398	2.7054	1.9195	2.8463	320.3611	2189.2896
Methanol (1), benzene (2)	2.1411	1.7905	2.1623	1.7925	1666.4410	227.2126
Methanol (1), ethyl acetate (2)	1.0016	1.0517	1.0017	1.0524	982.2689	–172.9317
Methanol (1), water (2)	0.7923	0.5434	0.8041	0.5619	82.9876	520.6458
Methyl acetate (1), methanol (2)	0.9605	1.0120	0.9614	1.0126	–93.8900	847.4348
1-Propanol (1), water (2)	2.7070	0.7172	2.9095	1.1572	906.5256	1396.6398
2-Propanol (1), water (2)	2.3319	0.8976	2.4702	1.0938	659.5473	1230.2080
Tetrahydrofuran (1), water (2)	2.8258	1.9450	3.0216	1.9436	1475.2583	1844.7926
Water (1), acetic acid (2)	0.4178	0.9533	0.4973	1.0623	705.5876	111.6579
Water (1), 1-butanol (2)	0.8608	3.2051	1.0996	4.1760	1549.6600	2050.2569
Water (1), formic acid (2)	–0.2966	–0.2715	–0.2935	–0.2757	–310.1060	1180.8040

*Abstracted from Gmehling and Onken, *Vapor-Liquid Equilibrium Data Collection,* DECHEMA Chemistry Data ser., vol. 1 (parts 1–10), Frankfurt, 1977.

TABLE 13-3 Activity-Coefficient Equations in Binary Form for Use with Parameters and Constants in Tables 13-2 and 13-4

Type of equation	Adjustable parameters	Equations in binary form
Margules	$\overline{A}_{12}$ $\overline{A}_{21}$	$\ln \gamma_1 = [\overline{A}_{12} + 2(\overline{A}_{21} - \overline{A}_{12})x_1]x_2^2$ $\ln \gamma_2 = [\overline{A}_{21} + 2(\overline{A}_{12} - \overline{A}_{21})x_2]x_1^2$
van Laar	A_{12}	$\ln \gamma_1 = A_{12}\left(\frac{A_{21}x_2}{A_{12}x_1 + A_{21}x_2}\right)^2$
	A_{21}	$\ln \gamma_2 = A_{21}\left(\frac{A_{12}x_1}{A_{12}x_1 + A_{21}x_2}\right)^2$
Wilson	$\lambda_{12} - \lambda_{11}$	$\ln \gamma_1 = -\ln(x_1 + \Lambda_{12}x_2) + x_2\left(\frac{\Lambda_{12}}{x_1 + \Lambda_{12}x_2} - \frac{\Lambda_{21}}{\Lambda_{21}x_1 + x_2}\right)$
	$\lambda_{21} - \lambda_{22}$	$\ln \gamma_2 = -\ln(x_2 + \Lambda_{21}x_1) - x_1\left(\frac{\Lambda_{12}}{x_1 + \Lambda_{12}x_2} - \frac{\Lambda_{21}}{\Lambda_{21}x_1 + x_2}\right)$

where $\Lambda_{12} = \frac{v_2^L}{v_1^L}\exp\left(-\frac{\lambda_{12} - \lambda_{11}}{RT}\right)$ $\Lambda_{21} = \frac{v_1^L}{v_2^L}\exp\left(-\frac{\lambda_{21} - \lambda_{22}}{RT}\right)$

v_i^L = molar volume of pure-liquid component i
λ_{ij} = interaction energy between components i and j, $\lambda_{ij} = \lambda_{ji}$

ing these parameters to predict K values and phase equilibria, are given in terms of the UNIQUAC equation by Prausnitz et al. (*Computer Calculations for Multicomponent Vapor-Liquid and Liquid-Liquid Equilibria,* Prentice-Hall, Englewood Cliffs, N.J., 1980) and in terms of the UNIFAC group contribution method by Fredenslund, Gmehling, and Rasmussen (*Vapor-Liquid Equilibria Using UNIFAC,* Elsevier, Amsterdam, 1980). Both use the method of Hayden and O'Connell [*Ind. Eng. Chem. Process Des. Dev.,* **14,** 209 (1975)] to compute $\hat{\Phi}_i^V$ in Eq. (13-4). When the system temperature is greater than the critical temperature of one or more components in the mixture, Prausnitz et al. utilize a Henry's-law constant $H_{i,M}$ in place of the product $\gamma_i^L\Phi_i^L$ in Eq. (13-4). Otherwise Φ_i^L is evaluated from vapor-pressure data with a Poynting saturated-vapor fugacity correction. When the total pressure is less than about 202.6 kPa (2 atm) and all components in the mixture have a critical temperature that is greater than the system temperature, then $\Phi_i^L = P_i^{sat}/P$ and $\hat{\Phi}_i^V = 1.0$. Equation (13-4) then reduces to

$$K_i = \gamma_i^L P_i^{sat}/P \tag{13-10}$$

which is referred to as a modified Raoult's-law K value. If, furthermore, the liquid phase is ideal, then $\gamma_i^L = 1.0$ and

$$K_i = P_i^{sat}/P \tag{13-11}$$

which is referred to as a Raoult's-law K value that is dependent solely on the vapor pressure P_i^{sat} of the component in the mixture. The UNIFAC method is being periodically updated with new group contributions, with a recent article being that of Hansen et al. [*Ind. Eng. Chem. Res.,* **30,** 2352 (1991)].

TABLE 13-4 Antoine Vapor-Pressure Constants and Liquid Molar Volume*

Species	Antoine constants† A	B	C	Applicable temperature region, °C	v^L, liquid molar volume, cm³/g·mol
Acetic acid	8.02100	1936.010	258.451	18–118	57.54
Acetone	7.11714	1210.595	229.664	(–13)–55	74.05
Benzene	6.87987	1196.760	219.161	8–80	89.41
1-Butanol	7.36366	1305.198	173.427	89–126	91.97
Carbon tetrachloride	6.84083	1177.910	220.576	(–20)–77	97.09
Chloroform	6.95465	1170.966	226.232	(–10)–60	80.67
Ethanol	7.58670	1281.590	193.768	78–203	58.68
Ethanol	8.11220	1592.864	226.184	20–93	58.68
Ethyl acetate	7.10179	1244.951	217.881	16–76	98.49
Formic acid	6.94459	1295.260	218.000	36–108	37.91
n-Hexane	6.91058	1189.640	226.280	(–30)–170	131.61
Methanol	8.08097	1582.271	239.726	15–84	40.73
Methyl acetate	7.06524	1157.630	219.726	2–56	79.84
1-Propanol	8.37895	1788.020	227.438	(–15)–98	75.14
2-Propanol	8.87829	2010.320	252.636	(–26)–83	76.92
Tetrahydrofuran	6.99515	1202.290	226.254	23–100	81.55
Water	8.07131	1730.630	233.426	1–100	18.07

*Abstracted from Gmehling and Onken, *Vapor-Liquid Equilibrium Data Collection,* DECHEMA Chemistry Data ser., vol. 1 (parts 1–10), Frankfurt, 1977.
†Antoine equation is $\log P^{sat} = A - B/(T + C)$ with P^{sat} in torr and T in °C.
NOTE: To convert degrees Celsius to degrees Fahrenheit, °F = 1.8°C + 32. To convert cubic centimeters per gram-mole to cubic feet per pound-mole, multiply by 0.016.

DEGREES OF FREEDOM AND DESIGN VARIABLES

DEFINITIONS

For separation processes, a design solution is possible if the number of independent equations equals the number of unknowns.

$$N_i = N_v - N_c$$

where N_v is the total number of variables (unknowns) involved in the process under consideration, N_c is the number of restricting relationships among the unknowns (independent equations), and N_i is termed the number of design variables. In the analogous phase-rule analysis, N_i is usually referred to as the degrees of freedom or variance. It is the number of variables that the designer must specify to define one unique operation (solution) of the process.

The variables N_t with which the designer of a separation process must be concerned are:

1. Stream concentrations (e.g., mole fractions)
2. Temperatures
3. Pressures
4. Stream flow rates
5. Repetition variables N_r

The first three are intensive variables. The fourth is an extensive variable that is not considered in the usual phase-rule analysis. The fifth is neither an intensive nor an extensive variable but is a single degree of freedom that the designer utilizes in specifying how often a particular element is repeated in a unit. For example, a distillation-column section is composed of a series of equilibrium stages, and when the designer specifies the number of stages that the section contains, he or she utilizes the single degree of freedom represented by the repetition variable ($N_r = 1.0$). If the distillation column contains more than one section (such as above and below a feed stage), the number of stages in each section must be specified and as many repetition variables exist as there are sections, that is, $N_r = 2$.

The various restricting relationships N_c can be classified as:

1. Inherent
2. Mass-balance
3. Energy-balance
4. Phase-distribution
5. Chemical-equilibrium

The inherent restrictions are usually the result of definitions and take the form of identities. For example, the concept of the equilibrium stage involves the inherent restrictions that $T^V = T^L$ and $P^V = P^L$ where the superscripts V and L refer to the equilibrium exit streams.

The mass-balance restrictions are the C balances written for the C components present in the system. (Since we will only deal with nonreactive mixtures, each chemical compound present is a phase-rule component.) An alternative is to write $(C - 1)$ component balances and one overall mass balance.

The phase-distribution restrictions reflect the requirement that $f_i^V = f_i^L$ at equilibrium where f is the fugacity. This may be expressed by Eq. (13-1). In vapor-liquid systems, it should always be recognized that all components appear in both phases to some extent and there will be such a restriction for each component in the system. In vapor-liquid-liquid systems, each component will have three such restrictions, but only two are independent. In general, when all components exist in all phases, the number of restricting relationships due to the distribution phenomenon will be $C(N_p - 1)$, where N_p is the number of phases present.

For the analysis here, the forms in which the restricting relationships are expressed are unimportant. Only the number of such restrictions is important.

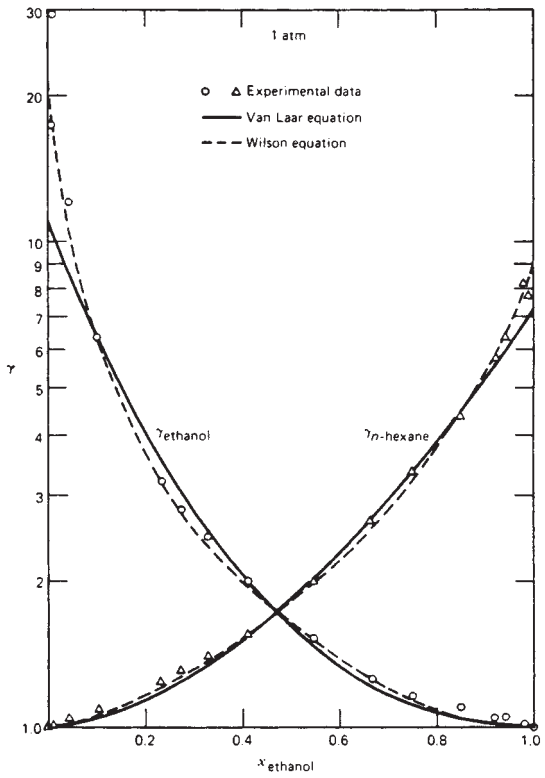

FIG. 13-20 Liquid-phase activity coefficients for an ethanol–*n*-hexane system. [*Henley and Seader,* Equilibrium-Stage Separation Operations in Chemical Engineering, *Wiley, New York, 1931; data of Sinor and Weber,* J. Chem. Eng. Data, **5,** *243–247 (1960).*]

ANALYSIS OF ELEMENTS

An *element* is defined as part of a more complex *unit.* The unit may be all or only part of an operation or the entire *process.* Our strategy will be to analyze all elements that appear in a separation process and determine the number of design variables associated with each. The appropriate elements can then be quickly combined to form the desired units and the various units combined to form the entire process. Allowance must of course be made for the connecting streams (*interstreams*) whose variables are counted twice when elements or units are joined.

The simplest element is a *single homogeneous stream.* The variables necessary to define it are:

	N_c^e
Concentrations	$C - 1$
Temperature	1
Pressure	1
Flow rate	1
	$C + 2$

There are no restricting relationships when the stream is considered only at a point. Henley and Seader (*Equilibrium-Stage Separation Operations in Chemical Engineering,* Wiley, New York, 1981) count all C concentrations as variables, but then have to include

$$\sum_i x_i = 1.0 \qquad \text{or} \qquad \sum_i y_i = 1.0$$

as a restriction.

A stream divider simply splits a stream into two or more streams of the same composition. Consider Fig. 13-21, which pictures the division of the condensed overhead liquid L_c into distillate D and

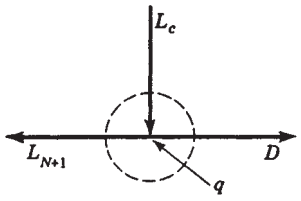

FIG. 13-21 Stream divider.

reflux L_{N+1}. The divider is permitted to operate nonadiabatically if desired. Three mass streams and one possible "energy stream" are involved; so

$$N_v^e = 3(C+2) + 1 = 3C + 7$$

Each mass stream contributes $C + 2$ variables, but an energy stream has only its rate q as a variable. The independent restrictions are as follows:

	N_c^e
Inherent	
T and P identities between L_{N+1} and D	2
Concentration identities between L_{N+1} and D	$C-1$
Mass balances	C
Energy balance	1
	$2C+2$

The number of design variables for the element is given by

$$N_i^e = N_v^e - N_c^e = (3C+7) - (2C+2) = C+5$$

Specification of the feed stream L_c($C + 2$ variables), the ratio L_{N+1}/D, the "heat leak" q, and the pressure of either stream leaving the divider utilizes these design variables and defines one unique operation of the divider.

A simple equilibrium stage (no feed or sidestreams) is depicted in Fig. 13-22. Four mass streams and a heat-leak (or heat-addition) stream provide the following number of variables:

$$N_v^e = 4(C+2) + 1 = 4C + 9$$

Vapor and liquid streams V_n and L_n respectively are in equilibrium with each other by definition and therefore are at the same T and P. These two inherent identities when added to C-component balances, one energy balance, and the C phase-distribution relationships give

$$N_c^e = 2C + 3$$

Then

$$N_i^e = N_v^e - N_c^e = (4C+9) - (2C+3) = 2C+6$$

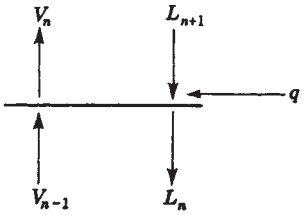

FIG. 13-22 Simple equilibrium stage.

These design variables can be utilized as follows:

Specifications	N_i^e
Specification of L_{n+1} stream	$C+2$
Specification of V_{n-1} stream	$C+2$
Pressure of either leaving stream	1
Heat leak q	1
	$2C+6$

The results of the analyses for all the various elements commonly encountered in distillation processes are summarized in Table 13-5. Details of the analyses are given by Smith (*Design of Equilibrium Stage Processes*, McGraw-Hill, New York, 1967) and in a somewhat different form by Henley and Seader (op. cit.).

ANALYSIS OF UNITS

A "unit" is defined as a combination of elements and may or may not constitute the entire process. By definition

$$N_v^u = N_r + \sum_i N_i^e$$

and

$$N_i^u = N_v^u - N_c^u$$

where N_c^u refers to *new* restricting relationships (identities) that may arise when elements are combined. N_c^u does not include any of the restrictions considered in calculating the N_i^e's for the various elements. It includes only the stream identities that exist in each interstream between two elements. The interstream variables ($C + 2$) were counted in each of the two elements when their respective N_i^e's were calculated. Therefore, ($C + 2$) new restricting relationships must be counted for each interstream in the combination of elements to prevent redundancy.

The simple absorber column shown in Fig. 13-23 will be analyzed here to illustrate the procedure. This unit consists of a series of simple equilibrium stages of the type in Fig. 13-22. Specification of the number of stages N utilizes the single repetition variable and

$$N_v^u = N_r + \sum_i N_i^e = 1 + N(2C+6)$$

since in Table 13-5 $N_i^e = 2C + 6$ for a simple equilibrium stage. There are $2(N - 1)$ interstreams, and therefore $2(N - 1)(C + 2)$ new identities (not previously counted) come into existence when elements are combined. Subtraction of these restrictions from N_v^u gives N_i^u, the design variables that must be specified.

$$N_i^u = N_v^u - N_c^u = N_r + \sum_i N_i^e - N_c^u$$
$$= [1 + N(2C+6)] - [2(N-1)(C+2)]$$
$$= 2C + 2N + 5$$

TABLE 13-5 Design Variables N_i^e for Various Elements

Element	N_v^e	N_c^e	N_i^e
Homogeneous stream	$C+2$	0	$C+2$
Stream divider	$3C+7$	$2C+2$	$C+5$
Stream mixer	$3C+7$	$C+1$	$2C+6$
Pump	$2C+5$	$C+1$	$C+4$
Heater	$2C+5$	$C+1$	$C+4$
Cooler	$2C+5$	$C+1$	$C+4$
Total condenser	$2C+5$	$C+1$	$C+4$
Total reboiler	$2C+5$	$C+1$	$C+4$
Partial condenser	$3C+7$	$2C+3$	$C+4$
Partial reboiler	$3C+7$	$2C+3$	$C+4$
Simple equilibrium state	$4C+9$	$2C+3$	$2C+6$
Feed stage	$5C+11$	$2C+3$	$3C+8$
Sidestream stage	$5C+11$	$3C+4$	$2C+7$
Adiabatic equilibrium flash	$3C+6$	$2C+3$	$C+3$
Nonadiabatic equilibrium flash	$3C+7$	$2C+3$	$C+4$

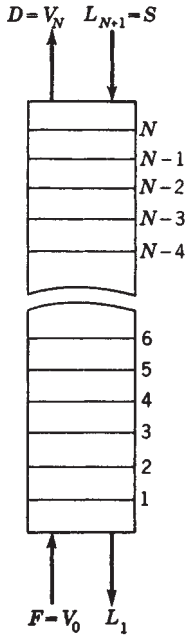

FIG. 13-23 Simple absorption.

These might be used as follows:

Specifications	N_i^u
Two feed streams	$2C + 4$
Number of stages N	1
Pressure of either stream leaving each stage	N
Heat leak for each stage	N
	$2C + 2N + 5$

A more complex unit is shown in Fig. 13-24, which is a schematic diagram of a *distillation column* with one feed, a total condenser, and a partial reboiler. Dotted lines encircle the six connected elements (or units) that constitute the distillation operation. The variables N_v^u that must be considered in the analysis of the entire process are just the sum of the N_i^e's for these six elements since here $N_r = 0$. Using Table 13-5,

Element (or unit)	$N_v^u = \sum_i N_i^e$
Total condenser	$C + 4$
Reflux divider	$C + 5$
$N - (M + 1)$ equilibrium stages	$2C + 2(N - M - 1) + 5$
Feed stage	$3C + 8$
$(M - 1)$ equilibrium stages	$2C + 2(M - 1) + 5$
Partial reboiler	$C + 4$
	$10C + 2N + 27$

Here, the two units of $N - (M + 1)$ and $(M - 1)$ stages are treated just like elements. Nine interstreams are created by the combination of elements; so

$$N_c^u = 9(C + 2) = 9C + 18$$

The number of design variables is

$$N_i^u = C + 2N + 9 \; N_v^u - N_c^u = (10C + 2N + 27) - (9C + 18)$$

One set of specifications that is particularly convenient for computer solutions is:

Specifications	N_i^u
Pressure of either stream leaving each stage (including reboiler)	N
Pressure of stream leaving condenser	1
Pressure of either stream leaving reflux divider	1
Heat leak for each stage (excluding reboiler)	$N - 1$
Heat leak for reflux divider	1
Feed stream	$C + 2$
Reflux temperature	1
Total number of stages N	1
Number of stages below feed M	1
Distillate rate D/F	1
Reflux rate (L_{N+1}/D)	1
	$C + 2N + 9$

Other specifications often used in place of one or more of the last four listed are the fractional recovery of one component in either D or B and/or the concentration of one component in either D or B.

OTHER UNITS AND COMPLEX PROCESSES

In Table 13-6, the number of design variables is summarized for several distillation-type separation operations, most of which are shown in Fig. 13-7. For columns not shown in Figs. 13-1 or 13-7 that

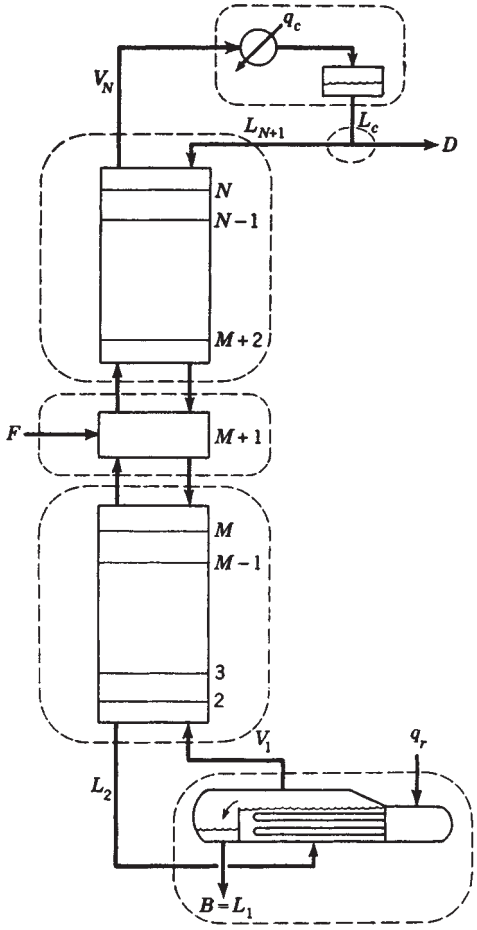

FIG. 13-24 Distillation column with one feed, a total condenser, and a partial reboiler.

involve additional feeds and/or sidestreams, add $(C + 3)$ degrees of freedom for each additional feed $(C + 2$ to define the feed and 1 to designate the feed stage) and 2 degrees of freedom for each sidestream (1 for the sidestream flow rate and 1 to designate the sidestream-stage location). Any number of elements or units can be combined to form complex processes. No new rules beyond those developed earlier are necessary for their analysis. When applied to the thermally coupled distillation process of Fig. 13-6*b*, the result is $N_i'' = 2(N + M) + C + 18$. Further examples are given in Henley and Seader (op. cit.). An alternative method for determining the degrees of freedom for equipment and processes is given by Pham [*Chem. Eng. Sci.*, **49,** 2507 (1994)].

TABLE 13-6 Design Variables N_i'' for Separation Units

Unit	N_i''*
Distillation (partial reboiler–total condenser)	$C + 2N + 9$
Distillation (partial reboiler–partial condenser)	$C + 2N + 6$
Absorption	$2C + 2N + 5$
Rectification (partial condenser)	$C + 2N + 3$
Stripping	$2C + 2N + 5$
Reboiled stripping (partial reboiler)	$C + 2N + 3$
Reboiled absorption (partial reboiler)	$2C + 2N + 6$
Refluxed stripping (total condenser)	$2C + 2N + 9$
Extractive distillation (partial reboiler–total condenser)	$2C + 2N + 12$

*N includes reboiler, but not condenser.

SINGLE-STAGE EQUILIBRIUM-FLASH CALCULATIONS

INTRODUCTION

The simplest continuous-distillation process is the adiabatic single-stage equilibrium-flash process pictured in Fig. 13-25. Feed temperature and the pressure drop across the valve are adjusted to vaporize the feed to the desired extent, while the drum provides disengaging space to allow the vapor to separate from the liquid. The expansion across the valve is at constant enthalpy, and this fact can be used to calculate T_2 (or T_1 to give a desired T_2).

From Table 13-5 it can be seen that the variables subject to the designer's control are $C + 3$ in number. The most common way to utilize these is to specify the feed rate, composition, and pressure $(C + 1$ variables) plus the drum temperature T_2 and pressure P_2. This operation will give one point on the *equilibrium-flash curve* shown in Fig. 13-26. This curve shows the relation at constant pressure between the fraction V/F of the feed flashed and the drum temperature. The temperature at $V/F = 0.0$ when the first bubble of vapor is about to form (saturated liquid) is the *bubble-point* temperature of the feed mixture, and the value at $V/F = 1.0$ when the first droplet of liquid is about to form (saturated liquid) is the *dew-point* temperature.

BUBBLE POINT AND DEW POINT

For a given drum pressure and feed composition, the bubble- and dew-point temperatures bracket the temperature range of the equilibrium flash. At the bubble-point temperature, the total vapor pressure exerted by the mixture becomes equal to the confining drum pressure, and it follows that $\sum y_i = 1.0$ in the bubble formed. Since $y_i = K_i x_i$ and since the x_i's still equal the feed concentrations (denoted by z_i's), calculation of the bubble-point temperature involves a trial-and-error search for the temperature which, at the specified pressure, makes $\sum K_i z_i = 1.0$. If instead the temperature is specified, one can find the bubble-point pressure that satisfies this relationship.

At the dew-point temperature y_i still equals z_i, and the relationship $\sum x_i = \sum z_i/K_i = 1.0$ must be satisfied. As in the case of the bubble point, a trial-and-error search for the dew-point temperature at a specified pressure is involved. Or, if the temperature is specified, the dew-point pressure can be calculated.

ISOTHERMAL FLASH

The calculation for a point on the flash curve that is intermediate between the bubble point and the dew point is referred to as an isothermal-flash calculation because T_2 is specified. Except for an ideal binary mixture, procedures for calculating an isothermal flash are iterative. A popular method is the following due to Rachford and Rice [*J. Pet. Technol.*, **4**(10), sec. 1, p. 19, and sec. 2, p. 3 (October 1952)]. The component mole balance $(Fz_i = Vy_i + Lx_i)$, phase-distribution relation $(K_i = y_i/x_i)$, and total mole balance $(F = V + L)$ can be combined to give

$$x_i = \frac{z_i}{1 + \dfrac{V}{F}(K_i - 1)} \tag{13-12}$$

$$y_i = \frac{K_i z_i}{1 + \dfrac{V}{F}(K_i - 1)} \tag{13-13}$$

Since $\sum x_i - \sum y_i = 0$,

$$f\{V\} = \sum_i \frac{z_i(1 - K_i)}{1 + \dfrac{V}{F}(K_i - 1)} = 0 \tag{13-14}$$

Equation (13-14) is solved iteratively for V/F, followed by the calculation of values of x_i and y_i from Eqs. (13-12) and (13-13) and L from the total mole balance. Any one of a number of numerical root-finding

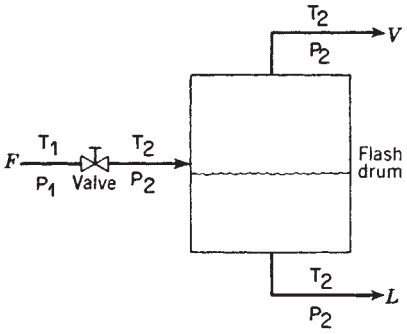

FIG. 13-25 Equilibrium-flash separator.

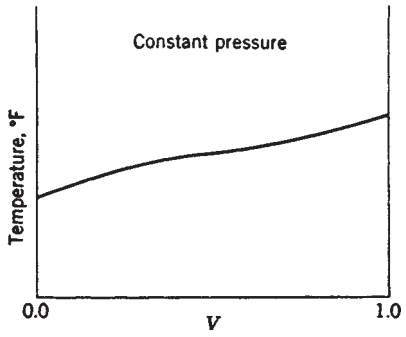

FIG. 13-26 Equilibrium-flash curve.

procedures such as the Newton-Raphson, secant, false-position, or bisection method can be used to solve Eq. (13-14). Values of K_i are constants if they are independent of liquid and vapor compositions. Then the resulting calculations are straightforward. Otherwise, the K_i values must be periodically updated for composition effects, perhaps after each iteration, using prorated values of x_i and y_i from Eqs. (13-12) and (13-13). Generally, the iterations are continued until the calculated value of V/F equals to within ± 0.0005 the value of V/F that was used to initiate that iteration. When converged, $\sum x_i$ and $\sum y_i$ will each be very close to a value of 1, and, if desired, T_1 can be computed from an energy balance around the valve if no heat exchanger is used. Alternatively, if T_1 is fixed as mentioned earlier, a heat exchanger must be added before, after, or in place of the valve with the required heat duty being calculated from an energy balance. The limits of applicability of Eqs. (13-12) to (13-14) are the bubble point, at which $V = 0$ and $x_i = z_i$, and the dew point, at which $L = 0$ and $y_i = z_i$, at which Eq. (13-2) reduces to the bubble-point equation

$$\sum_i K_i x_i = 1 \tag{13-15}$$

and the dew-point equation

$$\sum_i \frac{y_i}{K_i} = 1 \tag{13-16}$$

For a *binary feed,* specification of the flash-drum temperature and pressure fixes the equilibrium-phase concentrations, which are related to the K values by

$$x_1 = (1 - K_2)/(K_1 - K_2) \quad \text{and} \quad y_1 = (K_1K_2 - K_1)/(K_2 - K_1)$$

The mole balance can be rearranged to

$$\frac{V}{F} = \frac{z_1(K_1 - K_2)/(1.0 - K_2) - 1.0}{K_1 - 1.0}$$

If K_1 and K_2 are functions of temperature and pressure only (ideal solutions), the flash curve can be calculated directly without iteration.

ADIABATIC FLASH

In Fig. 13-25, if P_2 and the feed-stream conditions (i.e., F, z_i, T_1, P_1) are known, then the calculation of T_2, V, L, y_i, and x_i is referred to as an adiabatic flash. In addition to Eqs. (13-12) to (13-14) and the total mole balance, the following energy balance around both the valve and the flash drum combined must be included:

$$H^F F = H^V V + H^L L \tag{13-17}$$

Taking a basis of $F = 1.0$ mol and eliminating L with the total mole balance, Eq. (13-17) becomes

$$f_2\{V, T_2\} = H^F - V(H^V - H^L) - H^L = 0 \tag{13-18}$$

With T_2 now unknown, Eq. (13-17) becomes

$$f_1\{V, T_2\} = \sum_i \frac{z_i(1 - K_i)}{1 + V(K_i - 1)} = 0 \tag{13-19}$$

A number of iterative procedures have been developed for solving Eqs. (13-18) and (13-19) simultaneously for V and T_2. Frequently, and especially if the feed contains components of a narrow range of volatility, convergence is rapid for a tearing method in which a value of T_2 is assumed, Eq. (13-19) is solved iteratively by the isothermal-flash procedure, and, using that value of V, Eq. (13-18) is solved iteratively for a new approximation of T_2, which is then used to initiate the next cycle until T_2 and V converge. However, if the feed contains components of a wide range of volatility, it may be best to invert the sequence and assume a value for V, solve Eq. (13-19) for T_2, solve Eq. (13-18) for V, and then repeat the cycle. If K values and/or enthalpies are sensitive to the unknown phase compositions, it may be necessary simultaneously to solve Eqs. (13-18) and (13-19) by a Newton or other suitable iterative technique. Alternatively, the two-tier method of Boston and Britt [*Comput. Chem. Eng.,* **2,** 109 (1978)], which is also suitable for difficult isothermal-flash calculations, may be applied.

OTHER FLASH SPECIFICATIONS

Flash-drum specifications in addition to (P_2, T_2) and (P_2, adiabatic) are also possible but must be applied with care, as discussed by Michelsen [*Comp. Chem. Engng.,* **17,** 431 (1993)]. Most computer-aided process design and simulation programs permit a wide variety of flash specifications.

THREE-PHASE FLASH

Single-stage equilibrium-flash calculations become considerably more complex when an additional liquid phase can form, as from mixtures of water with hydrocarbons. Procedures for computing such situations are referred to as three-phase flash methods, which are given for the general case by Henley and Rosen (*Material and Energy Balance Computations,* Wiley, New York, 1968, chap. 8). When the two liquid phases are almost mutually insoluble, they can be considered separately and relatively simple procedures apply as discussed by Smith (*Design of Equilibrium Stage Processes,* McGraw-Hill, New York, 1963). Condensation of such mixtures may result in one liquid phase being formed before the other. Computer-aided process design and simulation programs all contain a Gibbs free-energy routine that can compute a three-phase flash by minimization of Gibbs free energy. Many difficult aspects of flash calculations are discussed by Michelsen [*Fluid Phase Equil.,* **9,** 1, 21 (1982)].

COMPLEX MIXTURES

Feed analyses in terms of component concentrations are usually not available for complex hydrocarbon mixtures with a final normal boiling point above about 38°C (100°F) (*n*-pentane). One method of handling such a feed is to break it down into pseudo components (narrow-boiling fractions) and then estimate the mole fraction and K value for each such component. Edmister [*Ind. Eng. Chem.,* **47,** 1685 (1955)] and Maxwell (*Data Book on Hydrocarbons,* Van Nostrand, Princeton, N.J., 1958) give charts that are useful for this estimation. Once K values are available, the calculation proceeds as described above for multicomponent mixtures. Another approach to complex mixtures is to obtain an American Society for Testing and Materials (ASTM) or true-boiling point (TBP) curve for the mixture and then use empirical correlations to construct the atmospheric-pressure equilibrium-flash curve (EFV), which can then be corrected to the desired operating pressure. A discussion of this method and the necessary charts are presented in a later subsection entitled "Petroleum and Complex-Mixture Distillation."

GRAPHICAL METHODS FOR BINARY DISTILLATION

INTRODUCTION

Multistage distillation under continuous, steady-state operating conditions is widely used in practice to separate a variety of mixtures. Table 13-7, taken from the study of Mix, Dweck, Weinberg, and Armstrong [*Am. Inst. Chem. Eng. J. Symp. Ser.* **76,** 192, 10 (1980)] lists key components for 27 industrial distillation processes. The design of multiequilibrium-stage columns can be accomplished by graphical techniques when the feed mixture contains only two components. The x-y diagram [McCabe and Thiele, *Ind. Eng. Chem.,* **17,** 605 (1925)] utilizes only equilibrium and mole-balance relationships but approaches rigorousness only for those systems in which energy effects on vapor and liquid rates leaving the stages are negligible. The enthalpy-concentration diagram [Ponchon, *Tech. Mod.,* **13,** 20, 55 (1921); and Savarit, *Arts Metiers,* **65,** 142, 178, 241, 266, 307 (1922)] utilizes the energy balance also and is rigorous when enough calorimetric data are available to construct the diagram without assumptions.

TABLE 13-7 Key Components for Distillation Processes of Industrial Importance

Key components	Typical number of trays
Hydrocarbon systems	
Ethylene-ethane	73
Propylene-propane	138
Propyne–1–3-butadiene	40
1–3 Butadiene–vinyl acetylene	130
Benzene-toluene	34, 53
Benzene–ethyl benzene	20
Benzene–diethyl benzene	50
Toluene–ethyl benzene	28
Toluene-xylenes	45
Ethyl benzene–styrene	34
o-Xylene–*m*-xylene	130
Organic systems	
Methanol-formaldehyde	23
Dichloroethane-trichloroethane	30
Acetic acid–acetic anhydride	50
Acetic anhydride–ethylene diacetate	32
Vinyl acetate–ethyl acetate	90
Ethylene glycol–diethylene glycol	16
Cumene-phenol	38
Phenol-acetophenone	39, 54
Aqueous systems	
HCN-water	15
Acetic acid–water	40
Methanol-water	60
Ethanol-water	60
Isopropanol-water	12
Vinyl acetate–water	35
Ethylene oxide–water	50
Ethylene glycol–water	16

The availability of computers has decreased our reliance on graphical methods. Nevertheless, diagrams are useful for quick approximations and for demonstrating the effect of various design variables. The *x-y* diagram is the most convenient for these purposes, and its use is developed in detail here. The use of the enthalpy-concentration diagram is given by Smith (*Design of Equilibrium Stage Processes*, McGraw-Hill, New York, 1963) and Henley and Seader (*Equilibrium-Stage Separation Operations in Chemical Engineering*, Wiley, New York, 1981).

PHASE EQUILIBRIUM DATA

Three types of binary equilibrium curves are shown in Fig. 13-27. The *y-x* diagram is almost always plotted for the component that is the more volatile (denoted by the subscript 1) in the region where distillation is to take place. Curve *A* shows the most usual case, in which component 1 remains more volatile over the entire composition range. Curve *B* is typical of many systems (ethanol-water, for example) in which the component that is more volatile at low values of x_1 becomes less volatile than the other component at high values of x_1. The vapor and liquid compositions are identical for the homogeneous azeotrope where curve *B* crosses the 45° diagonal. A heterogeneous azeotrope is formed with two liquid phases by curve *C*.

An azeotrope limits the separation that can be obtained between components by simple distillation. For the system described by curve *B*, the maximum overhead-product concentration that could be obtained from a feed with $x_1 = 0.25$ is the azeotropic composition. Similarly, a feed with $x_1 = 0.9$ could produce a bottom-product composition no lower than the azeotrope.

The phase rule permits only two variables to be specified arbitrarily in a binary two-phase system at equilibrium. Consequently, the curves in Fig. 13-27 can be plotted at either constant temperature or constant pressure but not both. The latter is more common, and data in Table 13-1 are for that case. The *y-x* diagram can be plotted in either mole, weight, or volume fractions. The units used later for the phase flow rates must, of course, agree with those used for the equilibrium data. Mole fractions, which are almost always used, are applied here.

It is sometimes permissible to assume constant *relative volatility* in order to approximate the equilibrium curve quickly. Then by applying Eq. (13-2) to components 1 and 2,

$$\alpha = K_1/K_2 = y_1x_2/x_1y_2$$

which, since $x_2 = 1 - x_1$ and $y_2 = 1 - y_1$, can be rewritten as

$$y_1 = \frac{x_1\alpha}{1 + (\alpha - 1)x_1} \tag{13-20}$$

for use in calculating points for the equilibrium curve.

McCABE-THIELE METHOD

Operating Lines The McCabe-Thiele method is based upon representation of the material-balance equations as operating lines on the *y-x* diagram. The lines are made straight (and the need for the energy balance obviated) by the assumption of *constant molar overflow*. The liquid-phase flow rate is assumed to be constant from tray to tray in each section of the column between addition (feed) and withdrawal (product) points. If the liquid rate is constant, the vapor rate must also be constant.

The constant-molar-overflow assumption represents several prior assumptions. The most important one is equal molar heats of vaporization for the two components. The other assumptions are adiabatic operation (no heat leaks) and no heat of mixing or sensible heat effects. These assumptions are most closely approximated for close-boiling isomers. The result of these assumptions on the calculation method can be illustrated with Fig. 13-28, which shows two material-balance envelopes cutting through the top section (above the top feed stream or sidestream) of the column. If L_{n+1} is assumed to be identical to L_{n-1} in rate, then $V_n = V_{n-2}$ and the component material balance for both envelopes 1 and 2 can be represented by

$$y_n = (L/V)x_{n+1} + (Dx_D/V) \tag{13-21}$$

where y and x have a stage subscript n or $n + 1$, but L and V need be identified only with the section of the column to which they apply. Equation (13-21) has the analytical form of a straight line where L/V is the slope and Dx_D/V is the y intercept at $x_1 = 0$.

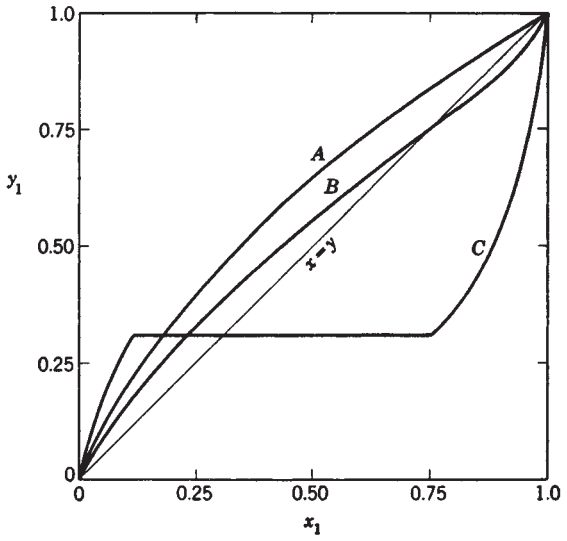

FIG. 13-27 Typical binary equilibrium curves. Curve *A*, system with normal volatility. Curve *B*, system with homogeneous azeotrope (one liquid phase). Curve *C*, system with heterogeneous azeotrope (two liquid phases in equilibrium with one vapor phase).

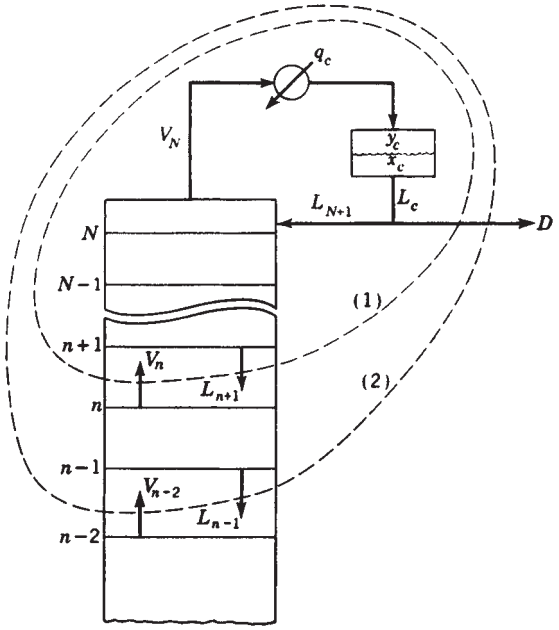

FIG. 13-28 Two material-balance envelopes in the top section of a distillation column.

The effect of a sidestream withdrawal point is illustrated by Fig. 13-29. The material-balance equation for the column section below the sidestream is

$$y_n = \frac{L'}{V'} x_{n+1} + \frac{Dx_D + Sx_S}{V'} \tag{13-22}$$

where the primes designate the L and V below the sidestream. Since the sidestream must be a saturated phase, $V = V'$ if a liquid side stream is withdrawn and $L = L'$ if it is a vapor.

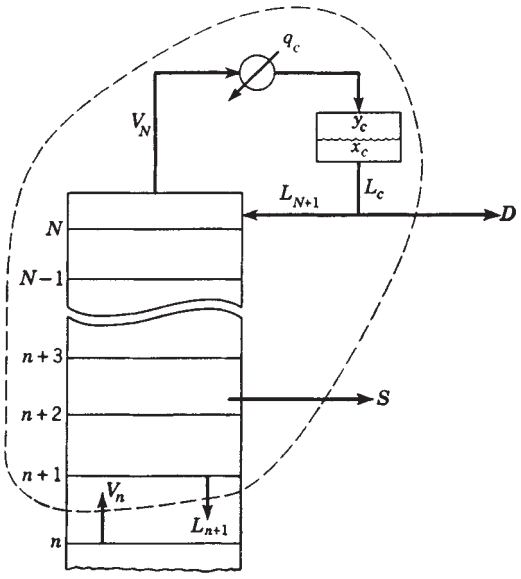

FIG. 13-29 Material-balance envelope which contains two external streams D and S, where S represents a sidestream product withdrawn above the feed plate.

If the sidestream in Fig. 13-29 had been a feed, the balance for the section below the feed would be

$$y_n = \frac{L'}{V'} x_{n+1} + \frac{Dx_D - Fx_F}{V'} \tag{13-23}$$

Similar equations can be written for the bottom section of the column. For the envelope shown in Fig. 13-30,

$$y_m = (L''/V'') x_{m+1} - (Bx_B/V) \tag{13-24}$$

where the subscript m is used to identify the stage number in the bottom section.

Equations such as (13-21) through (13-24) when plotted on the y-x diagram furnish a set of *operating lines.* A point on an operating line represents two *passing streams,* and the operating line itself is the locus of all possible pairs of passing streams within the column section to which the line applies.

An operating line can be located on the y-x diagram if (1) two points on the line are known or (2) one point and the slope are known. The known points on an operating line are usually its intersection with the y-x diagonal and/or its intersection with another operating line.

The slope L/V of the operating line is termed the *internal-reflux ratio.* This ratio in the operating-line equation for the top section of the column [see Eq. (13-21)] is related to the *external-reflux ratio* $R = L_{N+1}/D$ by

$$\frac{L}{V} = \frac{L_{N+1}}{V_N} = \frac{RD}{(1+R)D} = \frac{R}{1+R} \tag{13-25}$$

when the reflux stream L_{N+1} is a saturated liquid.

Thermal Condition of the Feed The slope of the operating line changes whenever a feed stream or a sidestream is passed. To calculate this change, it is convenient to introduce a quantity q which is defined by the following equations for a feed stream F:

$$L' = L + qF \tag{13-26}$$

$$V = V' + (1-q)F \tag{13-27}$$

The primes denote the streams below the stage to which the feed is introduced. The q is a measure of the thermal condition of the feed and represents the moles of saturated liquid formed in the feed stage

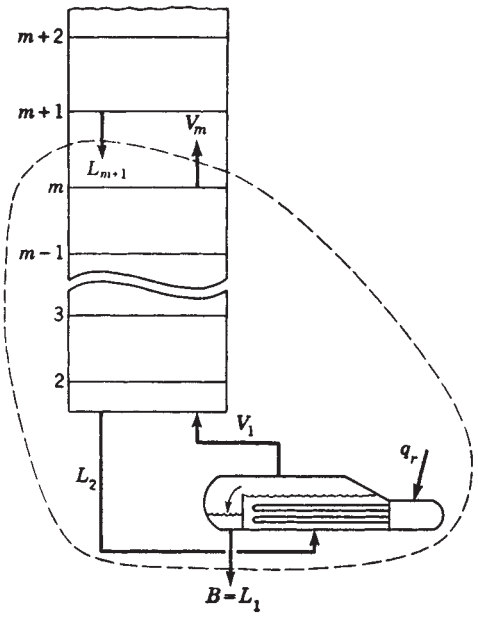

FIG. 13-30 Material-balance envelope around the bottom end of the column. The partial reboiler is equilibrium stage 1.

per mole of feed. It takes on the following values for various possible feed thermal conditions.

Subcooled-liquid feed: $q > 1$
Saturated-liquid feed: $q = 1$
Partially flashed feed: $1 > q > 0$
Saturated-vapor feed: $q = 0$
Superheated-vapor feed: $q < 0$

The q value for a particular feed can be estimated from

$$q = \frac{\text{energy to convert 1 mol of feed to saturated vapor}}{\text{molar heat of vaporization}}$$

Equations analogous to (13-26) and (13-27) can be written for a sidestream, but the q will be either 1 or 0 depending upon whether the sidestream is taken from the liquid or the vapor stream.

The q can be used to derive the "q-line equation" for a feed stream or a sidestream. The q line is the locus of all points of intersection of the two operating lines, which meet at the feed-stream or sidestream stage. This intersection must occur along that section of the q line between the equilibrium curve and the $y = x$ diagonal. At the point of intersection, the same y, x point must satisfy both the operating-line equation above the feed-stream (or sidestream) stage and the one below the feed-stream (or sidestream) stage. Subtracting one equation from the other gives for a feed stage

$$(V - V')y = (L - L')x + Fx_F$$

which when combined with Eqs. (13-26) and (13-27) gives the q-line equation

$$y = \frac{q}{q-1}x - \frac{x_F}{q-1} \tag{13-28}$$

A q-line construction for a partially flashed feed is given in Fig. 13-31. It is easily shown that the q line must intersect the diagonal at x_F. The slope of the q line is $q/(q-1)$. All five q-line cases are shown in Fig. 13-32.

The derivation of Eq. (13-28) assumes a single-feed column and no sidestream. However, the same result is obtained for other column configurations. Typical q-line constructions for sidestream stages are shown in Fig. 13-33. Note that the q line for a sidestream must always intersect the diagonal at the composition (y_1 or x_1) of the sidestream.

Figure 13-33 also shows the intersections of the operating lines with the diagonal construction line. The top operating line must always intersect the diagonal at the overhead-product composition x_D. This

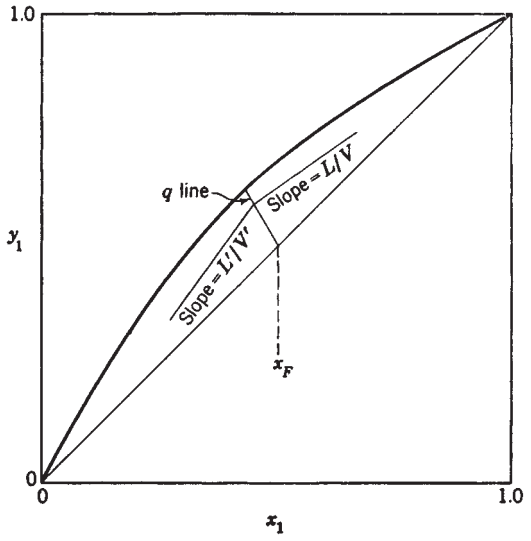

FIG. 13-31 Typical intersection of the two operating lines at the q line for a feed stage. The q line shown is for a partially flashed feed.

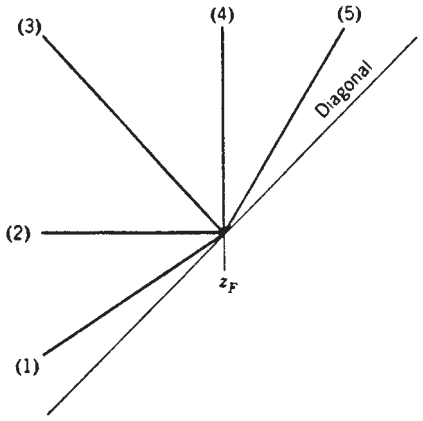

FIG. 13-32 All five cases of q lines; (1) superheated-vapor feed, (2) saturated-vapor feed, (3) partially vaporized feed, (4) saturated-liquid feed, and (5) subcooled-liquid feed. Slope of q line = $q/(q-1)$.

can be shown by substituting $y = x$ in Eq. (13-21) and using $V - L = D$ to reduce the resulting equation to $x = x_D$. Similarly (except for columns in which open steam is introduced at the bottom), the bottom operating line must always intersect the diagonal at the bottom-product composition x_B.

Equilibrium-Stage Construction The alternate use of the equilibrium curve and the operating line to "step off" equilibrium stages is illustrated in Fig. 13-34. The plotted portions of the equilibrium curve (curved) and the operating line (straight) cover the composition range existing in the column section shown in the lower right-hand corner. If y_n and x_n represent the compositions (in terms of the more volatile component) of the equilibrium vapor and liquid leaving stage n, then point (y_n, x_n) on the equilibrium curve must represent the equilibrium stage n. The operating line is the locus for compositions of all possible pairs of passing streams within the section and therefore a horizontal line (dotted) at y_n must pass through the point (y_n, x_{n+1}) on the operating line since y_n and x_{n+1} represent passing streams. Likewise, a vertical line (dashed) at x_n must intersect the operating line at point (y_{n-1}, x_n). The equilibrium stages above and below stage n can be located by a vertical line through (y_n, x_{n+1}) to find (y_{n+1}, x_{n+1}) and a horizontal line through (y_{n-1}, x_n) to find (y_{n-1}, x_{n-1}). It can be seen that one can work upward or downward through the column by alternating the use of equilibrium and operating lines.

Total-Column Construction The graphical construction for an entire column is shown in Fig. 13-35. The process, pictured in the lower right-hand corner of the diagram, is an existing column with a number of actual trays equivalent to eight equilibrium stages. A partial reboiler (equivalent to an equilibrium stage) and a total condenser are used. This column configuration was analyzed earlier (see Fig. 13-24) and shown to have $C + 2N + 9$ design variables (degrees of freedom) which must be specified to define one unique operation. These may be used as follows as the basis for a graphical solution:

Specifications	N_i^u
Stage pressures (including reboiler)	N
Condenser pressure	1
Stage heat leaks (except reboiler)	$N - 1$
Pressure and heat leak in reflux divider	2
Feed stream	$C + 2$
Feed-stage location	1
Total number of stages N	1
One overhead purity	1
Reflux temperature	1
External-reflux ratio	1
	$C + 2N + 9$

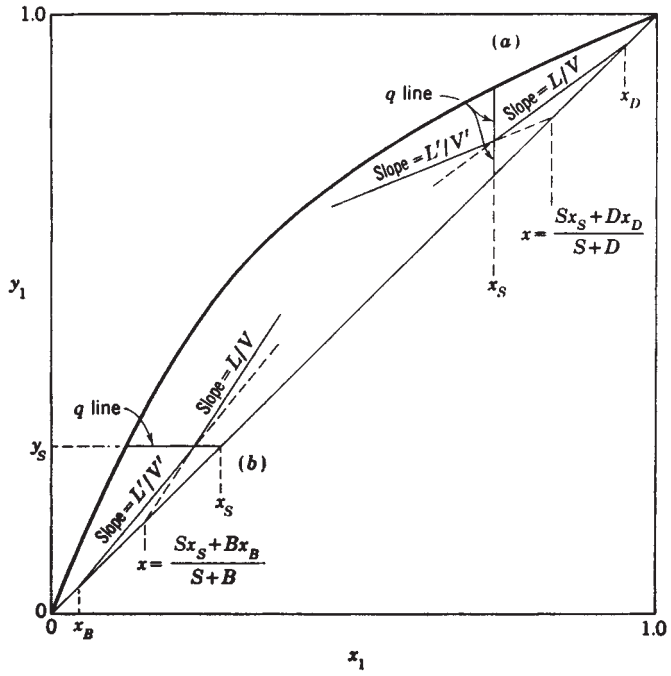

FIG. 13-33 Typical construction for a sidestream showing the intersection of the two operating lines with the q line and with the $x - y$ diagonal. (*a*) Liquid sidestream near the top of the column. (*b*) Vapor sidestream near the bottom of the column.

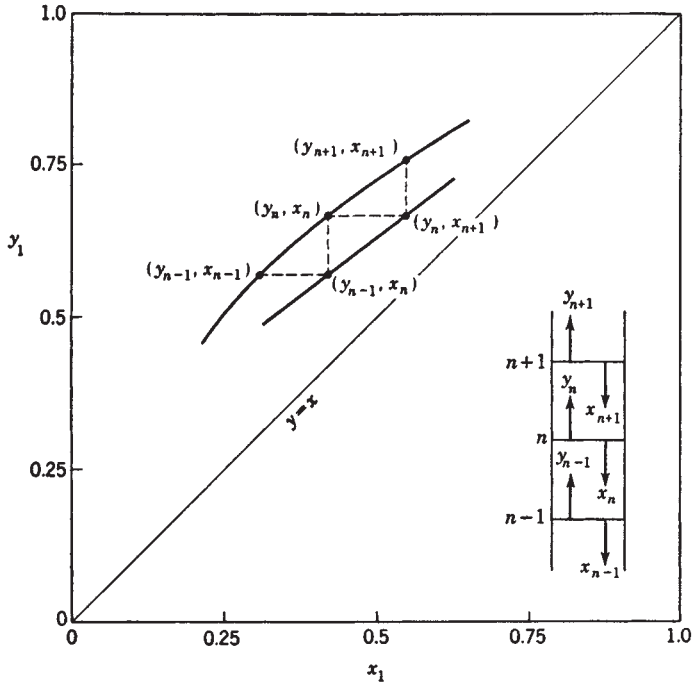

FIG. 13-34 Illustration of how equilibrium stages can be located on the x-y diagram through the alternating use of the equilibrium curve and the operating line.

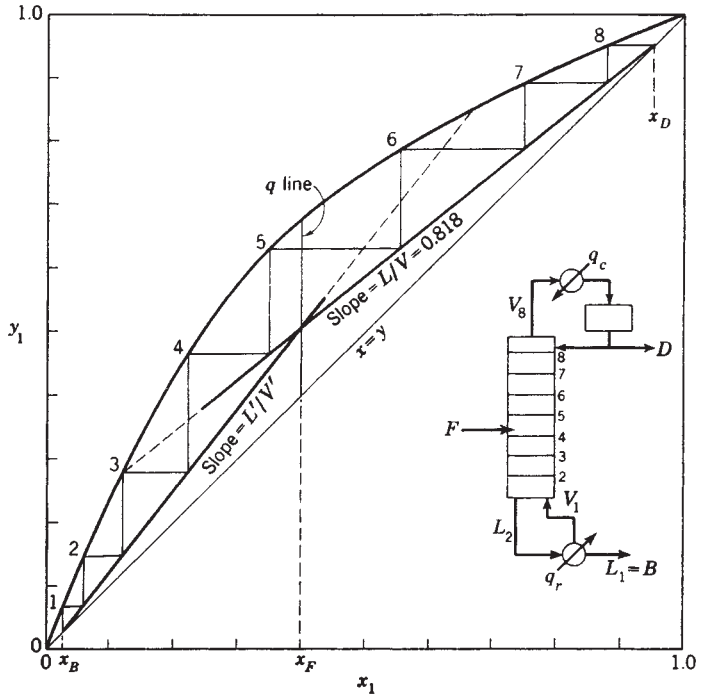

FIG. 13-35 Construction for a column with a bubble-point feed, a total condenser, and a partial reboiler.

Pressures can be specified at any level below the safe working pressure of the column. The condenser pressure will be set at 275.8 kPa (40 psia), and all pressure drops within the column will be neglected. The equilibrium curve in Fig. 13-35 represents data at that pressure. All heat leaks will be assumed to be zero. The feed composition is 40 mole percent of the more volatile component 1, and the feed rate is 0.126 (kg·mol)/s [1000 (lb·mol)/h] of saturated liquid ($q = 1$). The feed-stage location is fixed at stage 4 and the total number of stages at eight.

The overhead purity is specified as $x_D = 0.95$. The reflux temperature is the bubble-point temperature (saturated reflux), and the external-reflux ratio is set at $R = 4.5$.

Answers are desired to the following two questions. First, what bottom-product composition x_B will the column produce under these specifications? Second, what will be the top vapor rate V_N in this operation, and will it exceed the maximum vapor-rate capacity for this column, which is assumed to be 0.252 (kg·mol)/s [2000 (lb·mol)/h] at the top-tray conditions?

The solution is started by using Eq. (13-25) to convert the external-reflux ratio of 4.5 to an internal-reflux ratio of $L/V = 0.818$. The $x_D = 0.95$ value is then located on the diagonal, and the upper operating line is drawn as shown in Fig. 13-35.

If the x_B value were known, the bottom operating line could be immediately drawn from the x_B value on the diagonal up to its required intersection point with the upper operating line on the feed q line. In this problem, since the number of stages is fixed, the x_B which gives a lower operating line that will require exactly eight stages must be found by trial and error. An x_B value is assumed, and the resulting lower operating line is drawn. The stages can be stepped off by starting from either x_B or x_D; x_B was used in this case.

Note that the lower operating line is used until the fourth stage is passed, at which time the construction switches to the upper operating line. This is necessary because the vapor and liquid streams passing each other between the fourth and fifth stages must fall on the upper line.

The x_B that requires exactly eight equilibrium stages is $x_1 = 0.026$. An overall component balance gives $D = 0.051$ (kg·mol)/s [405 (lb·mol)/h]. Then,

$$V_N = V_B = L_{N+1} + D = D(R + 1) = 0.051(4.5 + 1.0)$$
$$= 0.280 \text{ (kg·mol)/s } [2230 \text{ (lb·mol)/h}]$$

which exceeds the column capacity of 0.252 (kg·mol)/s [2007 (lb·mol)/h]. This means that the column cannot provide an overhead-product yield of 40.5 percent at 95 percent purity. Either the purity specification must be reduced, or we must be satisfied with a lower yield. If the $x_D = 0.95$ specification is retained, the reflux rate must be reduced. This will cause the upper operating line to pivot upward around its fixed point of $x = 0.95$ on the diagonal. The new intersection of the upper line with the q line will lie closer to the equilibrium curve. The x_B value must then move upward along the diagonal because the eight stages will not "reach" as far as formerly. The higher x_B concentration will reduce the recovery of component 1 in the 95 percent overhead product.

Another entire column with a partially vaporized feed, a liquid-sidestream rate equal to D and withdrawn from the second stage from the top, and a total condenser is shown in Fig. 13-36. The specified concentrations are $x_F = 0.40$, $x_B = 0.05$, and $x_D = 0.95$. The specified L/V ratio in the top section is 0.818. These specifications permit the top operating line to be located and the two top stages stepped off to determine the liquid-sidestream composition $x_S = 0.746$. The operating line below the sidestream must intersect the diagonal at the "blend" of the sidestream and the overhead stream. Since S was specified to be equal to D in rate, the intersection point is

$$x = \frac{(1.0)(0.746) + (1.0)(0.95)}{1.0 + 1.0} = 0.848$$

This point plus the point of intersection of the two operating lines on the sidestream q line (vertical at $x_S = 0.746$) permits the location of the middle operating line. (The slope of the middle operating line could

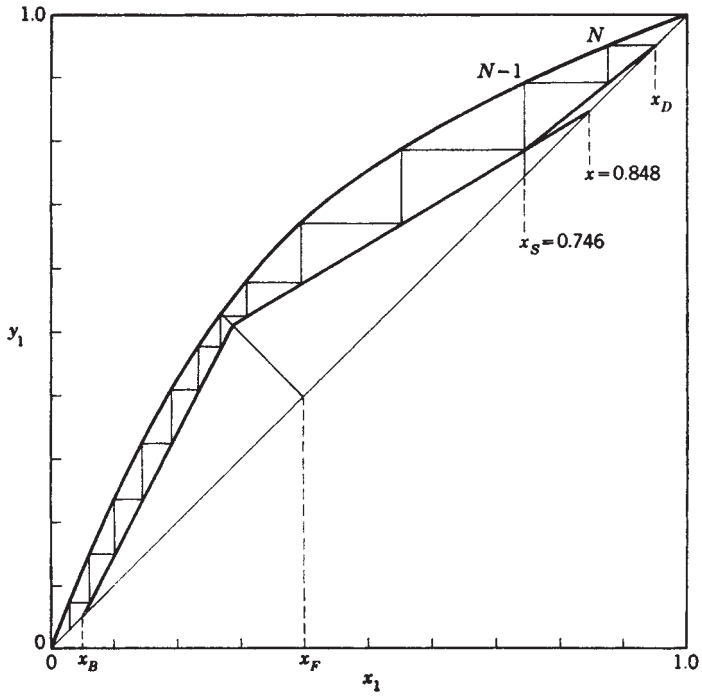

FIG. 13-36 Graphical solution for a column with a partially flashed feed, a liquid sidestream and a total condenser.

also have been used.) The lower operating line must run from the specified x_B value on the diagonal to the required point of intersection on the feed q line. The stages are stepped off from the top down in this case. The sixth stage from the top is the feed stage, and a total of about 11.4 stages is required to reach the specified $x_B = 0.05$.

Fractional equilibrium stages have meaning. The 11.4 will be divided by a tray efficiency, and the rounding to an integral number of actual trays should be done after that division. For example, if the average tray efficiency for the process being modeled in Fig. 13-36 were 80 percent, then the number of actual trays required would be 11.4/0.8 = 14.3, which would be rounded to 15.

Feed-Stage Location The *optimum* feed-stage location is that location which, with a given set of other operating specifications, will result in the widest separation between x_D and x_B for a given number of stages. Or, if the number of stages is not specified, the optimum feed location is the one that requires the lowest number of stages to accomplish a specified separation between x_D and x_B. Either of these criteria will always be satisfied if the operating line farthest from the equilibrium curve is used in each step as in Fig. 13-35.

It can be seen from Fig. 13-35 that the optimum feed location would have been the fifth tray for that operation. If a new column were being designed, that would have been the designer's choice. However, when an existing column is being modeled, the feed stage on the diagram should correspond as closely as possible to the actual feed tray in the column. It can be seen that a badly mislocated feed (a feed that requires one to remain with an operating line until it closely approaches the equilibrium curve) can be very wasteful insofar as the effectiveness of the stages is concerned.

Minimum Stages A column operating at total reflux is diagramed in Fig. 13-37*a*. Enough material has been charged to the column to fill the reboiler, the trays, and the overhead condensate drum to their working levels. The column is then operated with no feed and with all the condensed overhead stream returned as reflux ($L_{N+1} = V_N$ and $D = 0$). Also all the liquid reaching the reboiler is vaporized and returned to the column as vapor. Since F, D, and B are all zero, $L_{n+1} = V_n$ at all points in the column. With a slope of unity ($L/V = 1.0$), the operating line must coincide with the diagonal throughout the column. Total-reflux operation gives the minimum number of stages required to effect a specified separation between x_B and x_D.

Minimum Reflux The minimum-reflux ratio is defined as that ratio which if decreased by an infinitesimal amount would require an infinite number of stages to accomplish a specified separation between two components. The concept has meaning only if a separation between two components is specified and the number of stages is not specified. Figure 13-37*b* illustrates the minimum-reflux condition. As the reflux ratio is reduced, the two operating lines swing upward, pivoting around the specified x_B and x_D values, until one or both touch the equilibrium curve. For equilibrium curves shaped like the one shown, the contact occurs at the feed q line. Often an equilibrium curve will dip down closer to the diagonal at higher concentrations. In such cases, the upper operating line may make contact before its intersection point on the q line reaches the equilibrium curve. Wherever the contact appears, the intersection of the operating line with the equilibrium curve produces a pinch point which contains a very large number of stages, and a zone of constant composition is formed.

Intermediate Reboilers and Condensers A distillation column of the type shown in Fig. 13-2*a*, operating with an interreboiler and an intercondenser in addition to a reboiler and a condenser, is diagramed with the solid lines in Fig. 13-38. The dashed lines correspond to simple distillation with only a bottoms reboiler and an overhead condenser. Total boiling and condensing heat loads are the same for both columns. As shown by Kayihan [*Am. Inst. Chem. Eng. J. Symp. Ser.* **76,** 192, 1 (1980)], the addition of interreboilers and intercondensers increases thermodynamic efficiency but requires additional stages, as is clear from the positions of the operating lines in Fig. 13-38.

Optimum Reflux Ratio The general effect of the operating reflux ratio on fixed costs, operating costs, and the sum of these is shown in Fig. 13-39. In ordinary situations, the minimum on the total-cost curve will generally occur at an operating reflux ratio of from 1.1 to 1.5 times the minimum $R = L_{N+1}/D$ value, with the lower value corresponding to a value of the relative volatility close to 1.

Difficult Separations Some binary separations may pose special problems because of extreme purity requirements for one or both products or because of a relative volatility close to 1. The y-x diagram

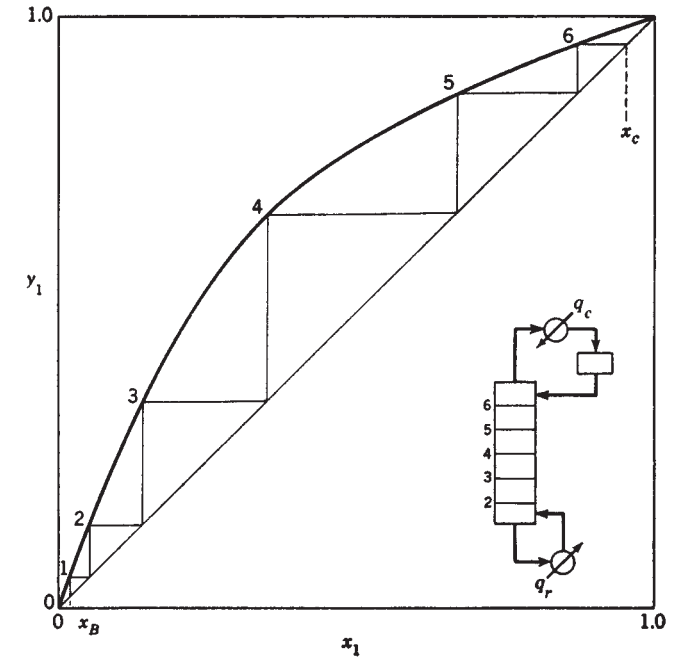

(a)

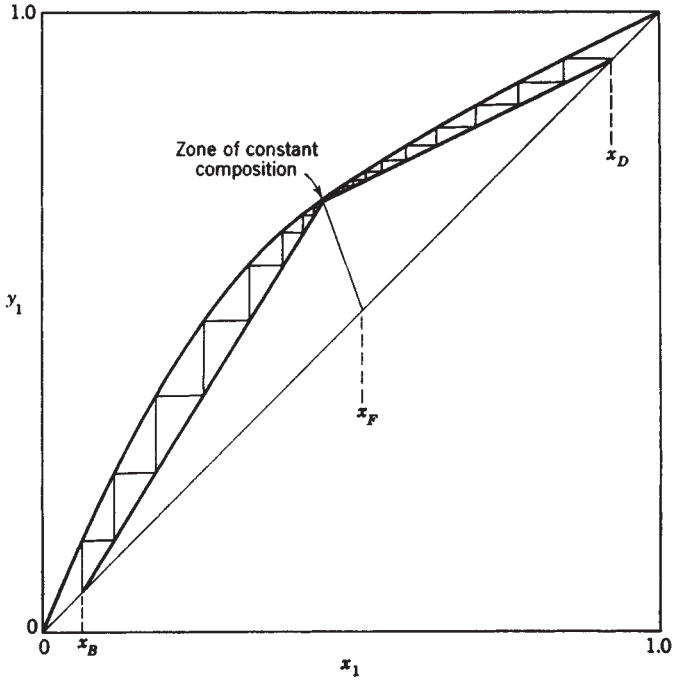

(b)

FIG. 13-37 McCabe-Thiele diagrams for limiting cases. (*a*) Minimum stages for a column operating at total reflux with no feeds or products. (*b*) Minimum reflux for a binary system of normal volatility.

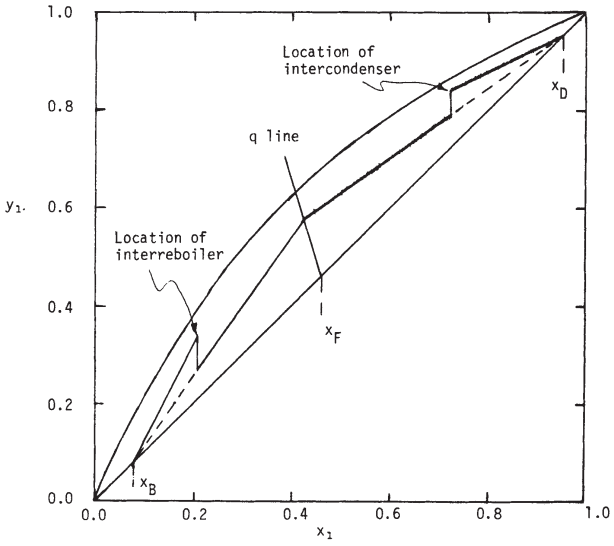

FIG. 13-38 McCabe-Thiele diagram for columns with and without an interreboiler and an intercondenser.

is convenient for stepping off stages at extreme purities if it is plotted on log-log paper. The equilibrium curve at very low x_1 values on ordinary graph paper can usually be assumed to be a straight line with an intercept term of zero which can be expressed as

$$y = (y/x)x + 0.0$$

where the slope y/x is a constant. The necessity for knowing the slope is eliminated by taking the logarithm of both sides

$$\log y = \log x + \log (y/x)$$

and plotting y versus x on a log-log plot to give a straight line with a slope of unity. The slope y/x is now an intercept term which need not be known. One point from the equilibrium curve is sufficient, therefore, to locate the equilibrium curve on the log-log plot. The operating line will be curved on the log-log plot and is located by plotting the appropriate material-balance equation. Both the equilibrium and the operating lines can be extended to any purity desired.

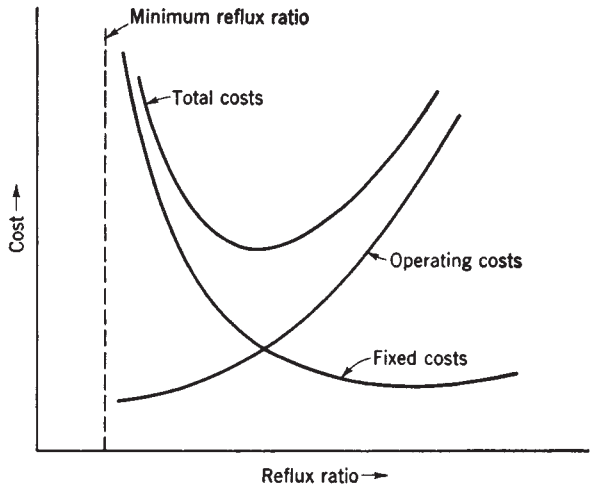

FIG. 13-39 Location of the optimum reflux for a given feed and specified separation.

A system with constant relative volatility can be handled conveniently by the equation of Smoker [*Trans. Am. Inst. Chem. Eng.*, **34,** 165 (1938)]. The derivation of the equation is shown, and its use is illustrated by Smith (op. cit.).

Stage Efficiency The use of the *Murphree plate efficiency* is particularly convenient on y-x diagrams. The Murphree efficiency is defined for the vapor phase as

$$\eta = (y_n - y_{n-1})/(y_n^* - y_{n-1}) \qquad (13\text{-}29)$$

where y_n^* is the composition of the vapor that would be in equilibrium with the liquid leaving stage n and is the value read from the equilibrium curve. The y_{n-1} and y_n are the actual (nonequilibrium) values for vapor streams leaving the $n-1$ and n stages respectively. Note that the y_{n-1} and y_n values assume that vapor streams are completely mixed and uniform in composition. An analogous efficiency can be defined for the liquid phase.

The application of a 50 percent Murphree vapor-phase efficiency on a y-x diagram is illustrated in Fig. 13-40. A "pseudo-equilibrium" curve is drawn halfway (on a vertical line) between the operating lines and the true-equilibrium curve. The true-equilibrium curve is used for the first stage (the partial reboiler is assumed to be an equilibrium stage), but for all other stages the vapor leaving each stage is assumed to approach the equilibrium value y_n^* only 50 percent of the way. Consequently, the steps in Fig. 13-40 represent actual trays.

Application of a constant efficiency to each stage as in Fig. 13-40 will not give, in general, the same answer as obtained when the number of equilibrium stages (obtained by using the true-equilibrium curve) is divided by the same efficiency factor.

The prediction and use of stage efficiencies are described in detail in Sec. 14.

Miscellaneous Operations The y-x diagrams for several other column configurations have not been presented here. The omitted items are *partial condensers, rectifying columns* (feed introduced to the bottom stage), *stripping columns* (feed introduced to the top stage), total reflux in the top section but not in the bottom section, multiple feeds, and introduction of *open steam* to the bottom stage to eliminate the reboiler. These configurations are discussed in Smith (op. cit.) and Henley and Seader (op. cit.), who also describe the more rigorous Ponchon-Savarit method, which is not included here.

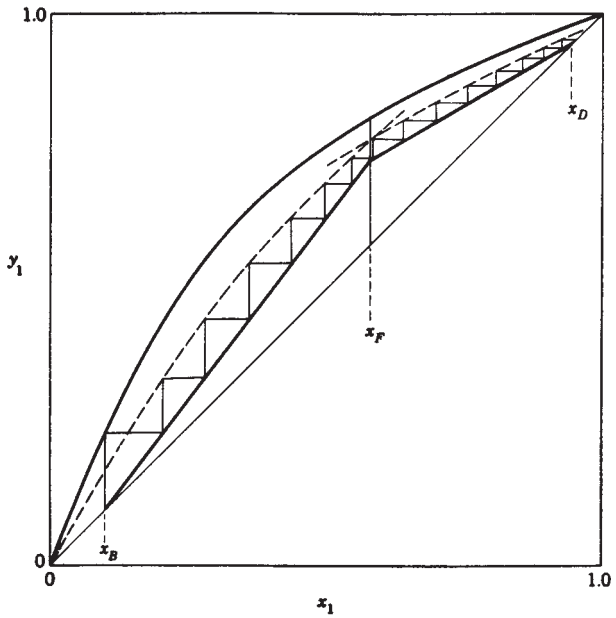

FIG. 13-40 Application of a 50 percent Murphree vapor-phase efficiency to each stage (excluding the reboiler) in the column. Each step in the diagram corresponds to an actual stage.

APPROXIMATE MULTICOMPONENT DISTILLATION METHODS

INTRODUCTION

Some approximate calculation methods for the solution of multicomponent, multistage separation problems continue to serve useful purposes even though computers are available to provide more rigorous solutions. The available phase equilibrium and enthalpy data may not be accurate enough to justify the longer rigorous methods. Or in extensive design and optimization studies, a large number of cases can be worked quickly and cheaply by an approximate method to define roughly the optimum specifications, which can then be investigated more exactly with a rigorous method.

Two approximate multicomponent shortcut methods for simple distillation are the Smith-Brinkley (SB) method, which is based on an analytical solution of the finite-difference equations that can be written for staged separation processes when stages and interstage flow rates are known or assumed and the Fenske-Underwood-Gilliland (FUG) method, which combines Fenske's total-reflux equation and Underwood's minimum-reflux equation with a graphical correlation by Gilliland that relates actual column performance to total- and minimum-reflux conditions for a specified separation between two key components. Thus, the SB and FUG methods are rating and design methods respectively. Both methods work best when mixtures are nearly ideal.

The SB method is not presented here, but is presented in detail in the sixth edition of *Perry's Chemical Engineers' Handbook.* Extensions of the SB method to nonideal mixtures and complex configurations are developed by Eckert and Hlavacek [*Chem. Eng. Sci.,* **33,** 77 (1978)] and Eckert [*Chem. Eng. Sci.,* **37,** 425 (1982)] respectively but are not discussed here. However, the approximate and very useful method of Kremser [*Nat. Pet. News,* **22**(21), 43 (May 21, 1930)] for application to absorbers and strippers is discussed at the end of this subsection.

FENSKE-UNDERWOOD-GILLILAND (FUG) SHORTCUT METHOD

In this approach, Fenske's equation [*Ind. Eng. Chem.,* **24,** 482 (1932)] is used to calculate N_m, which is the number of plates required to make a specified separation at total reflux, i.e., the minimum value of N. Underwood's equations [*J. Inst. Pet.,* **31,** 111 (1945); **32,** 598 (1946); **32,** 614 (1946); and *Chem. Eng. Prog.,* **44,** 603 (1948)] are used to estimate the minimum-reflux ratio R_m. The empirical correlation of Gilliland [*Ind. Eng. Chem.,* **32,** 1220 (1940)] shown in Fig. 13-41 then uses these values to give N for any specified R or R for any specified N. Limitations of the Gilliland correlation are discussed by Henley and Seader (*Equilibrium-Stage Separation Operations in Chemical Engineering,* Wiley, New York, 1981). The following equation, developed by Molokanov et al. [*Int. Chem. Eng.,* **12**(2), 209 (1972)] satisfies the end points and fits the Gilliland curve reasonably well:

$$\frac{N-N_m}{N+1} = 1 - \exp\left[\left(\frac{1+54.4\Psi}{11+117.2\Psi}\right)\left(\frac{\Psi-1}{\Psi^{0.5}}\right)\right] \qquad (13\text{-}30)$$

where $\Psi = (R-R_m)/(R+1)$.

The *Fenske total-reflux equation* can be written as

$$\left(\frac{x_i}{x_r}\right) = (\alpha_i)^{N_m}\left(\frac{x_i}{x_r}\right)_B \qquad (13\text{-}31)$$

or as

$$N_m = \frac{\log\left[\left(\frac{Dx_D}{Bx_B}\right)_i\left(\frac{Bx_B}{Dx_D}\right)_r\right]}{\log \alpha_i} \qquad (13\text{-}32)$$

where i is any component and r is an arbitrarily selected reference component in the definition of relative volatilities.

$$\alpha_i = K_i/K_r = y_i x_r/y_r x_i \qquad (13\text{-}33)$$

The particular value of α_i is the effective value used in Eqs. (13-36) and (13-34) defined in terms of values for each stage in the column by

$$\alpha^N = \alpha_N \alpha_{N-1} \cdots \alpha_2 \alpha_1 \qquad (13\text{-}34)$$

Equations (13-31) and (13-32) are rigorous relationships between the splits obtained for components i and r in a column at total reflux. However, the correct value of α_i must always be estimated, and this is where the approximation enters. It is usually estimated from

$$\alpha = (\alpha_{top}\alpha_{bottom})^{1/2} \qquad (13\text{-}35)$$

or

$$\alpha = (\alpha_{top}\alpha_{middle}\alpha_{bottom})^{1/3} \qquad (13\text{-}36)$$

A reasonably good estimate of the separation that will be accomplished in a plant column often can be obtained by specifying the split of one component (designated as the reference component r), setting N_m equal to from 40 to 60 percent of the number of equilibrium stages (not actual trays), and then using Eq. (13-32) to estimate the splits of all the other components. This is an iterative calculation because the component splits must first be arbitrarily assumed to give end compositions that can be used to give initial end-temperature estimates. The α_{top} and α_{bottom} values corresponding to these end temperatures are used in Eq. (13-35) to give α_i values for each component. The iteration is continued until the α_i values do not change from trial to trial.

The *Underwood minimum-reflux equations* of main interest are those that apply when some of the components do not appear in either the distillate or the bottoms products at minimum reflux. These equations are

$$\sum_i \frac{\alpha_i (x_{i,D})_m}{\alpha_i - \Theta} = R_m + 1 \qquad (13\text{-}37)$$

and

$$\sum_i \frac{\alpha_i x_{i,F}}{\alpha_i - \Theta} = 1 - q \qquad (13\text{-}38)$$

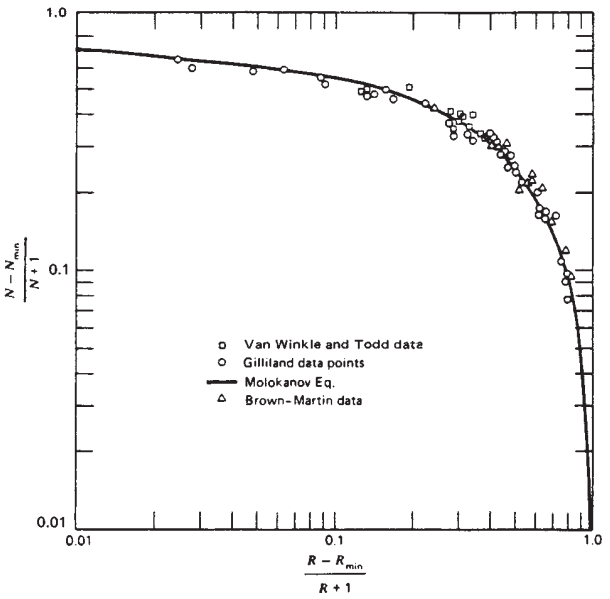

FIG. 13-41 Comparison of rigorous calculations with Gilliland correlation. [*Henley and Seader,* Equilibrium-Stage Separation Operations in Chemical Engineering, *Wiley, New York, 1981; data of Van Winkle and Todd,* Chem. Eng., **78**(21), *136 (Sept. 20, 1971); data of Gilliland,* Elements of Fractional Distillation, *4th ed., McGraw-Hill, New York, 1950; data of Brown and Martin,* Trans. Am. Inst. Chem. Eng., **35,** *679 (1939).*]

The relative volatilities α_i are defined by Eq. (13-33), R_m is the minimum-reflux ratio $(L_{N+1}/D)_{\min}$, and q describes the thermal condition of the feed (e.g., 1.0 for a bubble-point feed and 0.0 for a saturated-vapor feed). The $x_{i,F}$ values are available from the given feed composition. The Θ is the common root for the top-section equations and the bottom-section equations developed by Underwood for a column at minimum reflux with separate zones of constant composition in each section. The common root value must fall between α_{hk} and α_{lk}, where *hk* and *lk* stand for *heavy key* and *light key* respectively. The *key components* are the ones that the designer wants to separate. In the butane-pentane splitter problem used in Example 1, the light key is n-C_4 and the heavy key is i-C_5.

The α_i values in Eqs. (13-37) and (13-38) are effective values obtained from Eq. (13-35) or Eq. (13-36). Once these values are available, Θ can be calculated in a straightforward iteration from Eq. (13-38). Since the $(\alpha - \Theta)$ difference can be small, Θ should be determined to four decimal places to avoid numerical difficulties.

The $(x_{i,D})_m$ values in Eq. (13-37) are minimum-reflux values, i.e., the overhead concentration that would be produced by the column operating at the minimum reflux with an infinite number of stages. When the light key and the heavy key are adjacent in relative volatility and the specified split between them is sharp or the relative volatilities of the other components are not close to those of the two keys, only the two keys will distribute at minimum reflux and the $(x_{i,D})_m$ values are easily determined. This is often the case and is the only one considered here. Other cases in which some or all of the nonkey components distribute between distillate and bottom products are discussed in detail by Henley and Seader (op. cit.).

The FUG method is convenient for new-column design with the following specifications:

1. R/R_m, the ratio of reflux to minimum reflux
2. Split on the reference component (usually chosen as the heavy key)
3. Split on one other component (usually the light key)

However, the total number of equilibrium stages N, N/N_m, or the external-reflux ratio can be substituted for one of these three specifications. It should be noted that the feed location is automatically specified as the optimum one; this is assumed in the Underwood equations. The assumption of saturated reflux is also inherent in the Fenske and Underwood equations. An important limitation on the Underwood equations is the assumption of constant molar overflow. As discussed by Henley and Seader (op. cit.), this assumption can lead to a prediction of the minimum reflux that is considerably lower than the actual value. No such assumption is inherent in the Fenske equation. An exact calculational technique for minimum reflux is given by Tavana and Hansen [*Ind. Eng. Chem. Process Des. Dev.*, **18,** 154 (1979)]. A computer program for the FUG method is given by Chang [*Hydrocarbon Process.*, **60**(8), 79 (1980)]. The method is best applied to mixtures that form ideal or nearly ideal solutions.

Example 1: Calculation of FUG Method A large butane-pentane splitter is to be shut down for repairs. Some of its feed will be diverted temporarily to an available smaller column, which has only 11 trays plus a partial reboiler. The feed enters on the middle tray. Past experience on similar feeds indicates that the 11 trays plus the reboiler are roughly equivalent to 10 equilibrium stages and that the column has a maximum top-vapor capacity of 1.75 times the feed rate on a mole basis. The column will operate at a condenser pressure of 827.4 kPa (120 psia). The feed will be at its bubble point ($q = 1.0$) at the feed-tray conditions and has the following composition on the basis of 0.0126 (kg·mol)/*s* [100 (lb·mol)/h]:

Component	Fx_F
C_3	5
i-C_4	15
n-C_4	25
i-C_5	20
n-C_5	35
	100

The original column normally has less than 7 mol percent i-C_5 in the overhead and less than 3 mole percent n-C_4 in the bottoms product when operating at a distillate rate of $D/F = 0.489$. Can these product purities be produced on the smaller column at $D/F = 0.489$?

Pressure drops in the column will be neglected, and the K values will be read at 827 kPa (120 psia) in both column sections from the DePriester nomograph in Fig. 13-14*b*. When constant molar overflow is assumed in each section, the rates in pound-moles per hour in the upper and lower sections are as follows:

Top section	Bottom section
$D = (0.489)(100) = 48.9$	$B = 100 - 48.9 = 51.1$
$V = (1.75)(100) = 175$	$V' = V = 175$
$L = 175 - 48.9 = 126.1$	$L' = L + F = 226.1$
$V/L = 1.388$	$V'/L' = 0.7739$
$L/L' = 126.1/226.1 = 0.5577$	
$R = 126.1/48.9 = 2.579$	

NOTE: To convert pound-moles per hour to kilogram-moles per second, multiply by 1.26×10^{-4}.

Since the feed enters at the middle of the column, $M = 5$ and $M + 1 = 6$. Application of the FUG method is demonstrated on the splitter. Specifications necessary to model the existing column are:

1. $N = 10$, total number of equilibrium stages.
2. Optimum feed location (which may or may not reflect the actual location).
3. Maximum V/F at the top tray of 1.75.
4. Split on one component given in the following paragraphs.

The solution starts with an assumed arbitrary split of all the components to give estimates of top and bottom compositions that can be used to get initial end temperatures. The α_i's evaluated at these temperatures are averaged with an assumed feed-stage temperature (assumed to be the bubble point of the feed) by using Eq. (13-36). The initial assumption for the split on i-C_5 will be $Dx_D/Bx_B = 3.15/16.85$. As mentioned earlier, N_m usually ranges from $0.4N$ to $0.6N$, and the initial N_m value assumed here will be $(0.6)(10) = 6.0$. Equation (13-32) can be rewritten as

$$\left(\frac{Dx_D}{Fx_F - Dx_D}\right)_i = \alpha_i^{6.0}\left(\frac{3.15}{16.85}\right) = \alpha_i^{6.0}(0.1869)$$

or

$$Dx_{i,D} = \frac{0.1869\alpha_i^{6.0}}{1 + 0.1869\alpha_i^{6.0}} Fx_{i,F}$$

The evaluation of this equation for each component is as follows:

Component	α_i	$\alpha_i^{6.0}$	$0.1869\alpha_i^{6.0}$	Fx_F	Dx_D	Bx_B
C_3	5.00			5	5.0	0.0
i-C_4	2.63	330	61.7	15	14.8	0.2
n-C_4	2.01	66	12.3	25	25.1	1.9
i-C_5	1.00	1.00	0.187	20	3.15	16.85
n-C_5	0.843	0.36	0.0672	35	2.20	32.80
				100	48.25	51.75

The end temperatures corresponding to these product compositions are 344 K (159°F) and 386 K (236°F). These temperatures plus the feed bubble-point temperature of 358 K (185°F) provide a new set of α_i's which vary only slightly from those used earlier. Consequently, the $D = 48.25$ value is not expected to vary greatly and will be used to estimate a new i-C_5 split. The desired overhead concentration for i-C_5 is 7 percent; so it will be assumed that $Dx_D = (0.07)(48.25) = 3.4$ for i-C_5 and that the split on that component will be 3.4/16.6. The results obtained with the new α_i's and the new i-C_5 split are as follows:

Component	$\alpha_i^{6.0}$	$0.2048\alpha_i^{6.0}$	Fx_F	Dx_D	Bx_B	x_D	x_B
C_3			5	5.0	0.0	0.102	0.000
i-C_4	322	65.9	15	14.8	0.2	0.301	0.004
n-C_4	68	13.9	25	23.3	1.7	0.473	0.033
i-C_5	1.00	0.205	20	3.4	16.6	0.069	0.327
n-C_5	0.415	0.085	35	2.7	32.3	0.055	0.636
			100	49.2	50.8	1.000	1.000

The calculated i-C_5 concentration in the overhead stream is 6.9 percent, which is close enough to the 7.0 figure for now.

Table 13-8 shows subsequent calculations using the Underwood minimum-reflux equations. The α and x_D values in Table 13-8 are those from the Fenske

TABLE 13-8 Application of Underwood Equations

Component	x_F	α	αx_F	$\theta = 1.36$		$\theta = 1.365$		x_D	αx_D	$\alpha - \theta$	$\frac{\alpha x_D}{\alpha - \theta}$
				$\alpha - \theta$	$\frac{\alpha x_F}{\alpha - \theta}$	$\alpha - \theta$	$\frac{\alpha x_F}{\alpha - \theta}$				
C_3	0.05	4.99	0.2495	3.63	0.0687	3.625	0.0688	0.102	0.5090	3.6253	0.1404
i-C_4	0.15	2.62	0.3930	1.26	0.3119	1.255	0.3131	0.301	0.7886	1.2553	0.6282
n-C_4	0.25	2.02	0.5050	0.66	0.7651	0.655	0.7710	0.473	0.9555	0.6553	1.4581
i-C_5	0.20	1.00	0.2000	−0.36	−0.5556	−0.365	−0.5479	0.069	0.0690	−0.3647	−0.1892
n-C_5	0.35	0.864	0.3024	−0.496	−0.6097	−0.501	−0.6036	0.055	0.0475	−0.5007	−0.0949
	1.00				−0.0196		+0.0014	1.000			$1.9426 = R_m + 1$

Interpolation gives $\theta = 1.3647$.

total-reflux calculation. As noted earlier, the x_D values should be those at minimum reflux. This inconsistency may reduce the accuracy of the Underwood method, but to be useful a shortcut method must be fast, and it has not been shown that a more rigorous estimation of x_D values results in an overall improvement in accuracy. The calculated R_m is 0.9426. The actual reflux assumed is obtained from the specified maximum top vapor rate of 0.022 (kg·mol)/s [175 (lb·mol)/h] and the calculated D of 49.2 (from the Fenske equation).

$$L_{N+1} = V_N - D$$

$$R = V_N/D - 1 = 175/49.2 - 1 = 2.557$$

The $R_m = 0.9426$, $R = 2.557$, and $N = 10$ values are now used with the Gilliland correlation in Fig. 13-41 or Eq. (13-30) to check the initially assumed value of 6.0 for N_m. Equation (13-30) gives $N_m = 6.95$, which differs considerably from the assumed value.

Repetition of the calculations with $N_m = 7.0$ gives $R = 2.519$, $R_m = 0.9782$, and a calculated check value of $N_m = 6.85$, which is close enough. The final-product compositions and the α values used are as follows:

Component	α_i	Dx_D	Bx_B	x_D	x_B
C_3	4.98	5.00	0	0.1004	0.0
i-C_4	2.61	14.91	0.09	0.2996	0.0017
n-C_4	2.02	24.16	0.84	0.4852	0.0168
i-C_5	1.00	3.48	16.52	0.0700	0.3283
n-C_5	0.851	2.23	32.87	0.0448	0.6532
		49.78	50.32	1.0000	1.0000

These results indicate that the 7 percent i-C_5 in D and the 3 percent n-C_4 in B concentrations obtained in the original column can easily be obtained on the smaller column. Unfortunately, this disagrees somewhat with the answers obtained from a rigorous computer solution as shown in the following comparison:

	x_D		x_B	
Component	Rigorous	FUG	Rigorous	FUG
C_3	0.102	0.100	0.0	0.0
i-C_4	0.299	0.300	0.006	0.002
n-C_4	0.473	0.485	0.037	0.017
i-C_5	0.073	0.070	0.322	0.328
n-C_5	0.053	0.045	0.635	0.653
	1.000	1.000	1.000	1.000

KREMSER GROUP METHOD

Starting with the classical method of Kremser (op. cit.), approximate group methods of increasing complexity have been developed to calculate groups of equilibrium stages for a countercurrent cascade, such as is used in simple absorbers and strippers of the type depicted in Fig. 13-7*b* and *d*. However, none of these group methods can adequately account for stage temperatures that are considerably higher or lower than the two entering-stream temperatures for absorption and stripping respectively when appreciable composition changes occur. Therefore, only the simplest form of the Kremser method is presented here. Fortunately, rigorous computer methods described later can be applied when accurate results are required. The Kremser method is most useful for making preliminary estimates of absorbent and stripping-agent flow rates or equilibrium-stage requirements. The method can also be used to extrapolate quickly results of a rigorous solution to a different number of equilibrium stages.

Consider the general adiabatic countercurrent cascade of Fig. 13-42 where v and ℓ are molar component flow rates. Regardless of whether the cascade is an absorber or a stripper, components in the entering vapor will tend to be absorbed and components in the entering liquid will tend to be stripped. If more moles are stripped than absorbed, the cascade is a stripper; otherwise, the cascade is an absorber. The Kremser method is general and applies to either case. Application of component material-balance and phase equilibrium equations successively to stages 1 through $N - 1$, 1 through $N - 2$, etc., as shown by Henley and Seader (op. cit.), leads to the following equations originally derived by Kremser. For each component i,

$$(v_i)_N = (v_i)_0(\Phi_i)_A + (\ell_i)_{N+1}[1 - (\Phi_i)_S] \tag{13-39}$$

where

$$(\Phi_i)_A = \frac{(A_i)_e - 1}{(A_i)_e^{N+1} - 1} \tag{13-40}$$

is the fraction of component i in the entering vapor that is not absorbed.

$$(\Phi_i)_S = \frac{(S_i)_e - 1}{(S_i)_e^{N+1} - 1} \tag{13-41}$$

is the fraction of component i in the entering liquid that is not stripped.

$$(A_i)_e = (L/K_iV)_e \tag{13-42}$$

is the effective or average absorption factor for component i, and

$$(S_i)_e = 1/(A_i)_e \tag{13-43}$$

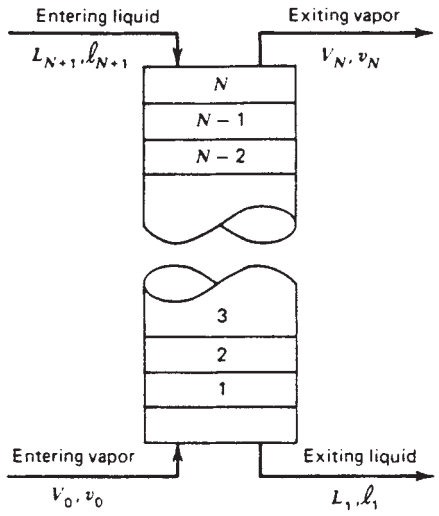

FIG. 13-42 General adiabatic countercurrent cascade for simple absorption or stripping.

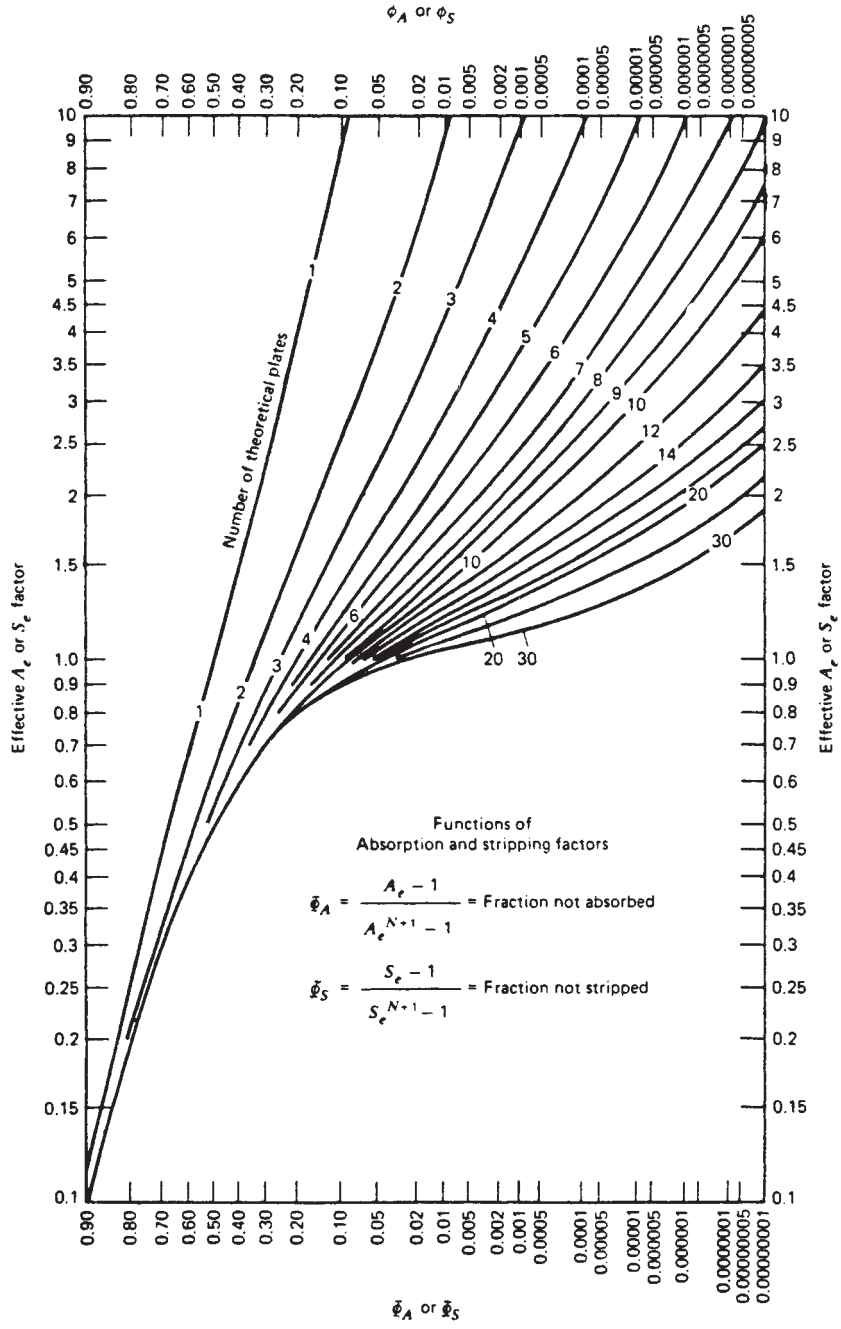

FIG. 13-43 Absorption and stripping factors. [*W. C. Edmister,* Am. Inst. Chem. Eng. J., *3, 165–171 (1957).*]

is the effective or average stripping factor for component *i*. When the entering streams are at the same temperature and pressure and negligible absorption and stripping occur, effective component absorption and stripping factors are determined simply by entering-stream conditions. Thus, if *K* values are composition-independent, then

$$(A_i)_e = 1/(S_i)_e = (L_{N+1}/K_i\{T_{N+1}, P_{N+1}\}V_0) \qquad (13\text{-}44)$$

When entering-stream temperatures differ and/or moderate to appreciable absorption and/or stripping occurs, values of A_i and S_i should be based on effective average values of L, V, and K_i in the cascade. However, even then Eq. (13-44) with T_{N+1} replaced by $(T_{N+1} + T_0)/2$ may be able to give a first-order approximation of $(A_i)_e$. In the case of an absorber, $L_{N+1} < L_e$ and $V_0 > V_e$ will be compensated to some extent by $K_i\{(T_{N+1} + T_0)/2, P)\} < K_i\{T_e, P\}$. A similar compensation, but in opposite directions, will occur in the case of a stripper.

Equations (13-40) and (13-41) are plotted in Fig. 13-43. Components having large values of A_e or S_e absorb or strip respectively to a large extent. Cooresponding values of Φ_A and Φ_S approach a value of 1 and are almost independent of the number of equilibrium stages.

An estimate of the minimum absorbent flow rate for a specified amount of absorption from the entering gas of some key component K for a cascade with an infinite number of equilibrium stages is obtained from Eq. (13-40) as

$$(L_{N+1})_{\min} = K_K V_0[1 - (\Phi_K)_A] \tag{13-45}$$

The corresponding estimate of minimum stripping-agent flow rate for a stripper is obtained as

$$(V_0)_{\min} = L_{N+1}[1 - (\Phi_K)_S]/K_K \tag{13-46}$$

Example 2: Calculation of Kremser Method For the simple absorber specified in Fig. 13-44, a rigorous calculation procedure as described below gives results in Table 13-9. Values of Φ were computed from component-product flow rates, and corresponding effective absorption and stripping factors were obtained by iterative calculations in using Eqs. (13-40) and (13-41) with $N = 6$. Use the Kremser method to estimate component-product rates if N is doubled to a value of 12.

Assume that values of A_e and S_e will not change with a change in N. Application of Eqs. (13-40), (13-41), and (13-39) gives the results in the last four columns of Table 13-10. Because of its small value of A_e, the extent of absorption of C_1 is unchanged. For the other components, somewhat increased amounts of absorption occur. The degree of stripping of the absorber oil is essentially unchanged. Overall, only an additional 0.5 percent of absorption occurs. The greatest increase in absorption occurs for n-C_4, to the extent of about 4 percent.

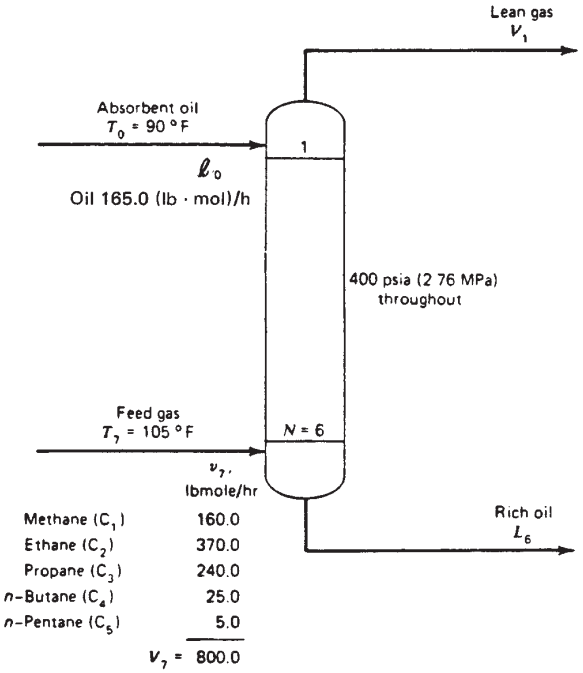

FIG. 13-44 Specifications for the absorber example.

TABLE 13-9 Results of Calculations for Simple Absorber of Fig. 13-44

	$N = 6$ (rigorous method)				$N = 12$ (Kremser method)					
	(lb · mol)/h						(lb · mol)/h			
Component	$(v_i)_6$	$(\ell_i)_1$	$(\Phi_i)_A$	$(\Phi_i)_S$	$(A_i)_e$	$(S_i)_e$	$(v_i)_{12}$	$(\ell_i)_1$	$(\Phi_i)_A$	$(\Phi_i)_S$
C_1	147.64	12.36	0.9228		0.0772		147.64	12.36	0.9228	
C_2	276.03	94.97	0.7460		0.2541		275.98	94.02	0.7459	
C_3	105.42	134.58	0.4393		0.5692		103.46	136.54	0.4311	
nC_4	1.15	23.85	0.0460		1.3693		0.16	24.84	0.0063	
nC_5	0.0015	4.9985	0.0003		3.6		0	5.0	0.0	
Absorber oil	0.05	164.95		0.9997		0.0003	0.05	164.95		0.9997
Totals	530.29	435.71					527.29	437.71		

NOTE: To convert pound-moles per hour to kilogram-moles per hour, multiply by 0.454.

TABLE 13-10 Top-Down Calculations for Example 3

Component	$R+1$	A_{10}	$\frac{\ell_{10}}{d}$	$\frac{\ell_{10}}{d}+1$	A_9	$\frac{\ell_9}{d}$	$\frac{\ell_9}{d}+1$	A_8	$\frac{\ell_8}{d}$	$\frac{\ell_8}{d}+1$	A_7	$\frac{\ell_7}{d}$
C_3	3.58	0.260	0.931	1.931	0.232	0.448	1.448	0.212	0.307	1.307	0.198	0.259
i-C_4	3.58	0.522	1.87	2.87	0.450	1.29	2.29	0.405	0.927	1.927	0.371	0.715
n-C_4	3.58	0.693	2.48	3.48	0.590	2.05	3.05	0.526	1.60	2.60	0.484	1.26
i-C_5	3.58	1.44	5.16	6.16	1.22	7.52	8.52	1.05	8.95	9.95	0.936	9.31
n-C_5	3.58	1.72	6.16	7.16	1.46	10.5	11.5	1.23	14.1	15.1	1.09	16.5

RIGOROUS METHODS FOR MULTICOMPONENT DISTILLATION-TYPE SEPARATIONS

INTRODUCTION

Availability of large digital computers has made possible rigorous solutions of equilibrium-stage models for multicomponent, multistage distillation-type columns to an exactness limited only by the accuracy of the phase equilibrium and enthalpy data utilized. Time and cost requirements for obtaining such solutions are very low compared with the cost of manual solutions. Methods are available that can accurately solve almost any type of distillation-type problem quickly and efficiently. The material presented here covers, in some detail, some of the more widely used computer algorithms as well as the classical Thiele-Geddes manual method. All are rating methods, in that the number of equilibrium stages and feed and withdrawal stages are specified. However, a successive-approximation design method that utilizes a rating method is given by Ricker and Grens [*Am. Inst. Chem. Eng. J.*, **20,** 238 (1974).] Those desiring further details are referred to the textbooks by Henley and Seader, King, and Holland cited under "General References" at the beginning of this section. These books, in turn, cite a myriad of references in chemical engineering journals. The mathematics involved is that of dealing

with sets of nonlinear algebraic equations. The general nature of the main mathematical problems is presented lucidly by Friday and Smith ["An Analysis of the Equilibrium Stage Separation Problem—Formulation and Convergence," *Am. Inst. Chem. Eng. J.*, **10,** 698 (1964)].

THIELE-GEDDES STAGE-BY-STAGE METHOD FOR SIMPLE DISTILLATION

Prior to the availability of digital computers, the most widely used manual methods for rigorous calculations of simple distillation were those of Lewis and Matheson (LM) [*Ind. Eng. Chem.*, **24,** 496 (1932)] and Thiele and Geddes (TG) [*Ind. Eng. Chem.*, **25,** 290 (1933)], in which the equilibrium-stage equations are solved one by one by using tearing techniques. The former is a design method, in which the number of stages is determined for a specified split between two key components. Thus, it is a rigorous analog of the FUG shortcut method. The TG method is a rating method in which distribution of components between distillate and bottoms is predicted for a specified number of stages. Thus, the TG method is a rigorous analog of the SB method.

Both the LM and the TG methods suffer from numerical difficulties that can prevent convergence in certain cases. The stage-to-stage calculation used in the LM method proceeds from the top down and from the bottom up and is subject to large truncation-error buildup if the components differ widely in volatility. The TG method avoids that difficulty, but numerical instabilities arise as soon as the stage-to-stage calculation crosses a feed stage. Then, a difference term appears in the equations, and sometimes this results in a serious loss of significant digits, making the TG method basically unsuited for multiple-feed columns.

All stage-to-stage methods that work from both ends of the column toward the middle suffer from two other disadvantages. First, the top-down and the bottom-up calculations must "mesh" somewhere in the column. Usually the mesh is made at a feed stage, and if more than one feed stage exists, a choice of mesh point must be made for each component. When the components vary widely in volatility, the same mesh point cannot be used for all components if serious numerical difficulties are to be avoided. Second, arbitrary procedures must be set up to handle *nondistributed* components. (A nondistributed component is one whose concentration in one of the end-product streams is smaller than the smallest number carried by the computer.) In the LM and TG equations, the concentrations for these components do not naturally take on nonzero values at the proper point as the calculations proceed through the column.

Because of all these numerical difficulties, neither the LM nor the TG stage-by-stage method is commonly implemented in modern computer algorithms. Nevertheless, the TG method is very instructive and is developed in the following example. For a single narrow-boiling feed, the TG manual method is quite efficient.

Example 3: Calculation of TG Method The TG method will be demonstrated by using the same example problem that was used above for the approximate methods. The example column was analyzed previously and found to have $C + 2N + 9$ design variables. The specifications to be used in this example were also listed at that time and included the total number of stages ($N = 10$), the feed-plate location ($M = 5$), the reflux temperature (corresponding to saturated liquid), the distillate rate ($D = 48.9$), and the top vapor rate ($V = 175$). As before, the pressure is uniform at 827 kPa (120 psia), but a pressure gradient could be easily handled if desired.

A temperature profile plus a vapor-rate profile through the column must be assumed to start the procedure. These variables are referred to as tear variables and must be iterated on until convergence is achieved in which their values no longer change from iteration to iteration and all equations are satisfied to an acceptable degree of tolerance. Each iteration down and then up through the column is referred to as a column iteration. A set of assumed values of the tear variables consistent with the specifications, plus the component K values at the assumed temperatures, is as follows, using assumed end and middle temperatures and K values from Fig. 13-14*b:*

				K				
Stage	V	L	T	C_3	i-C_4	n-C_4	i-C_5	n-C_5
10	175	126.1	163.5	2.77	1.38	1.04	0.500	0.420
9	↓	↓	178.5	3.10	1.60	1.22	0.590	0.495
8	↓	↓	191.3	3.40	1.78	1.37	0.685	0.585
7	↓	↓	202.0	3.63	1.94	1.49	0.770	0.660
6	↓	226.1	210.0	3.84	2.06	1.60	0.825	0.702
5	↓	↓	216.4	4.00	2.21	1.73	0.895	0.765
4	↓	↓	221.7	4.15	2.28	1.80	0.925	0.800
3	↓	↓	226.3	4.28	2.36	1.88	0.965	0.835
2	↓	↓	230.3	4.36	2.43	1.94	1.000	0.870
1	↓	51.1	234.0	4.42	2.50	1.99	1.030	0.890

Stage compositions in the TG method are obtained by stage-to-stage calculations from both ends toward the feed stage. With reference to Fig. 13-1, the calculations work with the ratios v_n/d, ℓ_n/d, v_m/b, and ℓ_m/b instead of v or ℓ directly. The working equations are derived as follows:

In the rectifying section, the equilibrium relationship for component i at any stage n can be expressed in terms of component flow rate in the distillate $d = Dx_D$ and component absorption factor $A_n = L_n/K_nV_n$.

$$\begin{aligned} x_n &= y_n/K_n \\ L_nx_n &= (L_n/K_nV_n)V_ny_n \\ \ell_n &= A_nv_n \\ \ell_n/d &= (v_n/d)A_n \end{aligned} \tag{13-47}$$

The general component-i balance around a section of stages from stage n to the top of the column is

$$v_n = \ell_{n+1} + d$$

or

$$v_n/d = (\ell_{n+1}/d) + 1 \tag{13-48}$$

Increasing the subscripts in Eq. (13-47) by 1 and substituting for ℓ_{n+1}/d in Eq. (13-48) gives the following combined equilibrium and material-balance relationship for component i:

$$v_n/d = (v_{n+1}/d)A_{n+1} + 1 \tag{13-49}$$

Or, if v_n/d is eliminated in Eq. (13-48)

$$\frac{\ell_n}{d} = A_n\left(\frac{\ell_{n+1}}{d} + 1\right) \tag{13-50}$$

Equation (13-50) is used to calculate, from the previous stage, the (ℓ/d) ratio on each stage in the rectifying section. The assumed temperature and phase-rate-profile assumptions conveniently fix all the A_n values for ideal solutions. The calculations are started by writing the equation for stage N:

$$\frac{\ell_N}{d} = A_N\left(\frac{\ell_{N+1}}{d} + 1\right) \tag{13-51}$$

For a total condenser, $x_D = x_{N+1}$ and

$$\ell_{N+1}/d = L_{N+1}/D = R \tag{13-52}$$

A knowledge of the reflux ratio (obtained from the specified distillate and top vapor rates) permits the calculation of $(\ell_N/d)_i$ from which $(\ell_{m-1}/d)_i$ is obtained, etc. Equation (13-50) is applied to each stage in succession until the ratio ℓ_{M+2}/d in the overflow from the stage above the feed stage is obtained. The calculations are then switched to the stripping section.

The equilibrium relationship for component i in the stripping section can be expressed in terms of component flow rate in the bottoms, $b = Bx_B$, and $S_m = K_mV_m/L_m$ as

$$\begin{aligned} y_m &= K_mx_m \\ V_my_m &= (K_mV_m/L_m)L_mx_m \\ v_m &= S_m\ell_m \\ v_m/b &= (\ell_m/b)S_m \end{aligned} \tag{13-53}$$

Combination with the material balance

$$(\ell_{m+1}/b) = v_m/b + 1 \tag{13-54}$$

gives

$$(\ell_{m+1}/b) = (\ell_m/b)S_m + 1 \tag{13-55}$$

The bottom-up calculations are started by writing Eq. (13-55) for stage 1 as

$$\ell_2/b = V_1K_1/B + 1 = S_1 + 1 \tag{13-56}$$

The S_m values all are fixed by assumed temperature and phase-rate profiles. Equation (13-55) is applied to each of the stripping stages in sequence until the ratio ℓ_{M+2}/b in the liquid entering the feed stage is obtained.

The manner in which rectifying and stripping-section calculations are meshed at the feed stage depends upon the thermal condition of the feed. Figure 13-45 shows three possible ways in which fresh feed can affect the L and V rates between the feed stage and stage $M + 2$. The superscript bar denotes the stream rate when the stream enters a stage, while the lack of a bar denotes the rate when the stream leaves a stage.

Top-down calculations for the example problem are shown in Table 13-10 and bottom-up calculations in Table 13-11. Top-down and bottom-up calculations have provided values of ℓ_{M+2}/d and ℓ_{M+2}/b respectively. For a bubble-point feed,

$$v_{M+1} = \bar{v}_{M+1}$$

and a combination of Eqs. (13-48) and (13-54) provides for each component i

$$\frac{b}{d} = \frac{v_{M+1}/d}{\bar{v}_{M+1}/b} = \frac{\ell_{M+2}/d + 1}{\ell_{M+2}/b - 1} \tag{13-57}$$

The b/d ratios obtained from this equation can then be used to calculate the individual b and d values as follows. Since

$$d + b = Fx_F \tag{13-58}$$

$$d = \frac{Fx_F}{1 + (b/d)}$$

and

$$b = (b/d)d \tag{13-59}$$

Calculated values of d from the first column iteration in the example problem are as follows:

Component	$\frac{\ell_7}{d} + 1$	$\frac{\ell_7}{b} - 1$	$\frac{b}{d}$	Fx_F	d
C_3	1.26	5450	0.000231	5	5.00
i-C_4	1.71	175	0.00977	15	14.85
n-C_4	2.26	47.7	0.0474	25	23.83
i-C_5	10.3	2.46	0.19	20	3.85
n-C_5	17.5	1.54	11.4	35	2.82
					50.4

The calculated D is 50.4 instead of 48.9. Before these incorrect d (and b) values are used to calculate the stage concentrations, followed by a new set of values of T, V, and L, convergence of the iteration is aided as follows by using the

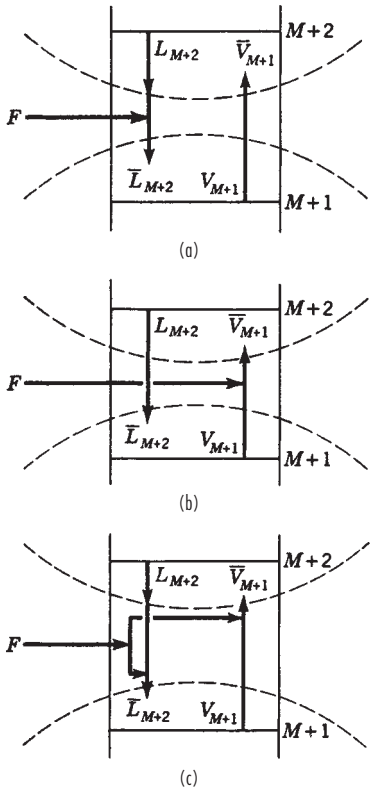

FIG. 13-45 Effect of feed on stream rates just above feed stage $M + 1$. (*a*) Subcooled or bubble-point feed. (*b*) Superheated or dew-point feed. (*c*) Partially flashed feed.

Θ method developed by Holland (*Fundamentals of Multicomponent Distillation,* McGraw-Hill, New York, 1981) and coworkers. A quantity θ is defined by

$$d' = \frac{Fx_F}{1 + (b/d)\Theta} \tag{13-60}$$

where values of d' are the ones that satisfy

$$\sum_i d' = D_{\text{specified}}$$

Comparison of Eqs. (13-57) and (13-60) shows that

$$b' = \Theta\,(b/d)d' \tag{13-61}$$

TABLE 13-11 Bottom-Up Calculations for Example 3

Component	S_1	$\frac{\ell_2}{b}$	S_2	$\frac{\ell_2}{b}S_2$	$\frac{\ell_3}{b}$	S_3	$\frac{\ell_3}{b}S_3$	$\frac{\ell_4}{b}$	S_4
C_3	15.1	16.1	3.37	54.3	55.3	3.31	183.0	184.0	3.21
i-C_4	8.56	9.56	1.88	18.0	19.0	1.83	34.8	35.8	1.76
n-C_4	6.81	7.81	1.50	11.7	12.7	1.45	18.4	19.4	1.39
i-C_5	3.53	4.53	0.774	3.51	4.51	0.747	3.37	4.37	0.716
n-C_5	3.05	4.05	0.673	2.73	3.73	0.646	2.41	3.41	0.619

Component	$\frac{\ell_4}{b}S_4$	$\frac{\ell_5}{b}$	S_5	$\frac{\ell_5}{b}S_5$	$\frac{\ell_6}{b}$	S_6	$\frac{\ell_6}{b}S_6$	$\frac{\ell_7}{b}$
C_3	590.6	591.6	3.10	1834	1835	2.97	5450	5451
i-C_4	63.0	64.0	1.71	109.4	110.4	1.59	175	176
n-C_4	27.0	28.0	1.34	37.5	38.5	1.24	47.7	48.7
i-C_5	3.13	4.13	0.693	2.86	3.86	0.638	2.46	3.46
n-C_5	2.11	3.11	0.592	1.84	2.84	0.543	1.54	2.54

The value of θ is found by solving the following nonlinear equation, where D is the specified distillate rate:

$$D - \sum_i \frac{Fx_F}{1 + (b/d)\Theta} = 0 \tag{13-62}$$

For the first column iteration, $\Theta = 1.25$ satisfies this equation. The b/d values and the Θ value are used in Eqs. (13-60) and (13-61) to give the following corrected end concentrations:

Component	$\frac{b}{d}$	d'	b'	x_D	x_1
C_3	0.000231	5.00	0.00144	0.102	0
i-C_4	0.00977	14.82	0.181	0.303	0.004
n-C_4	0.0474	23.60	1.40	0.482	0.027
i-C_5	4.19	3.21	16.79	0.066	0.329
n-C_5	11.4	2.30	32.7	0.047	0.640
		48.9	51.1	1.000	1.000

Stage-to-stage calculations shown in Tables 13-10 and 13-11 provide ℓ/d and ℓ/b values for each stage. These are used in the following equations to calculate normalized liquid concentrations for each component at each stage:

$$x_n = \frac{(\ell_n/d)d'}{\sum_i (\ell_n/d)d'} \tag{13-63}$$

$$x_m = \frac{(\ell_m/b)b'}{\sum_i (\ell_m/b)b'} \tag{13-64}$$

Application of these equations gives the results in Table 13-12. A set of T_n is calculated from the normalized x_n by bubble-point calculations. Corresponding values of y_n are obtained from $y_n = K_n x_n$. Once new x_n and T_n are available, new values of V_n are calculated from energy balances by using data from Maxwell (*Data Book on Hydrocarbons,* Van Nostrand, Princeton, N.J., 1950). First, an estimate of condenser duty is computed from an energy balance around the condenser,

$$Q_c = V_N(H_N^V - H_{N+1}^L)$$
$$= 175(18{,}900 - 10{,}750) = 1{,}426{,}000 \text{ Btu/h } (417.9 \text{ kW}) \tag{13-65}$$

The reboiler duty Q_r is obtained from an overall energy balance,

$$Q_r = DH_{N+1}^L + BH_1^L + Q_c - FH_F$$
$$= (48.9)(10{,}750) + (51.1)(17{,}080) + 1{,}426{,}000 - 100(13{,}540)$$
$$= 1{,}465{,}000 \text{ Btu/h } (429.3 \text{ kW}) \tag{13-66}$$

A new set of values of V_m is obtained from energy balances around the bottom section of the column,

$$V_m = \frac{Q_r + B(H_{M+1}^L - H_B^V)}{H_m^V - H_{m+1}^L} \tag{13-67}$$

Similar balances around the top section yield a new set of values of V_n. Corresponding values of L_n and L_m are obtained by material balances around the top and bottom sections respectively. The new V, L, and T profiles are listed in Table 13-13. In this example, they do not differ much from the initial guesses in Table 13-10.

It should be noted in Table 13-13 that it is not necessary to list two values of V, L, and T for the feed stage (stage 6) because the TC procedure gives a perfect match at the feed stage in each trial. This completes the first column iteration.

The new temperature and flow-rate profiles (which would be used as the assumptions to begin the second column iteration) are compared in Fig. 13-46 with the final solution. Both profiles are moving toward the final result.

Figure 13-47 shows the concentration profiles from the final solution. Note the discontinuities at the feed stage and the fact that feed-stage composition differs considerably from feed-stream composition. It can be seen in Fig. 13-47 from the n-C_4 and i-C_5 profiles that the separation between the keys improves rapidly with stage number; additional stages would be worthwhile.

Convergence to the final solution is rapid with the TG method for narrow-boiling feeds but may be slow for wide-boiling feeds. Generally, at least five column iterations are required. Convergence is obtained when successive sets of tear variables are identical to approximately four significant digits. This is accompanied by $\Theta = 1.0$, x = normalized x, and nearly identical successive values of Q_c as well as Q_r.

TABLE 13-12 Stage Compositions from the First Trial of Example 3

Component	x_1	$\frac{\ell_2}{b}b'$	x_2	$\frac{\ell_3}{b}b'$	x_3	$\frac{\ell_4}{b}b'$	x_4	$\frac{\ell_5}{b}b'$	x_5	$\frac{\ell_6}{b}b'$
C_3	0.000	0.0232	0.000	0.0796	0.000	0.279	0.001	0.852	0.004	2.65
i-C_4	0.004	1.73	0.008	3.44	0.016	6.48	0.030	11.6	0.052	20.0
n-C_4	0.027	10.9	0.049	17.8	0.081	27.2	0.124	39.2	0.176	53.9
i-C_5	0.329	76.1	0.344	75.7	0.346	73.4	0.335	69.3	0.311	64.8
n-C_5	0.640	132.4	0.599	122.0	0.557	111.5	0.510	101.7	0.447	92.9
	1.000	221.1	1.000	219.0	1.000	218.9	1.000	226.6	1.000	234.2

Component	x_6	$\frac{\ell_7}{d}d'$	x_7	$\frac{\ell_8}{d}d'$	x_8	$\frac{\ell_9}{d}d'$	x_9	$\frac{\ell_{10}}{d}d'$	x_{10}
C_3	0.011	1.295	0.012	1.535	0.013	2.240	0.019	4.66	0.038
i-C_4	0.085	10.6	0.097	13.7	0.120	19.1	0.162	27.7	0.228
n-C_4	0.230	29.7	0.271	37.8	0.331	48.4	0.410	58.5	0.481
i-C_5	0.277	29.9	0.273	28.7	0.252	24.1	0.204	16.6	0.136
n-C_5	0.397	37.9	0.347	32.4	0.284	24.1	0.204	14.2	0.117
	1.000	109.4	1.000	114.1	1.000	118.0	1.000	121.7	1.000

TABLE 13-13 New Temperature and Rate Profiles from the First Trial of Example 3

n	New T	$H_D^L - H_{n+1}^L$	$D(H_D^L - H_{n+1}^L) + Q_c$	$H_N^V - H_{n+1}^L$	V	L
10	160.0	0	1,426,000	8150	175.0	124.0
9	175.0	−1220	1,367,000	7900	172.9	119.6
8	186.0	−2190	1,319,000	7830	168.5	117.6
7	194.0	−3010	1,279,000	7680	166.5	114.2
6	200.0	−3490	1,256,000	7700	163.1	214.3

m	New T	$H_{m+1}^L - H_B^L$	$B(H_{m+1}^L - H_B^L) + Q_r$	$H_m^V - H_{m+1}^L$	V	L
5	211.0	−2480	1,338,000	8200	163.2	214.7
4	220.0	−1780	1,374,000	8400	163.6	215.5
3	228.0	−1130	1,407,000	8560	164.4	221.1
2	233.5	−560	1,438,000	8460	170.0	224.0
1	237.5	−210	1,454,000	8410	172.9	51.1

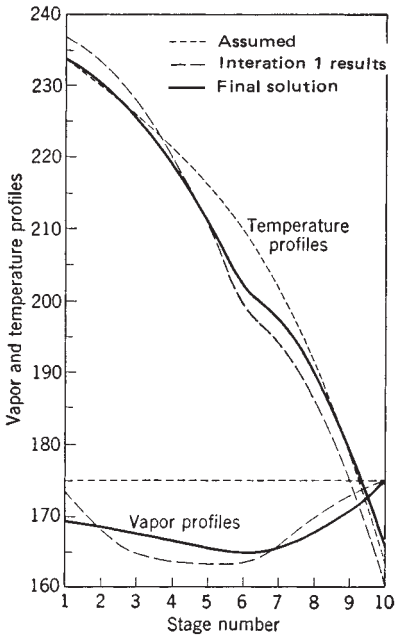

FIG. 13-46 Comparison of the assumed and calculated profiles from the first column iteration in Example 4 with the final computer solution.

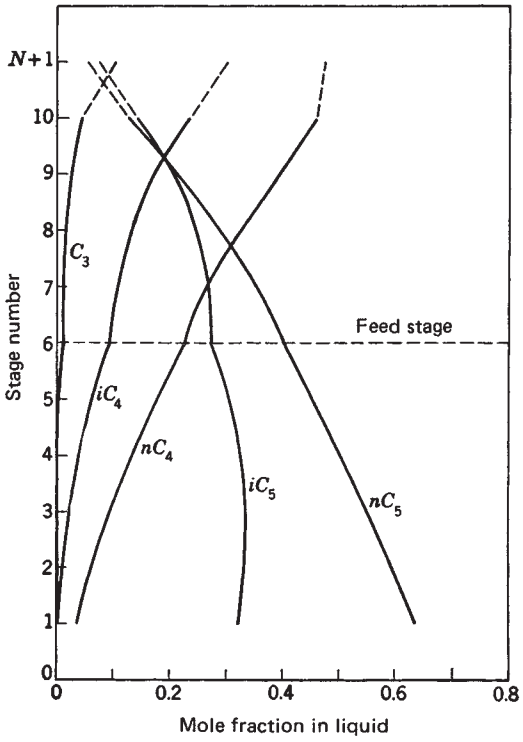

FIG. 13-47 Concentration profiles from the final solution of Example 4. The points at $N+1$ refer to the reflux composition, which is the same as the overhead vapor.

EQUATION-TEARING PROCEDURES USING THE TRIDIAGONAL-MATRIX ALGORITHM

As seen earlier, the manual Thiele-Geddes method involves solving the equilibrium-stage equations one at a time. More powerful, flexible, and reliable computer programs are based on the application of sparse matrix methods for solving simultaneously all or at least some of the equations. For cases in which combined column feeds represent mixtures that boil within either a narrow range (typical of many distillation operations) or a wide range (typical of absorbers and strippers) and in which great flexibility of problem specifications is not required, equation-tearing procedures that involve solving simultaneously certain subsets of the equations can be applied. Two such equation-tearing procedures are the bubble-point (BP) method for narrow-boiling mixtures suggested by Friday and Smith (op. cit.) and developed in detail by Wang and Henke [*Hydrocarbon Process.*, **45** (8), 155 (1966)], and the sum-rates (SR) method for wide-boiling mixtures proposed by Sujuta [*Hydrocarbon Process.*, **40**(12), 137 (1961)] and further developed by Burningham and Otto [*Hydrocarbon Process.*, **46**(10), 163 (1967)]. Both methods are described here. However, the BP method has been largely superseded by the more reliable and efficient simultaneous-correction and inside-out methods, which do, however, incorporate certain features of the BP method. Both the BP and SR methods start with the same primitive equations for the theoretical model of an equilibrium stage as presented next.

Consider a general, continuous-flow, steady-state, multicomponent, multistage separation operation. Assume that phase equilibrium between an exiting vapor phase and a single exiting liquid phase is achieved at each stage, that no chemical reactions occur, and that neither of the exiting phases entrains the other phase. A general schematic representation of such a stage j is shown in Fig. 13-48. Entering stage j is a single- or two-phase feed at molal flow rate F_j, temperature T_{Fj}, and pressure P_{Fj} and with overall composition in mole fractions $z_{i,j}$. Also entering stage j is interstage liquid from adjacent stage $j-1$ above at molal flow rate L_{j-1}, temperature T_{j-1}, pressure P_{j-1}, and mole fractions $x_{i,j-1}$. Similarly, interstage vapor from adjacent stage $j+1$ below enters at molal flow rate V_{j+1}, T_{j+1}, P_{j+1} and mole fractions $y_{i,j+1}$. Heat is transferred from (+) or to (−) stage j at rate Q_j to simulate a condenser, reboiler, intercooler, interheater, etc. Equilibrium vapor and liquid phases leave stage j at T_j and P_j and with mole fractions $y_{i,j}$ and $x_{i,j}$ respectively. The vapor may be partially withdrawn from the column as a sidestream at a molal flow rate W_j, with the remainder V_j sent to adjacent stage $j-1$ above. Similarly, exiting liquid may be split into a sidestream at a molal flow rate of U_j, with the remainder L_j sent to adjacent stage j below.

For each stage j, the following $2C+3$ component material-balance (M), phase-equilibrium (E), mole-fraction-summation (S), and energy-balance (H) equations apply, where C is the number of chemical species:

$$L_{j-1}x_{i,j-1} + V_{j+1}y_{i,j+1} + F_j z_{i,j} - (L_j + U_j)x_{i,j} - (V_j + W_j)y_{i,j} = 0 \quad (13\text{-}68)$$

$$y_{i,j} - K_{i,j}x_{i,j} = 0 \quad (13\text{-}69)$$

$$\sum_i y_{i,j} - 1.0 = 0 \quad (13\text{-}70)$$

$$\sum_i x_{i,j} - 1.0 = 0 \quad (13\text{-}71)$$

$$L_{j-1}H_{Lj-1} + V_{j+1}H_{Vj+1} + F_j H_{Fj} - (L_j + U_j)H_{Lj} - (V_j + W_j)H_{Vj} - Q_j = 0 \quad (13\text{-}72)$$

In general, K values and molal enthalpies in these MESH equations are complex implicit functions of stage temperature, stage pressure, and equilibrium mole fractions:

$$K_{i,j} = K_{i,j}\{T_j, P_j, x_j, y_j\}$$
$$H_{Vj} = H_{Vj}\{T_j, P_j, y_j\}$$
$$H_{Lj} = H_{Lj}\{T_j, P_j, x_j\}$$

where vectors x_j and y_j refer to all i values of $x_{i,j}$ and $y_{i,j}$ for the particular stage j. As shown in Fig. 13-49, a general countercurrent-flow col-

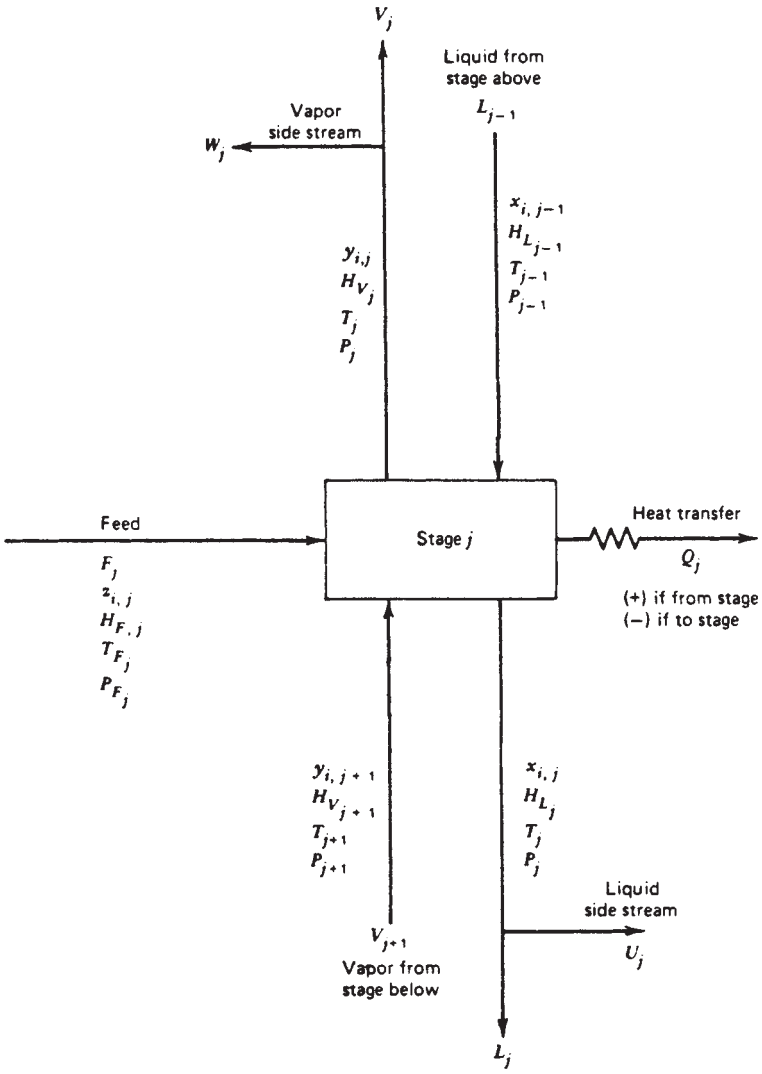

FIG. 13-48 General equilibrium stage.

umn of N stages can be formed from a collection of equilibrium stages of the type in Fig. 13-48. Note that streams L_0, V_{N+1}, W_1 and U_N are zero and do not appear in Fig. 13-49. Such a column is represented by $N(2C + 3)$ MESH equations in $[N(3C + 10) + 1]$ variables, and the difference or $[N(C + 7) + 1]$ variables must be specified. If the specified variables are the value of N and all values of $z_{i,j}$, F_j, T_{Fj}, P_{Fj}, P_j, U_j, W_j, and Q_j, then the remaining $N(2C + 3)$ unknowns are all values of $y_{i,j}$, $x_{i,j}$, L_j, V_j, and T_j. In this case, Eqs. (13-73), (13-74), and (13-77) are nonlinear in the unknowns and the MESH equations can not be solved directly. Even if a different set of variable specifications is made, the MESH equations still remain predominantly nonlinear in the unknowns. For the BP method as applied to distillation, specified variables are those listed except that bottoms rate L_N is specified rather than partial reboiler duty Q_N. This is equivalent by overall material balance to specifying vapor-distillate rate V_1 in the case of a partial condenser or liquid-distillate rate U_1 in the case of a total condenser. Also, reflux rate L_1 is specified rather than condenser duty Q_1. For the SR method as applied to absorption and stripping, the specified variables are those listed without exception.

Tridiagonal-Matrix Algorithm Both the BP and the SR equation-tearing methods compute liquid-phase mole fractions in the same way by first developing linear matrix equations in a manner shown by Amundson and Pontinen [*Ind. Eng. Chem.*, **50,** 730 (1958)]. Equations (13-69) and (13-68) are combined to eliminate $y_{i,j}$ and $y_{i,j+1}$ (however, the vector y_j still remains implicitly in $K_{i,j}$):

$$L_{j-1}x_{i,j-1} + V_{j+1}K_{i,j+1}x_{i,j+1} + F_j z_{i,j} - (L_j + U_j)x_{i,j} - (V_j + W_j)K_{i,j}x_{i,j} = 0 \quad (13\text{-}73)$$

Next, Eq. (13-68) is summed over the C components and over stages 1 through j and combined with Eqs. (13-70), (13-71), and $\sum_i z_{i,j} - 1.0 = 0$ to give a total material balance over stages 1 through j:

$$L_j = V_{j+1} + \sum_{m=1}^{j} (F_m - U_m - W_m) - V_1 \quad (13\text{-}74)$$

By combining Eq. (13-73) with Eq. (13-74), L_j is eliminated to give the following working equations for component material balances:

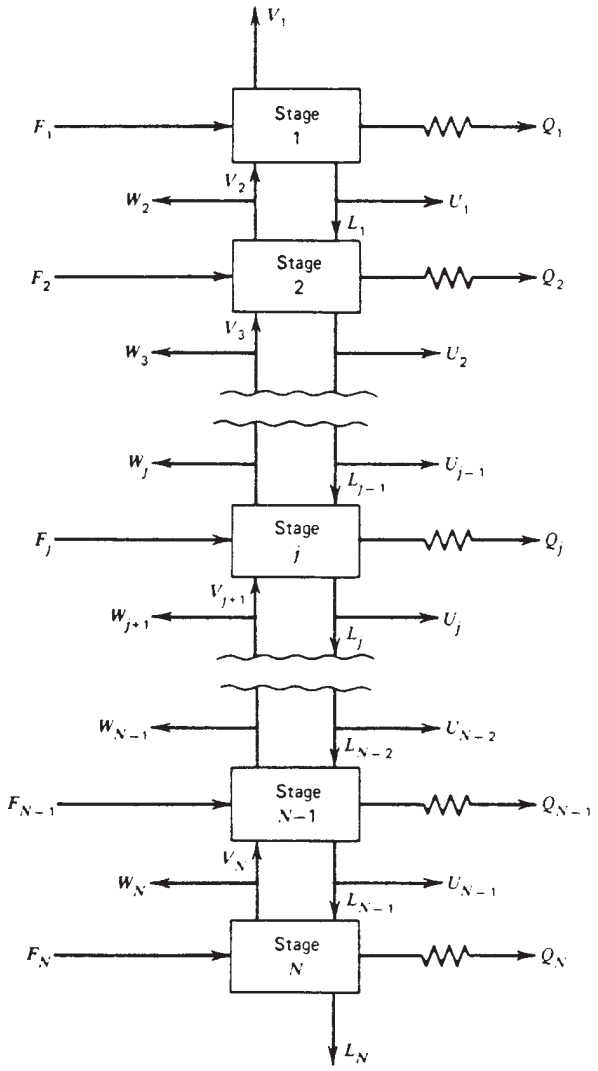

FIG. 13-49 General countercurrent cascade of N stages.

$$A_j x_{i,j-1} + B_{i,j} x_{i,j} + C_{i,j} x_{i,j+1} = D_{i,j} \tag{13-75}$$

where $$A_j = V_j + \sum_{m=1}^{j-1} (F_m - W_m - U_m) - V_i \qquad 2 \le j \le N \tag{13-76}$$

$$B_{i,j} = -\left[V_{j+1} + \sum_{m=1}^{j} (F_m - W_m - U_m) - V_1 + U_j + (V_j + W_j) K_{i,j} \right]$$

$$1 << j << N \tag{13-77}$$

$$C_{i,j} = V_{j+1} K_{i,j+1} \qquad 1 << j << N - 1 \tag{13-78}$$

$$D_{i,j} = -F_j z_{i,j} \qquad 1 << j << N \tag{13-79}$$

The NC equations (13-75) are linearized in terms of the NC unknowns $x_{i,j}$ by selecting unknowns V_j and T_j as tear variables and using values of vectors x_j and y_j from the previous iteration to compute values of $K_{i,j}$ for the current iteration. In this manner all values of A_j, $B_{i,j}$, and $C_{i,j}$ can be estimated. Values of $D_{i,j}$ are fixed by feed specifications. Furthermore, the NC equations (13-75) can be partitioned into C sets, one for each component, and solved separately for values of x_i, which pertains to all j values of $x_{i,j}$ for the particular species i. Each set of N equations is a special type of sparse matrix equation called a tridiagonal-matrix equation, which has the form shown in Fig. 13-50*a* for a five-stage example in which, for convenience, the subscript i has been dropped from the coefficients B, C, and D. For this type of sparse matrix equation, we can apply a highly efficient version of the gaussian elimination procedure called the Thomas algorithm, which avoids matrix inversion, eliminates the need to store the zero coefficients in the matrix, almost always avoids buildup of truncation errors, and rarely produces negative values of $x_{i,j}$.

The Thomas algorithm begins by a forward elimination, row by row starting down from the top row ($j = 1$, the condenser stage), to give the following replacements shown in Fig. 13-50*b*. For row 1:

$$p_1 = C_1/B_1,\ q_1 = D_1/B_1,\ B_1 \to 1,\ C_1 \to p_1,\ D_1 \to q_1$$

where $\to$ means "is replaced by."

For all subsequent rows:

$$p_j = C_j/(B_j - A_j p_{j-1}),\ q_j = (D_j - A_j q_{j-1})/(B_j - A_j p_{j-1}),$$
$$A_j \to 0,\ B_j \to 1,\ C_j \to p_j,\ D_j \to q_j$$

At the bottom row for component i, $x_N = q_N$. The remaining values of x_j for species i are computed recursively by backward substitution:

$$x_{j-1} = q_{j-1} - p_{j-1} x_j$$

BP Method for Distillation The bubble-point method for distillation, particularly when the components involved cover a relatively narrow range of volatility, proceeds iteratively by the following steps, where k is the iteration index for the entire distillation column.

1. Specify N and all values of $z_{i,j}$, F_j, T_{Fj}, P_{Fj}, P_j, U_j, W_j, and Q_j, except Q_1 and Q_N.
2. Specify type of condenser. If total ($U_1 \neq 0$), compute L_N from overall material balance; if partial ($U_1 = 0$), specify V_1 and compute L_N from overall material balance.
3. Specify reflux rate L_1, assuming no subcooling.
4. Compute $V_2 = V_1 + L_1 + U_1 - F_1$.
5. Provide initial guesses ($k = 0$) or values of all tear variables T_j and V_j ($j > 2$). Temperature guesses are readily obtained by linear interpolation between estimates of top- and bottom-stage temperatures. The bottom-stage temperature is estimated by making a bubble-point-temperature calculation by using an estimate of bottoms composition at the specified bottom-stage pressure. A similar calculation is made at the top stage by using an estimate of distillate composition; otherwise, for a partial condenser, a dew-point temperature calculation is made. An estimate of the vapor-rate profile is readily obtained by assuming constant molal overflow down the column.
6. Set index $k = 1$ to initiate the first column iteration.
7. Using specified stage pressures, current estimates of stage temperatures, and current estimates of stage vapor- and liquid-phase

$$\begin{bmatrix} B_1 & C_1 & 0 & 0 & 0 \\ A_2 & B_2 & C_2 & 0 & 0 \\ 0 & A_3 & B_3 & C_3 & 0 \\ 0 & 0 & A_4 & B_4 & C_4 \\ 0 & 0 & 0 & A_5 & B_5 \end{bmatrix} \begin{bmatrix} x_1 \\ x_2 \\ x_3 \\ x_4 \\ x_5 \end{bmatrix} = \begin{bmatrix} D_1 \\ D_2 \\ D_3 \\ D_4 \\ D_5 \end{bmatrix}$$

(a)

$$\begin{bmatrix} 1 & p_1 & 0 & 0 & 0 \\ 0 & 1 & p_2 & 0 & 0 \\ 0 & 0 & 1 & p_3 & 0 \\ 0 & 0 & 0 & 1 & p_4 \\ 0 & 0 & 0 & 0 & 1 \end{bmatrix} \begin{bmatrix} x_1 \\ x_2 \\ x_3 \\ x_4 \\ x_5 \end{bmatrix} = \begin{bmatrix} q_1 \\ q_2 \\ q_3 \\ q_4 \\ q_5 \end{bmatrix}$$

(b)

FIG. 13-50 Tridiagonal-matrix equation for a column with five theoretical stages. (*a*) Original equation. (*b*) After forward elimination.

compositions, estimate all $K_{i,j}$ values (for $k = 1$, initial estimates of stage phase compositions may be necessary if $K_{i,j}$ values are sensitive to phase compositions).

8. Compute values of $x_{i,j}$ by solving Eqs. (13-75) through (13-79) by the tridiagonal-matrix algorithm once for each component. Unless all mesh equations are converged, $\sum_i x_{i,j} \neq 1$ for each stage j.

9. To force $\sum_i x_{i,j} = 1$ at each stage j, normalize values by the replacement $x_{i,j} = x_{i,j} / \sum_i x_{i,j}$.

10. Compute a new set of values of $T_j^{(k)}$ tear variables by computing, one at a time, the bubble-point temperature at each stage based on the specified stage pressure and corresponding normalized $x_{i,j}$ values. The equation used is obtained by combining Eqs. (13-69) and (13-70) to eliminate $y_{i,j}$ to give

$$\sum_i K_{i,j}\{T_j, P_j, x_j, y_j\} = 1.0 \tag{13-80}$$

which is a nonlinear equation in $T_j^{(k)}$ and must be solved iteratively by some appropriate root-finding method, such as the Newton-Raphson or the Muller method.

11. Compute values of $y_{i,j}$ one at a time from Eq. (13-69).

12. Compute a new set of values of the V_j tear variables one at a time, starting with V_3, from an energy-balance equation that is obtained by combining Eqs. (13-72) and (13-74), eliminating L_{j-1} and L_j to give

$$V_j = (\tilde{C}_{j-1} - \tilde{A}_{j-1}V_{j-1})/\tilde{B}_{j-1} \tag{13-81}$$

where $\tilde{A}_{j-1} = H_{Lj-2} - H_{Vj-1}$

$$\tilde{B}_{j-1} = H_{Vj} - H_{Lj-1}$$

$$\tilde{C}_{j-1} = \left[\sum_{m=1}^{j-2}(F_m - W_m - U_m) - V_1\right](H_{Lj-1} - H_{Lj-2}) + F_{j-1}(H_{Lj-1} - H_{Fj-1}) + W_{j-1}(H_{Vj-1} - H_{Lj-1}) + Q_{j-1}$$

13. Check to determine if the new sets of tear variables $T_j^{(k)}$ and $V_j^{(k)}$ are within some prescribed tolerance of sets $T_j^{(k-1)}$ and $V_j^{(k-1)}$ used to initiate the current column iteration. A possible convergence criterion is

$$\sum_{j=1}^{N}\left[\frac{T_j^{(k)} - T_j^{(k-1)}}{T_j^{(k)}}\right]^2 + \sum_{j=3}^{N}\left[\frac{V_j^{(k)} - V_j^{(k-1)}}{V_j^{(k)}}\right]^2 \leq 10^{-7}N \tag{13-82}$$

but Wang and Henke (op. cit.) use

$$\sum_{j=1}^{N}[T_j^{(k)} - T_j^{(k-1)}]^2 \leq 0.01N \tag{13-83}$$

14. If the convergence criterion is met, compute values of L_j from Eq. (13-74) and values of Q_1 and Q_N from Eq. (13-72). Otherwise, set $k = k + 1$ and repeat steps 7 to 14.

Step 14 implies that if the calculations are not converged, values of $T_j^{(k)}$ computed in step 10 and values of $V_j^{(k)}$ computed in step 12 are used as values of the tear variables to initiate iteration $k + 1$. This is the method of successive substitution, which may require a large number of iterations and/or may result in oscillation. Alternatively, values of $T_j^{(k)}$ and $V_j^{(k)}$ can be adjusted prior to initiating iteration $k + 1$. Experience indicates that values of T_j should be reset if they tend to move outside of specified upper and lower bounds and that negative V_j values be reset to small positive values. Also, damping can be employed to prevent values of absolute T_j and V_j from changing by more than, say, 10 percent on successive iterations. Orbach and Crowe [*Can. J. Chem. Eng.*, **49,** 509 (1971)] show that the dominant eigenvalue method of adjusting values of T_j and V_j can generally accelerate convergence and is a worthwhile improvement to the BP method.

Example 4: Calculation of the BP Method Use the BP method with the SRK equation-of-state for K values and enthalpy departures to compute stage temperatures, interstage vapor and liquid flow rates and compositions, and reboiler and condenser duties for the light-hydrocarbon distillation-column specifications shown in Fig. 13-51 with feed at 260 psia. The specifications are selected to obtain three products: a vapor distillate rich in C_2 and C_3, a vapor sidestream rich in n-C_4, and a bottoms rich in n-C_5 and n-C_6.

Initial estimates provided for the tear variables were as follows compared with final converged values (after 23 iterations), where numbers in parentheses are consistent with specifications:

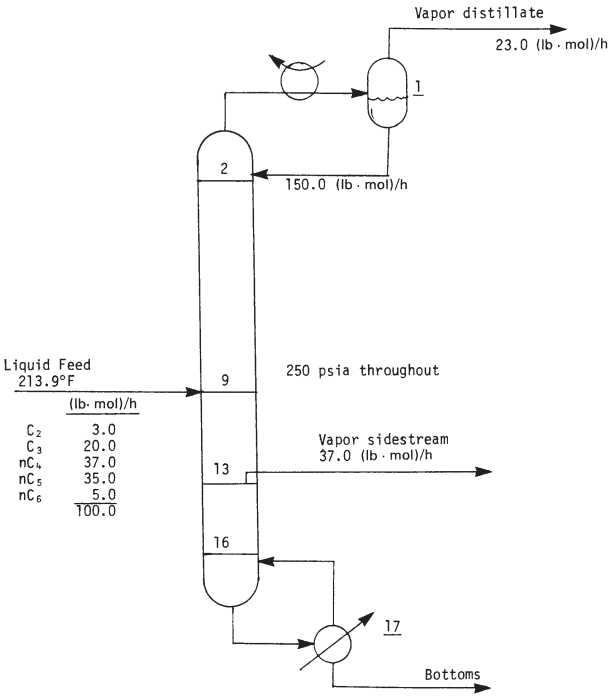

FIG. 13-51 Specifications for the calculation of distillation by the BP method.

Stage	$T^{(0)}$, °F	$T^{(23)}$, °F	$V^{(0)}$, (lb·mol)/h	$V^{(23)}$, (lb·mol)/h
1	110.00	124.4	(23)	23.0
2	121.87	141.0	(173)	173.0
3	133.75	157.4	173	167.3
4	145.62	172.6	173	162.8
5	157.50	184.9	173	160.4
6	169.37	194.5	173	159.5
7	181.25	202.6	173	158.4
8	193.12	211.1	173	155.8
9	205.00	221.9	173	151.4
10	216.87	229.9	173	155.8
11	228.75	236.5	173	160.2
12	240.62	242.9	173	162.9
13	252.50	250.2	173	164.0
14	264.37	258.1	210	200.8
15	276.25	267.4	210	199.4
16	288.12	278.1	210	197.9
17	300.00	290.5	210	196.4

NOTE: To convert degrees Fahrenheit to degrees Celsius, °C = (°F − 32)/1.8. To convert pound-moles per hour to kilogram-moles per second, multiply by 1.26×10^{-4}.

By employing successive substitution of the tear variables and the criterion of Eq. (13-83), convergence was achieved slowly, but without oscillation, in 23 iterations. Computed products are:

	Flow rate, (lb·mol)/h		
Component	Distillate	Sidestream	Bottoms
C_2	3.0	0.0	0.0
C_3	18.4	1.6	0.0
nC_4	1.6	25.7	9.7
nC_5	0.0	9.2	25.8
nC_6	0.0	0.5	4.5
	23.0	37.0	40.0

NOTE: To convert pound-moles per hour to kilogram-moles per second, multiply by 1.26×10^{-4}.

Examination of interstage-composition results showed that maximum nC_4 composition was achieved in the vapor leaving stage 12 rather than stage 13. Therefore, if the sidestream location were moved up one stage, a somewhat higher purity of nC_4 could probably be achieved in that stream. Further improvement in purity of the sidestream as well as the other two products could be achieved by increasing the reflux rate and/or number of stages. Computed condenser and reboiler duties were 268,000 and 418,000 W (914,000 and 1,425,000 Btu/h) respectively.

SR Method for Absorption and Stripping As shown by Friday and Smith (op. cit.), when an attempt is made to apply the BP method to absorption, stripping, or distillation, in which the volatility range of the chemical components in the column is very wide, calculations of stage temperatures from Eq. (13-80) become very sensitive to liquid compositions. This generally causes very oscillatory excursions in temperature from iteration to iteration, making it impossible to obtain convergence. A very successful modification of the BP method for such cases is the sum-rates method, in which new stage temperatures are computed instead from the energy-balance equation. Interstage vapor rates are computed by material balance from new interstage liquid rates that are obtained by multiplying the previous interstage liquid rates by corresponding unnormalized liquid mole-fraction summations computed from the tridiagonal-matrix algorithm. The SR method proceeds by the following steps:

1. Specify N and all values of $z_{i,j}$, F_j, T_{Fj}, P_{Fj}, P_j, U_j, W_j, and Q_j. For an adiabatic operation, all Q_j are zero.
2. Provide initial guesses ($k = 0$) for values of all tear variables T_j and V_j. Temperature guesses are readily obtained by linear interpolation between estimates of the top- and bottom-stage temperatures, taking the top as that of the liquid feed to the top stage and the bottom as that of the vapor feed to the bottom stage. An estimate of the vapor-rate profile is readily obtained by assuming constant molal overflow working up from the bottom in using the specified vapor feed or feeds. Compute corresponding initial values of L_j from Eq. (13-74).
3. Same as step 6 of the BP method.
4. Same as step 7 of the BP method.
5. Same as step 8 of the BP method.
6. Compute a new set of values of L_j from the sum-rates equation:

$$L_j^{(k+1)} = L_j^{(k)} \sum_i x_{i,j} \tag{13-84}$$

7. Compute a corresponding new set of V_j tear variables from the following total material balance, which is obtained by combining Eq. (13-74) with an overall material balance around the column:

$$V_j = L_{j-1} - L_N + \sum_{m=j}^{N} (F_m - W_m - U_m) \tag{13-85}$$

8. Same as step 9 of the BP method.
9. Same as step 11 of the BP method.
10. Normalize values of $y_{i,j}$.
11. Compute a new set of values of the T_j tear variables by solving simultaneously the set of N energy-balance equations (13-72), which are nonlinear in the temperatures that determine the enthalpy values. When linearized by a Newton iterative procedure, a tridiagonal-matrix equation that is solved by the Thomas algorithm is obtained. If we set g_j equal to Eq. (13-72), i.e., its residual, the linearized equations to be solved simultaneously are

$$\left(\frac{\partial g_1}{\partial T_1}\right)^{(r)} \Delta T_1 + \left(\frac{\partial g_1}{\partial T_2}\right)^{(r)} \Delta T_2 = -g_1^{(r)} \tag{13-86}$$

$$\left(\frac{\partial g_j}{\partial T_{j-1}}\right)^{(r)} \Delta T_{j-1} + \left(\frac{\partial g_j}{\partial T_j}\right)^{(r)} \Delta T_j + \left(\frac{\partial g_j}{\partial T_{j+1}}\right)^{(r)} \Delta T_{j+1} = -g_j^{(r)}$$

$$2 \le j \le N-1 \tag{13-87}$$

$$\left(\frac{\partial g_N}{\partial T_{N-1}}\right)^{(r)} \Delta T_{N-1} + \left(\frac{\partial g_j}{\partial T_N}\right)^{(r)} \Delta T_N = -g_N^{(r)} \tag{13-88}$$

where $\Delta T_j = T_j^{(r+1)} - T_j^{(r)}$, and thus $T_j^{(r+1)} = T_j^{(r)} + \Delta T_j$, and r is the iteration index. The partial derivatives depend upon the enthalpy correlations utilized and may be obtained analytically or numerically. Simultaneous Eqs. (13-86) to (13-88) are solved iteratively until corrections ΔT_j and, therefore, residual values of g_j approach zero.

12. Same as step 13 of the BP method.
13. If the convergence criterion is not met, set $k = k + 1$ and repeat steps 4 to 13.

With the SR method, convergence is often rapid even when successive substitution of T_j and V_j is used from one iteration to the next.

Example 5: Calculation of the SR Method Use the SR method with the PR equation of state for K values and enthalpy departures. The oil was taken as n-dodecane. To compute stage temperatures and interstage vapor and liquid flow rates and compositions for absorber-column specifications shown in Fig. 13-52. Note that a secondary absorber oil is used in addition to the main absorber oil and that heat is withdrawn from the seventh theoretical stage.

Initial estimates provided for the tear variables were as follows compared with final converged values obtained after five iterations:

Stage	$T^{(0)}$, °F	$T^{(5)}$, °F	$V^{(0)}$, (lb·mol)/h	$V^{(5)}$, (lb·mol)/h
1	80.00	84.6	450	323.9
2	81.43	85.5	450	367.7
3	82.86	86.3	450	371.3
4	84.29	85.3	450	374.7
5	85.71	86.0	450	388.6
6	87.14	86.6	450	393.0
7	88.57	85.2	450	398.2
8	90.00	92.7	450	410.4

NOTE: To convert degrees Fahrenheit to degrees Celsius, °C = (°F − 32)/1.8. To convert pound-moles per hour to kilogram-moles per second, multiply by 1.26×10^{-4}.

Convergence was achieved rapidly in five iterations by using Eq. (13-88) as the criterion. Computed compositions for lean gas and rich oil are:

	Flow rate, (lb·mol)/h	
Component	Lean gas	Rich oil
C_1	312.7	60.3
C_2	11.0	32.0
C_3	0.2	28.8
nC_4	0.0	19.0
nC_5	0.0	15.0
Oil	0.0	385.0
	323.9	540.1

NOTE: To convert pound-moles per hour to kilogram-moles per second, multiply by 1.26×10^{-4}.

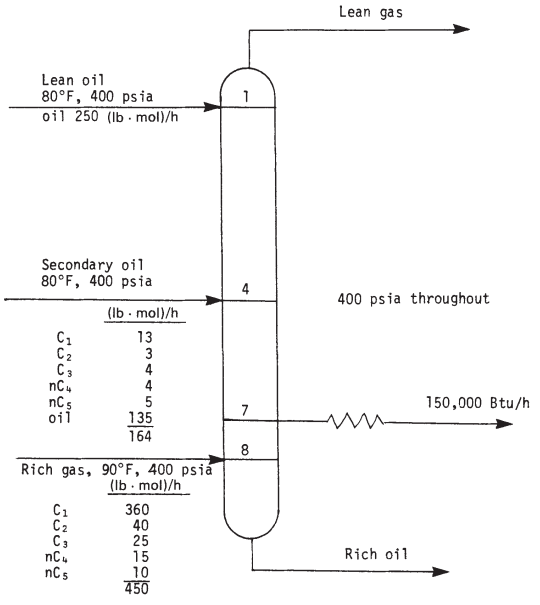

FIG. 13-52 Specifications for the calculation of an absorber by the SR method.

Approximately 0.016 (kg·mol)/s [126 (lb·mol)/h] of vapor is absorbed with an energy liberation of about 198,000 W (670,000 Btu/h), 20 percent of which is removed by the intercooler on stage 7. The temperature profile departs from a smooth curve at stages 4 and 7, where secondary oil enters and heat is removed respectively.

SIMULTANEOUS-CORRECTION PROCEDURES

The BP and SR tearing methods are generally successful only when applied respectively to the distillation of mixtures having a narrow boiling range and to absorbers and strippers. Furthermore, as shown earlier, specifications for these two tearing methods are very restricted. If one wishes to treat distillation of wide-boiling mixtures and other operations shown in Fig. 13-7 such as rectification, reboiled stripping, reboiled absorption, and refluxed stripping, it is usually necessary to utilize other procedures. One class of such procedures involves the solution of most or all of the MESH equations or their equivalent simultaneously by some iterative technique such as a Newton or a quasi-Newton method. Such simultaneous-correction (SC) methods are also useful for separations involving very nonideal liquid mixtures including extractive and azeotropic distillation or for cases in which considerable flexibility in specifications is desired.

The development of an SC procedure involves a number of important decisions: (1) What variables should be used? (2) What equations should be used? (3) How should variables be ordered? (4) How should equations be ordered? (5) How should flexibility in specifications be provided? (6) Which derivatives of physical properties should be retained? (7) How should equations be linearized? (8) If Newton or quasi-Newton linearization techniques are employed, how should the Jacobian be updated? (9) Should corrections to unknowns that are computed at each iteration be modified to dampen or accelerate the solution or be kept within certain bounds? (10) What convergence criterion should be applied?

Perhaps because of these many decisions, a large number of SC procedures have been published. Two quite different procedures that have achieved a significant degree of utilization in solving practical problems include the methods of Naphtali and Sandholm [*Am. Inst. Chem. Eng. J.*, **17,** 148 (1971)] and Goldstein and Stanfield [*Ind. Eng. Chem. Process Des. Dev.*, **9,** 78 (1970)]. The former procedure is of particular interest because, in principle, it can be applied to all cases. However, for situations involving large numbers of components, relatively small numbers of stages, and liquid solutions that are not too highly nonideal, the latter procedure is more efficient computationally.

Naphtali-Sandholm SC Method This method employs the equilibrium-stage model of Figs. 13-48 and 13-49 but reduces the number of variables by $2N$ so that only $N(2C + 1)$ equations in a like number of unknowns must be solved. In place of V_j, L_j, $x_{i,j}$, and $y_{i,j}$, component flow rates are used according to their definitions:

$$v_{i,j} = y_{i,j} V_j \tag{13-89}$$

$$\ell_{i,j} = x_{i,j} L_j \tag{13-90}$$

In addition, sidestream flow rates are replaced with sidestream flow ratios by

$$s_j = U_j / L_j \tag{13-91}$$

$$S_j = W_j / V_j \tag{13-92}$$

The MESH equations (13-68) to (13-72) then become the *MEH* functions:

$$M_{i,j} = \ell_{i,j}(1 + s_j) + v_{i,j}(1 + S_j) - \ell_{i,j-1} - v_{i,j+1} - f_{i,j} = 0 \tag{13-93}$$

where

$$f_{i,j} = F_j z_{i,j}$$

$$E_{i,j} = K_{i,j}\ell_{i,j}\left(\sum_a v_{a,j} \Big/ \sum_a \ell_{a,j}\right) - v_{i,j} = 0 \tag{13-94}$$

$$H_j = H_{Lj}(1 + s_j)\sum_i \ell_{i,j} + H_{Vj}(1 + S_j)\sum_i v_{i,j} - H_{Lj-1}\sum_i \ell_{i,j} - H_{Vj+1}\sum_i v_{i,j+1} - H_{Fj}\sum_i f_{i,j} - Q_j = 0 \tag{13-95}$$

where physical properties are not simplified:

$$K_{i,j} = K_{i,j}\{T_j, P_j, \ell_j, v_j\}$$

$$H_{Vj} = H_{Vj}\{T_j, P_j, v_j\}$$

$$H_{Lj} = H_{Lj}\{T_j, P_j, \ell_j\}$$

Let the order of corrections to the unknowns be according to stage number, which in terms of the corresponding unknowns is

$$\overline{\mathrm{X}} = [\overline{\mathrm{X}}_1, \overline{\mathrm{X}}_2, \ldots \overline{\mathrm{X}}_j, \ldots \overline{\mathrm{X}}_N]^T \tag{13-96}$$

where

$$\overline{\mathrm{X}}_j = [v_{1,j}, v_{2,j}, \ldots v_{C,j}, T_j, \ell_{1,j}, \ell_{2,j}, \ldots \ell_{C,j}]^T \tag{13-97}$$

Let the order of the linearized *MEH* functions also be according to stage number, which in terms of the corresponding nonlinear functions is

$$\overline{\mathrm{F}} = [\overline{\mathrm{F}}_1, \overline{\mathrm{F}}_2, \ldots \overline{\mathrm{F}}_j, \ldots \overline{\mathrm{F}}_N]^T \tag{13-98}$$

where

$$\overline{\mathrm{F}}_j = [H_j, M_{1,j}, M_{2,j}, \ldots M_{C,j}, E_{1j}, \ldots E_{C,j}]^T \tag{13-99}$$

Corrections to unknowns for the kth iteration are obtained from

$$\Delta\overline{\mathrm{X}}^{(k)} = -\left[\left(\frac{\partial\overline{\mathrm{F}}}{\partial\mathrm{X}}\right)^{-1}\right]^{(k)} \overline{\mathrm{F}}^{(k)} \tag{13-100}$$

The next approximations to the unknowns are obtained from

$$\overline{\mathrm{X}}^{(k+1)} = \overline{\mathrm{X}}^{(k)} + t\,\Delta\overline{\mathrm{X}}^{(k)} \tag{13-101}$$

where t is a damping ($0 < t < 1$) or acceleration ($t > 1$) factor. By ordering the corrections to the unknowns and the linearized functions in this manner, the resulting Jacobian of partial derivatives of all functions with respect to all unknowns is of a very convenient sparse matrix form of block tridiagonal structure.

$$\left(\frac{\overline{\overline{\mathrm{dF}}}}{\overline{\overline{\mathrm{dX}}}}\right) = \begin{bmatrix} \overline{\overline{\mathrm{B}}}_1 & \overline{\overline{\mathrm{C}}}_1 & 0 & 0 & .. & & & 0 \\ \overline{\overline{\mathrm{A}}}_2 & \overline{\overline{\mathrm{B}}}_2 & \overline{\overline{\mathrm{C}}}_2 & 0 & .. & & & 0 \\ 0^{*} & \overline{\overline{\mathrm{A}}}_3 & \overline{\overline{\mathrm{B}}}_3{}^{\dagger} & \overline{\overline{\mathrm{C}}}_3{}^{\ddagger} & & & & 0 \\ .. & & & & & & & .. \\ .. & & & & & & & .. \\ 0 & .. & & & & & & 0 \\ 0 & .. & & & 0 & \overline{\overline{\mathrm{A}}}^{*}_{N-1} & \overline{\overline{\mathrm{B}}}_{N-1}{}^{\dagger} & \overline{\overline{\mathrm{C}}}_{N-1}{}^{\ddagger} \\ 0 & .. & & & 0 & 0 & \overline{\overline{\mathrm{A}}}_N & \overline{\overline{\mathrm{B}}}_N \end{bmatrix} \tag{13-102}$$

Blocks $\overline{\overline{\mathrm{A}}}_j$, $\overline{\overline{\mathrm{B}}}_j$, and $\overline{\overline{\mathrm{C}}}_j$ are $(2C + 1)$ by $(2C + 1)$ submatrices of partial derivatives of the functions on stage j with respect to unknowns on stage $j - 1$, j, and $j + 1$ respectively. The solution to Eq. (13-100) is readily obtained by a matrix-algebra equivalent of the Thomas algorithm for a tridiagonal-matrix equation. Computer storage requirements are minimized by making the following replacements. Starting at top stage 1, using forward-block elimination,

$$\overline{\overline{\mathrm{C}}}_1 \to (\overline{\overline{\mathrm{B}}}_1)^{-1}\overline{\overline{\mathrm{C}}}_1,\ \overline{\mathrm{F}}_1 \to (\overline{\overline{\mathrm{B}}}_1)^{-1}\,\overline{\mathrm{F}}_1$$

and $\quad \overline{\overline{\mathrm{B}}}_1 \to I$ (the identity submatrix)

For stages j from 2 to $(N - 1)$,

$$\overline{\overline{\mathrm{C}}}_j \to (\overline{\overline{\mathrm{B}}}_j - \overline{\overline{\mathrm{A}}}_j\overline{\overline{\mathrm{C}}}_{j-1})^{-1}\overline{\overline{\mathrm{C}}}_j,$$

$$\overline{\mathrm{F}}_j \to (\overline{\overline{\mathrm{B}}}_j - \overline{\overline{\mathrm{A}}}_j\overline{\overline{\mathrm{C}}}_{j-1})^{-1}(\overline{\mathrm{F}} - \overline{\overline{\mathrm{A}}}_j\overline{\mathrm{F}}_{j-1}), \qquad \overline{\overline{\mathrm{A}}}_j \to 0, \qquad \overline{\overline{\mathrm{B}}}_j \to I$$

For final stage N,

$$\overline{\mathrm{F}}_N \to (\overline{\overline{\mathrm{B}}}_N - \overline{\overline{\mathrm{A}}}_N\overline{\overline{\mathrm{C}}}_{N-1})^{-1}(\overline{\mathrm{F}}_N - \overline{\overline{\mathrm{A}}}_N\overline{\mathrm{F}}_{N-1}), \qquad \overline{\overline{\mathrm{A}}}_N \to 0, \qquad \overline{\overline{\mathrm{B}}}_N \to I$$

This completes the forward steps to give $\Delta\overline{\mathrm{X}}_N = -\overline{\mathrm{F}}_N$. Remaining values of corrections $\Delta\overline{\mathrm{X}}_j$ are obtained by successive backward substitution from $\Delta\overline{\mathrm{X}}_j = -\overline{\mathrm{F}}_j \to -(\overline{\mathrm{F}}_j - \overline{\overline{\mathrm{C}}}_j\overline{\mathrm{F}}_{j+1})$. Matrix inversions are best done by *LU* decomposition. Efficiency is best for a small number of components C.

The Newton iteration is initiated by providing reasonable guesses for all unknowns. However, these can be generated from guesses of just T, T_N, and one interstage value of F_j or L_j. Remaining values of T_j are obtained by linear interpolation. By assuming constant molal over-

flow, calculations are readily made of remaining values of V_j and L_j, from which initial values of $v_{i,j}$ and $\ell_{i,j}$ are obtained from Eqs. (13-89) and (13-90) after obtaining approximations of $x_{i,j}$ and $y_{i,j}$ from steps 4, 5, 8, 9, and 10 of the SR method. Alternatively, a much cruder but often sufficient estimate of $x_{i,j}$ and $y_{i,j}$ is obtained by flashing the combined column feeds at average column pressure and a vapor-to-liquid ratio that approximates the ratio of overhead plus vapor-sidestream flows to bottoms plus liquid-sidestream flows. Resulting compositions are used as the initial estimate for every stage.

At the conclusion of each iteration, convergence is checked by employing an approximate criterion such as

$$\tau = \sum_j \left\{ \left(\frac{H_j}{\xi} \right)^2 + \sum_i [(M_{i,j})^2 + (E_{i,j})^2] \right\} \le \epsilon \qquad (13\text{-}103)$$

where ξ is a scale factor that is of the order of the average molal heat of vaporization. If we take

$$\epsilon = N(2C + 1) \left(\sum_j F_j^2 \right) 10^{-10} \qquad (13\text{-}104)$$

converged values of the unknowns will generally be accurate, on the average, to from four or more significant digits.

During early iterations, particularly when initial estimates of the unknowns are poor, τ and corrections to the unknowns will be very large. It is then preferred to utilize a small value of t in Eq. (13-101) so as to dampen changes to unknowns and prevent wild oscillations. However, the use of values of t much less than 0.25 may slow or prevent convergence.

It is also best to reset to zero or small values any negative values of component flow rates before initiating the next iteration. When the neighborhood of the solution is reached, τ will often decrease by one or more orders of magnitude at each iteration, and it is best to set $t = 1$. Because the Newton method is quadratically convergent in the neighborhood of the solution, usually only three or four additional iterations will be required to reach the convergence criterion. Prior to that, it is not uncommon for τ to increase somewhat from one iteration to the next. If the Jacobian tends toward a singular condition, it may be necessary to restart the procedure with different initial guesses or adjust the Jacobian in some manner.

Standard specifications for the Naphtali-Sandholm method are Q_j (including zero values) at each stage at which heat transfer occurs and sidestream flow ratio s_j or S_j (including zero values) at each stage at which a sidestream is withdrawn. However, the desirable block tridiagonal structure of the jacobian matrix can still be preserved when substitute specifications are made if they are associated with the same stage or an adjacent stage. For example, suppose that for a reboiled absorber, as in Fig. 13-7*f*, it is desired to specify a boil-up ratio rather than reboiler duty. Equation (13-95) for function H_N is removed from the $N(2C + 1)$ set of equations and is replaced by the equation

$$\tilde{H}_N = \sum_i v_{i,N} - (V_N/L_N) \sum_i \ell_{i,N} = 0 \qquad (13\text{-}105)$$

where the value of (V_N/L_N) is specified. Following convergence of the calculations, Q_N is computed from the removed equation.

All of the major computer-aided design and simulation programs have a simultaneous-correction algorithm. A Naphtali-Sandholm type of program, particularly suited for applications to distillation, extractive distillation, and azeotropic distillation, has been published by Fredenslund, Gmehling, and Rasmussen (*Vapor-Liquid Equilibria Using UNIFAC, a Group Contribution Method,* Elsevier, Amsterdam, 1977). Christiansen, Michelsen, and Fredenslund [*Comput. Chem. Eng.*, **3,** 535 (1979)] apply a modified Naphtali-Sandholm type of method to the distillation of natural-gas liquids, even near the critical region, using thermodynamic properties computed from the Soave-Redlich-Kwong equation of state. Block and Hegner [*Am. Inst. Chem. Eng. J.*, **22,** 582 (1976)] extended the Naphtali-Sandholm method to staged separators involving two liquid phases (liquid-liquid extraction) and three coexisting phases (three-phase distillation).

Example 6: Calculation of Naphtali-Sandholm SC Method Use the Naphtali-Sandholm SC method to compute stage temperatures and interstage vapor and liquid flow rates and compositions for the reboiled-stripper specifications shown in Fig. 13-53. The specified bottoms rate is equivalent to removing most of the nC_5 and nC_6 and some of the nC_7 in the bottoms.

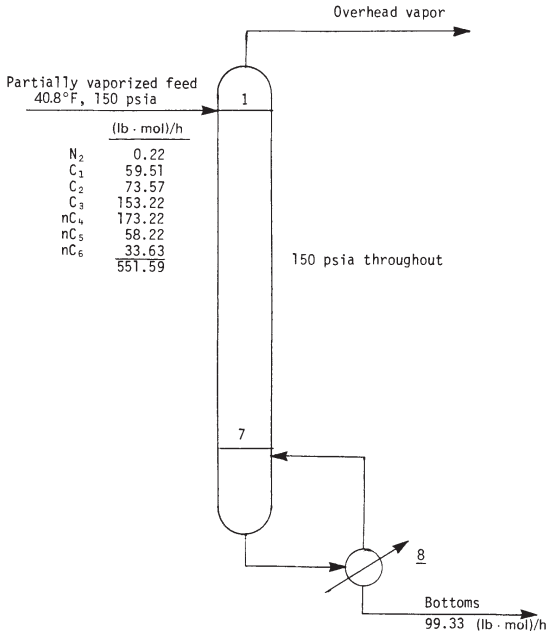

FIG. 13-53 Specifications for the calculation of a reboiled stripper by the Naphtali-Sandholm method.

Calculations were made with the Grayson-Streed modification of the Chao-Seader method for *K* values and the Lee-Kesler method for enthalpy departures. Initial estimates for stage temperatures and flow rates were as follows, where numbers in parentheses are consistent with specifications:

		(lb·mol)/h	
Stage	*T*, °F	*V*	*L*
1	130	(452.26)	550
8	250		

NOTE: To convert degrees Fahrenheit to degrees Celsius, °C = (°F − 32)/1.8. To convert pound-moles per hour to kilogram-moles per second, multiply by 1.26×10^{-4}.

For specified feed temperature and pressure, an isothermal flash of the feed gave 13.35 percent vaporization.

Convergence was achieved in 3 iterations. Converged values of temperatures, total flows, and component flow rates are tabulated in Table 13-14. Computed reboiler duty is 1,295,000 W (4,421,000 Btu/h). Computed temperature, total vapor flow, and component flow profiles, shown in Fig. 13-54, are not of the shapes that might be expected. Vapor and liquid flow rates for nC_4 change dramatically from stage to stage.

INSIDE-OUT METHODS

The BP, SR, and SC methods described above expend a large percentage of their computational effort during each iteration in the calculation of K values, enthalpies, and derivatives thereof. An algorithm designed to significantly reduce that effort was developed by Boston and Sullivan [*Can. J. Chem. Engr.*, **52,** 52 (1974)]. The MESH equations are solved in an inner loop using simple, approximate equations for *K* values and enthalpies. The empirical constants in these equations are determined and infrequently updated from the more rigorous, but complex, *K* value and enthalpy correlations in an outer loop, using calculated compositions and temperatures from the inner loop. Thus, the method is referred to as the inside-out method. The iteration variables for the outer loop are the constants in the approximate thermodynamic-property equations in the inner loop. The iteration variables for the inner loop are related to stage *j*

TABLE 13-14 Converged Results for Reboiled Stripper of Fig. 13-53

Stg	Temp °F	Pres psia	Net flows Liquid lb·mol/h	Net flows Vapor lb·mol/h	Feeds lb·mol/h	Product lb·mol/h	Duties MMBtu/h
1	130.5	150.00	566.13		551.59	452.26	
2	170.0	150.00	622.63	466.80			
3	184.4	150.00	638.20	523.30			
4	192.7	150.00	637.73	538.87			
5	200.6	150.00	626.86	538.40			
6	211.8	150.00	608.02	527.53			
7	228.5	150.00	586.11	508.69			
8	251.3	150.00		486.78		99.33	4.421

Tray compositions

Stage #1	130.49°F Vap lb·mol/h	150.00 psia Liq lb·mol/h
Nitrogen	0.22000	0.03033
Methane	59.51000	4.72506
Ethane	73.56996	20.85994
Propane	153.18130	115.69593
n-Butane	150.43202	318.78543
n-Pentane	12.75881	70.16827
n-Hexane	2.58982	35.86041
Total lb·mol/h	452.2619	566.1254

Stage #2	170.01°F Vap lb·mol/h	150.00 psia Liq lb·mol/h
Nitrogen	0.03033	0.00517
Methane	4.72506	0.36256
Ethane	20.85991	5.14611
Propane	115.65723	66.94922
n-Butane	295.99744	428.55569
n-Pentane	24.70708	83.84168
n-Hexane	4.82023	37.77268
Total lb·mol/h	466.7973	622.6332

Stage #3	184.42°F Vap lb·mol/h	150.00 psia Liq lb·mol/h
Nitrogen	0.00517	0.00085
Methane	0.36256	0.02460
Ethane	5.14608	1.08705
Propane	66.91052	31.95980
n-Butane	405.76770	466.08041
n-Pentane	38.38049	99.77217
n-Hexane	6.73250	39.27149
Total lb·mol/h	523.3050	638.1964

Stage #4	192.68°F Vap lb·mol/h	150.00 psia Liq lb·mol/h
Nitrogen	0.00085	0.00014
Methane	0.02460	0.00159
Ethane	1.08701	0.21493
Propane	31.92111	14.00705
n-Butane	443.29239	457.42691
n-Pentane	54.31099	124.43126
n-Hexane	8.23131	41.64842
Total lb·mol/h	538.8683	637.7303

Tray compositions

Stage #5	200.64°F Vap lb·mol/h	150.00 psia Liq lb·mol/h
Nitrogen	0.00014	0.00002
Methane	0.00159	0.00010
Ethane	0.21490	0.04043
Propane	13.96836	5.73731
n-Butane	434.63895	410.72699
n-Pentane	78.97008	162.79074
n-Hexane	10.60824	47.56607
Total lb·mol/h	538.4022	626.8616

Stage #6	211.75°F Vap lb·mol/h	150.00 psia Liq lb·mol/h
Nitrogen	0.00002	0.00000
Methane	0.00010	0.00001
Ethane	0.04039	0.00719
Propane	5.69862	2.17265
n-Butane	387.93896	329.74094
n-Pentane	117.32958	212.37617
n-Hexane	16.52589	63.72279
Total lb·mol/h	527.5336	608.0197

Stage #7	228.46°F Vap lb·mol/h	150.00 psia Liq lb·mol/h
Nitrogen	0.00000	0.00000
Methane	0.00001	0.00000
Ethane	0.00716	0.00119
Propane	2.13396	0.74298
n-Butane	306.95294	227.83710
n-Pentane	166.91501	254.54031
n-Hexane	32.68262	102.98384
Total lb·mol/h	508.6917	586.1054

Stage #8	251.31°F Vap lb·mol/h	150.00 psia Liq lb·mol/h
Nitrogen	0.00000	0.00000
Methane	0.00000	0.00000
Ethane	0.00116	0.00003
Propane	0.70429	0.03869
n-Butane	205.04907	22.78802
n-Pentane	209.07915	45.46117
n-Hexane	71.94367	31.04017
Total lb·mol/h	486.7773	99.3281

stripping factors, $K_{ij}V_j/L_j$, for components i, which make use of volatility and energy parameters. Otherwise, the inner-loop calculations utilize computational features of the BP, SR, and SC methods, to compute stage temperatures, compositions, and flow rates. The inside-out method takes advantage of the following observations: (1) relative volatilities vary from iteration to iteration much less than the K values, (2) enthalpy of vaporization varies from iteration to iteration much less than phase enthalpies, and (3) component stripping factors combine effects of temperature and liquid and vapor flows at each stage.

As an example of how the approximate thermodynamic-property equations are handled in the inner loop, consider the calculation of K values. The approximate models for nearly ideal liquid solutions are the following empirical Clausius-Clapeyron form of the K value in terms of a base or reference component, b, and the definition of the relative volatility, α.

$$K_{b,j} = \exp(A_j - B_j/T_j) \tag{13-106}$$

$$K_{i,j} = \alpha_{i,j} K_{b,j} \tag{13-107}$$

Values of A and B for the base component are back-calculated for each stage in the outer loop from a suitable K-value correlation (e.g. the SRK equation, which is also used to compute the K values of the other components on each of the other stages so that values of α_{ij} can be computed). The values of A, B, and α are passed from the outer loop to the inner loop, where they are used to formulate the phase equilibria equation:

$$v_{i,j} = \alpha_{i,j} S_{b,j} l_{i,j} \tag{13-108}$$

where

$$S_{b,j} = K_{ij} V_j / L_j \tag{13-109}$$

The initial version of the inside-out method was developed for rapid calculations of simple and complex distillation, absorption, and

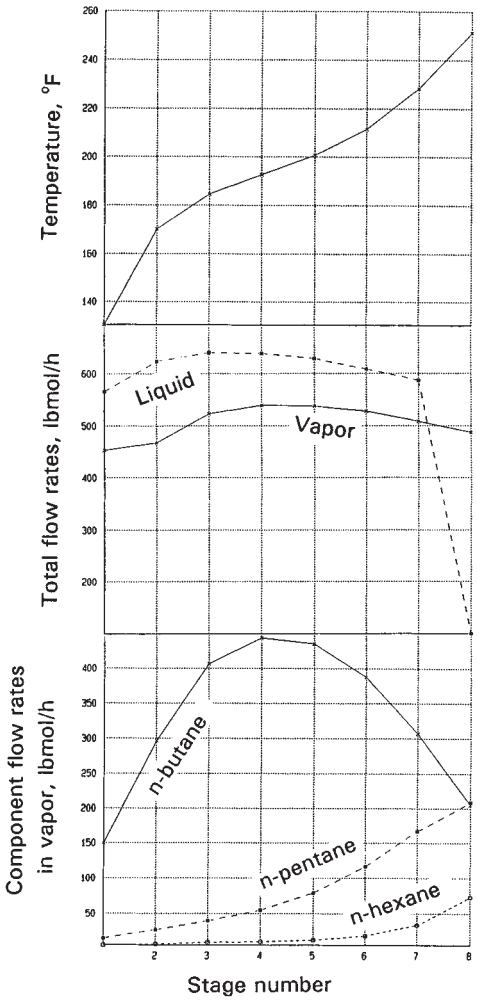

FIG. 13-54 Converged profiles for the reboiled stripper of Fig. 13-53.

stripping operations for hydrocarbon mixtures. However extensions and improvements in the method by Boston and coworkers [*Comput. Chem. Engng.*, **2,** 109 (1978), *ACS Symp. Ser.* No. 124, 135 (1980), *Comput. Chem. Engng.*, **8,** 105 (1984), and *Chem. Eng. Prog.*, **86** (8), 45–54 (1990)] and by Russell [*Chem. Eng.*, **90,** (20), 53 (1983)] and Jelinek [*Comput. Chem. Engng.*, **12,** 195 (1988)] now make it possible to apply the method to reboiled absorption, reboiled stripping, extractive and azeotropic distillation, three-phase systems, reactive distillation, highly nonideal systems, and interlinked distillation systems with pumparounds, bypasses, and external heat exchangers. Inside-out methods are incorporated into most of the computer-aided process design and simulation programs and are now the methods of choice for design and simulation, as stated by Haas, who in Chap. 4 of Kister (op. cit.) presents details of two of the several inside-out algorithms.

Example 7: Calculation of Inside-Out Method For the conditions of the simple distillation column shown in Fig. 13-55, obtain a converged solution by the inside-out method, using the SRK equation-of-state for thermodynamic properties (in the outer loop).

A computer solution was obtained as follows. The only initial assumptions are a condenser outlet temperature of 65°F and a bottoms-product temperature of 165°F. The bubble-point temperature of the feed is computed as 123.5°F. In the initialization procedure, the constants A and B in (13-106) for inner-loop calculations, with T in °R, are determined from the SRK equation, with the following results:

Stage	T, °F	A	B	K_b
1	65	6.870	3708	0.8219
2	95	6.962	4031	0.7374
3	118	7.080	4356	0.6341
4	142	7.039	4466	0.6785
5	165	6.998	4576	0.7205

Values of enthalpy constants for approximate equations are not tabulated here but are also computed for each stage based on the initial temperature distribution.

In the inner-loop calculation sequence, component flow rates are computed from the MESH equations by the tridiagonal matrix method. The resulting bottoms-product flow rate deviates somewhat from the specified value of 50 lb·mol/h. However, by modifying the component stripping factors with a base stripping factor, S_b, in (13-109) of 1.1863, the error in the bottoms flow rate is reduced to 0.73 percent.

The initial inside-loop error from the solution of the normalized energy-balance equations, is found to be only 0.04624. This is reduced to 0.000401 after two iterations through the inner loop.

At this point in the inside-out method, the revised column profiles of temperature and phase compositions are used in the outer loop with the complex SRK thermodynamic models to compute updates of the approximate K and H constants. Then only one inner-loop iteration is required to obtain satisfactory convergence of the energy equations. The K and H constants are again updated in the outer loop. After one inner-loop iteration, the approximate K and H constants are found to be sufficiently close to the SRK values that overall convergence is achieved. Thus, a total of only 3 outer-loop iterations and 4 inner-loop iterations are required.

To illustrate the efficiency of the inside-out method to converge this example, the results from each of the three outer-loop iterations are summarized in the following tables:

Outer-loop iteration	Stage temperatures, °F				
	T_1	T_2	T_3	T_4	T_5
Initial guess	65	—	—	—	165
1	82.36	118.14	146.79	172.66	193.20
2	83.58	119.50	147.98	172.57	192.53
3	83.67	119.54	147.95	172.43	192.43

Outer-loop iteration	Total liquid flows, lb·moles/hr				
	L_1	L_2	L_3	L_4	L_5
Specification	100	—	—	—	—
1	100.00	89.68	187.22	189.39	50.00
2	100.03	89.83	188.84	190.59	49.99
3	100.0	89.87	188.96	190.56	50.00

Outer-loop iteration	Component flows in bottoms product, lb·moles/hr			
	C_3	nC_4	nC_5	L_5
1	0.687	12.045	37.268	50.000
2	0.947	12.341	36.697	49.985
3	0.955	12.363	36.683	50.001

From these tables, it is seen that the stage temperatures and total liquid flows are already close to the converged solution after only one outer-loop iteration. However, the composition of the bottoms product, specifically with respect to the lightest component, C_3, is not close to the converged solution until after two iterations. The inside-out method does not always converge so dramatically, but is usually quite efficient.

HOMOTOPY-CONTINUATION METHODS

Although the SC and inside-out methods are reasonably robust, they are not guaranteed to converge and sometimes fail, particularly for very nonideal liquid solutions and when initial guesses are poor. A much more robust, but more time-consuming, method is differential arclength homotopy continuation, the basic principles and applications of which are discussed by Wayburn and Seader [*Comp. Chem. Engng.*, **11,** 7–25 (1987); *Proceedings Second Intern. Conf. Foundations of Computer-Aided Process Design,* CACHE, Austin, TX, 765–

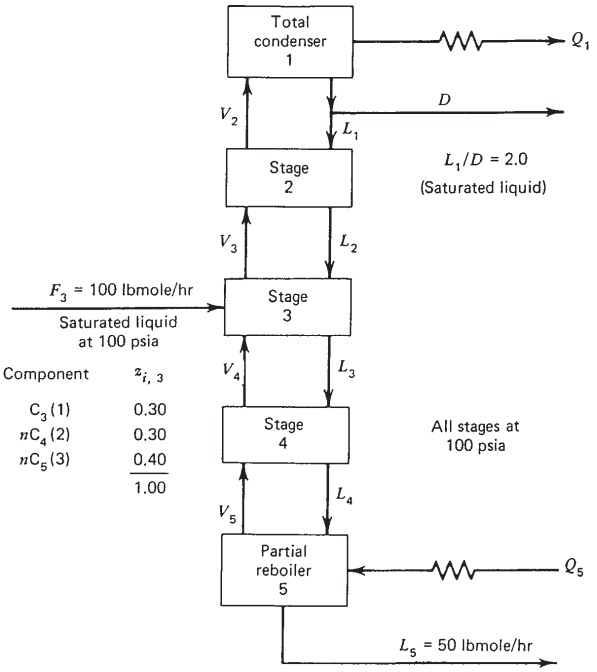

FIG. 13-55 Specifications for distillation column of Example 7.

862 (1984); *AIChE monograph Series,* AIChE, New York, **81,** No. 15 (1985)]. Homotopy methods begin from a known solution of a companion set of equations and follow a path to the desired solution of the set of equations to be solved. In most cases, the path exists and can be followed. In one implementation, the set of equations to be solved, call it $f(x)$, and the companion set of equations, call it $g(x)$, are connected together by a set of mathematical homotopy equations:

$$h(x,t) = t\,f(x) + (1-t)g(x) = 0 \qquad (13\text{-}110)$$

where t is a homotopy parameter. An appropriate function is selected for $g(x)$ such as $f(x) - f(x_0)$, where x_0 are the initial guesses, which can be selected arbitrarily. At the beginning of the path, $t = 0$ and Eq. (13-110) becomes $h(x,t) = f(x) - f(x_0) = 0$ or $f(x) = f(x_0)$. The homotopy parameter is then gradually moved from 0 to 1. At a value of $t = 1$, Eq. (13-110) becomes $h(x,t) = f(x) = 0$, which corresponds to the desired solution.

The movement along the path is accomplished by a predictor-corrector continuation procedure, where the corrector is often a numerical Euler integration step of the differential-arclength form of Eq. (13-110) along the arclength of the path (rather than a step in t), as proposed by Klopfenstein [*J. Assoc. Comput. Mach.,* **8,** 366 (1961)]. The arclength of the path is preferred, over the homotopy parameter, as a continuation parameter because the path may make one or more turns in the homotopy parameter, making it difficult to take an integration step. The predictor step is accompanied by a truncation error that is reduced in the corrector step, which employs Newton's method with Eq. (13-110) to return to the path. If the predictor steps along the path are not too large, the corrector steps always converge.

Another implementation of homotopy-continuation methods is the use of problem-dependent homotopies that exploit some physical aspect of the problem. Vickery and Taylor [*AIChE J.,* **32,** 547 (1986)] utilized thermodynamic homotopies for K values and enthalpies to gradually move these properties from ideal to actual values so as to solve the MESH equations when very nonideal liquid solutions were involved. Taylor, Wayburn, and Vickery [*I. Chem. E. Symp. Ser.* No. 104, B305 (1987)] used a pseudo-Murphree efficiency homotopy to move the solution of the MESH equations from a low efficiency, where little separation occurs, to a higher and more reasonable efficiency.

Continuation methods, also called *imbedding* and *path-following* methods, were first applied to the solution of separation models involving large numbers of nonlinear equations by Salgovic, Hlavacek, and Ilavsky [*Chem. Eng. Sci.,* **36,** 1599 (1981)] and by Byrne and Baird [*Comp. Chem. Engng.,* **9,** 593 (1985)]. Since then, they have been applied successfully to problems involving interlinked distillation (Wayburn and Seader, op. cit.), azeotropic and three-phase distillation [Kovach, III and Seider, *Comp. Chem. Engng.,* **11,** 593 (1987)], and reactive distillation [Chang and Seader, *Comp. Chem. Engng.,* **12,** 1243 (1988)], when SC and inside-out methods have failed. Today, many computer-aided distillation-design and simulation packages include continuation techniques to make the codes more robust.

STAGE EFFICIENCY

The mathematical models presented earlier for rigorous calculations of multistage, multicomponent distillation-type separations assume that equilibrium with respect to both heat and mass transfer is attained at each stage. Unless temperature changes significantly from stage to stage, the assumption that vapor and liquid phases exiting from a stage are at the same temperature is generally valid. However, in most cases, equilibrium with respect to mass transfer is not a valid assumption. If all feed components have the same mass-transfer efficiency, the number of actual stages or trays is simply related to the number of equilibrium stages used in the modeling calculations by an overall stage efficiency. For distillation, as discussed in Sec. 14, this efficiency for well-designed trays typically varies from 40 to 120 percent; the higher value being achieved in some large-diameter towers because of a cross-flow effect. Efficiencies for absorption and extractive distillation can be lower than 40 percent.

When it is desired to compute, with rigorous methods, actual rather than equilibrium stages, Eqs. (13-69) and (13-94) can be modified to include the Murphree vapor-phase efficiency $\eta_{i,j}$, defined by Eq. (13-29). This is particularly desirable for multistage operations involving feeds containing components of a wide range of volatility and/or concentration, in which only a rectification (absorption) or stripping action is provided and all components are not sharply separated. In those cases, the use of a different Murphree efficiency for each component and each tray may be necessary to compute recovery accurately.

Departures from the equilibrium-stage model may also occur when entrainment of liquid droplets in the rising vapor or occlusion of vapor in the liquid flow in the downcomer is significant. The former condition may occur at high vapor loading when flooding is approached. The latter condition is possible at high operating pressures when vapor and liquid densities are not drastically different. Entrainment and occlusion effects are not strictly due to mass-transfer inefficiency and are best taken into account by including entrainment terms in the modeling equations, as shown by Loud and Waggoner [*Ind. Eng. Chem. Process Des. Dev.,* **17,** 149 (1978)].

RATE-BASED MODELS

Although the widely used equilibrium-stage models for distillation, described above, have proved to be quite adequate for binary and close-boiling, ideal and near-ideal multicomponent vapor-liquid mixtures, their deficiencies for general multicomponent mixtures have long been recognized. Even Murphree [*Ind. Eng. Chem.,* **17,** 747–750 and 960–964 (1925)], who formulated the widely used plate efficiencies that carry his name, pointed out clearly their deficiencies for multicomponent mixtures and when efficiencies are small. Later, Walter and Sherwood [*Ind. Eng. Chem.,* **33,** 493 (1941)] showed that experimentally measured efficiencies could cover an enormous range, with some values less than 10 percent, and Krishna et al. [*Trans. Inst. Chem. Engr.,* **55,** 178 (1977)] showed theoretically that the component mass-transfer coupling effects discovered by Toor [*AIChE J.,* **3,** 198 (1957)] could cause the rate of mass transfer for components having small concentration driving forces to be controlled by the other species, with the result that Murphree vapor efficiencies could cover the entire range of values from minus infinity to plus infinity.

The first major step toward the development of a more realistic rate-based (nonequilibrium) model for distillation was taken by Krishnamurthy and Taylor [*AIChE J.*, **31,** 449–465 (1985)]. More recently, Taylor, Kooijman, and Hung [*Comp. Chem. Engng.*, **18,** 205–217 (1994)] extended the initial development so as to add the effects of tray-pressure drop, entrainment, occlusion, and interlinks with other columns. In the augmented MESH equations, which they refer to as the MERSHQ equations, they replace the conventional mass and energy balances around each stage by two balances each, one for the vapor phase and one for the liquid phase. Each of the component-material balances contains a term for the rate of mass transfer between the two phases; the energy balances contain a term for the rate of heat transfer between phases. Thus, each pair of phase balances is coupled by mass or heat-transfer rates, which are estimated from constitutive equations that account, in as rigorous a manner as possible, for bulk transport, species interactions, and coupling effects. The heat and mass-transfer coefficients in these equations are obtained from empirical correlations of experimental data and the Chilton-Colburn analogy. Equilibrium between the two phases is assumed at the phase interface. Thus, the rate-based model deals with both transport and thermodynamics. Although tray efficiencies are not part of the modeling equations, efficiencies can be back-calculated from the results of the simulation. Various options for vapor and liquid flow configurations are employed in the model, including plug flow and perfectly mixed flow on each tray.

A schematic diagram of the nonequilibrium stage for the Taylor et al. model is shown in Fig. 13-56. Entering the stage are the following material streams: F^V = vapor feed; F^L = liquid feed; V_{j+1} = vapor from stage below together with fractional-liquid entrainment, ϕ^L_{j+1}; L_{j-1} = liquid from stage above with fractional-vapor occlusion, ϕ^V_{j-1}; G^V = vapor interlink; and G^L = liquid interlink. Leaving the stage are the following material streams: V_j = vapor with fractional withdrawal as sidestream, r^V_j, and fractional-liquid entrainment, ϕ^L_j; and L_j = liquid with fractional withdrawal as sidestream, r^L_j, and fractional-vapor occlusion, ϕ^V_j. Also leaving the stage are heat-transfer streams, Q^V_j and Q^L_j. The rate of heat transfer from the vapor phase to the liquid phase is E_j and the rate of component mass transfer from the vapor phase to the liquid phase is N_{ij}.

The nonequilibrium-model equations for the stage in Fig. 13-56 are as follows in residual form, where i = component ($i = 1$ to C), j = stage number ($j = 1$ to N), and ν = a stage in another column that supplies an interlink.

Material Balances (2*C* + 2 Equations) Component for the vapor phase:

$$M^V_{ij} \equiv (1 + r^V_j + \phi^V_j)V_j y_{ij} - V_{j+1}y_{i,j+1} - \phi^V_{j-1}V_{j-1}y_{i,j-1} - f^V_{ij} - \sum_{\nu=1}^{n} G^V_{ij\nu} + N_{ij} = 0 \qquad i = 1, 2, \ldots, c \tag{13-111}$$

Component for the liquid phase:

$$M^L_{ij} \equiv (1 + r^L_j + \phi^L_j)L_j x_{ij} - L_{j-1}x_{i,j-1} - \phi^L_{j+1}L_{j+1}x_{i,j+1} - f^L_{ij} - \sum_{\nu=1}^{n} G^L_{ij\nu} - N_{ij} = 0 \qquad i = 1, 2, \ldots, c \tag{13-112}$$

Total for the vapor phase:

$$M^V_{tj} \equiv (1 + r^V_j + \phi^V_j)V_j - V_{j+1} - \phi^L_{j-1}V_{j-1} - F^V_j - \sum_{i=1}^{c}\sum_{\nu=1}^{n} G^V_{ij\nu} + N_{tj} = 0 \tag{13-113}$$

Total for the liquid phase:

$$M^L_{tj} \equiv (1 + r^L_j + \phi^L_j)L_j - L_{j-1} - \phi^L_{j+1}L_{j+1} - F^L_j - \sum_{i=1}^{c}\sum_{\nu=1}^{n} G^L_{ij\nu} - N_{tj} = 0 \tag{13-114}$$

Energy Balances (3 Equations) For the vapor phase:

$$E^V_j \equiv (1 + r^V_j + \phi^V_j)V_j H^V_j - V_{j+1}H^V_{j+1} - \phi^V_{j-1}V_{j-1}H^V_{j-1} - F^V_j H^{VF}_j - \sum_{\nu=1}^{n} G^V_{j\nu}H^V_{j\nu} + Q^V_j + e^V_j = 0 \tag{13-115}$$

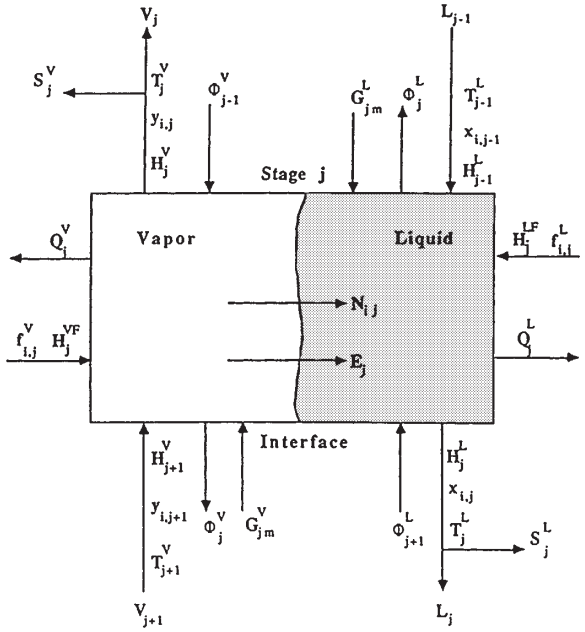

FIG. 13-56 Schematic diagram of a nonequilibrium stage.

For the liquid phase:

$$E^L_j \equiv (1 + r^L_j + \phi^L_j)L_j H^L_j - L_{j-1}H^L_{j-1} - \phi^L_{j+1}L_{j+1}H^L_{j+1} - F^L_j H^{LF}_j - \sum_{\nu=1}^{n} G^L_{j\nu}H^L_{j\nu} + Q^L_j - e^L_j = 0 \tag{13-116}$$

Continuity across the phase interface:

$$E^I_j \equiv e^V_j - e^L_j = 0 \tag{13-117}$$

Mass-Transfer Rates (2*C* − 2 Equations) Component in the vapor phase:

$$R^V_{ij} \equiv N_{ij} - N^V_{ij} = 0 \qquad i = 1, 2, \ldots, c-1 \tag{13-118}$$

Component in the liquid phase:

$$R^L_{ij} \equiv N_{ij} - N^L_{ij} = 0 \qquad i = 1, 2, \ldots, c-1 \tag{13-119}$$

Summation of Mole Fractions (2 Equations) Vapor-phase interface:

$$S^{VI}_j \equiv \sum_{i=1}^{c} y^I_{ij} - 1 = 0 \tag{13-120}$$

Liquid-phase interface:

$$S^{LI}_j \equiv \sum_{i=1}^{c} x^I_{ij} - 1 = 0 \tag{13-121}$$

Hydraulic Equation for Stage Pressure Drop (1 Equation) Vapor-phase pressure drop:

$$P_j \equiv p_j - p_{j-1} - (\Delta p_{j-1}) = 0 \tag{13-122}$$

Interface Equilibrium (*C* Equations) Component vapor-liquid equilibrium:

$$Q^I_{ij} \equiv K_{ij}x^I_{ij} - y^I_{ij} = 0 \qquad i = 1, 2, \ldots, c \tag{13-123}$$

Equations (13-111) to (13-114), (13-118) and (13-119), contain terms, N_{ij}, for rates of mass transfer of components from the vapor phase to the liquid phase (rates are negative if transfer is from the liquid phase to the vapor phase). These rates are estimated from diffusive and bulk-flow contributions, where the former are based on interfacial area, average mole-fraction driving forces, and mass-

transfer coefficients that account for coupling effects through binary-pair coefficients. Although the stage shown in Fig. 13-56 appears to apply to a trayed column, the model also applies for a section of a packed column. Accordingly, empirical correlations for the interfacial area and binary-pair mass-transfer coefficients cover bubble-cap trays, sieve trays, valve trays, dumped packings, and structured packings. The average mole-fraction driving forces for diffusion depend upon the assumed vapor and liquid-flow patterns. In the mixed-flow model, both phases are completely mixed. This is the simplest model and is usually suitable for small-diameter trayed columns. In the plug-flow model, both phases move in plug flow. This model is applicable to packed columns and certain trayed columns.

Equations (13-115) to (13-117) contain terms, e_j, for rates of heat transfer from the vapor phase to the liquid phase. These rates are estimated from convective and bulk-flow contributions, where the former are based on interfacial area, average-temperature driving forces, and convective heat-transfer coefficients, which are determined from the Chilton-Colburn analogy for the vapor phase and from the penetration theory for the liquid phase.

The K values (vapor-liquid equilibrium ratios) in Equation (13-123) are estimated from the same equation-of-state or activity-coefficient models that are used with equilibrium-stage models. Tray or packed-section pressure drops are estimated from suitable correlations of the type discussed by Kister (op. cit.).

From the above list of rate-based model equations, it is seen that they total $5C + 6$ for each tray, compared to $2C + 1$ or $2C + 3$ (depending on whether mole fractions or component flow rates are used for composition variables) for each stage in the equilibrium-stage model. Therefore, more computer time is required to solve the rate-based model, which is generally converged by an SC approach of the Newton type.

A potential limitation of the application to design of a rate-based model compared to the equilibrium-stage model is that the latter can be computed independently of the geometry of the column because no transport equations are included in the model. Thus, the sizing of the column is decoupled from the determination of column operating conditions. However, this limitation of the early rate-based models has now been eliminated by incorporating a design mode that simultaneously designs trays and packed sections.

A study of industrial applications by Taylor, Kooijman, and Woodman [IChemE. Symp. Ser. Distillation and Absorption 1992, A415–A427 (1992)] concluded that rate-based models are particularly desirable when simulating or designing: (1) packed columns, (2) systems with strongly nonideal liquid solutions, (3) systems with trace components that need to be tracked closely, (4) columns with rapidly changing profiles, (5) systems where tray-efficiency data are lacking. Besides the extended model just described, a number of other investigators, as summarized by Taylor, Kooijman, and Hung (op. cit.), have developed rate-based models for specific applications and other purposes, including cryogenic distillation, crude distillation, vacuum distillation, catalytic distillation, three-phase distillation, dynamic distillation, and liquid-liquid extraction. Commercial computerized rate-based models are available in two simulation programs: RATEFRAC in ASPEN PLUS from Aspen Technology, Inc., Cambridge, Massachusetts and NEQ2 in ChemSep from R. Taylor and H. A. Kooijman of Clarkson University. Rate-based models could usher in a new era in trayed and packed-column design and simulation.

Example 8: Calculation of Rate-Based Distillation The separation of 655 lb·mol/h of a bubble-point mixture of 16 mol % toluene, 9.5 mol % methanol, 53.3 mol % styrene, and 21.2 mol % ethylbenzene is to be carried out in a 9.84-ft diameter sieve-tray column having 40 sieve trays with 2-inch high weirs and on 24-inch tray spacing. The column is equipped with a total condenser and a partial reboiler. The feed will enter the column on the 21st tray from the top, where the column pressure will be 93 kPa, The bottom-tray pressure is 101 kPa and the top-tray pressure is 86 kPa. The distillate rate will be set at 167 lb·mol/h in an attempt to obtain a sharp separation between toluene-methanol, which will tend to accumulate in the distillate, and styrene and ethylbenzene. A reflux ratio of 4.8 will be used. Plug flow of vapor and complete mixing of liquid will be assumed on each tray. K values will be computed from the UNIFAC activity-coefficient method and the Chan-Fair correlation will be used to estimate mass-transfer coefficients. Predict, with a rate-based model, the separation that will be achieved and back-calculate from the computed tray compositions, the component vapor-phase Murphree-tray efficiencies.

The calculations were made with the RATEFRAC program and comparisons were made with the companion RADFRAC program, which utilizes the inside-out method for an equilibrium-based model.

The rate-based model gave a distillate with 0.023 mol % ethylbenzene and 0.0003 mol % styrene, and a bottoms product with essentially no methanol and 0.008 mol % toluene. Murphree tray efficiencies for toluene, styrene, and ethylbenzene varied somewhat from tray to tray, but were confined mainly between 86 and 93 percent. Methanol tray efficiencies varied widely, mainly from 19 to 105 percent, with high values in the rectifying section and low values in the stripping section. Temperature differences between vapor and liquid phases leaving a tray were not larger than 5°F.

Based on an average tray efficiency of 90 percent for the hydrocarbons, the equilibrium-based model calculations were made with 36 equilibrium stages. The results for the distillate and bottoms compositions, which were very close to those computed by the rate-based method, were a distillate with 0.018 mol % ethylbenzene and less than 0.0006 mol % styrene, and a bottoms product with only a trace of methanol and 0.006 mol % toluene.

ENHANCED DISTILLATION

INTRODUCTION

In distillation operations, separation results from differences in vapor- and liquid-phase compositions arising from the partial vaporization of a liquid mixture or the partial condensation of a vapor mixture. The vapor phase becomes enriched in the more volatile components while the liquid phase is depleted of those same components. In many situations, however, the change in composition between the vapor and liquid phases in equilibrium becomes small (so-called "pinched condition"), and a large number of successive partial vaporizations and partial condensations is required to achieve the desired separation. Alternatively, the vapor and liquid phases may have identical compositions, because of the formation of an azeotrope, and no separation by simple distillation is possible.

Several enhanced distillation-based separation techniques have been developed for close-boiling or low-relative-volatility systems, and for systems exhibiting azeotropic behavior. All of these special techniques are ultimately based on the same differences in the vapor and liquid compositions as ordinary distillation, but, in addition, they rely on some additional mechanism to further modify the vapor-liquid behavior of the key components. These enhanced techniques can be classified according to their effect on the relationship between the vapor and liquid compositions:

1. *Azeotropic distillation and pressure-swing distillation.* Methods that cause or exploit azeotrope formation or behavior to alter the boiling characteristics and separability of the mixture.
2. *Extractive distillation and salt distillation.* Methods that primarily modify liquid-phase behavior to alter the relative volatility of the components of the mixture.
3. *Reactive distillation.* Methods that use chemical reaction to modify the composition of the mixture or, alternatively, use existing vapor-liquid differences between reaction products and reactants to enhance the performance of a reaction.

AZEOTROPISM

At low-to-moderate pressure ranges typical of most industrial applications, the fundamental composition relationship between the vapor and liquid phases in equilibrium can be expressed as a function of the total

system pressure, the vapor pressure of each pure component, and the liquid-phase activity coefficient of each component i in the mixture:

$$y_i P = x_i \gamma_i P_i^{sat} \qquad (13\text{-}124)$$

In systems that exhibit ideal liquid-phase behavior, the activity coefficients, γ_i, are equal to unity and Eq. (13-124) simplifies to Raoult's law. For nonideal liquid-phase behavior, a system is said to show negative deviations from Raoult's law if $\gamma_i < 1$, and conversely, positive deviations from Raoult's law if $\gamma_i > 1$. In sufficiently nonideal systems, the deviations may be so large the temperature-composition phase diagrams exhibit extrema, as shown in each of the three parts of Fig. 13-57. At such maxima or minima, the equilibrium vapor and liquid compositions are identical. Thus,

$$y_i = x_i \qquad \text{for all } i = 1, \ldots n \qquad (13\text{-}125)$$

and the system is said to form an azeotrope (from the Greek, meaning *to boil unchanged*). Azeotropic systems show a minimum in the *T-x,y* diagram when the deviations from Raoult's law are positive (Fig. 13-57*a*) and a maximum in the *T-x,y* diagram when the deviations from Raoult's law are negative (Fig. 13-57*b*). If at these two conditions, a single liquid phase is in equilibrium with the vapor phase, the azeotrope is homogeneous. If multiple liquid-phase behavior is exhibited at the azeotropic condition, the azeotrope is heterogeneous. For heterogeneous azeotropes, the vapor-phase composition is equal to the overall composition of the two (or more) liquid phases (Fig. 13-57*c*). Mixtures with only small deviations from Raoult's law may form an azeotrope only if the components are close-boiling. As the boiling-point difference between the components increases, the composition of the azeotrope shifts closer to one of the pure components (toward the lower-boiling pure component for minimum-boiling azeotropes, and toward the higher-boiling pure component for maximum-boiling azeotropes). Mixtures of components whose boiling points differ by more than about 30°C generally do not exhibit azeotropes distinguishable from the pure components even if large deviations from Raoult's law are present. As a qualitative guide to liquid-phase activity-coefficient behavior, Robbins [*Chem. Eng. Prog.*, **76** (10) 58 (1980)] developed a matrix of chemical families, shown in Table 13-15, which indicates expected deviations from Raoult's law.

The formation of two liquid phases within some temperature range for close-boiling mixtures is generally an indication that the system will also exhibit a minimum-boiling azeotrope, since two liquid phases may form when deviations from Raoult's law are extremely positive. The fact that immiscibility does occur, however, does not guarantee that the azeotrope will be heterogeneous. The azeotropic temperature is sometimes outside the range of temperatures at which a system exhibits two liquid phases. Moreover, the azeotropic composition may not necessarily fall within the composition range of the two-liquid-phase region even when within the appropriate temperature range

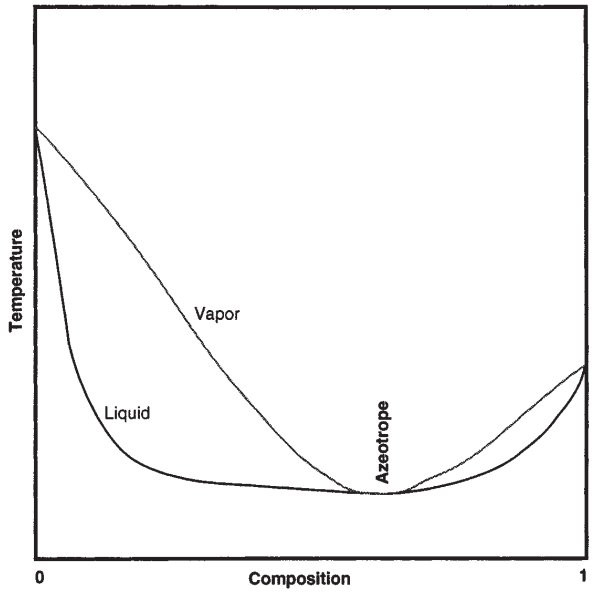

FIG. 13-57 Schematic isobaric-phase diagrams for binary azeotropic mixtures. (*a*) Homogeneous minimum-boiling azeotropes.

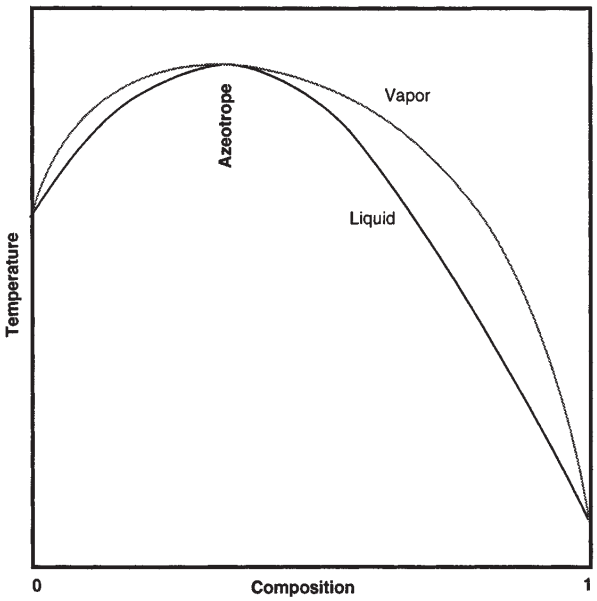

FIG. 13-57 (*Continued*) Schematic isobaric-phase diagrams for binary azeotropic mixtures. (*b*) Homogeneous maximum-boiling azeotrope.

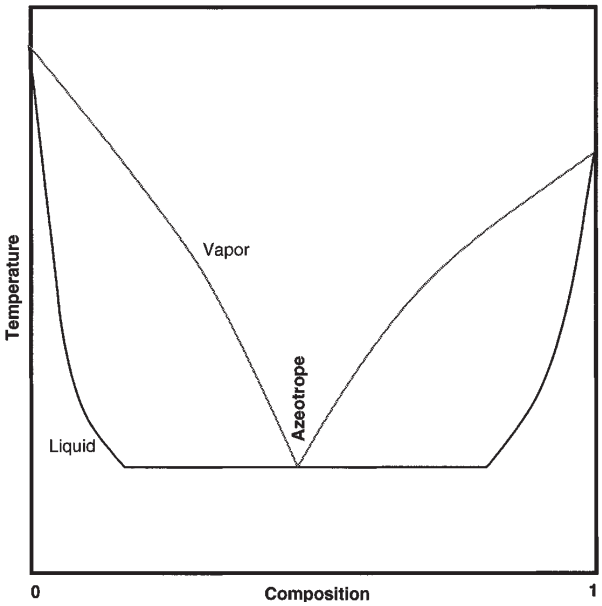

FIG. 13-57 (*Continued*) Schematic isobaric-phase diagrams for binary azeotropic mixtures. (*c*) Heterogeneous azeotrope.

TABLE 13-15 Solute-Solvent Group Interactions

Solute class	Group	Solvent class 1	2	3	4	5	6	7	8	9	10	11	12
	H-donor												
1	Phenol	0	0	–	0	–	–	–	–	–	–	–	–
2	Acid, thiol	0	0	–	0	–	–	0	0	0	0	–	–
3	Alcohol, water	–	–	0	+	+	0	–	–	–	–	–	–
4	Active-H on multihalo paraffin	0	0	+	0	–	–	–	–	–	–	0	–
	H-acceptor												
5	Ketone, amide with no H on N, sulfone, phosphine oxide	–	–	+	–	0	+	–	–	–	+	–	–
6	Tertamine	–	–	0	–	+	0	–	–	0	+	0	0
7	Secamine	–	0	–	–	+	+	0	0	0	0	0	–
8	Pri amine, ammonia, amide with 2H on N	–	0	–	–	+	+	0	0	–	+	–	–
9	Ether, oxide, sulfoxide	–	0	+	–	+	0	0	–	0	+	0	–
10	Ester, aldehyde, carbonate, phosphate, nitrate, nitrite, nitrile, intramolecular bonding, e.g., *o*-nitro phenol	–	0	+	–	+	+	0	–	–	0	–	–
11	Aromatic, olefin, halogen aromatic, multihalo paraffin without active H, monohalo paraffin	+	+	+	0	+	0	0	–	0	+	0	0
	Non-H-bonding												
12	Paraffin, carbon disulfide	+	+	+	+	+	0	+	+	+	+	0	0

SOURCE: Robbins, L. A., *Chem. Eng. Prog.,* **76**(10), 58–61 (1980), by permission.

for liquid-liquid behavior, as is for example the case for the methyl acetate-water and tetrahydrofuran-water systems. Homogeneous azeotropes that are completely miscible at all temperatures usually occur between species with very close boiling points and rather small liquid-phase nonidealities. Moreover, since strong positive deviations from Raoult's law are required for liquid-liquid phase splitting, maximum-boiling azeotropes ($\gamma_i < 1$) are never heterogeneous.

Additional general information on the thermodynamics of phase equilibria and azeotropy is available in Swietoslawski (*Azeotropy and Polyazeotropy,* Pergamon, London, 1963), Van Winkle (*Distillation,* McGraw-Hill, New York, 1967), Smith and Van Ness (*Introduction to Chemical Engineering Thermodynamics,* McGraw-Hill, New York, 1975), Wizniak [*Chem. Eng. Sci.,* **38,** 969 (1983)], and Walas (*Phase Equilibria in Chemical Engineering,* Butterworths, Boston, 1985). Horsley (*Azeotropic Data-III,* American Chemical Society, Washington, 1983) compiled an extensive list of binary and some ternary and higher experimental azeotropic boiling-point and composition data. Another source for azeotrope data and activity coefficient model parameters is the multivolume *Vapor-Liquid Equilibrium Data Collection* (DECHEMA, Frankfort 1977), a compendium of published experimental VLE data. Most of the data have been tested for thermodynamic consistency and have been fit to the Wilson, UNIQUAC, Van Laar, Margules, and NRTL equations. An extensive two-volume compilation of data for 18,800 systems involving 1,700 compounds, entitled *Azeotropic Data* by Gmehling et al., was published in 1994 by VCH Publishers, Deerfield Beach, Florida. A computational method for determining the temperatures and compositions of all azeotropes of a multicomponent mixture, from liquid-phase activity-coefficient correlations, by a differential arclength homotopy continuation method is given by Fidkowski, Malone, and Doherty [*Computers and Chem. Eng.,* **17,** 1141 (1993)].

RESIDUE CURVE MAPS AND DISTILLATION REGION DIAGRAMS

The simplest form of distillation involves boiling a multicomponent liquid mixture batchwise in a single-stage still pot. At any instant in time the vapor being generated and removed from the pot is assumed to be in equilibrium with the remaining liquid (assumed to be perfectly mixed) in the still. Because the vapor is richer in the more volatile components than the liquid, the composition and temperature of the liquid remaining in the still changes continuously over time and moves progressively toward less volatile compositions and higher temperatures until the last drop is vaporized. For some mixtures, this last composition is the highest-boiling pure component in the system. For other mixtures, this final composition may be a maximum-boiling azeotrope. For yet other systems, the final composition varies depending on the initial composition of the mixture charged to the still.

A residue curve is a tracing of this change in perfectly mixed liquid composition for simple single-stage batch distillation with respect to time. Arrows are sometimes added, pointing in the direction of increasing time, increasing temperature, and decreasing volatility. Because simple, batch distillation can be described mathematically by

$$dx_i/d\xi = x_i - y_i \qquad \text{for all } i = 1, \ldots n \tag{13-126}$$

where ξ is a nonlinear time scale, residue curves may also be extrapolated backward in time to give more volatile compositions which would produce a residue equal to the specified initial composition. A *residue curve map* (RCM) is generated by varying the initial composition and extrapolating Eq. (13-126) both forward and backward in time [Doherty and Perkins, *Chem. Eng. Sci.,* **33,** 281 (1978)]. Unlike a binary *y-x* plot, relative-volatility information is not presented. Therefore, it is difficult to determine the ease of separation from a residue curve map alone.

Residue curve maps can be constructed for mixtures of any number of components, but can be pictured graphically only for up to four components. For a binary mixture, a *T-x,y* diagram suffices; the system is simple enough that vapor-phase information can be included without confusion. With a ternary mixture, liquid-phase compositions are plotted on a triangular diagram, similar to that used in liquid-liquid extraction. Four-component systems can be plotted in a 3-dimensional tetrahedron. The vertices of the triangular diagram or tetrahedron represent the pure components. Any binary, ternary, and quaternary azeotropes are placed at the appropriate compositions on the edges and/or interior of the triangle and tetrahedron.

The simplest form of ternary RCM, as exemplified for the ideal normal-paraffin system of pentane-hexane-heptane, is illustrated in Fig. 13-58*a*, using a right-triangle diagram. Maps for all other nonazeotropic ternary mixtures are qualitatively similar. Each of the infinite number of possible residue curves originates at the pentane vertex, travels toward and then away from the hexane vertex, and terminates at the heptane vertex.

The family of all residue curves that originate at one composition and terminate at another composition defines a region. Systems that do not involve azeotropes have only one region—the entire composition space. However, for many systems, not all residue curves originate or terminate at the same two compositions. Such systems will have more that one region. The demarcation between regions in which adjacent residue curves originate from different compositions or terminate at different compositions is called a *separatrix.* Separatrices are related to the existence of azeotropes. In the composition space for a binary system, the separatrix is a point (the azeotropic composition). With three components, the separatrix becomes a (generally curved) line, with four components the separatrix becomes a surface, and so on.

All pure components and azeotropes in a system lie on region boundaries. Within each region, the most volatile composition on the boundary (either a pure component or a minimum-boiling azeotrope and the origin of all residue curves) is called the *low-boiling node.* The least-volatile composition on the boundary (again either a pure component or a maximum-boiling azeotrope and the terminus of all residue curves) is called the *high-boiling node.* All other pure components and azeotropes are called *intermediate-boiling saddles* (because no residue curves originate or terminate at these compositions). Adjacent regions may share nodes and saddles. Pure components and azeotropes are labeled as nodes and saddles as a result of the boiling points of all of the components and azeotropes in a system. If one species is removed, the labeling of all remaining pure components and azeotropes, particularly those that were saddles, may change. Region-defining separatrices always originate or terminate at saddle azeotropes, but never at saddle-pure components. Saddle-ternary azeotropes are particularly interesting because they are less obvious to determine experimentally (being neither minimum-boiling nor maximum-boiling), and have only recently begun to be recorded in the literature. (Gmehling et al., Azeotropic Data, VCH Publishers, Deerfield Beach, Florida, 1994). However, their presence in a mixture implies separatrices, which may have an important impact on the design of a separation system.

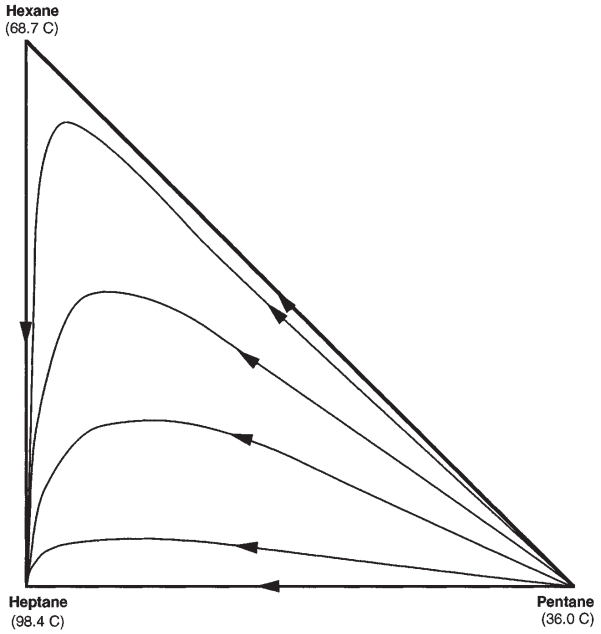

FIG. 13-58 Residue curve maps. (*a*) Nonazeotropic pentane-hexane-heptane system.

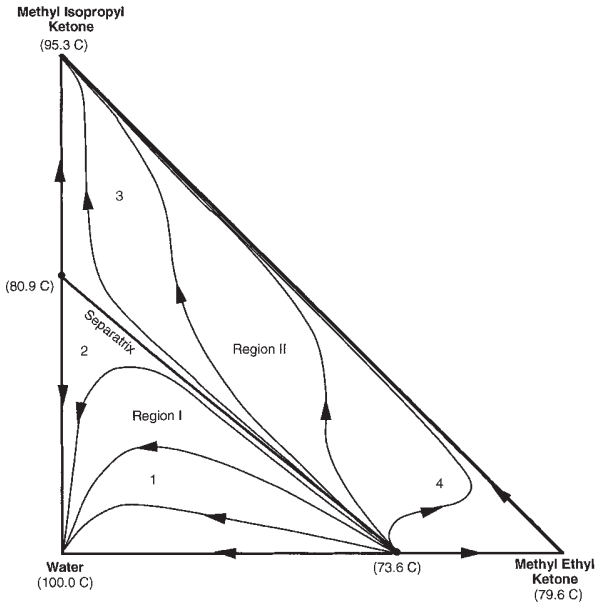

FIG. 13-58 (*Continued*) Residue curve maps. (*b*) MEK-MIPK-water system containing two minumum-boiling binary azeotropes.

Both *methylethylketone* (MEK) and *methylisopropylketone* (MIPK) form minimum-boiling azeotropes with water (Fig. 13-58b). In this ternary system, a separatrix connects the binary azeotropes and divides the RCM into two regions. The high-boiling node of Region I is pure water, while the low-boiling node is the MEK-water azeotrope.

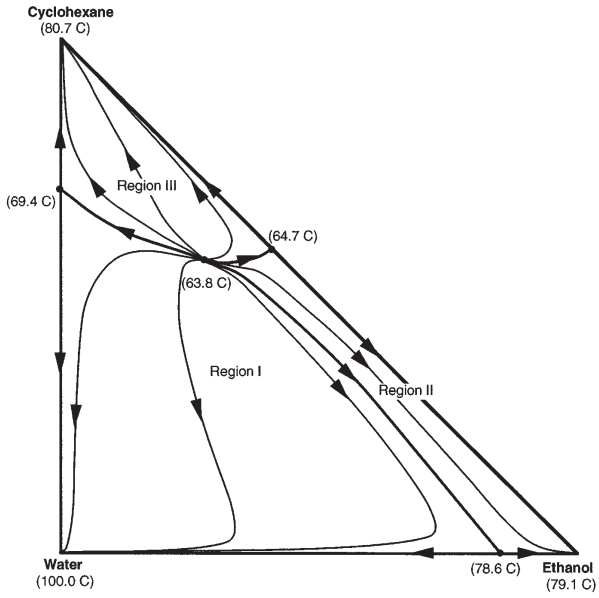

FIG. 13-58 (*Continued*) Residue curve maps. (*c*) Ethanol-cyclohexane-water system containing four minimum-boiling azeotropes and three distillation regions.

In Region II, the high- and low-boiling nodes are MIPK and the MEK-water azeotrope, respectively. The more complicated cyclohexane-ethanol-water system (Fig. 13-58c) has three separatrices and three regions, all of which share the ternary azeotrope as the low-boiling node.

The liquid-composition profiles in continuous staged or packed distillation columns operating at infinite reflux and boilup are closely approximated by simple distillation-residue curves [Van Dongen and Doherty, *Ind. Eng. Chem. Fundam.*, **24,** 454 (1985)]. Residue curves are also indicative of many aspects of the general behavior of continuous columns operating at more practical reflux ratios. For example, to a first approximation, the composition of the distillate and bottoms of a single-feed, continuous distillation column lie on the same residue curve. Therefore, for systems with separatrices and multiple regions, distillation-composition profiles are constrained to lie in specific regions. The precise boundaries of these distillation regions are a function of reflux ratio, but they are closely approximated by the RCM separatrices. If a RCM separatrix exists in a system, a corresponding distillation boundary will also exist. Separatrices and distillation boundaries correspond exactly at all pure components and azeotropes.

Residue curves can be constructed from experimental data or can be calculated analytically if equation-of-state or activity-coefficient expressions are available (e.g., Wilson binary-interaction parameters, UNIFAC groups). However, considerable information on system behavior can still be deduced from a simple semi-qualitative sketch of the RCM separatrices or distillation boundaries based only on pure component and azeotrope boiling-point data and approximate azeotrope compositions. Rules for constructing such qualitative *distillation region diagrams* (DRD) are given by Foucher et al. [*Ind. Eng. Chem. Res.*, **30,** 760–772, 2364 (1991)]. For ternary systems containing no more than one ternary azeotrope, and no more than one binary azeotrope between each pair of components, 125 such DRD are mathematically possible, although only a dozen or so represent most systems commonly encountered in practice.

Figure 13.59 illustrates all of the 125 possible DRD for ternary systems. Azeotropes are schematically depicted generally to have equimolar composition, distillation boundaries are shown as straight lines, and the arrows on the distillation boundaries indicate increasing temperature. These DRD are indexed in Table 13-16 according to a temperature-profile sequence of position numbers, defined in a keyed-triangular diagram at the bottom of the table, arranged by increasing the boiling point. Positions 1, 3, and 5 are the pure components in order of decreasing volatility. Positions 2, 4, and 6 are binary azeotropes at the positions shown in the keyed triangle, and position 7 is the ternary azeotrope. Azeotrope position numbers are deleted from the temperature profile if the corresponding azeotrope is known not to exist. It should be noted that not every conceivable temperature profile corresponds to a thermodynamically consistent system, and such combinations have been excluded from the index. As is evident from the index, some DRD are consistent with more than one temperature profile. Also, some temperature profiles are consistent with more than one DRD. In such cases, the correct diagram for a system must be determined from residue curves obtained from experimental or calculated data.

Schematic DRD shown in Fig. 13-59 are particularly useful in determining the implications of possibly unknown ternary saddle azeotropes by postulating position 7 at interior positions in the temperature profile. It should also be noted that some combinations of binary azeotropes require the existence of a ternary saddle azeotrope. As an example, consider the system acetone (56.4°C), chloroform (61.2°C), and methanol (64.7°C). Methanol forms minimum-boiling azeotropes with both acetone (54.6°C) and chloroform (53.5°C), and acetone-chloroform forms a maximum-boiling azeotrope (64.5°C). Experimentally there are no data for maximum or minimum-boiling ternary azeotropes. The temperature profile for this system is 461325, which from Table 13-16 is consistent with DRD 040 and DRD 042. However, Table 13-16 also indicates that the pure component and binary azeotrope data are consistent with three temperature profiles involving a ternary saddle azeotrope, namely 4671325, 4617325, and 4613725. All three of these temperature profiles correspond to DRD 107. Experimental residue curve trajectories for the acetone-chloroform-methanol system, as shown in Fig. 13-60, suggest the existence of a ternary saddle azeotrope and DRD 107 as the correct approximation of the distillation regions. Ewell and Welch [*Ind. Eng. Chem.*, **37,** 1224 (1945)] confirm such a ternary saddle at 57.5°C.

APPLICATIONS OF RCM AND DRD

Residue curve maps and distillation region diagrams are very powerful tools for understanding all types of batch and continuous distillation operations, particularly when combined with other information such as liquid-liquid binodal curves. Applications include:

1. *System visualization.* Location of distillation boundaries, azeotropes, distillation regions, feasible products, and liquid-liquid regions.
2. *Evaluation of laboratory data.* Location and confirmation of saddle ternary azeotropes and a check of thermodynamic consistency of data.
3. *Process synthesis.* Concept development, construction of flowsheets for new processes, and redesign or modification of existing process flowsheets.
4. *Process modeling.* Identification of infeasible or problematic column specifications that could cause simulation convergence difficulties or failure, and determination of initial estimates of column parameters including feed-stage location, number of stages in the stripping and enriching sections, reflux ratio, and product compositions.
5. *Control analysis/design.* Analysis of column balances and profiles to aid in control system design and operation.
6. *Process trouble shooting.* Analysis of separation system operation and malfunction, examination of composition profiles, and tracking of trace impurities with implications for corrosion and process specifications.

Material balances for mixing or continuous separation operations are represented graphically on triangular composition diagrams such as residue curve maps or distillation region diagrams by straight lines connecting pertinent compositions. Overall flow rates are found by the inverse-lever-arm rule. Distillation material balance lines are governed by two constraints:

1. The bottoms, distillate, and overall feed compositions must lie on the same straight line.
2. The bottoms and distillate compositions must lie (to a very close approximation) on the same residue curve.

Since residue curves do not by definition cross separatrices, the distillate and bottoms compositions must be in the same distillation region with the mass balance line intersecting a residue curve in two places. Mass balance lines for mixing and for other separations not involving vapor-liquid equilibria, such as extraction and decantation, are of course not limited by distillation boundaries.

For a given multicomponent mixture, a single-feed distillation column can be designed with sufficient stages, reflux, and material balance control to produce separations ranging from the *direct* mode of operation (low-boiling node taken as distillate) to the *indirect* mode (high-boiling node taken as bottoms). The bow-tie shaped set of reachable compositions for single-feed distillation is roughly bounded by the material balance lines corresponding to the sharpest direct separation and the sharpest indirect separation possible. The exact shape of the reachable composition space is further limited by the requirement that the distillate and bottoms lie on the same residue curve [Wahnschafft, et al., *Ind. Eng. Chem. Res.*, **31,** 2345 (1992)]. Since residue curves are deflected by saddles, it is generally not possible to obtain a saddle product (pure component or azeotrope) from a simple single-feed column.

Consider the recovery of MIPK from an MEK-MIPK-water mixture. The bow-tie approximation of reachable compositions for several feeds are shown in Fig 13-61*a* and the exact reachable compositions are shown in Fig. 13-61*b*. From Feed F3, which is situated in a different distillation region than the desired product, pure MIPK cannot be obtained at all. With the upper edge of the bow-tie region for Feed F1 along the MEK-MIPK (water-free) face of the composition triangle, and part of the lower edge along the MEK-water (MIPK-free) face, there are conditions under which both the water in the bottoms MIPK product can be driven to low levels (high-product purity) and MIPK in

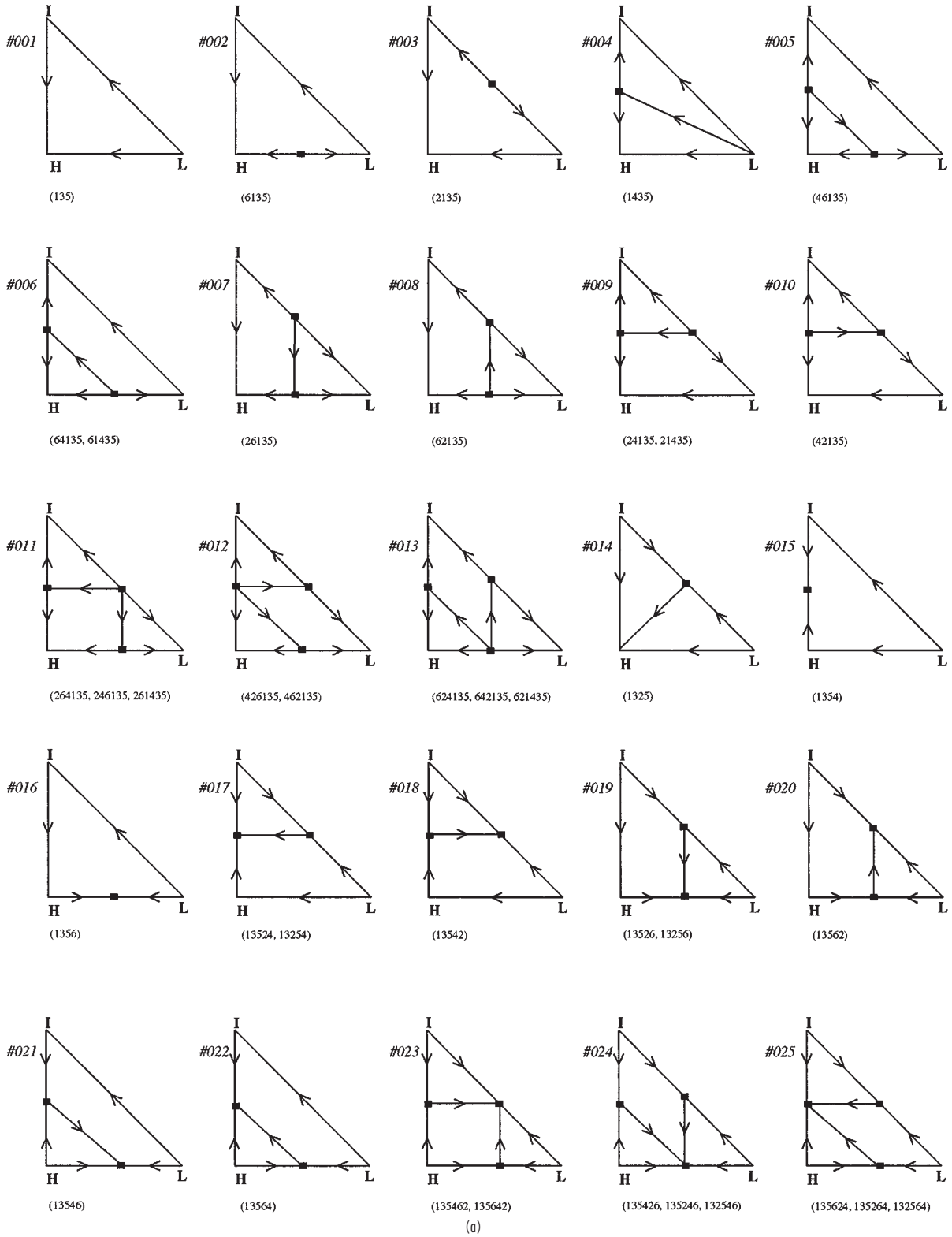

FIG. 13-59 Distillation region diagrams for ternary mixtures.

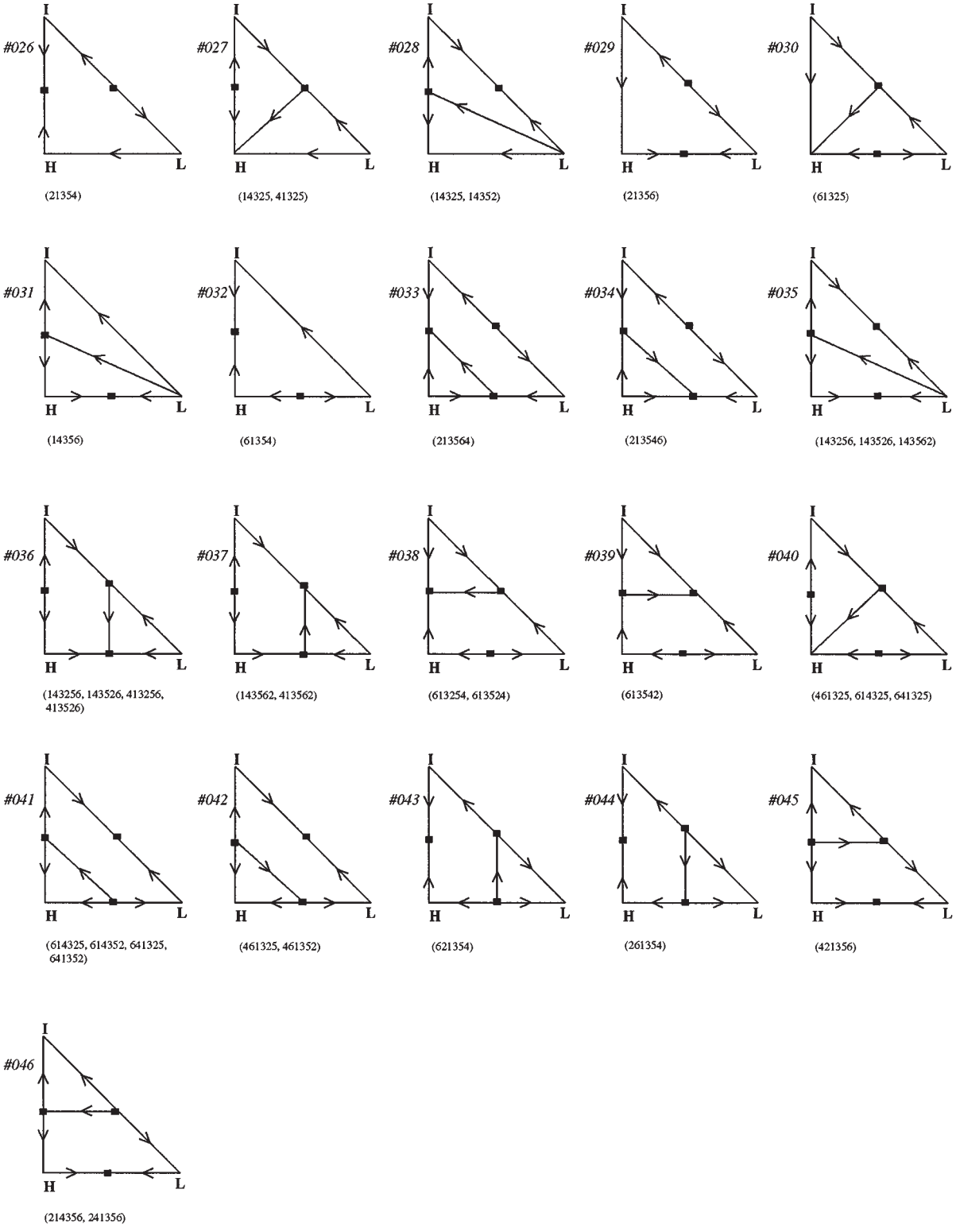

(b)

FIG. 13-59 (*Continued*) Distillation region diagrams for ternary mixtures.

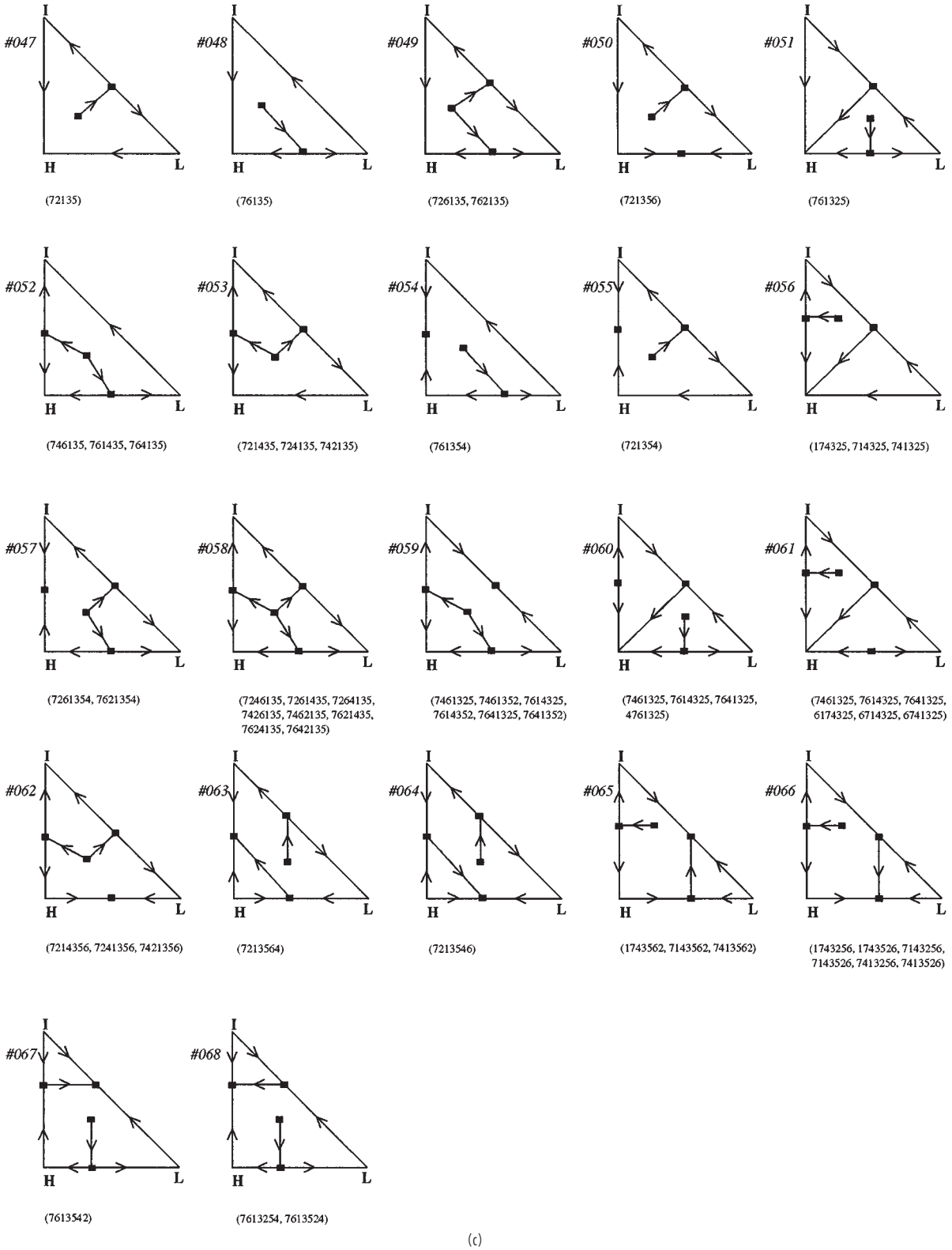

(c)

FIG. 13-59 (*Continued*) Distillation region diagrams for ternary mixtures.

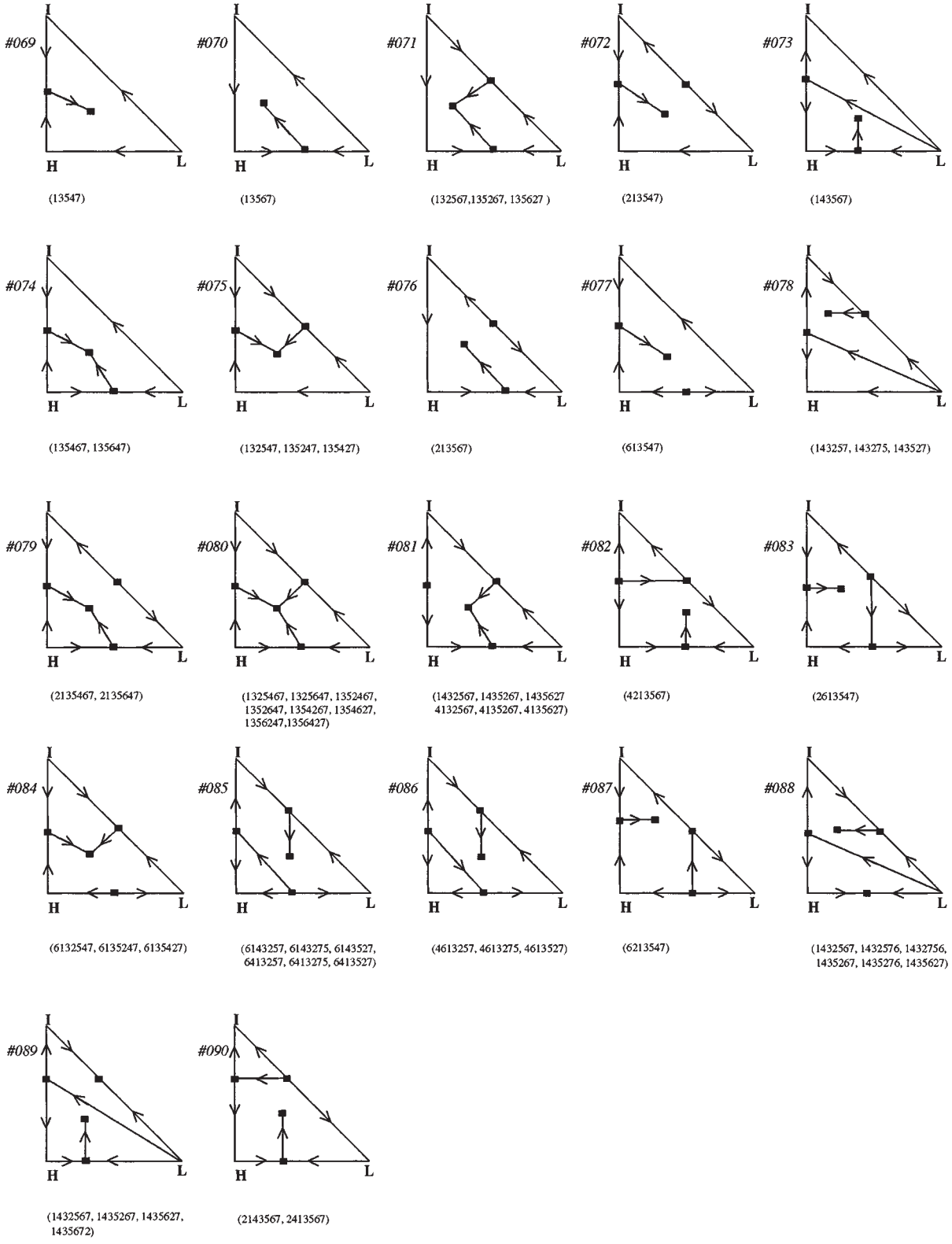

(d)

FIG. 13-59 (*Continued*) Distillation region diagrams for ternary mixtures.

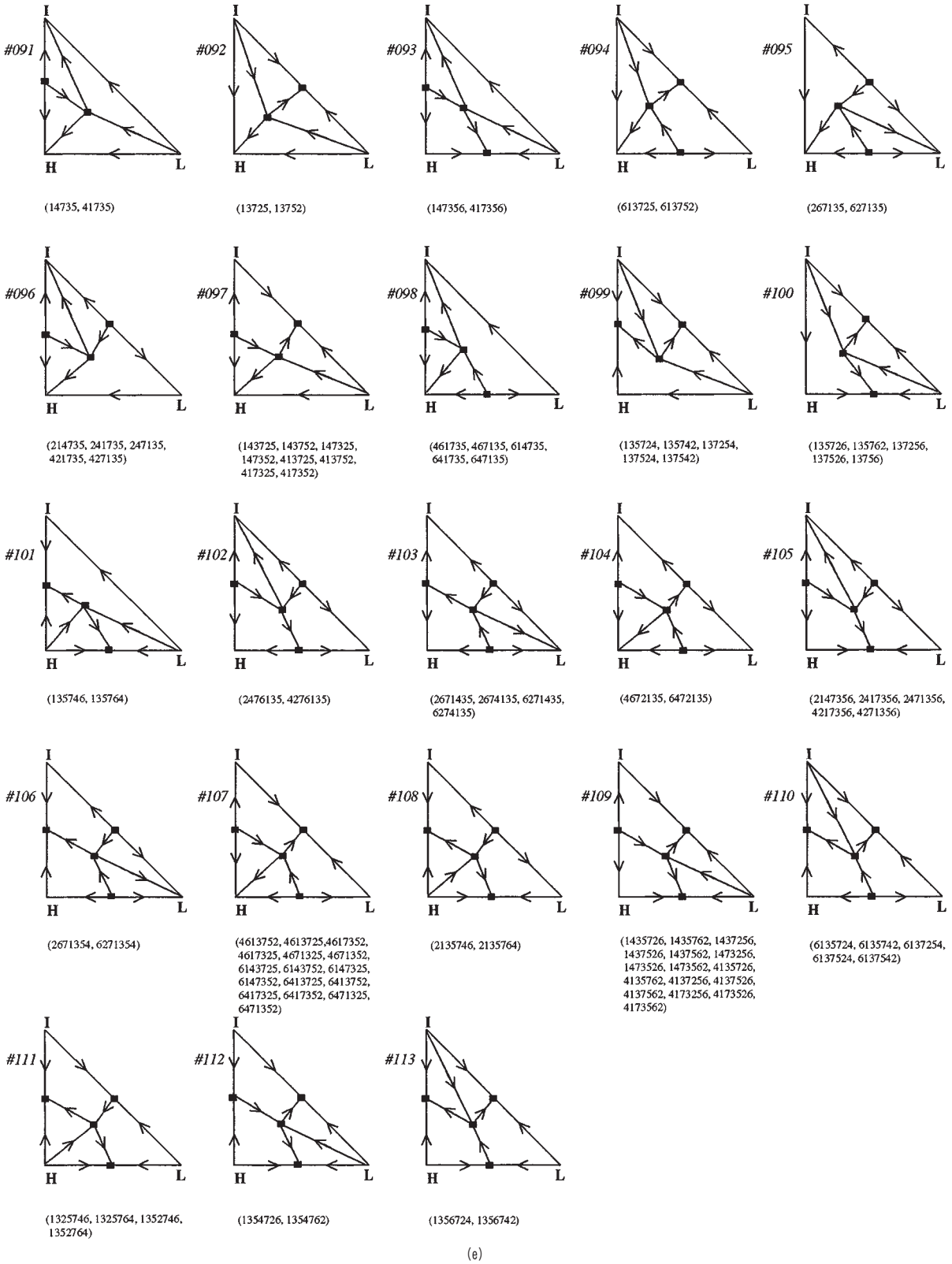

(e)

FIG. 13-59 (*Continued*) Distillation region diagrams for ternary mixtures.

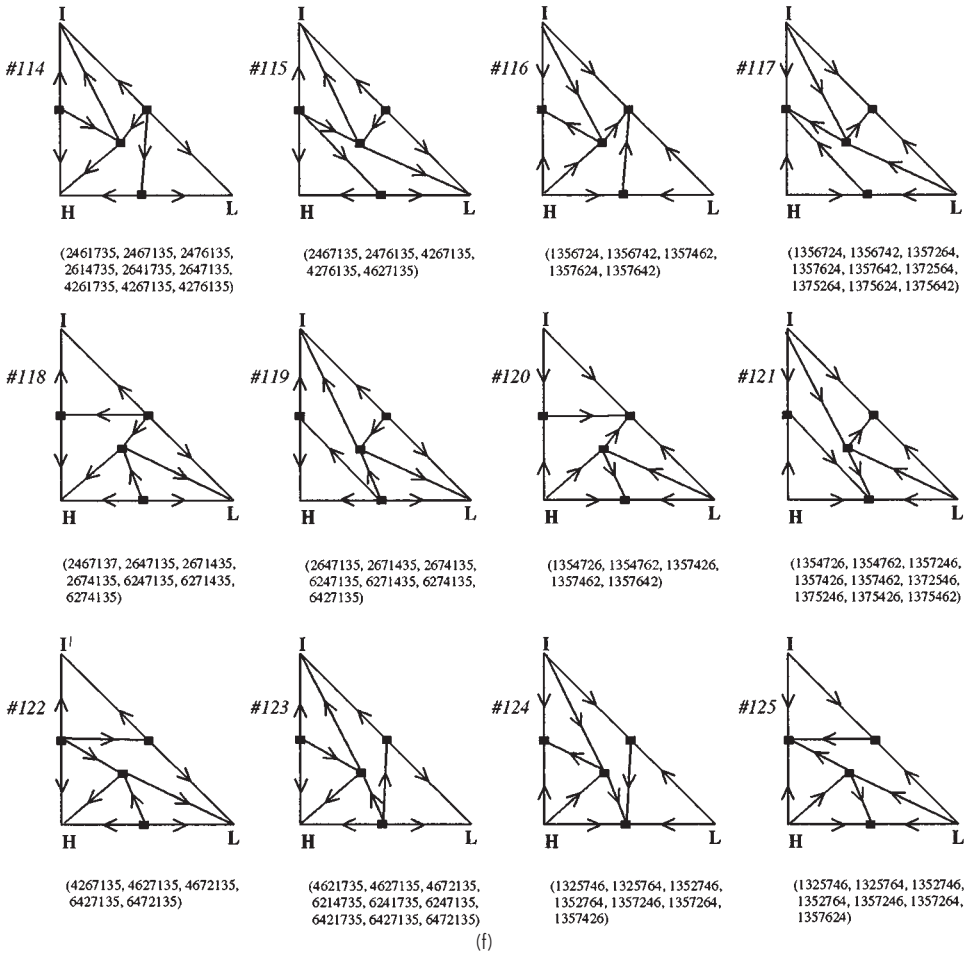

FIG. 13-59 (*Continued*) Distillation region diagrams for ternary mixtures.

the distillate can also be driven to low levels (high-product recovery), although achieving such an operation depends on having an adequate number of stages and reflux ratio.

The bow-tie region for Feed F2 is significantly different, with the upper edge along the water-MIPK (MEK-free) face of the triangle and the lower edge along the distillation boundary. From this feed it is not possible to achieve a high-purity MIPK specification while simultaneously obtaining high MIPK recovery. If the column is operated to get a high purity of MIPK, then the material balance line runs into the distillation boundary. Alternatively, if the column is operated to obtain a high recovery of MIPK (by removing the MEK-water azeotrope as distillate), the material balance requires the bottoms to lie on the water-MIPK face of the triangle.

The number of saddles in a particular distillation region can have significant impact on column-profile behavior, process stability, and convergence behavior in process simulation of the system. Referring to the MIPK-MEK-water system in Fig. 13-58*b,* Region I contains one saddle (MIPK-water azeotrope), while Region II contains two saddles (pure MEK and the MIPK-water azeotrope). These are three- and "four-sided" regions respectively. In a three-sided region, all residue curves track toward the solitary saddle. However, in a four (or more) sided region with saddles on either side of a node, some residue curves will tend to track toward one saddle, while others track toward another opposite saddle. For example, residue curve 1 in Region I originates from the MEK-water azeotrope low-boiling node and travels first toward the single saddle of the region (MIPK-water azeotrope) before ending at the water high-boiling node. Likewise, residue curve 2 and all other residue curves in Region I follow the same general path.

In Region II, residue curve 3 originates from the MEK-water azeotrope, travels toward the MIPK-water saddle azeotrope, and ends at pure MIPK. However, residue curve 4 follows a completely different path, traveling toward the pure MEK saddle before ending at pure MIPK. Some multicomponent columns have been designed for operation in four-sided regions with the feed composition adjusted so that both the high-boiling and low-boiling nodes can be obtained simultaneously as products. However, small perturbations in feed composition or reflux can result in feasible operation on many different residue curves that originate and terminate at these compositions. Multiple steady states and composition profiles that shift dramatically from tracking toward one saddle to the other are possible [Kovach, and Seider, *AIChE J.,* **33,** 1300 (1987). Consider a column operating in Region II of the MIPK-MEK-water diagram. Fig. 13-62 shows the composition and temperature profiles for the column operating at three different sets of operating conditions and two feed locations as given in Table 13-17. The desired product specification is 97 mol % MIPK, no more than 3 mol % MEK, and less than 10 ppm residual water. For Case A (Fig. 13-62*a*), the column profile tracks up the water-free side of the diagram. A pinched zone (area of little change in tray temperature and composition) occurs between the feed tray (tray

TABLE 13-16 Temperature Profile—DRD # Table*

Temp. Profile	DRD #	Temp. Profile	DRD #	Temp. Profile	DRD #	Temp. Profile	DRD #	Temp. Profile	DRD #	Temp. Profile	DRD #
135	001	137524	099	624135	013	1357462	120	2671435	103	6247135	118
1325	014	137526	100	627135	095		121		119		119
1354	015	137542	099	641325	041		116		118		123
1356	016	137562	100		040	1357624	117	2674135	118	6271354	106
1435	004	143256	035	641352	041		116		119	6271435	118
2135	003		036	641735	098		125		103		103
6135	002	143257	078	642135	013	1357642	120	4132567	081		119
13254	017	143275	078	647135	098		117	4135267	081	6274135	103
13256	019	143526	036	714325	056		116	4135627	081		118
13524	017		035	721354	055	1372546	121	4135726	109		119
13526	019	143527	078	721356	050	1372564	117	4135762	109	6413257	085
13542	018	143562	035	721435	053	1375246	121	4137256	109	6413275	085
13546	021		037	724135	053	1375264	117	4137526	109	6413527	085
13547	069	143567	073	726135	049	1375426	121	4137562	109	6413725	107
13562	020	143725	097	741325	056	1375462	121	4173256	109	6413752	107
13564	022	143752	097	742135	053	1375624	117	4173526	109	6417325	107
13567	070	147325	097	746135	052	1375642	117	4173562	109	6417352	107
13725	092	147352	097	761325	051	1432567	089	4213567	082	6421735	123
13752	092	147356	093	761354	054		088	4217356	105	6427135	122
14325	028	174325	056	761435	052		081	4261735	114		123
027		213546	034	762135	049	1432576	088	4267135	122		119
14352	028	213547	072	764135	052	1432756	088		115	6471325	107
14356	031	213564	033	1325467	080	1435267	081		114	6471352	107
14735	091	213567	076	1325647	080		089	4271356	105	6472135	104
21354	026	214356	046	1325746	111		088	4276135	114		122
21356	029	214735	096		124	1435276	088		102		123
21435	009	241356	046		125	1435627	089		115	6714325	061
24135	009	241735	096	1325764	111		081	4613257	086	6741325	061
26135	007	246135	011		124		088	4613275	086	7143256	066
41325	027	247135	096		125	1435672	089	4613527	086	7143526	066
41735	091	261354	044	1352467	080	1435726	109	4613725	107	7143562	065
42135	010	261435	011	1352647	080	1435762	109	4613752	107	7213546	064
46135	005	264135	011	1352746	125	1437256	109	4617325	107	7213564	063
61325	030	267135	095		111	1437526	109	4617352	107	7214356	062
61354	032	413256	036		124	1437562	109	4621735	123	7241356	062
61435	006	413526	036	1352764	124	1473256	109	4627135	123	7246135	058
62135	008	413562	037		111	1473526	109		115	7261354	057
64135	006	413725	097		125	1473562	109		122	7261435	058
72135	047	413752	097	1354267	080	1743256	066	4671325	107	7264135	058
76135	048	417325	097	1354627	080	1743526	066	4671352	107	7413256	066
132546	024	417352	097	1354726	120	1743562	065	4672135	104	7413526	066
132547	075	417356	093		121	2135467	079		122	7413562	065
132564	025	421356	045		112	2135647	079		123	7421356	062
132567	071	421735	096	1354762	121	2135746	108	4761325	060	7426135	058
135246	024	426135	012		120	2135764	108	6132547	084	7461325	060
135247	075	427135	096		112	2143567	090	6135247	084		059
135264	025	461325	040	1356247	080	2147356	105	6135427	084		061
135267	071		042	1356427	080	2413567	090	6135724	110	7461352	059
135426	024	461352	042	1356724	113	2417356	105	6135742	110	7462135	058
135427	075	461735	098		117	2461735	114	6137254	110	7613254	068
135462	023	462135	012		116	2467135	114	6137524	110	7613524	068
135467	074	467135	098	1356742	116		115	6137542	110	7613542	067
135624	025	613254	038		117		118	6143257	085	7614325	061
135627	071	613524	038		113	2471356	105	6143275	085		060
135642	023	613542	039	1357246	121	2476135	115	6143527	085		059
135647	074	613547	077		125		114	6143725	107	7614352	059
135724	099	613725	094		124		102	6143752	107	7621354	057
135726	100	613752	094	1357264	117	2613547	083	6147325	107	7621435	058
135742	099	614325	041		125	2614735	114	6147352	107	7624135	058
135746	101		040		124	2641735	114	6174325	061	7641325	061
135762	100	614735	098	1357426	121	2647135	118	6213547	087		060
135764	101	621354	043		120		119	6214735	123		059
137254	099	614352	041		124		114	6214735	123	7641352	059
137256	100	621435	013			2671354	106	6241735	123	7642135	058

Ternary DRD table lookup procedure:

1. Classify a system by writing down each position number in ascending order of boiling points.
   - A position number is not written down if there is no azeotrope at that position.
   - The resulting sequence of numbers is known as the *temperature profile.*
   - Each temperature profile will have a minimum of three numbers and a maximum of seven numbers.
   - List multiple temperature profiles when you have incomplete azeotropic data.
   - All seven position numbers are shown on the diagram.
2. Using the table, look up the temperature profile(s) to find the corresponding DRD #.

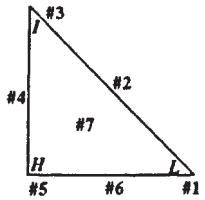

* Table 13-16 and Fig. 13-59 developed by Eric J. Peterson, Eastman Chemical Co.

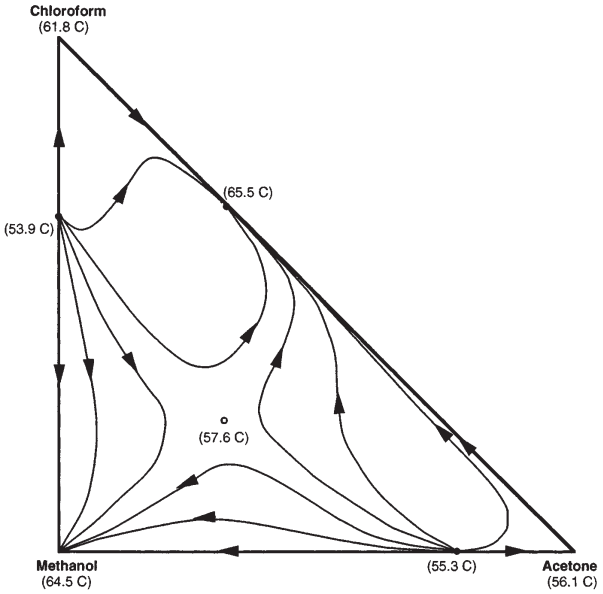

FIG. 13-60 Residue curves for acetone-chloroform-methanol system suggesting a ternary saddle azeotrope.

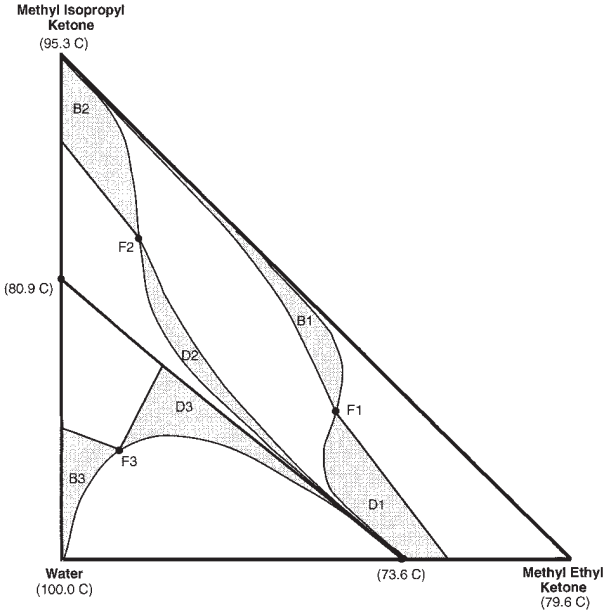

FIG. 13-61 (*Continued*) MEK-MIPK-water system. (*b*) Exact-reachable compositions.

4) and tray 18. The temperature remains constant at about 93°C throughout the pinch. Product specifications are met.

When the feed composition becomes enriched in water, as with Case B, the column profile changes drastically (Fig. 13-62*b*). At the same reflux and boil-up, the column no longer meets specifications. The MIPK product is lean in MIPK and too rich in water. The profile now tracks generally up the left side of Region II. Note also the dramatic change in the temperature profile. A pinched zone still exists between trays 4 and 18, but the tray temperature in the zone has dropped to 80°C (from 93°C). Most of the trays are required to move through the vicinity of the saddle. Typically, pinches (if they exist) occur close to saddles and nodes.

In Case C (Fig. 13-62*c*), increasing the boil-up ratio to 6 brings the MIPK product back within specifications, but the production rate and recovery have dropped off. In addition, the profile has switched back to the right side of the region; the temperatures on trays in the pinched zone (trays 4–18) are back to 93°C. Such a drastic fluctuation in tray temperature with a relatively minor adjustment of the manipulated variable (boil-up in this case), can make control difficult. This is especially true if the control strategy involves maintaining a constant temperature on one of the trays between tray 4 and 18. If a tray is selected that exhibits wide temperature swings, the control system may have a difficult time compensating for disturbances. Such columns are also often difficult to model with a process simulator. Design algorithms often rely on perturbation of a variable (such as reflux or reboil) while checking for convergence of column heat and material balances. In situations where the column profile is altered drastically by minor changes in the perturbed variable, the simulator may be close to a feasible solution, but successive iterations may appear to be very far apart. The convergence routine may continue to oscillate between column profiles and never reach a solution. Likewise, when an attempt is made to design a column to obtain product compositions in different distillation regions, the simulation will never converge.

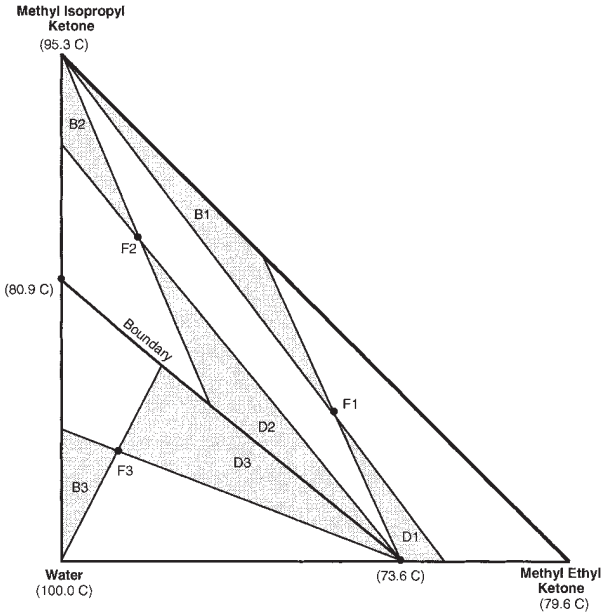

FIG. 13-61 MEK-MIPK-water system. (*a*) Approximate bow-tie reachable compositions by simple distillation.

EXTENSION TO BATCH DISTILLATION

Although batch distillation is covered in a subsequent separate section, it is appropriate to consider the application of RCM and DRD to batch distillation at this time. With a conventional batch-rectification column, a charge of starting material is heated and fractionated, with a vapor product removed continuously. The composition of the vapor product changes continuously and at times drastically as the lighter component(s) are exhausted from the still. Between points of drastic change in the vapor composition, a "cut" is often made. Successive cuts can be removed until the still is nearly dry. The sequence, number, and limiting composition of each cut is dependent on the form of

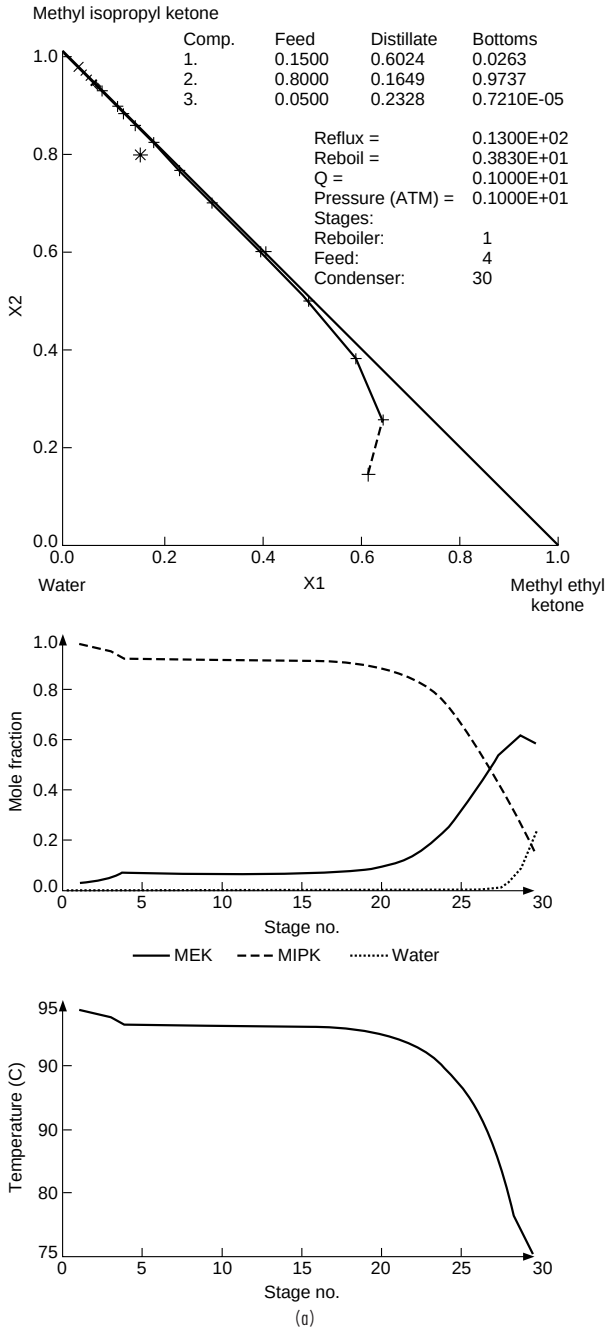

FIG. 13-62 Sensitivity of composition and temperature profiles for MEK-MIPK-water system.

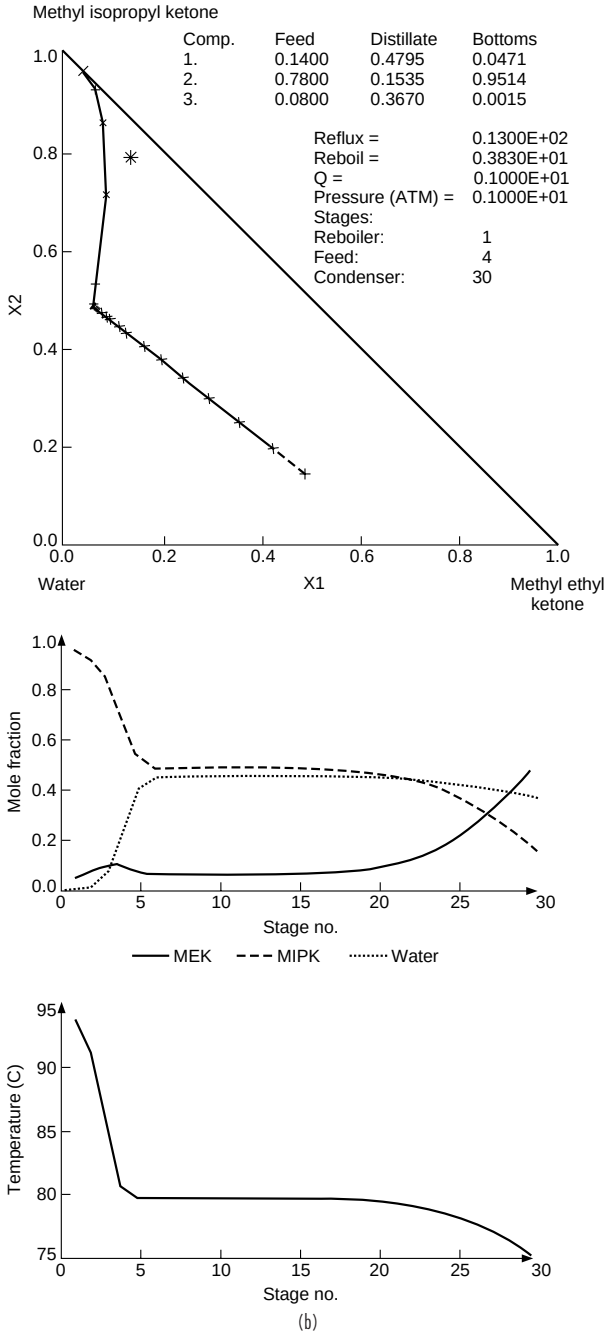

FIG. 13-62 (*Continued*) Sensitivity of composition and temperature profiles for MEK-MIPK-water system.

the residue curve map and the composition of the initial charge to the still. As with continuous distillation operation, the set of reachable products (cuts) for a given charge to a batch distillation is constrained by the residue-curve-map separatrices, which cannot normally be crossed.

Given a sufficient number of stages and reflux, the vapor composition can be made to closely approach direct-mode, continuous operation in which the lowest-boiling species is taken overhead. As the low-boiling component is removed, the still composition moves along a straight material-balance line through the initial feed composition and the low-boiling node away from the initial composition until it reaches the edge of the composition triangle or a separatrix. The path then follows the edge or separatrix to the high-boiling node of the region. At each turn a new cut is taken. Examples for the acetone-chloroform-methanol and MEK-water-MIPK systems are given in Fig. 13-63 [Bernot et al., *Chem. Eng. Sci.*, **45,** 1207 (1990)].

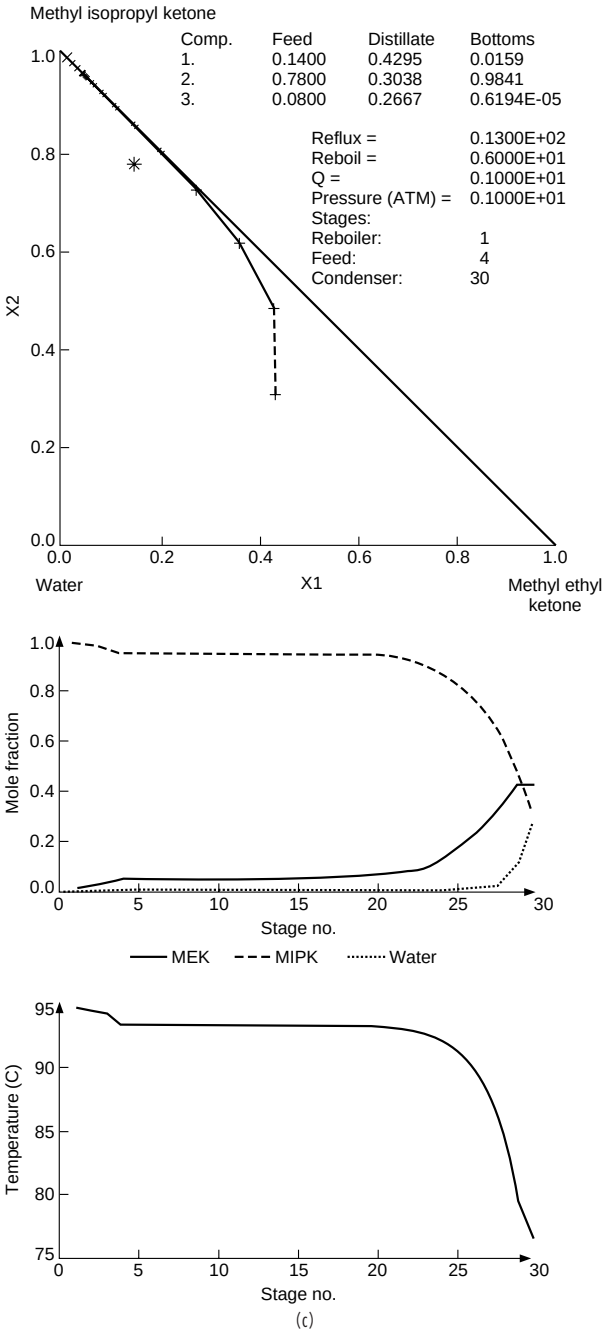

(c)

FIG. 13-62 (*Continued*) Sensitivity of composition and temperature profiles for MEK-MIPK-water system.

AZEOTROPIC DISTILLATION

Introduction The term azeotropic distillation has been applied to a broad class of fractional distillation-based separation techniques in that specific azeotropic behavior is exploited to effect a separation. The agent that causes the specific azeotropic behavior, often called the *entrainer*, may already be present in the feed mixture (a self-entraining mixture) or may be an added mass-separation agent. Azeotropic distillation techniques are used throughout the petrochemical and chemical processing industries for the separation of close-boiling, pinched, or azeotropic systems for which simple distillation is either too expensive or impossible. With an azeotropic feed mixture, presence of the azeotroping agent results in the formation of a more favorable azeotropic pattern for the desired separation. For a close-boiling or pinched feed mixture, the azeotroping agent changes the dimensionality of the system and allows separation to occur along a less-pinched path. Within the general heading of azeotropic distillation techniques, several approaches have been followed in devising azeotropic distillation flowsheets including:

1. Choosing an entrainer to give a residue curve map with specific distillation regions and node temperatures.
2. Exploiting changes in azeotropic composition with total system pressure.
3. Exploiting curvature of distillation region boundaries.
4. Choosing an entrainer to cause azeotrope formation in combination with liquid-liquid immiscibility.

The first three of these are solely VLE-based approaches, involving a series of simple distillation operations and recycles. The final approach also relies on distillation (VLE), but also exploits another physical phenomena, liquid-liquid phase formation (phase splitting), to assist in entrainer recovery. This approach is the most powerful and versatile. Examples of industrial uses of azeotropic distillation grouped by method are given in Table 13-18.

TABLE 13-17 Sets of Operating Conditions for Fig. 13-62

Case	Reflux ratio	Reboil ratio		Feed composition	Distillate composition	Bottoms composition
A	13	3.8	MEK	0.15	0.60	0.03
			MIPK	0.80	0.16	0.97
			water	0.05	0.24	7 ppm
B	13	3.8	MEK	0.14	0.48	0.05
			MIPK	0.78	0.15	0.95
			water	0.08	0.37	20,000 ppm
C	13	6	MEK	0.14	0.43	0.02
			MIPK	0.78	0.30	0.98
			water	0.08	0.27	6.5 ppm

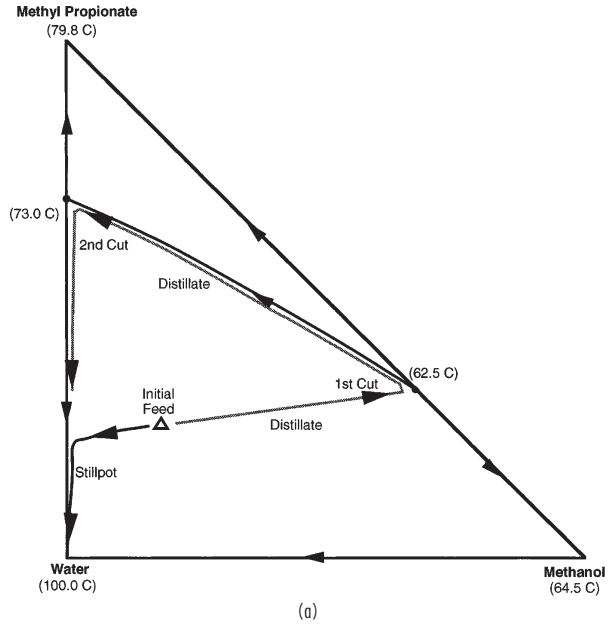

(a)

FIG. 13-63 Batch distillation paths. (*a*) Methanol-methyl propionate-water system.

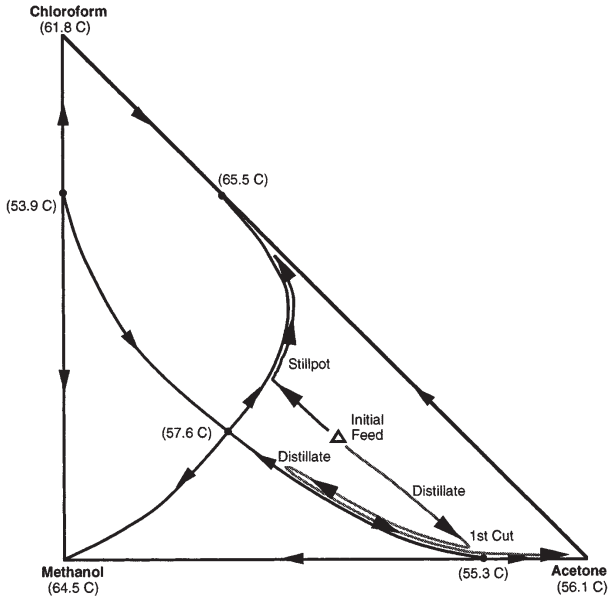

(b)

FIG. 13-63 (*Continued*) Batch distillation paths. (*b*) Methanol-acetone-chloroform system.

The choice of the appropriate azeotropic distillation method and the resulting flowsheet for the separation of a particular mixture are strong functions of the separation objective. For example, it may be desirable to recover all constituents of the original feed mixture as pure components, or only some as pure components and some as azeotropic mixtures suitable for recycle. Not every objective may be obtainable by azeotropic distillation for a given mixture and portfolio of candidate entrainers.

Exploitation of Homogeneous Azeotropes Homogeneous azeotropic distillation refers to a flowsheet structure in which azeotrope formation is exploited or avoided in order to accomplish the desired separation in one or more distillation columns. The azeotropes in the system either do not exhibit two-liquid-phase behavior or the liquid-phase behavior is not or cannot be exploited in the separation sequence. The structure of a particular sequence will depend on the geometry of the residue curve map or distillation region diagram for the feed mixture-entrainer system. Two approaches are possible:

1. Selection of an entrainer such that the desired products all lie within a single distillation region (the products may be pure components or azeotropic mixtures).
2. Selection of an entrainer such that although the desired products lie in different regions, some type of boundary-crossing mechanism is employed.

As mentioned previously, ternary mixtures can be represented by 125 different residue curve maps or distillation region diagrams. However, feasible distillation sequences using the first approach can be developed for breaking homogeneous binary azeotropes by the addition of a third component only for those more restricted systems that do not have a distillation boundary connected to the azeotrope and for which one of the original components is a node. For example, from

TABLE 13-18 Examples of Azeotropic Distillation

System	Type	Entrainer(s)	Remark
	Exploitation of homogeneous azeotropes		
No known industrial examples			
	Exploitation of pressure sensitivity		
THF-water	Minimum boiling azeotrope	None	Alternative to extractive distillation
Methyl acetate-methanol	Minimum boiling azeotrope	None	Element of recovery system for alternative to production of methyl acetate by reactive distillation; alternative to azeotropic, extractive distillation
Alcohol-ketone systems	Minimum boiling azeotropes	None	
Ethanol-water	Minimum boiling azeotrope	None	Alternative to extractive distillation, salt extractive distillation, heterogeneous azeotropic distillation; must reduce pressure to less than 11.5kPa for azeotrope to disappear
	Exploitation of boundary curvature		
Hydrochloric acid-water	Maximum boiling azeotrope	Sulfuric acid	Alternative to salt extractive distillation
Nitric acid-water	Maximum-boiling azeotrope	Sulfuric acid	Alternative to salt extractive distillation
	Exploitation of azeotropy and liquid phase immiscibility		
Ethanol-water	Minimum boiling azeotrope	Cyclohexane, benzene, heptane, hexane, toluene, gasolene, diethyl ether	Alternative to extractive distillation, pressure-swing distillation
Acetic acid-water	Pinched system	Ethyl acetate, propyl acetate, diethyl ether, dichloroethane, butyl acetate	
Butanol-water	Minimum boiling azeotrope	Self-entraining	
Acetic acid-water-vinyl acetate	Pinched, azeotropic system	Self-entraining	
Methyl acetate-methanol	Minimum boiling azeotrope	Toluene, methyl isobutyl ketone	Element of recovery system for alternative to production of methyl acetate by reactive distillation; alternative to extractive pressure-swing distillation
Diethoxymethanol-water-ethanol	Minimum-boiling azeotropes	Self-entraining	
Pyridine-water	Minimum-boiling azeotrope	Benzene	Alternative to extractive distillation
Hydrocarbon-water	Minimum-boiling azeotrope	Self-entraining	

Fig. 13-59, the following eight residue curve maps are suitable for breaking homogeneous minimum-boiling azeotropes: DRD 002, 027, 030, 040, 051, 056, 060, and 061 as collected in Fig. 13-64*a*. To produce the necessary distillation region diagrams, an entrainer must be found that is either: (1) an intermediate boiler that forms no azeotropes (DRD 002), or (2) lowest boiling or intermediate boiling and forms a maximum-boiling azeotrope with the lower-boiling original component. In these cases, the entrainer may also optionally form a minimum-boiling azeotrope with the higher boiling of the original components or a minimum-boiling ternary azeotrope. In all cases, after the addition of the entrainer, the higher-boiling original component is a node and is removed as bottoms product from a first column operated in the indirect mode with the lower-boiling original component recovered as distillate in a second column.

The seven residue curve maps suitable for breaking homogeneous maximum-boiling azeotropes (DRD 028, 031, 035, 073, 078, 088, 089) are shown in Fig. 13-64*b*. In this case, the entrainer must form a minimum-boiling azeotrope with the higher-boiling original component and either a maximum-boiling azeotrope or no azeotrope with the lower-boiling original component. In all cases, after the addition of the entrainer, the lower-boiling original component is a node and is removed as distillate from a first column operated in the direct mode with the higher-boiling original component recovered as bottoms product in a second column.

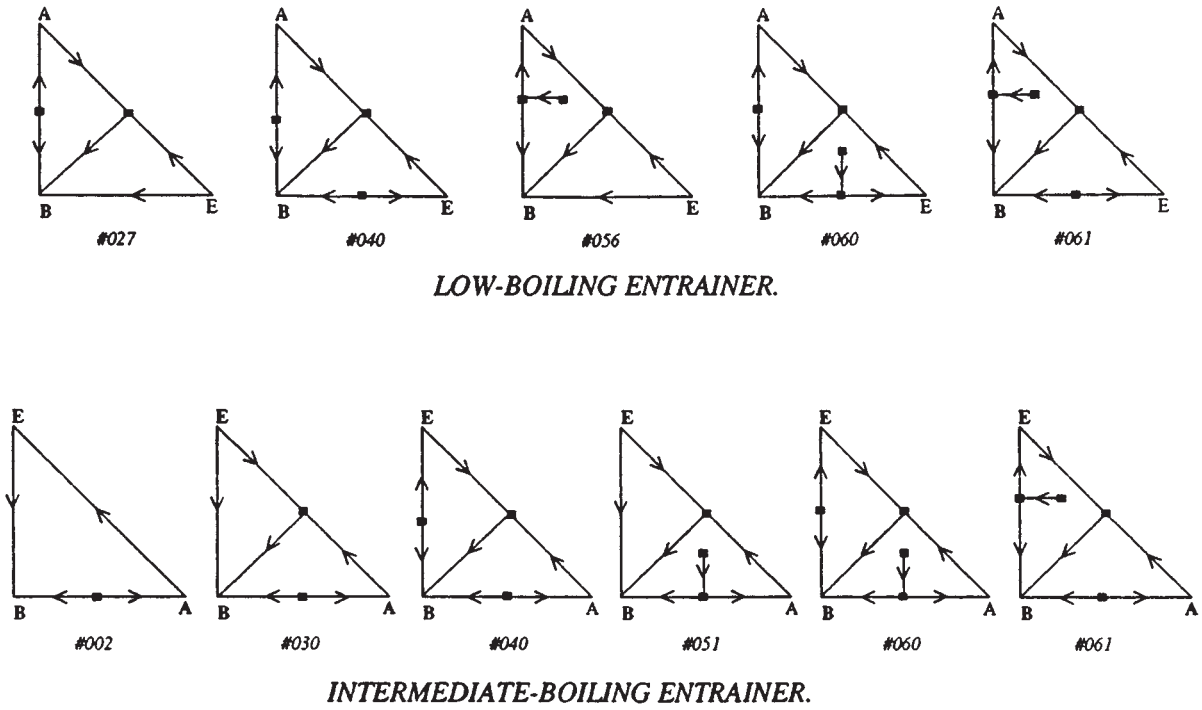

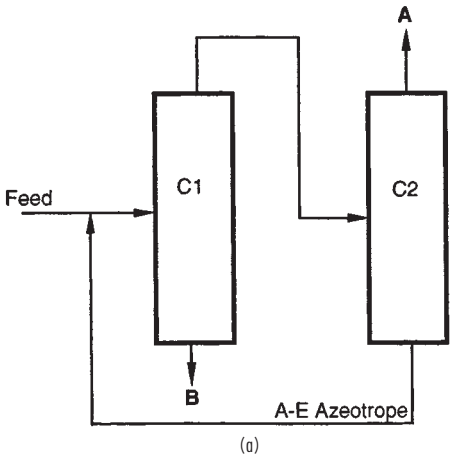

FIG. 13-64 Feasible distillation region diagrams for breaking homogeneous binary azeotrope A-B. (*a*) Low-boiling entrances.

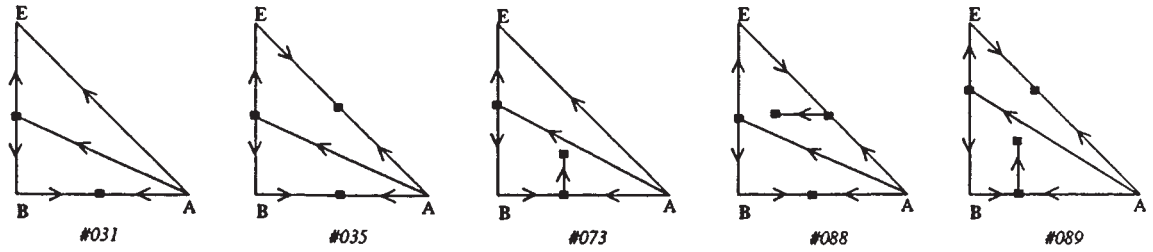

INTERMEDIATE-BOILING ENTRAINER.

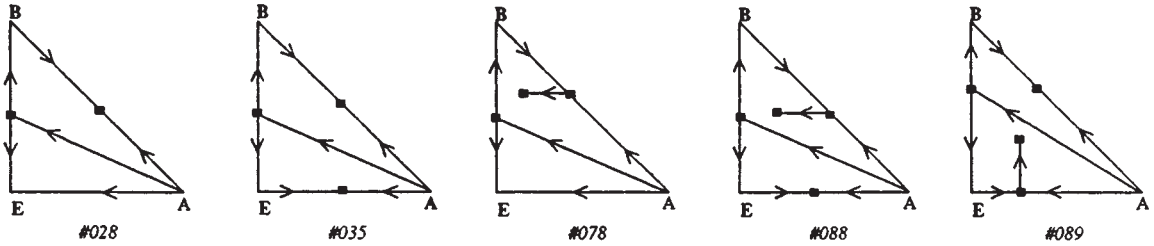

HIGH-BOILING ENTRAINER.

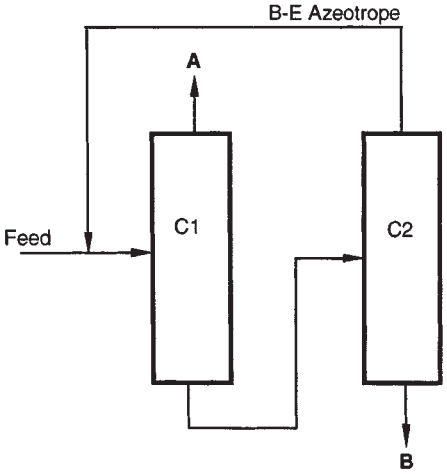

(b)

FIG. 13-64 (*Continued*) Feasible distillation region diagrams for breaking homogeneous binary azeotrope A-B. (*b*) Intermediate-boiling entrances.

In one sense, the restrictions on the boiling point and azeotrope formation of the entrainer act as efficient screening criteria for entrainer selection. Entrainers that do not show appropriate boiling-point characteristics can be discarded without detailed analysis. However, in another sense, although theoretically feasible, the above sequences suffer from serious drawbacks that limit their practical application. DRD 002 requires that the entrainer be an intermediate-boiling component that forms no azeotropes. Unfortunately these are often difficult criteria to meet, as any intermediate boiler will be closer-boiling to both of the original components and, therefore, will be more likely to be at least pinched or even form azeotropes. The remaining feasible distillation region diagrams require that the entrainer form a maximum-boiling azeotrope with the lower-boiling original component. Because maximum-boiling azeotropes are relatively rare, finding a suitable entrainer may be difficult.

For example, the dehydration of organics that form homogeneous azeotropes with water is a common industrial problem. It is extremely difficult to find an intermediate-boiling entrainer that also does not form an azeotrope with water. Furthermore, the resulting separation is likely to be close-boiling or pinched throughout most of the column, requiring a large number of stages. However, consider the separation of valeric acid (187.0°C) and water. This system exhibits an azeotrope

(99.8°C). Ignoring for the moment potentially severe corrosion problems, formic acid (100.7°C), which is an intermediate boiler and which forms a maximum-boiling azeotrope with water (107.1°C), is a candidate entrainer (DRD 030, Fig. 13-65*a*). In the conceptual sequence shown in Fig. 13-65*b*, a recycle of the formic acid-water maximum-boiling azeotrope is added to the original valeric acid-water feed, which may be of any composition. Using the indirect mode of operation, high-boiling node valeric acid is removed in high purity and high recovery as bottoms in a first column, which by mass balance produces a formic acid-water distillate. This binary mixture is fed to a second column that produces pure water as distillate and the formic acid-water azeotrope as bottoms for recycle to the first column. The inventory of formic acid is an important optimization variable in this theoretically feasible but difficult separation scheme.

Exploitation of Pressure Sensitivity The breaking of homogeneous azeotropes that are part of a distillation boundary (that is, into products in different distillation regions) requires that the boundary be "crossed." This may be done by mixing some external stream with the original feed stream in one region such that the resulting composition is in another region for further processing. However, the external stream must be completely regenerated, and mass-balance observed. For example, it is not possible to break a homogeneous binary azeotrope simply by adding one of the products to cross the azeotropic composition.

The composition of many azeotropes varies with the system pressure (Horsley, *Azeotropic Data-III*, American Chemical Society, Washington, 1983 and Gmehling et al., *Azeotropic Data*, VCH Publishers, Deerfield Beach, Florida, 1994). This effect can be exploited to separate azeotropic mixtures by so-called pressure-swing distillation if at some pressure the azeotrope simply disappears, as for example does the ethanol-water azeotrope at pressures below 11.5 kPa. However, pressure sensitivity can still be exploited if the azeotropic composition and related distillation boundary change sufficiently over a moderate change in total system pressure. A composition in one region under one set of conditions, could be in a different region under a different set of conditions. A two-column sequence for separating a binary maximum-boiling azeotrope is shown in Fig. 13-66 for a system in which the azeotropic composition at pressure P1 is richer in component B than the azeotropic composition at pressure P2. The first column, operating at pressure P1, is fed a mixture of fresh feed and recycle stream from the second column such that the overall composition lies on the A side of the azeotropic composition at P1. Pure component A is recovered as distillate and a mixture near the azeotropic composition is produced as bottoms. The pressure of this bottoms stream is changed to P2 and fed to the second column. This feed is on the B side of the azeotropic composition at P2. Pure component B is now recovered as the distillate and the azeotropic bottoms composition is recycled to the first column. An analogous flowsheet can be used for separating binary-homogeneous minimum-boiling azeotropes. In this case the pure components are recovered as bot-

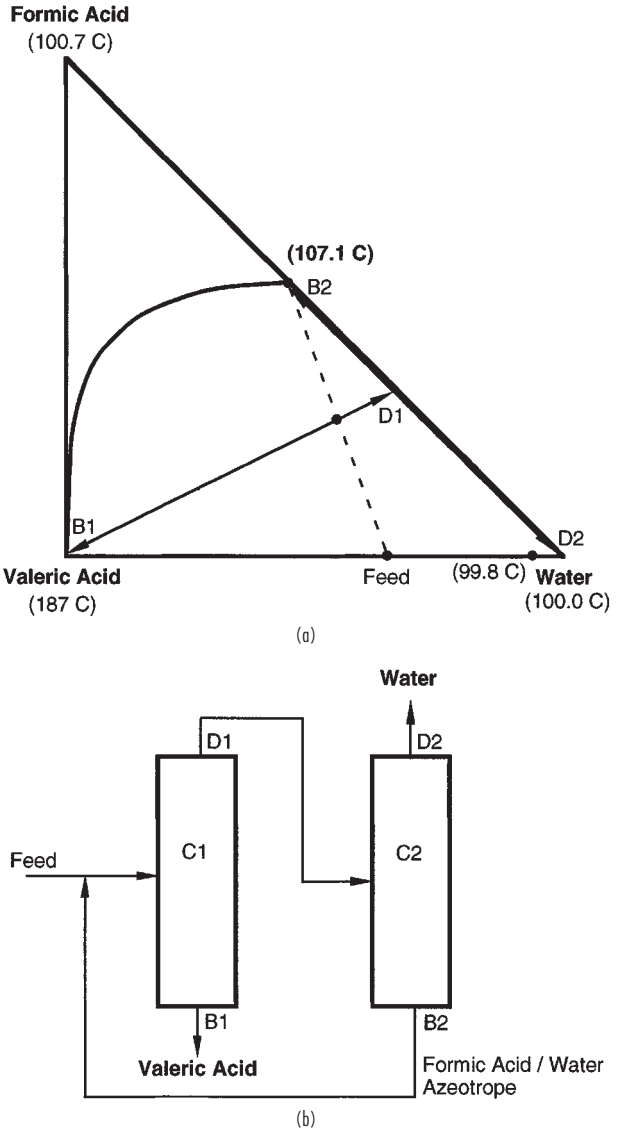

FIG. 13-65 Valeric acid-water separation with formic acid. (*a*) Mass balances on distillation region diagram. (*b*) Conceptual sequence.

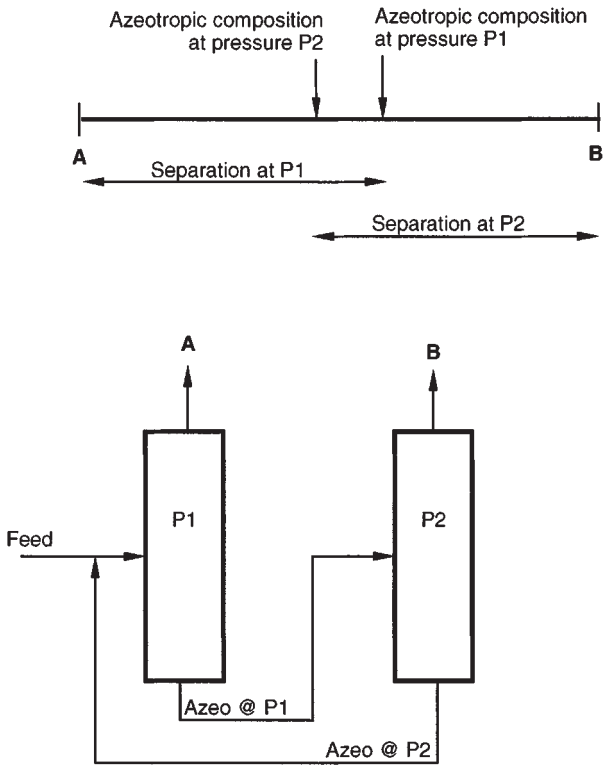

FIG. 13-66 Conceptual sequence for separating maximum-boiling binary azeotrope with pressure swing distillation.

toms in both columns and the distillate from each column is recycled to the other column.

For pressure-swing distillation to be practical, the azeotropic composition must vary at least 5 percent, (preferably 10 percent or more) over a moderate pressure range (not more than ten atmospheres between the two pressures). With a very large pressure range, refrigeration may be required for condensation of the low-pressure distillate or an impractically high reboiler temperature may result in the high-pressure column. The smaller the variation of azeotrope composition over the pressure range, the larger will be the recycle streams between the two columns. In particular, for minimum-boiling azeotropes, the pressure-swing distillation approach requires high energy usage and high capital costs (large-diameter columns) because both recycled azeotropic compositions must be taken overhead. Often one lobe of an azeotropic VLE diagram is pinched regardless of pressure; and, therefore, one of the columns will require a large number of stages to produce the corresponding pure-component product.

General information on pressure-swing distillation can be found in Van Winkle (*Distillation,* McGraw-Hill, New York, 1967), Wankat (*Equilibrium-Staged Separations,* Elsevier, New York, 1988), and Knapp and Doherty [*Ind. Eng. Chem. Res.*, **31,** 346 (1992)]. Only a relatively small fraction of azeotropes are sufficiently pressure sensitive for a pressure-swing process to be economical. Some applications include the minimum-boiling azeotrope tetrahydrofuran-water [Tanabe et al., U.S. Patent 4,093,633 (1978)], and maximum-boiling azeotropes of hydrogen chloride-water and formic acid-water (Horsley, *Azeotropic Data-III,* American Chemical Society, Washington, 1983). Since separatrices also move with pressure-sensitive azeotropes, the pressure-swing principle can also be used for overcoming distillation boundaries in multicomponent azeotropic mixtures.

Exploitation of Boundary Curvature A second approach to boundary crossing exploits boundary curvature in order to produce compositions in different distillation regions. When distillation boundaries exhibit extreme curvature, it may be possible to design a column such that the distillate and bottoms are on the same residue curve in one distillation region, while the feed (which is not required to lie on the column-composition profile) is in another distillation region. In order for such a column to meet material-balance constraints (i.e., bottom, distillate, feed on a straight line), the feed must be located in a region where the boundary is concave.

As an example, Van Dongen [Ph.D. Thesis, University of Massachusetts, (1983)] considered the separation of a methanol-methyl acetate mixture, which forms a homogeneous azeotrope, using *n*-hexane as an entrainer. The separatrices for this system (Fig. 13-67*a*) are somewhat curved. A separation sequence that exploits this boundary curvature is shown in Fig. 13-67*b.* Recycled methanol-methyl acetate binary azeotrope and methanol-methyl acetate-hexane ternary azeotrope are added to the original feed F0 to produce a net-feed composition F1 for column C1 designed to lie on a line between pure methanol and the curved part of the boundary between Regions I and II. C1 is operated in the indirect mode producing the high-boiling node methanol as a bottoms product, and by mass balance, a distillate near the curved boundary. The distillate, although in Region I, becomes feed F2 to column C2 which is operated in the direct mode entirely in Region II, producing the low-boiling node ternary azeotrope as distillate and by mass balance, a methanol-methyl acetate mixture as bottoms. This bottoms mixture is on the opposite side of the methanol-methyl acetate azeotrope at the original feed F0. The bottoms from C2 is finally fed to binary distillation column C3, which produces pure methyl acetate as bottoms product and the methanol-methyl acetate azeotrope as distillate. The distillates from C2 and C3 are recycled to C1. The distillate and bottoms compositions for C2 lie on the same residue curve, and the composition profile lies entirely within Region II, even though its feed composition is in Region I.

Exploitation of boundary curvature for breaking azeotropes is very similar to exploiting pressure sensitivity from a mass-balance point of view, and suffers from the same disadvantages. Separation schemes have large recycle flows, and in the case of minimum-boiling azeotropes, the recycle streams are distillates. However, in the case of maximum-boiling azeotropes, these recycles are underflows and

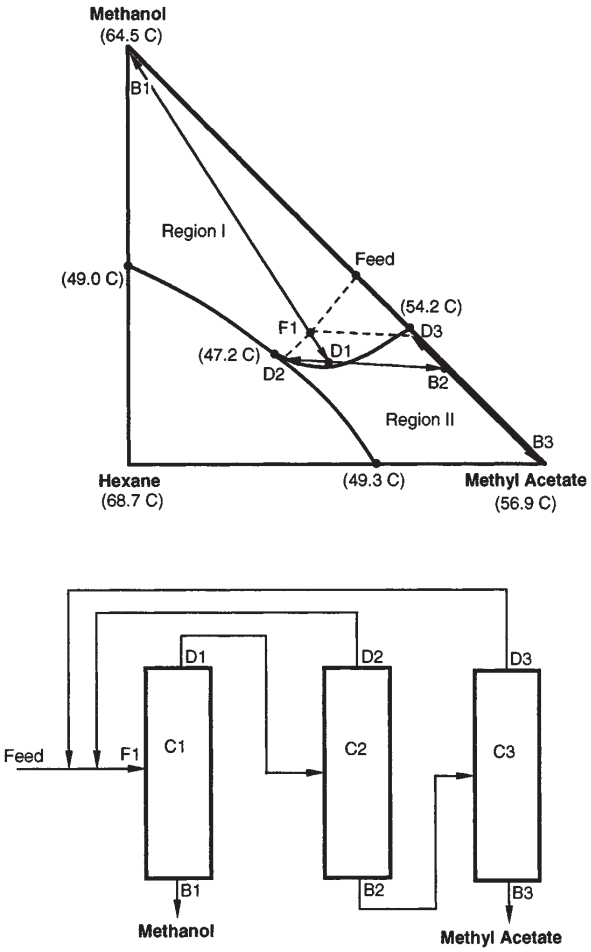

FIG. 13-67 Separation of methanol-methyl acetate by exploitation of distillation boundary curvature.

the economics are improved. One such application, illustrated in Fig. 13-68, is the separation of the nitric acid-water azeotrope by adding sulfuric acid. Recycled sulfuric acid is added to a nitric acid-water mixture near the azeotropic composition to produce a net feed in Region I. The first column, operated in the direct mode, produces a nitric-acid distillate and a bottoms product, by mass balance, near the distillation boundary. In this case, sulfuric acid associates with water so strongly and the separatrix is so curved and nearly tangent to the water-sulfuric acid edge of the composition diagram that the second column operating in the indirect mode in Region II, producing sulfuric acid as bottoms product also produces a distillate close enough to the water specification that a third column is not required (Thiemann et al., in *Ullmann's Encyclopedia of Industrial Chemistry,* Fifth Edition, Volume **A17,** VCH Verlagsgesellschaft mbH, Weinheim, 1991).

Exploitation of Azeotropy and Liquid-Phase Immiscibility One powerful and versatile separation approach exploits several physical phenomena simultaneously including enhanced vapor-liquid behavior, where possible, and liquid-liquid behavior to bypass difficult distillation separations. For example, the overall separation of close-boiling mixtures can be made easier by the addition of an entrainer that forms a heterogeneous minimum-boiling azeotrope with one (generally the lower-boiling) of the key components. Two-liquid-phase formation provides a means of breaking this azeotrope, thus simplifying the entrainer recovery and recycle process. Moreover,

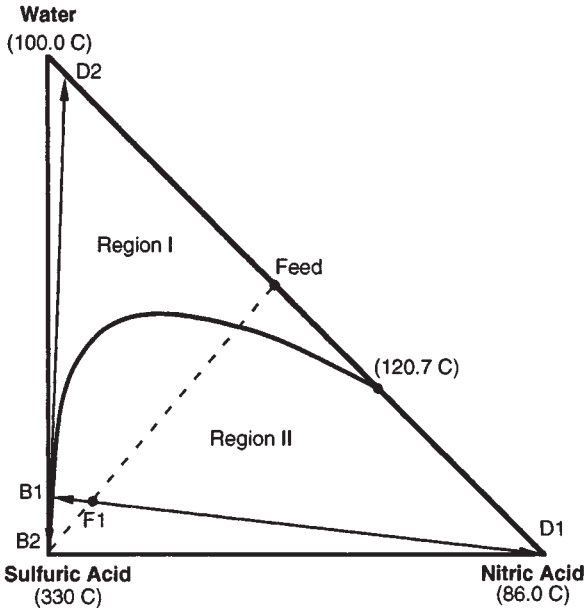

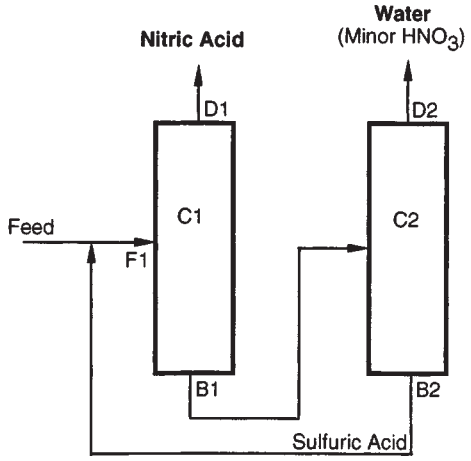

FIG. 13-68 Separation of nitric acid-water system with sulfuric acid in a two-column sequence exploiting extreme boundary curvature.

since liquid-liquid tie lines are unaffected by distillation boundaries (and the separate liquid phases are often located in different distillation regions), liquid-liquid phase splitting is a powerful mechanism for crossing distillation boundaries. The phase separator is usually a simple decanter, but sometimes a multistage extractor is substituted. The decanter or extractor can also be replaced by some other non-VLE-based separation technique such as membrane permeation, chromatography, adsorption, or crystallization. In addition, sequences may include additional separation operations (distillations or other methods) for preconcentration of the feed mixture, entrainer recovery, and final-product purification.

The simplest case of combining VLE and LLE is the separation of a binary heterogeneous azeotropic mixture. One example is the dehydration of 1-butanol, a self-entraining system, in which butanol (117.7°C) and water form a minimum-boiling heterogeneous azeotrope (93.0°C). As shown in Fig. 13-69, the fresh feed may be added to either column C1 or C2, depending on whether the feed is on the organic-rich side or the water-rich side of the azeotrope. The feed may also be added into the decanter directly if it doesn't move the overall composition of the decanter outside of the two-liquid-phase region. Column C1 produces anhydrous butanol as a bottoms product and a composition close to the butanol-water azeotrope as the distillate. After condensation, the azeotrope rapidly phase separates in the decanter. The upper layer, consisting of 78 wt % butanol, is refluxed totally to C1 for further butanol recovery. The water layer, consisting of 92 wt % water, is fed to C2. This column produces pure water as a bottoms product and, again, a composition close to the azeotrope as distillate for recycle to the decanter. Sparged steam may be used in C2, saving the cost of a reboiler. A similar flowsheet can be used for dehydration of hydrocarbons and other species that are largely immiscible with water.

A second example of the use of liquid-liquid immiscibilities in an azeotropic-distillation sequence is the separation of the ethanol-water minimum-boiling azeotrope. For this separation, a number of entrainers have been proposed, which are usually chosen to be immiscible with water, form a ternary minimum-boiling (preferably heterogeneous) azeotrope with ethanol and water (and, therefore, usually also binary minimum-boiling azeotropes with both ethanol and water). All such systems correspond to DRD 058, although the labeling of the vertices depends on whether the entrainer is lower boiling than ethanol, intermediate boiling, or higher boiling than water. The residue curve map for the case for cyclohexane as entrainer was illustrated in Fig. 13-58c. One three-column distillation sequence is shown in Fig. 13-70. Other two-, three-, or four-column sequences have been described by Knapp and Doherty (*Kirk-Othmer Encyclopedia of Chemical Technology,* Fourth Edition, Vol. **8,** Wiley, New York, 1993).

Fresh aqueous ethanol feed is first preconcentrated to nearly the azeotropic composition in column C3, while producing a water bottoms product. The distillate from C3 is sent to column C1, which is refluxed with the entire organic (entrainer-rich) layer, recycled from a decanter. Mixing of these two streams is the key to this sequence as it allows the overall feed composition to cross the distillation boundary into Region II. column C1 is operated to recover pure high-boiling node ethanol as a bottoms product and to produce a distillate close to the ternary azeotrope. If the ternary azeotrope is heterogeneous (as it

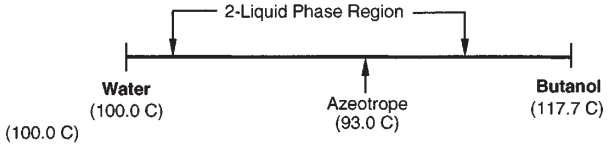

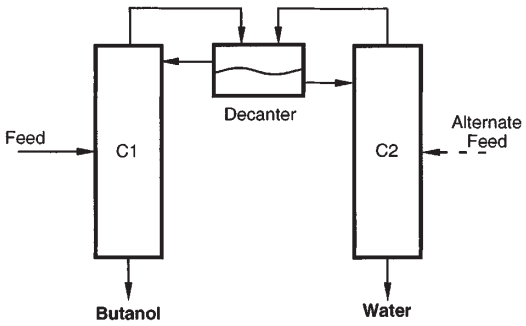

FIG. 13-69 Separation of butanol-water with heterogeneous azeotropic distillation.

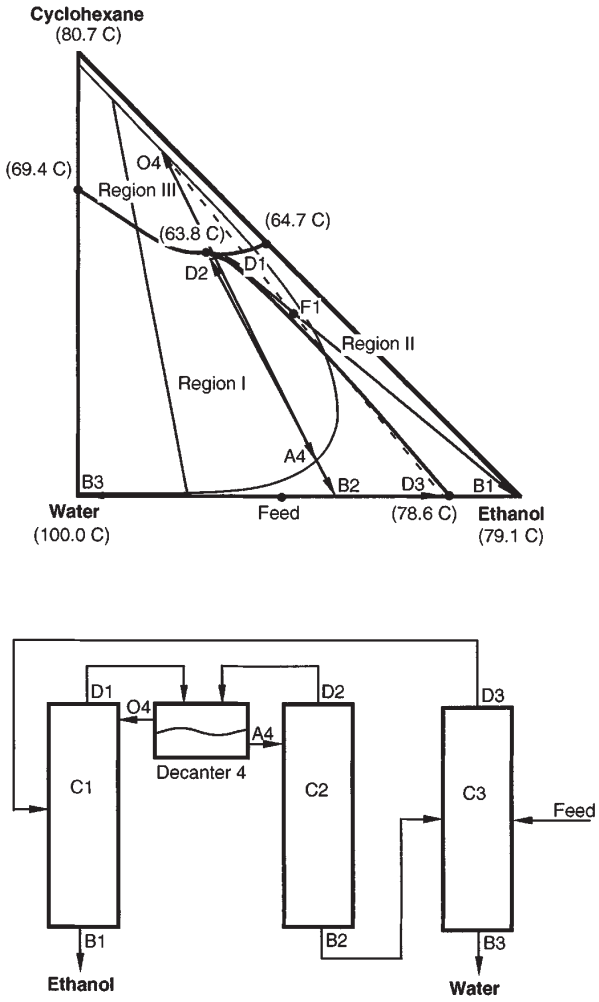

FIG. 13-70 Three-column sequence for ethanol dehydration with cyclohexane (operating column C2 in the direct mode).

is in this case), it is sent to the decanter for phase separation. If the ternary azeotrope is homogeneous (as it is in the alternative case of ethyl acetate as the entrainer) the distillate is first mixed with water before being sent to the decanter. The inventory of entrainer is adjusted to allow C1 to operate essentially between two nodes, although such practice, as discussed previously, is relatively susceptible to instabilities from minor feed or reflux perturbations. Refluxing a fraction of the water-rich decanter layer results in an additional degree of freedom to mitigate against variability in the feed composition. The remaining portion of the water layer from the decanter is stripped of residual cyclohexane in column C2, which may be operated either in the direct mode (producing low-boiling node ternary azeotrope as distillate and, by mass balance, an ethanol-water bottoms for recycle to C3 or, in the indirect mode (producing high-boiling node water as bottoms and, by mass balance, a ternary distillate near the distillation boundary. The distillate may be recycled to the decanter, the top of C2, or C2 feed.

Design and Operation of Azeotropic Distillation Columns Simulation and design of azeotropic distillation columns is a difficult computational problem, but one that is readily handled, in most cases, by widely available commercial computer process simulation packages [Glasscock and Hale, *Chem. Eng.,* **101**(11), 82 (1994)]. Most simulators are capable of modeling the steady state and dynamic behavior of both homogeneous azeotropic distillation systems and those systems involving two-liquid phase behavior within the column, if accurate thermodynamic data and activity-coefficient or equation-of-state models are available. However, VLE and VLLE estimated or extrapolated from binary data or predicted from such methods as UNIFAC may not be able to accurately locate boundaries and predict the extent of liquid immiscibilities. Moreover, different activity-coefficient models fit to the same experimental data often give very different results for the shape of boundaries and liquid-liquid regions. Therefore the design of separation schemes relying on boundary curvature should not be attempted unless accurate, reliable experimental equilibrium data are available.

Two liquid phases can occur within a column in the distillation of heterogeneous systems. Older references, for example Robinson and Gilliland (*Elements of Fractional Distillation*, McGraw-Hill, New York, 1950) state that the presence of two liquid phases in a column should be avoided as much as possible because performance may be reduced. However, more recent studies indicate that problems with two-phase flow have been overstated [Herron et al., *AIChE J.* **34,** 1267 (1988) and Harrison, *Chem. Eng. Prog.,* **86**(11), 80 (1990)]. Based on case-history data and experimental evidence, there is no reason to expect unusual capacity or pressure-drop limitations, and standard correlations for these parameters should give acceptable results. Because of the violent nature of the gas/liquid/liquid mixing on trays, trayed column efficiencies are relatively unaffected by liquid-liquid phase behavior. The falling-film nature of gas/liquid/liquid contact in packing, however, makes that situation more uncertain. Reduced efficiencies may be expected in systems where one of the keys distributes between the phases.

EXTRACTIVE DISTILLATION

Introduction Extractive distillation is a partial vaporization process in the presence of a miscible, high-boiling, non-volatile mass-separation agent, normally called the *solvent*, which is added to an azeotropic or nonazeotropic feed mixture to alter the volatilities of the key components without the formation of any additional azeotropes. Extractive distillation is used throughout the petrochemical- and chemical-processing industries for the separation of close-boiling, pinched, or azeotropic systems for which simple single-feed distillation is either too expensive or impossible. It can also be used to obtain products which are residue-curve saddles, a task not generally possible with single-feed distillation.

Fig. 13-71 illustrates the classical implementation of an extractive distillation process for the separation of a binary system. The configuration consists of a double-feed extractive column and a solvent-recovery column. The components *A* and *B* may have a low relative volatility or form a minimum-boiling azeotrope. The solvent is introduced into the extractive column at a high concentration a few stages below the condenser, but above the primary-feed stage. Since the solvent is chosen to be nonvolatile it remains at a relatively high concentration in the liquid phase throughout the sections of the column below the solvent-feed stage.

One of the components, *A* (not necessarily the most volatile species of the original mixture), is withdrawn as an essentially pure distillate stream. Because the solvent is nonvolatile, at most a few stages above the solvent-feed stage are sufficient to rectify the solvent from the distillate. The bottoms product, consisting of *B* and the solvent, is sent to the recovery column. The distillate from the recovery column is pure *B*, and the solvent-bottoms product is recycled back to the extractive column.

Extractive distillation works by the exploitation of the selective solvent-induced enhancements or moderations of the liquid-phase nonidealities of the components to be separated. The solvent selectively alters the activity coefficients of the components being separated. To do this, a high concentration of solvent is necessary. Several features are essential:

1. The solvent must be chosen to affect the liquid-phase behavior of the key components differently, otherwise no enhancement in separability will occur.

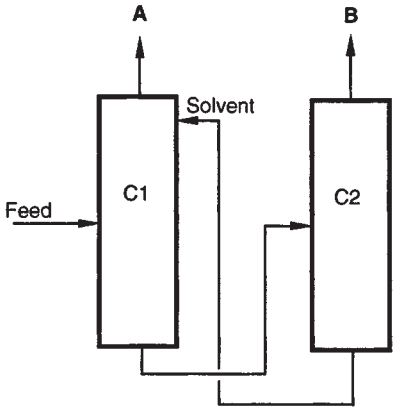

FIG. 13-71 Typical extracting distillation sequence. Component *A* is less associated with the solvent.

2. The solvent must be higher boiling than the key components of the separation and must be relatively nonvolatile in the extractive column, in order to remain largely in the liquid phase.
3. The solvent should not form additional azeotropes with the components in the mixture to be separated.
4. The extractive column must be a double-feed column, with the solvent feed above the primary feed; the column must have an extractive section.

As a consequence of these restrictions, separations of binary systems by extractive distillation correspond to only two possible three-component distillation region diagrams, depending on whether the binary system is pinched or close boiling (DRD 001), or forms a minimum-boiling azeotrope (DRD 003). The addition of high-boiling solvents can also facilitate the breaking of maximum-boiling azeotropes (DRD 014), for example splitting the nitric acid-water azeotrope with sulfuric acid. However, as explained in the section on azeotropic distillation, this type of separation might better be characterized as exploitation of extreme boundary curvature rather than extractive distillation, as the important liquid-phase activity-coefficient modification occurs in the bottom of the column. Although many references show sulfuric acid being introduced high in the column, two separate feeds are in fact not required.

Examples of industrial uses of extractive distillation grouped by distillation region diagram type are given in Table 13-19. Achievable compositions in dual-feed extractive distillation columns are very different from the bow-tie regions for single-feed columns. Either pure component (the higher-boiling of which is a saddle) for close-boiling systems, and either pure component (both of which are saddles) for minimum-boiling azeotropic systems can be obtained as distillate.

Extractive distillation is generally only applicable to systems in which the components to be separated contain one or more different functional groups. Extractive distillation is usually uneconomical for separating stereoisomers, homologs, or homology or structural isomers containing the same functional groups, unless the differences in structure also contribute to significantly different polarity, dipole moment, or hydrophobic character. One such counter-example is the separation of ethanol from isopropanol, where the addition of methyl benzoate raises the relative volatility from 1.09 to 1.27 [Berg et al., *Chem. Eng. Comm.*, **66,** 1 (1988)].

Solvent Effects in Extractive Distillation In the distillation of ideal or nonazeotropic mixtures, the component with the lowest pure-component boiling point is always recovered primarily in the distillate, while the highest boiler is recovered primarily in the bottoms. The situation is not as straightforward for an extractive-distillation operation. With some solvents, the component with the lower pure-component boiling point will be recovered in the distillate as in ordinary distillation. For another solvent, the expected order is reversed, and the component with the higher pure-component boiling point will be recovered in the distillate. The possibility that the expected relative volatility may be reversed by the addition of solvent is entirely a function of the way the solvent interacts with and modifies the activity coefficients and, thus, the volatility of the components in the mixture.

In normal applications of extractive distillation (i.e., pinched, close-boiling, or azeotropic systems), the relative volatilities between the light and heavy key components will be unity or close to unity. Assuming an ideal vapor phase and subcritical components, the relative volatility between the light and heavy keys of the desired separation can be written as the product of the ratios of the pure-component vapor pressures and activity-coefficient ratios whether the solvent is present or not:

$$\alpha_{L,H} = \left(\frac{P_L^{sat}}{P_H^{sat}}\right)\left(\frac{\gamma_L}{\gamma_H}\right) \tag{13-127}$$

where *L* and *H* denote the lower-boiling and higher-boiling pure component, respectively.

The addition of the solvent has an indirect effect on the vapor-pressure ratio. Because the solvent is high boiling and is generally added at a relatively high mole ratio to the primary-feed mixture, the temperature of an extractive-distillation process tends to increase over that of a simple distillation of the original binary mixture (unless the system pressure is lowered). The result is a corresponding increase in the vapor pressure of both key components. However, the rise in operating temperature generally *does not* result in a significant modification of the relative volatility, because the ratio of vapor pressures often remains approximately constant, unless the slopes of the vapor-pressure curves differ significantly. The ratio of the vapor pressures typically remains greater than unity, following the "natural" volatility of the system.

Since activity coefficients have a strong dependence on composition, the effect of the solvent on the activity coefficients is generally more pronounced. However, the magnitude and direction of change is highly dependent on the solvent concentration, as well as the liquid-phase interactions between the key components and the solvent. The solvent acts to lessen the nonidealities of the key component whose liquid-phase behavior is similar to the solvent, while enhancing the nonideal behavior of the dissimilar key.

The solvent and the key component that show most similar liquid-phase behavior tend to exhibit little molecular interactions. These components form an ideal or nearly ideal liquid solution. The activity coefficient of this key approaches unity, or may even show negative deviations from Raoult's law if solvating or complexing interactions occur. On the other hand, the dissimilar key and the solvent demonstrate unfavorable molecular interactions, and the activity coefficient of this key increases. The positive deviations from Raoult's law are further enhanced by the diluting effect of the high-solvent concentration, and the value of the activity coefficient of this key may approach the infinite dilution value, often a very large number.

The natural relative volatility of the system is enhanced when the activity coefficient of the lower-boiling pure component is increased by the solvent addition (γ_L/γ_H increases and $P_L^{sat}/P_H^{sat} > 1$). In this case, the lower-boiling pure component will be recovered in the distillate as expected. In order for the higher-boiling pure component to be recovered in the distillate, the addition of the solvent must decrease the ratio γ_L/γ_H such that the product of the γ_L/γ_H and P_L^{sat}/P_H^{sat} (i.e., $\alpha_{L,H}$) in the presence of the solvent is less than unity. Generally, the latter is more difficult and requires higher solvent-to-feed ratios. It is normally better to select a solvent that forces the lower-boiling component overhead.

The effect of solvent concentration on the activity coefficients of the key components is shown in Fig. 13-72 for the system methanol-acetone with either water or methylisopropylketone (MIPK) as solvent. For an initial-feed mixture of 50 mol % methanol and 50 mol % acetone (no solvent present), the ratio of activity coefficients of methanol and acetone is close to unity. With water as the solvent, the activity coefficient of the similar key (methanol) rises slightly as the solvent concentration increases, while the coefficient of acetone approaches the relatively large infinite-dilution value. With methylisopropylketone as the solvent, acetone is the similar key and its activity coefficient drops toward unity as the solvent concentration increases, while the activity coefficient of the methanol increases.

TABLE 13-19 Examples of Extractive Distillation, Salt Extractive Distillation

System	Type	Solvent(s)	Remark
Ethanol-water	Minimum-boiling azeotrope	Ethylene glycol, acetate salts for salt process	Alternative to azeotropic distillation, pressure swing distillation
Benzene-cyclohexane	Minimum-boiling azeotrope	Aniline	
Ethyl acetate-ethanol	Minimum-boiling azeotrope	Higher esters or alcohols, aromatics	Process similar for other alcohol-ester systems
THF-water	Minimum-boiling azeotrope	Propylene glycol	Alternative to pressure swing distillation
Acetone-methanol	Minimum-boiling azeotrope	Water, aniline, ethylene glycol	
Isoprene-pentane	Minimum-boiling azeotrope	Furfural, DMF, acetonitrile	
Pyridine-water	Minimum-boiling azeotrope	Bisphenol	
Methyl acetate-methanol	Minimum-boiling azeotrope	Ethylene glycol monomethyl ether	Element of recovery system for alternative to production of methyl acetate by reactive distillation; alternative to azeotropic, pressure, swing distillation
C4 alkenes/C4 alkanes/ C4 dienes	Close-boiling and minimum-boiling azeotropes	Furfural, DMF, acetonitrile, *n*-methylpyrolidone	
C5 alkenes/C5 alkanes/ C5 dienes	Close-boiling and minimum-boiling azeotropes	Furfural, DMF, acetonitrile, *n*-methylpyrolidone	
Heptane isomers-cyclohexane	Close-boiling	Aniline, phenol	
Heptane isomers-toluene	Close-boiling and minimum-boiling azeotropes	Aniline, phenol	
Vinyl acetate-ethyl acetate	Close-boiling	Phenol, aromatics	Alternative to simple distillation
Propane-propylene	Close-boiling	Acrylonitrile	Alternative to simple distillation, adsorption
Ethanol-isopropanol	Close-boiling	Methyl benzoate	Alternative to simple distillation
Hydrochloric acid-water	Maximum-boiling azeotrope	Sulfuric acid, calcium chloride for salt process	Sulfuric acid process relies heavily on boundary curvature
Nitric acid-water	Maximum-boiling azeotrope	Sulfuric acid, magnesium nitrate for salt process	Sulfuric acid process relies heavily on boundary curvature

Several methods are available for determining whether the lower- or higher-boiling pure component will be recovered in the distillate. For a series of solvent concentrations, the *y-x* phase diagram of the low-boiling and high-boiling keys can be plotted on a solvent-free basis. At a particular solvent concentration (dependent on the selected solvent and keys), the azeotropic point in the pseudobinary plot disappears at one of the pure component corners. The component corresponding to the corner where the azeotrope disappears is recovered in the distillate [Knapp and Doherty, in *Kirk-Othmer Encyclopedia of Chemical Technology,* Fourth Edition, Vol. **8,** Wiley, New York (1993)]. LaRoche et al. [*Can. J. Chem. Eng.*, **69,** 1302 (1991)] present a related method in which the $\alpha_{L,H} = 1$ line is plotted on the ternary composition diagram. If the $\alpha_{L,H} = 1$ line intersects the lower-boiling pure component-solvent face, then the lower-boiling component will be recovered in the distillate and vice versa if the $\alpha_{L,H} = 1$ line intersects the higher-boiling pure component-solvent face. A very simple method, if a rigorous residue curve map is available, is to examine the shape and inflection of the residue curves as they approach the pure solvent vertex. Whichever solvent-key component face the residue curves predominantly tend toward as they approach the solvent vertex is the key component that will be recovered in the bottoms with the solvent. In Fig. 13-73*a*, all residue curves approaching the water (solvent) vertex are inflected toward the methanol-water face, with the result that methanol will be recovered in the bottoms and acetone in the distillate. Alternatively, with MIPK as the solvent the residue curves (Fig. 13-73*b*), all residue curves show inflection toward the acetone-MIPK face, indicating that acetone will be recovered in the bottoms and methanol in the distillate.

Extractive Distillation Design and Optimization Extractive distillation column composition profiles have a very characteristic

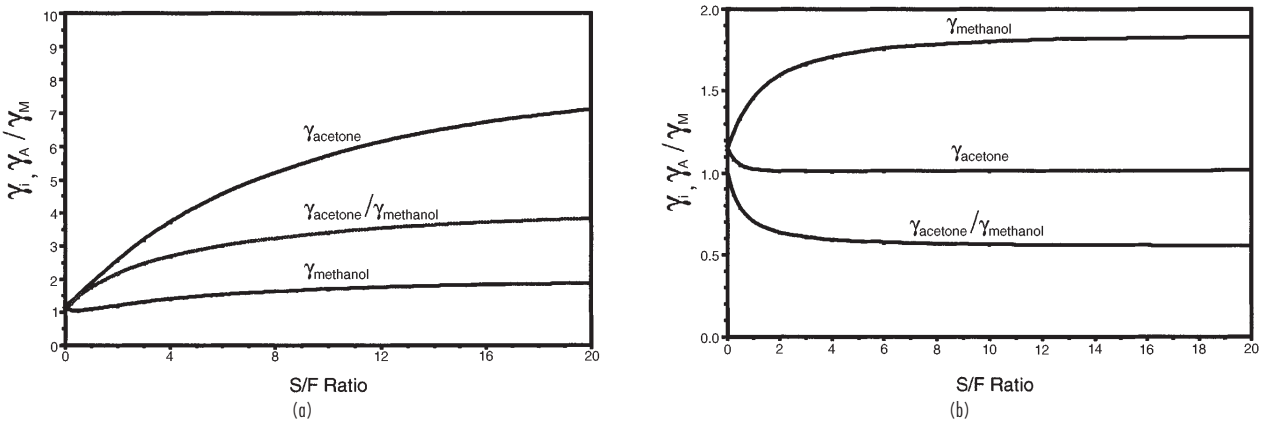

FIG. 13-72 Effect of solvent concentration on activity coefficients for acetone-methanol system. (*a*) water solvent. (*b*) MIPK solvent.

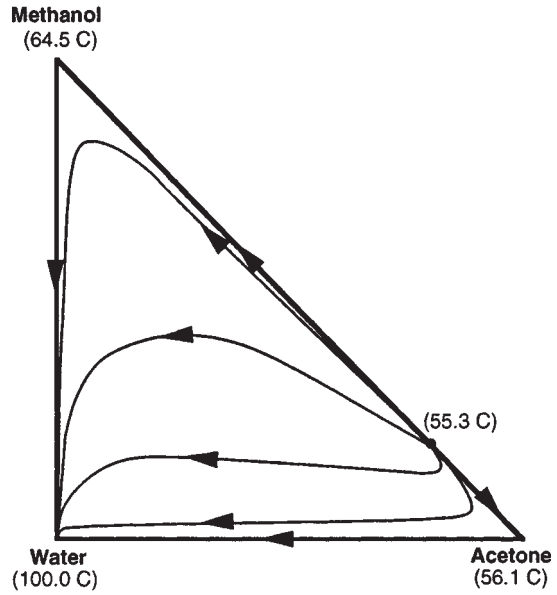

FIG. 13-73 Residue curve maps for acetone-methanol systems. (*a*) With water. (*b*) With MIPK.

shape on a ternary diagram. The composition profile for the separation of methanol-acetone with water is given in Fig. 13-74. Stripping and rectifying profiles start at the bottoms and distillate compositions respectively, track generally along the faces of the composition triangle, and then turn toward the high-boiling (solvent) node and low-boiling node, respectively. For a feasible single-feed design these profiles must cross at some point. However, in an extractive distillation they cannot cross. The extractive-section profile acts at the bridge between these two sections. Most of the key-component separation occurs in this section in the presence of high-solvent concentration.

The variable that has the most significant impact on the economics of an extractive distillation is the solvent-to-feed (*S/F*) ratio. For close-boiling or pinched nonazeotropic mixtures, no minimum-solvent flow rate is required to effect the separation, as the separation is always theoretically possible (if not economical) in the absence of the solvent. However, the extent of enhancement of the relative volatility is largely determined by the solvent concentration and hence the *S/F* ratio. The relative volatility tends to increase as the *S/F* ratio increases. Thus, a given separation can be accomplished in fewer equilibrium stages. As an illustration, the total number of theoretical stages required as a function of *S/F* ratio is plotted in Fig. 13-75*a* for the separation of the nonazeotropic mixture of vinyl acetate and ethyl acetate using phenol as the solvent.

For the separation of a minimum-boiling binary azeotrope by extractive distillation, there is clearly a minimum-solvent flow rate below which the separation is impossible (due to the azeotrope). For azeotropic separations, the number of equilibrium stages is infinite at or below $(S/F)_{min}$ and decreases rapidly with increasing solvent, and then may asymptote, or rise slowly. The relationship between the total number of stages and the *S/F* ratio for a given purity and recovery for the azeotropic acetone-methanol system with water as solvent is shown in Fig 13-75*b*. A rough idea of $(S/F)_{min}$ can be determined from a pseudobinary diagram or by plotting the $\alpha_{L,H} = 1$ line on a ternary diagram. The solvent composition at which the azeotrope disappears in a corner of the pseudobinary diagram is an indication of $(S/F)_{min}$ [LaRoche et al., *Can. J. Chem. Eng.*, **69,** 1302 (1991)]. Typically, operating *S/F* ratios for economically acceptable solvents is between two and five. Higher *S/F* ratios tend to increase the diameter of both the extractive column and the solvent-recovery columns, but reduce the required number of equilibrium stages and minimum-reflux ratio. Moreover, higher *S/F* ratios lead to higher reboiler temperatures, resulting in the use of higher-cost utilities, higher utility usages, and greater risk of degradation.

Knight and Doherty [*Ind. Eng. Chem. Fundam.*, **28,** 564 (1989)] have published rigorous methods for computing minimum reflux for extractive distillation, with an operating reflux of 1.2 to 1.5 times the minimum value usually acceptable. Interestingly, unlike other forms of distillation, in extractive distillation the distillate purity or recovery does not increase monotonically with increasing reflux ratio for a given number of stages. Above a maximum-reflux ratio the separation can

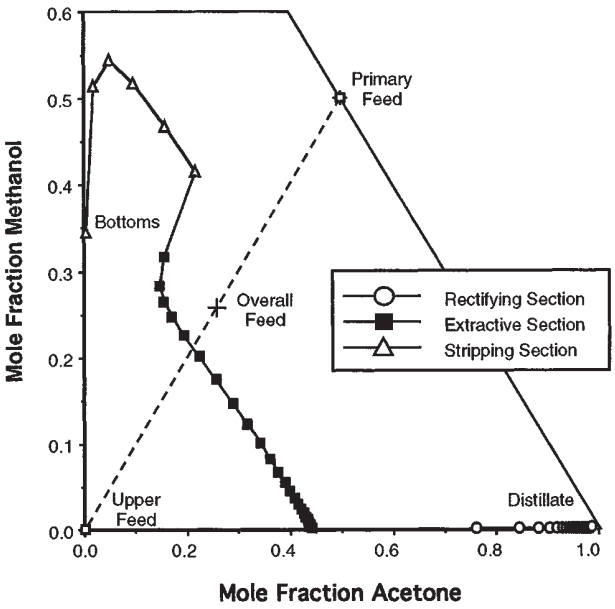

FIG. 13-74 Extractive distillation column composition profile for the separation of acetone-methanol with water.

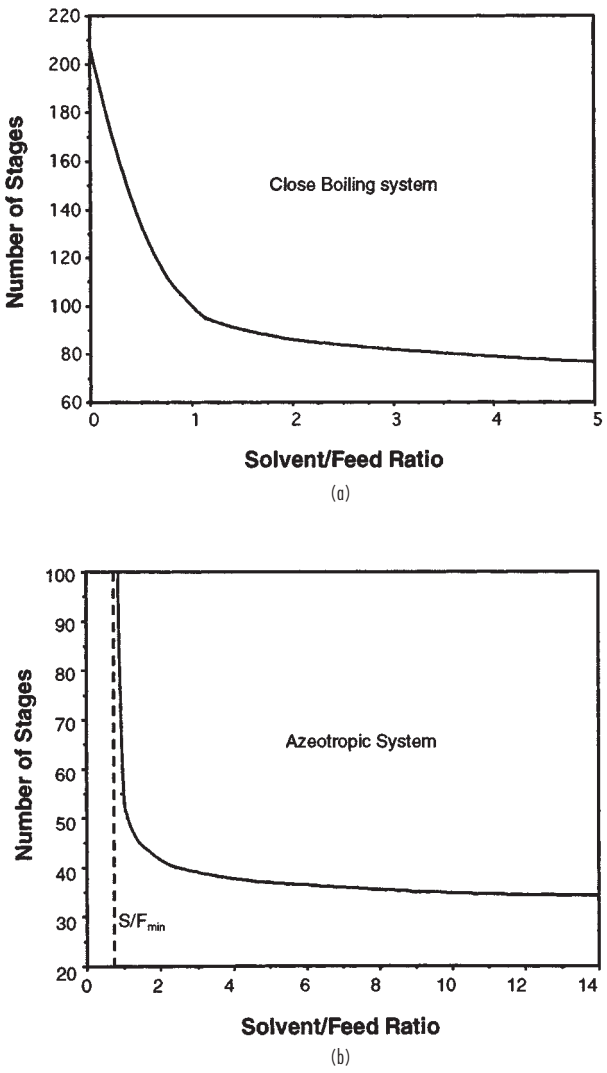

FIG. 13-75 Number of theoretical stages versus solvent-to-feed ratio for extractive distillation. (*a*) Close-boiling vinyl acetate-ethyl acetate system with phenol solvent. (*b*) Azeotropic acetone-methanol system with water solvent.

no longer be achieved and the distillate purity actually decreases for a given number of stages [LaRoche et al., *AIChE J.*, **38,** 1309 (1992)]. The difference between R_{min} and R_{max} increases as the *S*/*F* ratio increases. Large amounts of reflux lowers the solvent concentration in the upper section of the column, degrading rather than enhancing column performance. Because the reflux ratio goes through a maximum, the conventional-control strategy of increasing reflux to maintain purity can be detrimental rather than beneficial. However R_{max} generally occurs at impractically high reflux ratios and is typically not of major concern.

The thermal quality of the solvent feed has no effect on the value of $(S/F)_{min}$, but does affect the minimum reflux to some extent, especially as the (S/F) ratio increases. R_{max} occurs at higher values of the reflux ratio as the upper-feed quality decreases; a subcooled upper feed provides additional refluxing capacity and less external reflux is required for the same separation. It is also sometimes advantageous to introduce the primary feed to the extractive distillation column as a vapor to help maintain a higher solvent concentration on the feed tray and the trays immediately below.

Robinson and Gilliland (*Elements of Fractional Distillation*, McGraw-Hill, New York, 1950), Smith (*Design of Equilibrium Stage Processes*, McGraw-Hill, New York, 1963), Van Winkle (*Distillation*, McGraw-Hill, New York, 1967), and Walas (*Chemical Process Equipment*, Butterworths, Boston, 1988) discuss rigorous stage-by-stage design techniques as well as shortcut and graphical methods for determining minimum stages, $(S/F)_{min}$, minimum reflux, and the optimum locations of the solvent and primary feed points. More recently Knapp and Doherty [*AIChE J.*, **40,** 243 (1994)] have published column-design methods based on geometric arguments and fixed-point analysis. Most commercial simulators are capable of solving multiple-feed extractive distillation heat and material balances, but do not include straightforward techniques for calculating $(S/F)_{min}$, minimum or maximum reflux.

Solvent Screening and Selection Choosing an effective solvent can have the most profound effect on the economics of an extractive distillation process. The approach most often adopted is to first generate a short list of potential solvents using simple qualitative screening and selection methods. Experimental verification is best undertaken only after a list of promising candidate solvents has been generated and some chance at economic viability has been demonstrated via preliminary process modeling.

Solvent selection and screening approaches can be divided into two levels of analysis. The first level focuses on identification of functional groups or chemical families that are likely to give favorable solvent-key component molecular interactions. The second level of analysis identifies and compares individual-candidate solvents. The various methods of analysis are described briefly and illustrated with an example of choosing a solvent for the methanol-acetone separation.

First Level: Broad Screening by Functional Group or Chemical Family

Homologous series. Select candidate solvents from the high-boiling homologous series of both light and heavy key components. Favor homologs of the heavy key, as this tends to enhance the natural relative volatility of the system. Homologous components tend to form ideal solutions and are unlikely to form azeotropes [Scheibel, *Chem. Eng. Prog.* **44**(12), 927 (1948)].

Robbins chart. Select candidate solvents from groups in the Robbins Chart (Table 13-15) that tend to give positive (or no) deviations from Raoult's law for the key component desired in the distillate and negative (or no) deviations for the other key.

Hydrogen-bonding characteristics. Select candidate solvents from groups that are likely to cause the formation of hydrogen bonds with the key component to be removed in the bottoms, or disruption of hydrogen bonds with the key to be removed in the distillate. Formation and disruption of hydrogen bonds are often associated with strong negative and positive deviations, respectively from Raoult's law. Several authors have developed charts indicating expected hydrogen bonding interactions between families of compounds [Ewell et al., *Ind. Eng. Chem.*, **36,** 871 (1944), Gilmont et al., *Ind. Eng. Chem.*, **53,** 223 (1961), and Berg, *Chem. Eng. Prog.*, **65**(9), 52 (1969)]. Table 13-20 presents a hydrogen-bonding classification of chemical families and a summary of deviations from Raoult's law.

Polarity characteristics. Select candidate solvents from chemical groups that tend to show higher polarity than one key component or lower polarity than the other key. Polarity effects are often cited as a factor in causing deviations from Raoult's law [Hopkins and Fritsch, *Chem. Eng. Prog.*, **51**(8), (1954), Carlson et al., *Ind. Eng. Chem.*, **46,** 350 (1954), and Prausnitz and Anderson, *AIChE J.*, **7,** 96 (1961)]. The general trend in polarity based on the functional group of a molecule is given in Table 13-21. The chart is best for molecules of similar size. A more quantitative measure of the polarity of a molecule is the polarity contribution to the three-term Hansen solubility parameter. A tabulation of calculated three-term solubility parameters is provided by Barton (*CRC Handbook of Solubility Parameters and other Cohesion Parameters*, CRC Press, Boca Raton, 1991), along with a group-contribution method for calculating the three-term solubility parameters of compounds not listed in the reference.

Second Level: Identification of Individual Candidate Solvents

Boiling point characteristics. Select only candidate solvents that boil at least 30–40°C above the key components to ensure that the sol-

TABLE 13-20 Hydrogen Bonding Classification of Chemical Families

Class	Chemical family			
H-Bonding, Strongly Associative (HBSA)	Water Primary amides Secondary amides	Polyacids Dicarboxylic acids Monohydroxy acids	Polyphenols Oximes Hydroxylamines	Amino alcohols Polyols
H-Bond Acceptor-Donor (HBAD)	Phenols Aromatic acids Aromatic amines Alpha H nitriles	Imines Monocarboxylic acids Other monoacids Peracids	Alpha H nitros Azines Primary amines Secondary amines	*n*-alcohols Other alcohols Ether alcohols
H-Bond Acceptor (HBA)	Acyl chlorides Acyl fluorides Hetero nitrogen aromatics Hetero oxygen aromatics	Tertiary amides Tertiary amines Other nitriles Other nitros Isocyanates Peroxides	Aldehydes Anhydrides Cyclo ketones Aliphatic ketones Esters Ethers	Aromatic esters Aromatic nitriles Aromatic ethers Sulfones Sulfolanes
π-Bonding Acceptor (π-HBA)	Alkynes Alkenes	Aromatics Unsaturated esters		
H-Bond Donor (HBD)	Inorganic acids Active H chlorides	Active H fluorides Active H iodides	Active H bromides	
Non-Bonding (NB)	Paraffins Nonactive H chlorides	Nonactive H fluorides Sulfides	Nonactive H iodides Disulfides	Nonactive H bromides Thiols

Deviations from Raoult's Law

H-Bonding classes	Type of deviations	Comments
HBSA + NB HBAD + NB	Alway positive dev., HBSA + NB often limited miscibility	H-bonds broken by interactions
HBA + HBD	Always negative dev.	H-bonds formed by interactions
HBSA + HBD HBAD + HBD	Always positive deviations, HBSA + HBD often limited miscibility	H-bonds broken and formed; dissociation of HBSA or HBAD liquid most important effect
HBSA + HBSA HBSA + HBAD HBSA + HBA HBAD + HBAD HBAD + HBA	Usually positive deviations; some give maximum-boiling azeotropes	H-bonds broken and formed
HBA + HBA HBA + NB HBD + HBD HBD + NB NB + NB	Ideal, quasi-ideal systems; always positive or no deviations; azeotropes, if any, minimum-boiling	No H-bonding involved

NOTE: π-HBA is *enhanced* version of HBA.

vent is relatively nonvolatile and remains largely in the liquid phase. With this boiling point difference, the solvent should also not form azeotropes with the other components.

Selectivity at infinite dilution. Rank candidate solvents according to their selectivity at infinite dilution. The selectivity at infinite dilution is defined as the ratio of the activity coefficients at infinite dilution of the two key components in the solvent. Since solvent effects tend to increase as solvent concentration increases, the infinite-dilution selectivity gives an upper bound on the efficacy of a solvent. Infinite-dilution activity coefficients can be predicted using such methods as UNIFAC, ASOG, MOSCED (Reid et al., *Properties of Gases and Liquids*, Fourth Edition, McGraw-Hill, New York, 1987). They can be found experimentally using a rapid gas-liquid chromatography method based on relative retention times in candidate solvents (Tassios in *Extractive and Azeotropic Distillation*, Advances in Chemistry Series 115, American Chemical Society, Washington, 1972) and they can be correlated to bubble-point data [Kojima and Ochi, *J. Chem. Eng. Japan*, **7**(2), 71 (1974)]. DECHEMA [*Vapor-Liquid Equilibrium Data Collection*, Frankfort (1977)], has also published a compilation of experimental infinite-dilution activity coefficients.

Experimental measurement of relative volatility. Rank candidate solvents by the increase in relative volatility caused by the addition of the solvent. One technique is to experimentally measure the relative volatility of a fixed-composition key component-solvent mixture (often a 1/1 ratio of each key, with a 1/1 to 3/1 solvent/key ratio) for various solvents. [Carlson et al., *Ind. Eng. Chem.*, **46,** 350 (1954)]. The Othmer equilibrium still is the apparatus of choice for these measurements [Zudkevitch, *Chem. Eng. Comm.*, **116,** 41 (1992)].

Methanol and acetone boil at 64.5°C and 56.1°C, respectively and form a minimum-boiling azeotrope at 55.3°C. The natural volatility of the system is acetone > methanol, so the favored solvents most likely will be those that cause the acetone to be recovered in the distillate. However, for the purposes of the example, a solvent that reverses the natural volatility will also be identified. First, examining the polarity of

TABLE 13-21 Relative Polarities of Functional Groups

MOST POLAR	Water
↓	Organic acids
↓	Amines
↓	Polyols
↓	Alcohols
↓	Esters
↓	Ketones
↓	Aldehydes
↓	Ethers
↓	Aromatics
↓	Olefins
LEAST POLAR	Paraffins
Effect of branching	
MOST POLAR	Normal
	Secondary
LEAST POLAR	Tertiary

ketones and alcohols (Table 13-21), solvents favored for the recovery of methanol in the bottoms would come from groups more polar than methanol, such as acids, water, and polyols. Turning to the Robbins Chart (Table 13-15), favorable groups are amines, alcohols, polyols, and water since these show expected positive deviations for acetone and zero or negative deviations for methanol. For reversing the natural volatility, solvents should be chosen that are less polar than acetone, such as ethers, hydrocarbons, and aromatics. Unfortunately, both ethers and hydrocarbons are expected to give positive deviations for both acetone and methanol, so should be discarded. Halohydrocarbons and ketones are expected to give positive deviations for methanol and either negative or no deviations for acetone. The other qualitative indicators show that both homologous series (ketones and alcohols) look promising. Thus, after discounting halohydrocarbons for environmental reasons, the best solvents will probably come from alcohols, polyols, and water for recovering methanol in the bottoms and ketones for recovering acetone in the bottoms. Table 13-22 shows the boiling points and experimental or estimated infinite-dilution activity coefficients for several candidate solvents from the aforementioned groups. Methylethylketone boils too low, as does ethanol, and also forms an azeotrope with methanol. These two candidates can be discarded. Other members of the homologous series, along with water and ethylene glycol, have acceptable boiling points (at least 30°C higher than keys). Of these, water (the solvent used industrially) clearly has the largest effect on the activity coefficients, followed by ethylene glycol. Although inferior to water or ethylene glycol, both MIPK and MIBK would probably be acceptable for reversing the natural volatility of the system.

Extractive Distillation by Salt Effects A second method of modifying the liquid-phase behavior (and thus the relative volatility) of a mixture in order to effect a separation is by the addition of a nonvolatile, soluble, ionic salt. The process is analogous to extractive distillation with a high-boiling liquid. In the simplest case, for the separation of a binary mixture, the salt is fed at the top of the column by dissolving it in the hot reflux stream before introduction into the column. In order to function effectively the salt must be adequately soluble in both components throughout the range of compositions encountered in the column. Since the salt is essentially completely nonvolatile, it remains in the liquid phase on each tray and alters the relative volatility throughout the length of the column. No rectification section is needed above the salt feed. The bottoms product is recovered from the salt solution by evaporation or drying, and the salt is recycled. The ions of a salt are typically capable of causing much larger and more selective effects on liquid-phase behavior than the molecules of a liquid solvent. As a result, salt-to-feed ratios less than 0.1 are typical.

The use of a salting agent presents a number of problems not associated with a liquid solvent, such as the difficulty of transporting and metering a solid or saturated salt solution, slow mixing or dissolution rate of the salt, limits to solubility in the feed components, and potential for corrosion. However, in the limited number of systems for which an effective salt can be found, the energy usage, equipment size, capital investment, and ultimate separation cost can be significantly reduced compared to extractive distillation using a liquid solvent [Furter, *Chem. Eng. Commun.,* **116,** 35 (1992)]. Applications of salt extractive distillation include acetate salts to produce absolute ethanol, magnesium nitrate for the production of concentrated nitric acid as an alternative to the sulfuric-acid solvent process, and calcium chloride to produce anhydrous hydrogen chloride. Other examples are noted by Furter [*Can. J. Chem. Eng.*, **55,** 229 (1977)].

One problem limiting the consideration of salt extractive distillation is the fact that the performance and solubility of a salt in a particular system is difficult to predict without experimental data. Some recent advances have been made in modeling the VLE behavior of organic-aqueous-salt solutions using modified UNIFAC, NRTL, UNIQUAC, and other approaches [Kumar, *Sep. Sci. Tech.,* **28**(1), 799 (1993)].

TABLE 13-22 Comparison of Candidate Solvents for Methanol/Acetone Extractive Distillation

Solvent	Boiling pt. (°C)	Azeotrope formation	$\gamma^{\infty}_{Acetone}$	γ^{∞}_{MeOH}	$\gamma^{\infty}_{Acetone}/\gamma^{\infty}_{MeOH}$
MEK	79.6	With MeOH	1.01	1.88	0.537
MIPK	102.0	No	1.01	1.89	0.534
MIBK	115.9	No	1.06	2.05	0.517
Ethanol	78.3	No	1.85	1.04	1.78
1-Propanol	97.2	No	1.90	1.20	1.58
1-Butanol	117.8	No	1.93	1.33	1.45
Water	100.0	No	11.77	2.34	5.03
EG	197.2	No	3.71	1.25	2.97

$\gamma^{\infty}_{Acetone} = 1.79$ (in MeOH)
$\gamma^{\infty}_{MeOH} = 1.81$ (in acetone)

REACTIVE DISTILLATION

Introduction Reactive distillation is a unit operation in which chemical reaction and distillative separation are carried out simultaneously within a fractional distillation apparatus. Reactive distillation may be advantageous for liquid-phase reaction systems when the reaction must be carried out with a large excess of one or more of the reactants, when a reaction can be driven to completion by removal of one or more of the products as they are formed, or when the product recovery or by-product recycle scheme is complicated or made infeasible by azeotrope formation.

For consecutive reactions in which the desired product is formed in an intermediate step, excess reactant can be used to suppress additional series reactions by keeping the intermediate-species concentration low. A reactive distillation can achieve the same end by removing the desired intermediate from the reaction zone as it is formed. Similarly, if the equilibrium constant of a reversible reaction is small, high conversions can be achieved by use of a large excess of reactant. Alternatively, by Le Chatelier's principle, the reaction can be driven to completion by removal of one or more of the products as they are formed. Typically, reactants can be kept much closer to stoichiometric proportions in a reactive distillation. When a reaction mixture exhibits azeotropism, the recovery of products and recycle of excess reagents can be quite complicated and expensive. Reactive distillation can provide a means of breaking azeotropes by altering or eliminating the condition for azeotrope formation in the reaction zone through the combined effects of vaporization-condensation and consumption-production of the species in the mixture. Alternatively, a reaction may be used to convert the species into components that are more easily distilled. In each of these situations, the conversion and selectivity often can be improved markedly, with much lower-reactant inventories and recycle rates, and much simpler recovery schemes. The capital savings can be quite dramatic. A list of applications of reactive distillation appearing in the literature is given in Table 13-23.

Although reactive distillation has many potential applications, it is not appropriate for all situations. Since it is in essence a distillation process, it has the same range of applicability as other distillation operations. Distillation-based equipment is not designed to effectively handle solids, supercritical components (where no separate vapor and liquid phases exist), gas-phase reactions, or high-temperature or high-pressure reactions such as hydrogenation, steam reforming, gasification, and hydrodealkylation.

Simulation, Modeling, and Design Feasibility Because reaction and separation phenomena are closely coupled in a reactive distillation process, simulation and design is significantly more complex than that of sequential reaction and separation processes. In spite of the complexity, however, most commercial computer process modeling packages offer reliable and flexible routines for simulating steady-state reactive distillation columns, with either equilibrium or kinetically controlled reaction models. [Venkataraman et al., *Chem. Eng. Prog.,* **86**(6), 45 (1990)]. As with other enhanced distillation processes, the results are very sensitive to the thermodynamics model chosen and the accuracy of the VLE data used to generate model parameters. Of equal, if not more significance is the accuracy of data on reaction rate as a function of temperature. Very different conclusions can be drawn about the feasibility of a reactive distillation if the reaction is assumed to reach chemical equilibrium on each stage of the column or if the reaction is assumed to be kinetically controlled [Barbosa and Doherty, *Chem. Eng. Sci.,* **43,** 541 (1988)]. Tray holdup

TABLE 13-23 Applications of Reactive Distillation

Process	Reaction type	Reference
Methyl acetate from methanol and acetic acid	Esterification	Agreda et al., *Chem. Eng. Prog.,* **86**(2), 40 (1990)
General process for ester formation	Esterification	Simons, "Esterification" in Encyclopedia of Chemical Processing and Design, Vol 19, Dekker, New York, 1983
Dibutyl phthalate from butanol and phthalic acid	Esterification	Berman et al., *Ind. Eng. Chem.*, **40,** 2139 (1948)
Ethyl acetate from ethanol and butyl acetate	Transesterification	Davies and Jeffreys, *Trans. Inst. Chem. Eng.,* **51,** 275 (1973)
Recovery of acetic acid and methanol from methyl acetate by-product of vinyl acetate production	Hydrolysis	Fuchigami, *J. Chem. Eng. Jap.,* **23,** 354 (1990)
Nylon 6,6 prepolymer from adipic acid and hexamethylenediamine	Amidation	Jaswal and Pugi, U.S. Patent 3,900,450 (1975)
MTBE from isobutene and methanol	Etherification	DeGarmo et al., *Chem. Eng. Prog.,* **88**(3), 43 (1992)
TAME frompentenes and methanol	Etherification	Brockwell et al., *Hyd. Proc.,* **70**(9), 133 (1991)
Separation of close boiling 3- and 4-picoline by complexation with organic acids	Acid-base	Duprat and Gau, *Can. J. Chem. Eng.,* **69,** 1320 (1991)
Separation of close-boiling meta and para xylenes by formation of tert-butyl meta-xylene	Transalkylation	Saito et al., *J. Chem. Eng. Jap.,* **4,** 37 (1971)
Cumene from propylene and benzene	Alkylation	Shoemaker and Jones, *Hyd. Proc.,* **67**(6), 57 (1987)
General process for the alkylation of aromatics with olefins	Alkylation	Crossland, U.S. Patent 5,043,506 (1991)
Production of specific higher and lower alkenes from butenes	Diproportionation	Jung et al., U.S. Patent 4,709,115 (1987)
4-Nitrochlorobenzene from chlorobenzene and nitric acid	Nitration	Belson, *Ind. Eng. Chem. Res.,* **29,** 1562 (1990)
Production of methylal and high purity formaldehyde		Masamoto and Matsuzaki, *J. Chem. Eng. Jap.,* **27,** 1 (1994)

and stage requirements are two important variables directly affected by the form of the reaction model chosen.

When an equilibrium reaction occurs in a vapor-liquid system, the phase compositions depend not only on the relative volatility of the components in the mixture, but also on the consumption (and production) of species. Thus, the condition for azeotropy in a nonreactive system ($y_i = x_i$, for all i) no longer holds true in a reactive system and must be modified to include reaction stoichiometry:

$$\frac{y_1 - x_1}{v_1 - v_T x_1} = \frac{y_i - x_i}{v_i - v_T x_i} \qquad \text{for all } i = 1, n \qquad (13\text{-}128)$$

where $$v_T = \sum_{i=1}^{n} v_i$$

x_i = mole fraction of component i in the liquid phase
y_i = mole fraction of component i in the vapor phase
v_i = stoichiometric coefficient of component i (negative for reactants, positive for products)

Phase compositions that satisfy Eq. (13-128) are stationary points on a phase diagram and have been labeled *reactive azeotropes* by Barbosa and Doherty [*Chem. Eng. Sci.,* **43,** 529 (1988)]. At a reactive azeotrope the mass exchange between the vapor and liquid phase and the generation (or consumption) of each species is balanced such that the composition of neither phase changes. Reactive azeotropes show the same distillation properties as ordinary azeotropes and therefore affect what products are achievable. Reactive azeotropes are not easily visualized in conventional y-x coordinates but become apparent upon a transformation of coordinates which depends on the number of reactions, the order of each reaction (e.g., $A + B \leftrightarrow C$ or $A + B \leftrightarrow C + D$), presence of nonreacting components, and the extent of reaction. The general vector-matrix form of the transform for C reacting components, with R reactions, and I nonreacting components has been derived by Ung and Doherty [*Chem. Eng. Sci.,* **50,** 23 (1995)]. For the transformed mole fraction of component i in the liquid phase, X_i, they give

$$X_i = \left[\frac{x_i - v_i^T (v_{Ref})^{-1} x_{Ref}}{1 - v_{TOT}^T (v_{Ref})^{-1} x_{Ref}} \right], \qquad i = 1, \ldots . \text{C-R} \qquad (13\text{-}129)$$

where v_i^T = row vector of stoichiometric coefficients of component i for each reaction
v_{Ref} = square matrix of stoichiometric coefficients for R reference components in R reactions
x_{Ref} = column vector of mole fractions for the R reference components in the liquid phase
v_{TOT}^T = row vector composed of the sum of the stoichiometric coefficients for each reaction

An equation identical to (13-129) defines the transformed mole fraction of component i in the vapor phase, Y_i, where the terms in x are replaced by terms in y.

The transformed variables describe the system composition with or without reaction and sum to unity as do x_i and y_i. The condition for azeotropy becomes $X_i = Y_i$. Barbosa and Doherty have shown that phase and distillation diagrams constructed using the transformed composition coordinates have the same properties as phase and distillation region diagrams for nonreactive systems and similarly can be used to assist in design feasibility and operability studies [*Chem. Eng. Sci.,* **43,** 529, 1523, and 2377 (1988a,b,c)]. A residue curve map in transformed coordinates for the reactive system methanol-acetic acid-methyl acetate-water is shown in Fig. 13-76. Note that the nonreactive azeotrope between water and methyl acetate has disappeared, while the methyl acetate-methanol azeotrope remains intact. Only

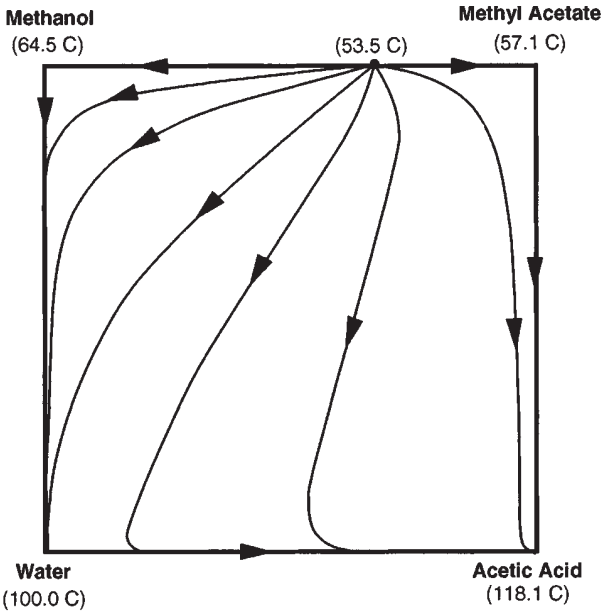

FIG. 13-76 Residue curve map for the reactive system methanol-acetic acid-methyl acetate-water in chemical equilibrium.

those azeotropes containing either all the required reactants or products will be altered by the reaction (water and methyl acetate can back-react to form acetic acid and methanol, whereas methanol and methyl acetate cannot further react in the absence of either water or acetic acid). This reactive system consists of only one distillation region in which the methanol-methyl acetate azeotrope is the low-boiling and acetic acid is the high-boiling node.

The situation becomes more complicated when the reaction is kinetically controlled and does not come to complete-chemical equilibrium under the conditions of temperature, liquid holdup, and rate of vaporization in the column reactor. Venimadhavan et al. [*AIChE J.*, **40,** 1814 (1994)] and Rev [*Ind. Eng. Chem. Res.*, **33,** 2174 (1994)] show that the existence and location of reactive azeotropes is a function of approach to equilibrium as well as the evaporation rate.

Mechanical Design and Implementation Issues The choice of catalyst has a significant impact on the mechanical design and operation of the reactive column. The catalyst must allow the reaction to occur at reasonable rates at the relatively low temperatures and pressures common in distillation operations (typically less than 10 atmospheres and between 50°C and 250°C). Selection of a homogeneous catalyst, such as a high-boiling mineral acid, allows the use of more traditional tray designs and internals (albeit designed with allowance for high-liquid holdups). With a homogeneous catalyst, lifetime is not a problem, as it is added (and withdrawn) continuously. Alternatively, heterogeneous solid catalysts require either complicated mechanical means for continuous replenishment or relatively long lifetimes in order to avoid constant maintenance. As with other multiphase reactors, use of a solid catalyst adds an additional resistance to mass transfer from the bulk liquid (or vapor) to the catalyst surface, which may be the limiting resistance. The catalyst containment system must be designed to ensure adequate liquid-solid contacting and minimize bypassing. A number of specialized column internal designs, catalyst containment methods, and catalyst replenishment systems have been proposed for both homogeneous and heterogeneous catalysts. A partial list of these methods is given in Table 13-24.

Heat management is another important consideration in the implementation of a reactive distillation process. Conventional reactors for highly exothermic or endothermic reactions are often designed as modified shell-and-tube heat exchangers for efficient heat transfer. However, a trayed or packed distillation column is a rather poor mechanical design for the management of the heat of reaction. Although heat can be removed or added in the condenser or reboiler easily, the only mechanism for heat transfer in the column proper is through vaporization (or condensation). For highly exothermic reactions, a large excess of reactants may be required as a heat sink, necessitating high-reflux rates and larger-diameter columns to return the vaporized reactants back to the reaction zone. Often a prereactor of conventional design is used to accomplish most of the reaction and heat removal before feeding to the reactive column for final conversion, as exemplified in most processes for the production of tertiary amyl methyl ether (TAME) [Brockwell et al., *Hyd. Proc.*, **70**(9), 133 (1991)]. Highly endothermic reactions may require intermediate reboilers. None of these heat-management issues preclude the use of reactive distillation, but must be taken into account during the design phase. Comparison of heat of reaction and average heat of vaporization data for a system, as in Fig. 13-77, gives some indication of potential heat imbalances [Sundmacher et al., *Chem. Eng. Comm.*, **127,** 151 (1994)]. The heat neutral systems ($-\Delta H_{\text{react}} \approx \Delta H_{\text{vap(avg)}}$) such as methyl acetate and other esters can be accomplished in one reactive column, whereas the MTBE and TAME processes, with higher heats of reaction than vaporization, often include an additional prereactor. One exception is the catalytic distillation process for cumene production, which is accomplished without a prereactor. Three moles of benzene reactant are vaporized (and refluxed) for every mole of cumene produced. The relatively high heat of reaction is advantageous in this case as it reduces the overall heat duty of the process by about 30 percent [Shoemaker and Jones, *Hyd. Proc.*, **57**(6), 57 (1987)].

Process Applications The production of esters from alcohols and carboxylic acids illustrates many of the principles of reactive distillation as applied to equilibrium-limited systems. The equilibrium constants for esterification reactions are usually relatively close to unity. Large excesses of alcohols must be used to obtain acceptable yields with large recycles. In a reactive-distillation scheme, the reac-

TABLE 13-24 Catalyst Systems for Reactive Distillation

Description	Application	Reference
	Homogeneous catalysis	
Liquid-phase mineral-acid catalyst added to column or reboiler	Esterifications Dibutyl phlalate Methyl acetate	Keyes, *Ind. Eng. Chem.*, **24,** 1096 (1932) Berman et al., *Ind. Eng. Chem.*, **40,** 2139 (1948) Agreda et al., U.S. Patent 4,435,595 (1984)
	Heterogeneous catalysis	
Catalyst-resin beads placed in cloth bags attached to fiberglass strip. Strip wound around helical stainless steel mesh spacer	Etherifications Cumene	Smith et al., U.S. Patent 4,443,559 (1981) Shoemaker and Jones, *Hyd.* **57**(6), 57 (1987)
Ion exchange resin beads used as column packing	Hydrolysis of methyl acetate	Fuchigami, *J. Chem. Eng. Jap.*, **23,** 354 (1990)
Molecular sieves placed in bags or porous containers	Alkylation of aromatics	Crossland, U.S. Patent 5,043,506 (1991)
Ion exchange resins formed into Raschig rings	MTBE	Flato and Hoffman, *Chem. Eng. Tech.*, **15,** 193 (1992)
Granular catalyst resin loaded in corrugated sheet casings	Dimethyl acetals of formaldehyde	Zhang et al., Chinese Patent 1,065,412 (1992)
Trays modified to hold catalyst bed	MTBE	Sanfilippo et al., Eur. Pat. Appl. EP 470,625 (1992)
Distillation trays consturcted of porous catalytically active material and reinforcing resins	None specified	Wang et al., Chinese Patent 1,060,228 (1992)
Method described for removing or replacing catalyst on trays as a liquid slurry	None specified	Jones, U.S. Patent, 5,133,942 (1992)
Catalyst bed placed in downcomer, designed to prevent vapor flow through bed	Etherifications, alkylations	Asselineau, Eur. Pat. Appl. EP 547,939 (1993)
Slotted plate for catalyst support designed with openings for vapor flow	None specified	Evans and Stark, Eur. Pat. Appl. EP 571,163 (1993)
Ion exchanger fibers (reinforced ion exchange polymer) used as solid-acid catalyst	Hydrolysis of methyl acetate	Hirata et al., Jap. Patent 05,212,290 (1993)
High-liquid holdup trays designed with catalyst bed extending below tray level, perforated for vapor-liquid contact	None specified	Yeoman et al., Int. Pat. Appl., WO 9408679 (1994)
Catalyst bed placed in downcomer, in-line withdrawal/addition system	None specified	Carland, U.S. Patent, 5,308,451 (1994)

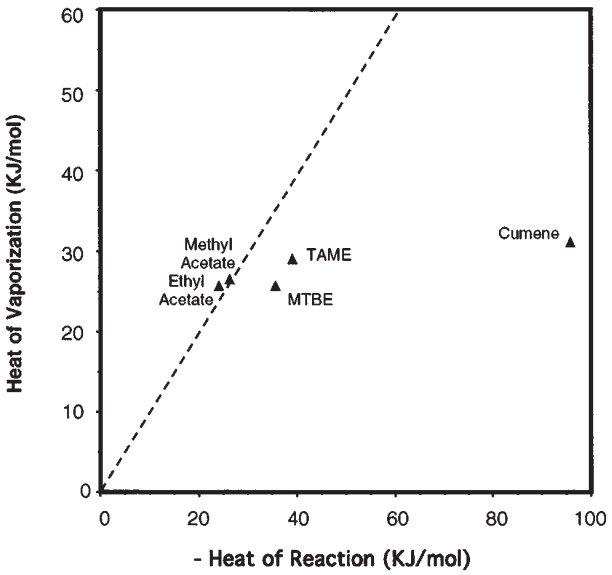

FIG. 13-77 Similarity of heats of reaction and vaporization for compounds made by reactive distillation.

tion is driven to completion by removal of the water of esterification. The method used for removal of the water depends on the boiling points, compositions, and liquid-phase behavior of any azeotropes formed between the products and reactants and largely dictates the structure of the reactive-distillation flowsheet.

When the ester forms a binary low-boiling azeotrope with water or a ternary alcohol-ester-water azeotrope and that azeotrope is heterogeneous (or can be moved into the two-liquid-phase region), the continuous flowsheet illustrated in Fig. 13-78 can be used. Such a flowsheet works for the production of ethyl acetate and higher homologs. In this process scheme, acetic acid and the alcohol are continuously fed to the reboiler of the esterification column, along with a homogeneous strong-acid catalyst. Since the catalyst is largely nonvolatile, the reboiler acts as the primary reaction site. The alcohol is usually fed in slight excess to ensure complete reaction of the acid and to compensate for alcohol losses through distillation of the water-ester-(alcohol) azeotrope. The esterification column is operated such that the low-boiling, water-laden azeotrope is taken as the distillation product. Upon cooling, the distillate separates into two liquid phases. The aqueous layer is steam-stripped, with the organics recycled to the decanter or reactor. The ester layer from the decanter contains some water and possibly alcohol. Part of this layer may be refluxed to the esterification column. The remainder is fed to a low-boiler column where the water-ester and alcohol-ester azeotropes are removed overhead and recycled to the decanter or reactor. The dry, alcohol-free ester is then optionally taken overhead in a final refining column.

Methyl acetate cannot be produced in high purity using the simple esterification scheme described above. The methyl acetate-methanol-water system does not exhibit a ternary minimum-boiling azeotrope, the methyl acetate-methanol azeotrope is lower boiling than the water-methyl acetate azeotrope, a distillation boundary extends between these two binary azeotropes, and the heterogeneous region does not include either azeotrope, nor does it cross the distillation boundary. Consequently, the water of esterification cannot be removed effectively and methyl acetate cannot be separated from the methanol and water azeotropes by a simple decantation in the same manner as outlined above. Conventional sequential reaction-separation processes rely on large excesses of acetic acid to drive the reaction to higher conversion to methyl acetate, necessitating a capital- and energy-intensive acetic acid-water separation and large recycle streams. The crude methyl acetate product, contaminated with water and methanol, can be purified by a

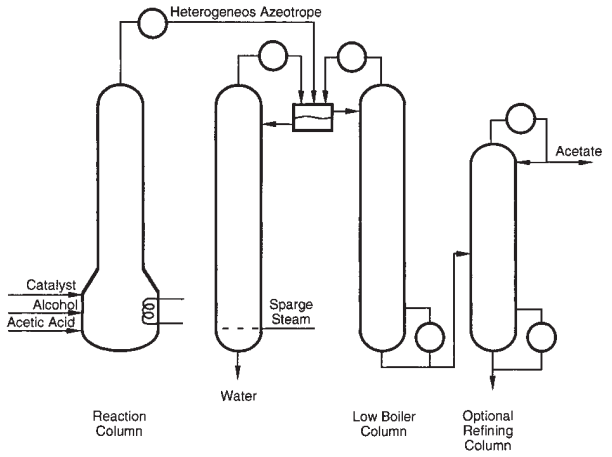

FIG. 13-78 Flowsheet for exters which form a heterogeneous minimum-boiling azeotrope with water.

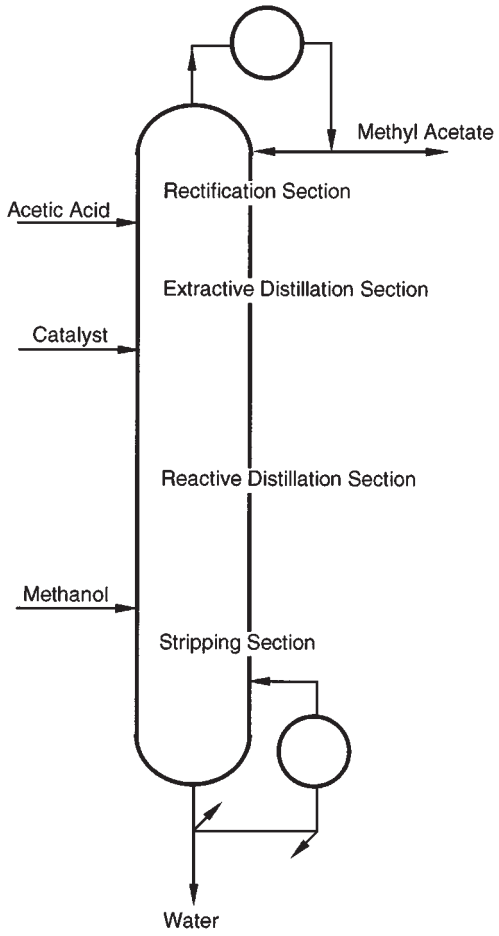

FIG. 13-79 Integrated reactive-extractive distillation column for the production of methyl acetate.

number of the enhanced distillation techniques such as pressure-swing distillation [Harrison, US Patent 2,704,271 (1955)], extractive distillation with ethylene glycol monomethylether as the solvent [Kumerle, German Patent 1,070,165 (1959)], or azeotropic distillation with an aromatic or ketone entrainer [Yeomans, Eur. Patent Appl. 060717 and 060719 (1982)]. The end result is a capital- and energy-intensive process typically requiring multiple reactors and distillation columns.

The reactive-distillation process (Fig. 13-79) provides a mechanism for overcoming both the limitations on conversion due to chemical equilibrium as well as the difficulties in purification imposed by the water-methyl acetate and methanol-methyl acetate azeotropes [Agreda et al., *Chem. Eng. Prog.*, **86**(2), 40 (1990)]. Conceptually, this flowsheet can be thought of as four heat-integrated distillation columns (one of which is also a reactor) stacked on top of each other. The primary reaction zone consists of a series of countercurrent flashing stages in the middle of the column. Adequate residence time for the reaction is provided by high-liquid-holdup bubble-cap trays with specially designed downcomer sumps to further increase tray holdup. A nonvolatile homogeneous catalyst is fed at the top of the reactive section and exits with the underflow water by-product. The extractive-distillation section, immediately above the reactive section, is critical in achieving high-methyl-acetate purity. As shown in Fig. 13-76, simultaneous reaction and distillation eliminates the water-methyl acetate azeotrope (and the distillation boundary of the nonreactive system). However, pure methyl acetate remains a saddle in the reactive system, and cannot be obtained as a pure component by simple reactive distillation. The acetic acid feed acts as a solvent in an extractive-distillation section placed above the reaction section, breaking the methanol-methyl acetate azeotrope, and yielding a pure methyl acetate distillate product. The uppermost rectification stages serve to remove any acetic acid from the methyl acetate product and the bottommost stripping section removes any methanol and methyl acetate from the water by-product. The countercurrent flow of the reactants results in high local excesses at each end of the reactive section, even though the overall feed to the reactive column is stoichiometric. Therefore, the large excess of acetic acid at the top of the reactive section prevents methanol from reaching the distillate, while, similarly, methanol at the bottom of the reactive section keeps acetic acid from the water bottoms. Temperature and composition profiles for this reactive-extractive-distillation column are shown in Fig. 13-80*a* and *b*, respectively.

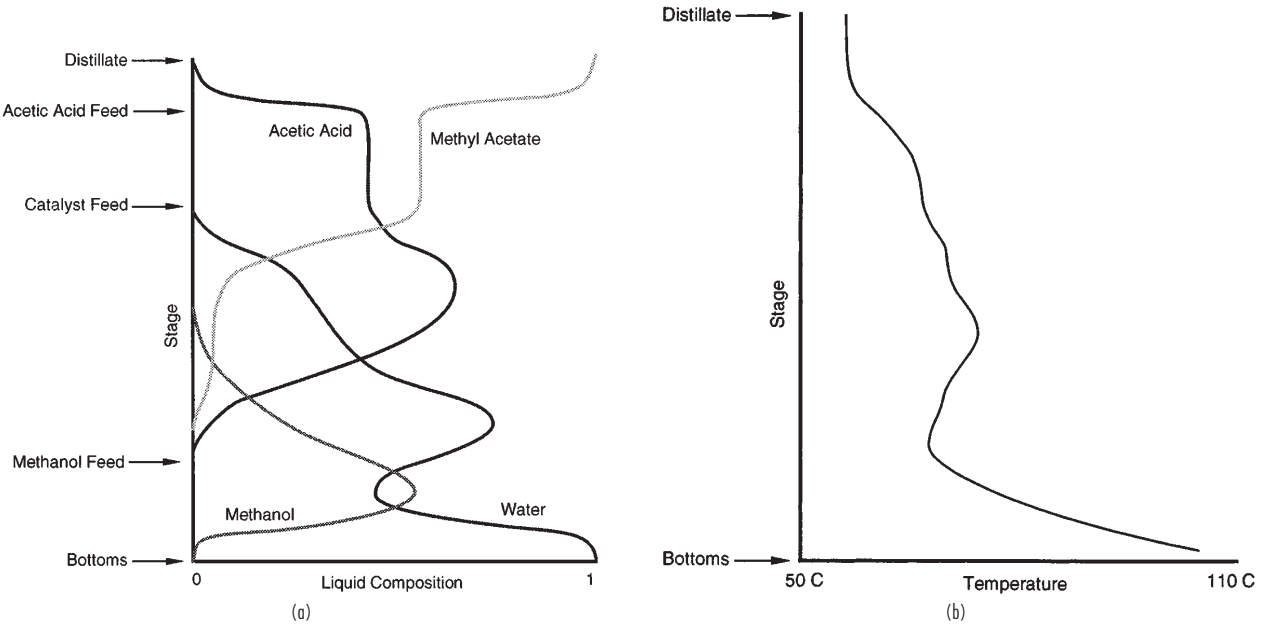

FIG. 13-80 Reactive extracting distillation for methyl acetate production. (*a*) Composition profile. (*b*) Temperature profile.

PETROLEUM AND COMPLEX-MIXTURE DISTILLATION

INTRODUCTION

Although the principles of multicomponent distillation apply to petroleum, synthetic crude oil, and other complex mixtures, this subject warrants special consideration for the following reasons:

1. Such feedstocks are of exceedingly complex composition, consisting, in the case of petroleum, of many different types of hydrocarbons and perhaps of inorganic and other organic compounds. The number of carbon atoms in the components may range from 1 to more than 50, so that the compounds may exhibit atmospheric-pressure boiling points from −162°C (−259°F) to more than 538°C (1000°F). In a given boiling range, the number of different compounds that exhibit only small differences in volatility multiplies rapidly with increasing boiling point. For example, 16 of the 18 octane isomers boil within a range of only 12°C (22°F).
2. Products from the distillation of complex mixtures are in themselves complex mixtures. The character and yields of these products vary widely, depending upon the source of the feedstock. Even crude oils from the same locality may exhibit marked variations.
3. The scale of petroleum-distillation operations is generally large, and, as discussed in detail by Nelson (*Petroleum Refinery Engineering*, 4th ed., McGraw-Hill, New York, 1958) and Watkins (*Petroleum Refinery Distillation*, 2d ed., Gulf, Houston, 1979), such operations are common in several petroleum-refinery processes including atmospheric distillation of crude oil, vacuum distillation of bottoms residuum obtained from atmospheric distillation, main fractionation of gaseous

effluent from catalytic cracking of various petroleum fractions, and main fractionation of effluent from thermal coking of various petroleum fractions. These distillation operations are conducted in large pieces of equipment that can consume large quantities of energy. Therefore, optimization of design and operation is very important and frequently leads to a relatively complex equipment configuration.

CHARACTERIZATION OF PETROLEUM AND PETROLEUM FRACTIONS

Although much progress has been made in identifying the chemical species present in petroleum, it is generally sufficient for purposes of design and analysis of plant operation of distillation to characterize petroleum and petroleum fractions by gravity, laboratory-distillation curves, component analysis of light ends, and hydrocarbon-type analysis of middle and heavy ends. From such data, as discussed in the *Technical Data Book—Petroleum Refining* [American Petroleum Institute (API), Washington], five different average boiling points and an index of paraffinicity can be determined; these are then used to predict the physical properties of complex mixtures by a number of well-accepted correlations, whose use will be explained in detail and illustrated with examples. Many other characterizing properties or attributes such as sulfur content, pour point, water and sediment content, salt content, metals content, Reid vapor pressure, Saybolt Universal viscosity, aniline point, octane number, freezing point, cloud point, smoke point, diesel index, refractive index, cetane index, neutralization number, wax content, carbon content, and penetration are generally measured for a crude oil or certain of its fractions according to well-specified ASTM tests. But these attributes are of much less interest here even though feedstocks and products may be required to meet certain specified values of the attributes.

Gravity of a crude-oil or petroleum fraction is generally measured by the ASTM D 287 test or the equivalent ASTM D 1298 test and may be reported as specific gravity (SG) 60/60°F [measured at 60°F (15.6°C) and referred to water at 60°F (15.6°C)] or, more commonly, as API gravity, which is defined as

$$\text{API gravity} = 141.5/(\text{SG } 60/60°\text{F}) - 131.5 \qquad (13\text{-}130)$$

Water, thus, has an API gravity of 10.0, and most crude oils and petroleum fractions have values of API gravity in the range of 10 to 80. Light hydrocarbons (*n*-pentane and lighter) have values of API gravity ranging upward from 92.8.

The volatility of crude-oil and petroleum fractions is characterized in terms of one or more laboratory distillation tests that are summarized in Table 13-25. The ASTM D 86 and D 1160 tests are reasonably rapid batch laboratory distillations involving the equivalent of approximately one equilibrium stage and no reflux except for that caused by heat losses. Apparatus typical of the D 86 test is shown in Fig. 13-81 and consists of a heated 100-mL or 125-mL Engler flask containing a calibrated thermometer of suitable range to measure the temperature of the vapor at the inlet to the condensing tube, an inclined brass condenser in a cooling bath using a suitable coolant, and a graduated cylinder for collecting the distillate. A stem correction is not applied to the temperature reading. Related tests using similar apparatuses are the D 216 test for natural gasoline and the Engler distillation.

In the widely used ASTM D 86 test, 100 mL of sample is charged to the flask and heated at a sufficient rate to produce the first drop of distillate from the lower end of the condenser tube in from 5 to 15 min, depending on the nature of the sample. The temperature of the vapor at that instant is recorded as the initial boiling point (IBP). Heating is continued at a rate such that the time from the IBP to 5 volume percent recovered of the sample in the cylinder is 60 to 75 s. Again, vapor temperature is recorded. Then, successive vapor temperatures are recorded for from 10 to 90 percent recovered in intervals of 10, and at 95 percent recovered, with the heating rate adjusted so that 4 to 5 mL are collected per minute. At 95 percent recovered, the burner flame is increased if necessary to achieve a maximum vapor temperature referred to as the end point (EP) in from 3 to 5 additional min. The percent recovery is reported as the maximum percent recovered in the cylinder. Any residue remaining in the flask is reported as percent residue, and percent loss is reported as the difference between 100 mL and the sum of the percent recovery and percent residue. If the atmosphere test pressure P is other than 101.3 kPa (760 torr), temperature readings may be adjusted to that pressure by the Sidney Young equation, which for degrees Fahrenheit is

$$T_{760} = T_P + 0.00012(760 - P)(460 + T_P) \qquad (13\text{-}131)$$

Another pressure correction for percent loss can also be applied, as described in the ASTM test method.

Results of a typical ASTM distillation test for an automotive gasoline are given in Table 13-26, in which temperatures have already been corrected to a pressure of 101.3 kPa (760 torr). It is generally assumed that percent loss corresponds to volatile noncondensables that are distilled off at the beginning of the test. In that case, the percent recovered values in Table 13-26 do not correspond to percent evaporated values, which are of greater scientific value. Therefore, it is common to adjust the reported temperatures according to a linear interpolation procedure given in the ASTM test method to obtain corrected temperatures in terms of percent evaporated at the standard intervals as included in Table 13-26. In the example, the corrections are not large because the loss is only 1.5 volume percent.

Although most crude petroleum can be heated to 600°F (316°C) without noticeable cracking, when ASTM temperatures exceed 475°F (246°C), fumes may be evolved, indicating decomposition, which may cause thermometer readings to be low. In that case, the following correction attributed to S. T. Hadden may be applied:

$$\Delta T_{\text{corr}} = 10^{-1.587 + 0.0047357T}$$

where T = measured temperature, °F
ΔT_{corr} = correction to be added to T, °F

At 500 and 600°F (260 and 316°C), the corrections are 6 and 18°F (3.3 and 10°C) respectively.

As discussed by Nelson (op. cit.), virtually no fractionation occurs in an ASTM distillation. Thus, components in the mixture do distill one by one in the order of their boiling points but as mixtures of successively higher boiling points. The IBP, EP, and intermediate points have little theoretical significance, and, in fact, components boiling below the IBP and above the EP are present in the sample. Never-

TABLE 13-25 Laboratory Distillation Tests

Test name	Reference	Main applicability
ASTM (atmospheric)	ASTM D 86	Petroleum fractions or products, including gasolines, turbine fuels, naphthas, kerosines, gas oils, distillate fuel oils, and solvents that do not tend to decompose when vaporized at 760 mmHg
ASTM [vacuum, often 10 torr (1.3 kPa)]	ASTM D 1160	Heavy petroleum fractions or products that tend to decompose in the ASTM D 86 test but can be partially or completely vaporized at a maximum liquid temperature of 750°F (400°C) at pressures down to 1 torr (0.13 kPa)
TBP [atmospheric or 10 torr (1.3 kPa)]	Nelson,* ASTM D 2892	Crude oil and petroleum fractions
Simulated TBP (gas chromatography)	ASTM D 2887	Crude oil and petroleum fractions
EFV (atmospheric, superatmospheric, or subatmospheric)	Nelson†	Crude oil and petroleum fractions

*Nelson, *Petroleum Refinery Engineering*, 4th ed., McGraw-Hill, New York, 1958, pp. 95–99.
†Ibid., pp. 104–105.

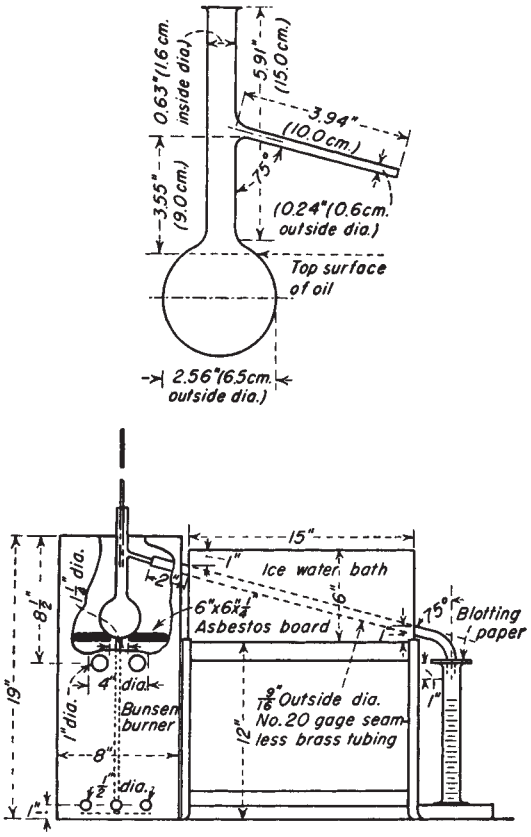

FIG. 13-81 ASTM distillation apparatus; detail of distilling flask is shown in the upper figure.

theless, because ASTM distillations are quickly conducted, have been successfully automated, require only a small sample, and are quite reproducible, they are widely used for comparison and as a basis for specifications on a large number of petroleum intermediates and products, including many solvents and fuels. Typical ASTM curves for several such products are shown in Fig. 13-82.

TABLE 13-26 Typical ASTM D 86 Test Results for Automobile Gasoline Pressure, 760 torr (101.3 kPa)

Percent recovered basis (as measured)			Percent evaporated basis (as corrected)		
Percent recovered	*T*, °F	Percent evaporated	Percent evaporated	*T*, °F	Percent recovered
0(IBP)	98	1.5	1.5	98	(IBP)
5	114	6.5	5	109	3.5
10	120	11.5	10	118	8.5
20	150	21.5	20	146	18.5
30	171	31.5	30	168	28.5
40	193	41.5	40	190	38.5
50	215	51.5	50	212	48.5
60	243	61.5	60	239	58.5
70	268	71.5	70	264	68.5
80	300	81.5	80	295	78.5
90	340	91.5	90	334	88.5
95	368	96.5	95	360	93.5
EP	408			408	(EP)

NOTE: Percent recovery = 97.5; percent residue = 1.0; percent loss = 1.5. To convert degrees Fahrenheit to degrees Celsius, °C = (°F − 32)/1.8.

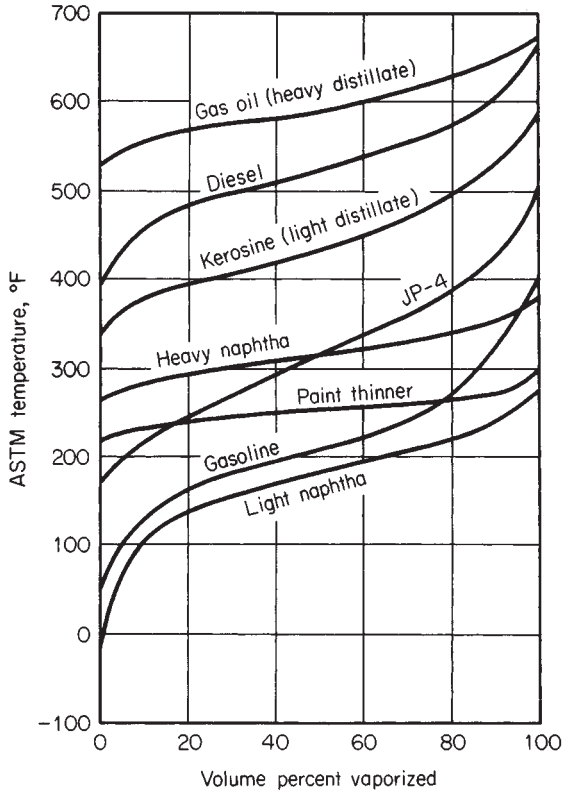

FIG. 13-82 Representative ASTM D 86 distillation curves.

Data from a true-boiling-point (TBP) distillation test provides a much better theoretical basis for characterization. If the sample contains compounds that have moderate differences in boiling points such as in a light gasoline containing light hydrocarbons (e.g., isobutane, *n*-butane, isopentane, etc.), a plot of overhead-vapor-distillate temperature versus percent distilled in a TBP test would appear in the form of steps as in Fig. 13-83. However, if the sample has a higher average boiling range when the number of close-boiling isomers increases, the steps become indistinct and a TBP curve such as that in Fig. 13-84 results. Because the degree of separation for a TBP distillation test is much higher than for an ASTM distillation test, the IBP is lower and the EP is higher for the TBP method as compared with the ASTM method, as shown in Fig. 13-84.

A standard TBP laboratory-distillation-test method has not been well accepted. Instead, as discussed by Nelson (op. cit., pp. 95–99),

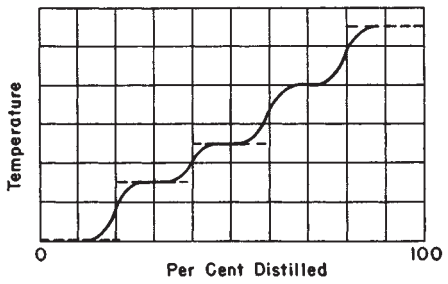

FIG. 13-83 Variation of boiling temperature with percent distilled in true-boiling-point distillation of light hydrocarbons.

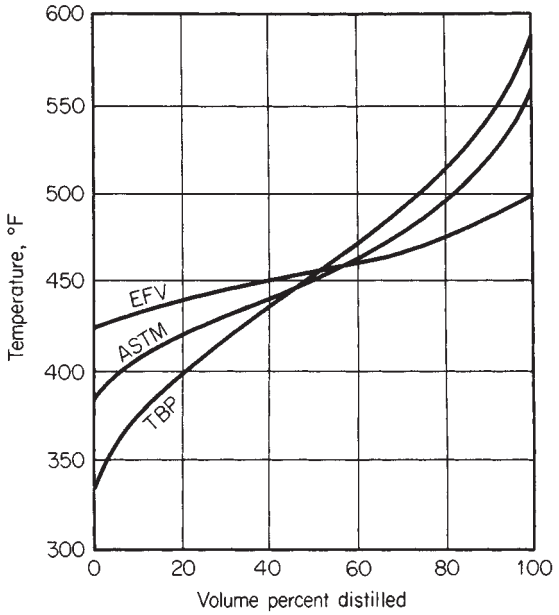

FIG. 13-84 Comparison of ASTM, TBP, and EFV distillation curves for kerosine.

batch distillation equipment that can achieve a good degree of fractionation is usually considered suitable. In general, TBP distillations are conducted in columns with 15 to 100 theoretical stages at reflux ratios of 5 or greater. Thus, the new ASTM D 2892 test method, which involves a column with from 14 to 17 theoretical stages and a reflux ratio of 5, essentially meets the minimum requirements. Distillate may be collected at a constant or a variable rate. Operation may be at 101.3-kPa (760 torr) pressure or at a vacuum at the top of the column as low as 0.067 kPa (0.5 torr) for high-boiling fractions, with 1.3 kPa (10 torr) being common. Results from vacuum operation are extrapolated to 101.3 kPa (760 torr) by the vapor-pressure correlation of Maxwell and Bonner [*Ind. Eng. Chem.,* **49,** 1187 (1957)], which is given in great detail in the API *Technical Data Book—Petroleum Refining* (op. cit.) and in the ASTM D 2892 test method. It includes a correction for the nature of the sample (paraffin, olefin, napthene, and aromatic content) in terms of the UOP characterization factor, UOP-K, as given by

$$\text{UOP-K} = (T_B)^{1/3}/\text{SG} \qquad (13\text{-}132)$$

where T_B = mean average boiling point, °R, which is the arithmetic average of the molal average boiling point and the cubic volumetric average boiling point. Values of UOP-K for *n*-hexane, 1-hexene, cyclohexene, and benzene are 12.82, 12.49, 10.99, and 9.73 respectively. Thus, paraffins with their lower values of specific gravity tend to have high values, and aromatics tend to have low values of UOP-K. A movement toward an international TBP standard is discussed by Vercier and Mouton [*Oil Gas J.,* **77**(38), 121 (1979)].

A crude-oil assay always includes a whole crude API gravity and a TBP curve. As discussed by Nelson (op. cit., pp. 89–90) and as shown in Fig. 13-85, a reasonably consistent correlation (based on more than 350 distillation curves) exists between whole crude API gravity and the TBP distillation curve at 101.3 kPa (760 torr). Exceptions not correlated by Fig. 13-85 are highly paraffinic or naphthenic crude oils.

An alternative to TBP distillation is simulated distillation by gas chromatography. As described by Green, Schmauch, and Worman [*Anal. Chem.,* **36,** 1512 (1965)] and Worman and Green [*Anal. Chem.,* **37,** 1620 (1965)], the method is equivalent to a 100-theoretical-plate TBP distillation, is very rapid, reproducible, and easily automated, requires only a small microliter sample, and can better define initial and final boiling points. The ASTM D 2887 standard test method is based on such a simulated distillation and is applicable to samples having a boiling range greater than 55°C (100°F) for temperature determinations as high as 538°C (1000°F). Typically, the test is conducted with a gas chromatograph having a thermal-conductivity detector, a programmed temperature capability, helium or hydrogen carrier gas, and column packing of silicone gum rubber on a crushed-fire-brick or diatomaceous-earth support.

It is important to note that simulated distillation does not always separate hydrocarbons in the order of their boiling point. For example, high-boiling multiple-ring-type compounds may be eluted earlier than normal paraffins (used as the calibration standard) of the same boiling point. Gas chromatography is also used in the ASTM D 2427 test method to determine quantitatively ethane through pentane hydrocarbons.

A third fundamental type of laboratory distillation, which is the most tedious to perform of the three types of laboratory distillations, is equilibrium-flash distillation (EFV), for which no standard test exists. The sample is heated in such a manner that the total vapor produced remains in contact with the total remaining liquid until the desired temperature is reached at a set pressure. The volume percent vaporized at these conditions is recorded. To determine the complete flash curve, a series of runs at a fixed pressure is conducted over a range of temperature sufficient to cover the range of vaporization from 0 to 100 percent. As seen in Fig. 13-84, the component separation achieved by an EFV distillation is much less than by the ASTM or TBP distillation tests. The initial and final EFV points are the bubble point and the dew point respectively of the sample. If desired, EFV curves can be established at a series of pressures.

Because of the time and expense involved in conducting laboratory distillation tests of all three basic types, it has become increasingly common to use empirical correlations to estimate the other two distillation curves when either the ASTM, TBP, or EFV curve is available. Preferred correlations given in the API *Technical Data Book—Petroleum Refining* (op. cit.) are based on the work of Edmister and Pollock [*Chem. Eng. Prog.,* **44,** 905 (1948)], Edmister and Okamoto [*Pet. Refiner,* **38**(8), 117 (1959); **38**(9), 271 (1959)], Maxwell (*Data Book on*

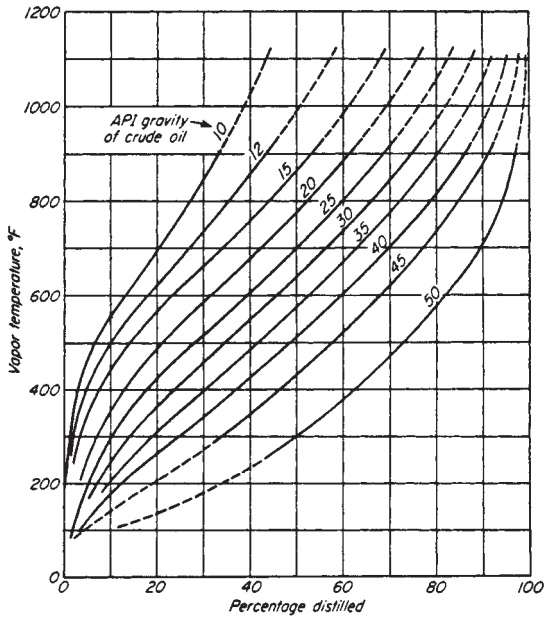

FIG. 13-85 Average true-boiling-point distillation curves of crude oils. (*From W. E. Edmister,* Applied Hydrocarbon Thermodynamics, *vol. 1, 1st ed., 1961 Gulf Publishing Company, Houston, Texas, Used with permission. All rights reserved.*)

Hydrocarbons, Van Nostrand, Princeton, N.J., 1950), and Chu and Staffel [*J. Inst. Pet.,* **41,** 92 (1955)]. Because of the lack of sufficiently precise and consistent data on which to develop the correlations, they are, at best, first approximations and should be used with caution. Also, they do not apply to mixtures containing only a few components of widely different boiling points. Perhaps the most useful correlation of the group is Fig. 13-86 for converting between ASTM D 86 and TBP distillations of petroleum fractions at 101.3 kPa (760 torr). The ASTM D 2889 test method, which presents a standard method for calculating EFV curves from the results of an ASTM D 86 test for a petroleum fraction having a 10 to 90 volume percent boiling range of less than 55°C (100°F), is also quite useful.

APPLICATIONS OF PETROLEUM DISTILLATION

Typical equipment configurations for the distillation of crude oil and other complex hydrocarbon mixtures in a crude unit, a catalytic-cracking unit, and a delayed-coking unit of a petroleum refinery are shown in Figs. 13-87, 13-88, and 13-89. The initial separation of crude oil into fractions is conducted in two main columns, shown in Fig. 13-87. In the first column, called the atmospheric tower or topping still, partially vaporized crude oil, from which water, sediment, and salt have been removed, is mainly rectified, at a feed-tray pressure of no more than about 276 kPa (40 psia), to yield a noncondensable light-hydrocarbon gas, a light naphtha, a heavy naphtha, a light distillate (kerosine), a heavy distillate (diesel oil), and a bottoms residual of components whose TBP exceeds approximately 427°C (800°F). Alternatively, other fractions, shown in Fig. 13-82, may be withdrawn. To control the IBP of the ASTM D 86 curves, each of the sidestreams of the atmospheric tower and the vacuum and main fractionators of Figs. 13-87, 13-88, and 13-89 may be sent to side-cut strippers, which use a partial reboiler or steam stripping. Additional stripping by steam is commonly used in the bottom of the atmospheric tower as well as in the vacuum tower and other main fractionators.

Additional distillate in the TBP range of approximately 427 to 593°C (800 to 1100°F) is recovered from bottoms residuum of the atmospheric tower by rectification in a vacuum tower, also shown in Fig. 13-87, at the minimum practical overhead condenser pressure, which is typically 1.3 kPa (10 torr). Use of special low-pressure-drop trays or column packing permits feed-tray pressure to be approximately 5.3 to 6.7 kPa (40 to 50 torr) to obtain the maximum degree of vaporization. Vacuum towers may be designed or operated to produce several different products including heavy distillates, gas-oil feedstocks for catalytic cracking, lubricating oils, bunker fuel, and bottoms residua of asphalt (5 to 8° API gravity) or pitch (0 to 5° API gravity). The catalytic-cracking process of Fig. 13-88 produces a superheated vapor at approximately 538°C (1000°F) and 172 to 207 kPa (25 to 30 psia) of a TBP range that covers hydrogen to compounds with normal boiling points above 482°C (900°F). This gas is sent directly to a main fractionator for rectification to obtain products that are typically gas and naphtha [204°C (400°F) ASTM EP approximately], which are often fractionated further to produce relatively pure light hydrocarbons and gasoline; a light cycle oil [typically 204 to 371°C (400 to 700°F) ASTM D 86 range], which may be used for heating oil, hydrocracked, or recycled to the catalytic cracker; an intermediate cycle oil [typically 371 to 482°C (700 to 900°F) ASTM D 86 range], which is generally recycled to the catalytic cracker to extinction; and a heavy gas oil or bottom slurry oil.

Vacuum-column bottoms, bottoms residuum from the main fractionation of a catalytic cracker, and other residua can be further processed at approximately 510°C (950°F) and 448 kPa (65 psia) in a delayed coker unit, as shown in Fig. 13-89 to produce petroleum coke and gas of TBP range that covers methane (with perhaps a small amount of hydrogen) to compounds with normal boiling points that may exceed 649°C (1200°F). The gas is sent directly to a main fractionator that is similar to the type used in conjunction with a catalytic cracker, except that in the delayed-coking operation the liquid to be coked first enters into and passes down through the bottom trays of the main fractionator to be preheated by and to scrub coker vapor of entrained coke particles and condensables for recycling to the delayed coker. Products produced from the main fractionator are similar, except for more unsaturated cyclic compounds, to those produced in a catalytic-cracking unit and include gas and coker naphtha, which are further processed to separate out light hydrocarbons and a coker naphtha that generally needs hydrotreating; and light and heavy coker gas oils, both of which may require hydrocracking to become suitable blending stocks.

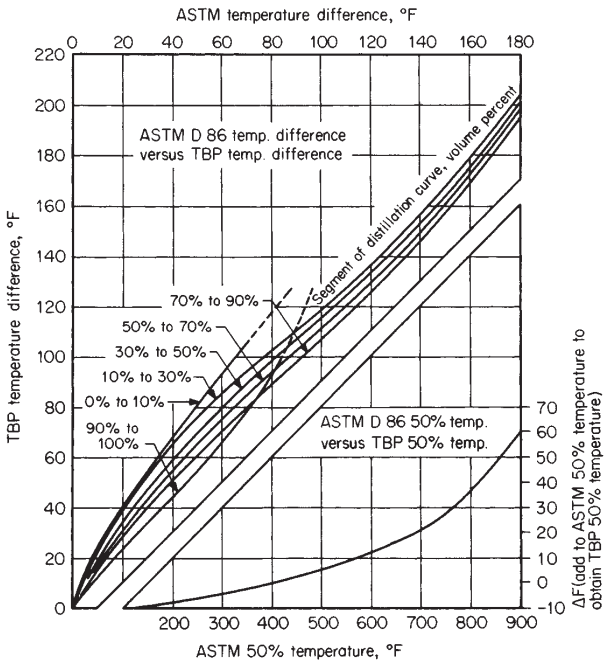

FIG. 13-86 Relationship between ASTM and TBP distillation curves. (*From W. C. Edmister,* Applied Hydrocarbon Thermodynamics, *vol. 1, 1st ed., 1961 Gulf Publishing Company, Houston, Texas. Used with permission. All rights reserved.*)

DESIGN PROCEDURES

Two general procedures are available for designing fractionators that process petroleum, synthetic crude oils, and complex mixtures. The first, which was originally developed for crude units by Packie [*Trans. Am. Inst. Chem. Eng. J.,* **37,** 51 (1941)], extended to main fractionators by Houghland, Lemieux, and Schreiner [*Proc. API,* sec. III, *Refining,* 385 (1954)], and further elaborated and described in great detail by Watkins (op. cit.), utilizes material and energy balances, with empirical correlations to establish tray requirements, and is essentially a hand-calculation procedure that is a valuable learning experience and is suitable for preliminary designs. Also, when backed by sufficient experience from previous designs, this procedure is adequate for final design.

In the second procedure, which is best applied with a digital computer, the complex mixture being distilled is represented by actual components at the light end and by perhaps 30 pseudo components (e.g., petroleum fractions) over the remaining portion of the TBP distillation curve for the column feed. Each of the pseudo components is characterized by a TBP range, an average normal boiling point, an average API gravity, and an average molecular weight. Rigorous material-balance, energy-balance, and phase equilibrium calculations are then made by an appropriate equation-tearing method as shown by Cecchetti et al. [*Hydrocarbon Process.,* **42**(9), 159 (1963)] or a simultaneous-correction procedure as shown, e.g., by Goldstein and Stanfield [*Ind. Eng. Chem. Process Des. Dev.,* **9,** 78 (1970) and Hess et al. [*Hydrocarbon Process.,* **56**(5), 241 (1977)]. Highly developed procedures of the latter type, suitable for preliminary or final design are included in most com-

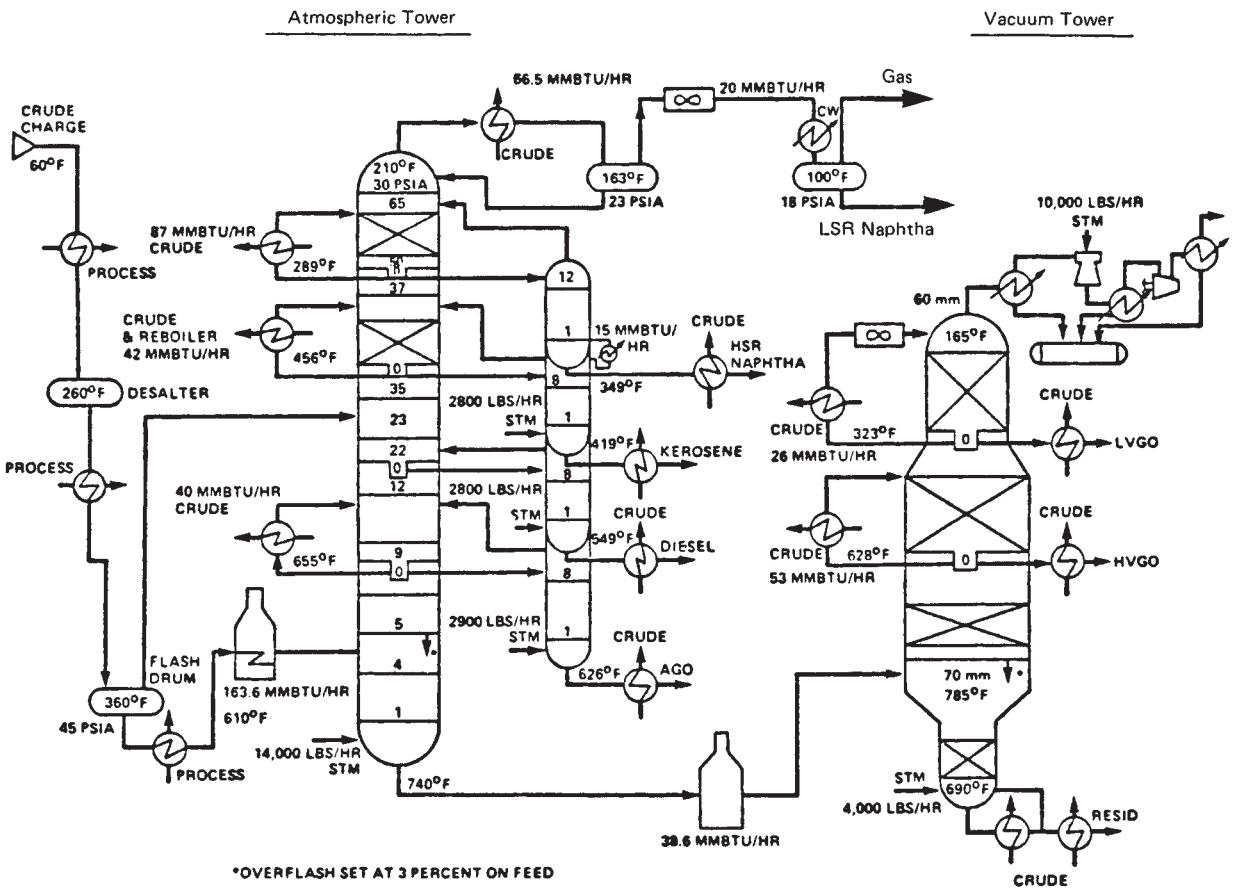

FIG. 13-87 Crude unit with atmospheric and vacuum towers. [*Kleinschrodt and Hammer, "Exchange Networks for Crude Units".* Chem. Eng. Prog., **79**(7), *33 (1983).*]

puter-aided steady-state process design and simulation programs as a special case of interlinked distillation, wherein the crude tower or fractionator is converged simultaneously with the sidecut-stripper columns.

Regardless of the procedure used, certain initial steps must be taken for the determination or specification of certain product properties and yields based on the TBP distillation curve of the column feed, method of providing column reflux, column-operating pressure, type of condenser, and type of side-cut strippers and stripping requirements. These steps are developed and illustrated with several detailed examples by Watkins (op. cit.). Only one example, modified from one given by Watkins, is considered briefly here to indicate the approach taken during the initial steps.

For the atmospheric tower shown in Fig. 13-90, suppose distillation specifications are as follows:

Feed: 50,000 bbl (at 42 U.S. gal each) per stream day (BPSD) of 31.6° API crude oil.

Measured light-ends analysis of feed:

Component	Volume percent of crude oil
Ethane	0.04
Propane	0.37
Isobutane	0.27
n-Butane	0.89
Isopentane	0.77
n-Pentane	1.13
	3.47

Measured TBP and API gravity of feed, computed atmospheric pressure EFV (from API *Technical Data Book*), and molecular weight of feed:

Volume percent vaporized	TBP, °F	EFV, °F	°API	Molecular weight
0	–130	179		
5	148	275	75.0	91
10	213	317	61.3	106
20	327	394	50.0	137
30	430	468	41.8	177
40	534	544	36.9	223
50	639	619	30.7	273
60	747	696	26.3	327
70	867	777	22.7	392
80	1013	866	19.1	480

Product specifications:

	ASTM D 86, °F		
Desired cut	5%	50%	95%
Overhead (*OV*)			253
Heavy naphtha (*HN*)	278	314	363
Light distillate (*LD*)	398	453	536
Heavy distillate (*HD*)	546	589	
Bottoms (*B*)			

NOTE: To convert degrees Fahrenheit to degrees Celsius, °C = (°F – 32)/1.8.

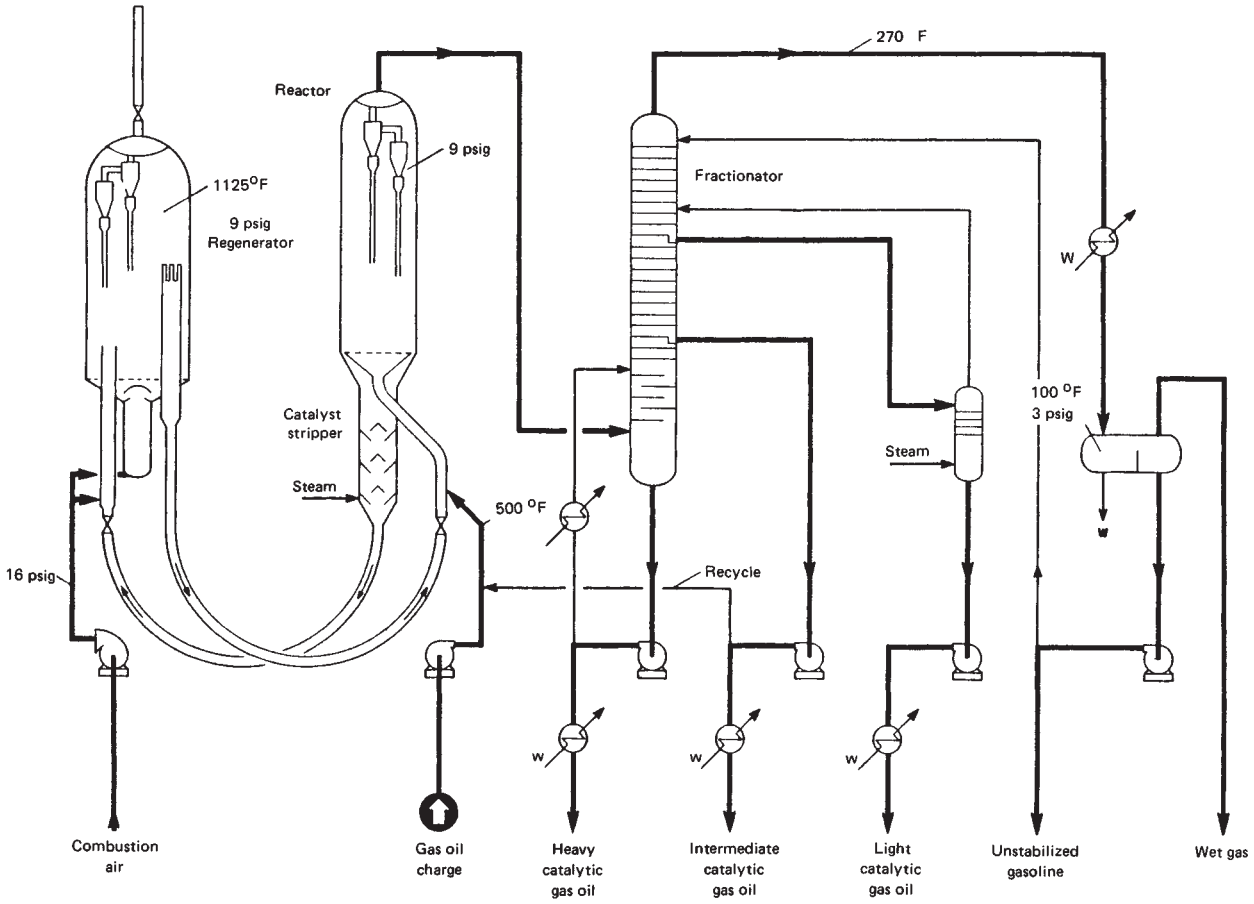

FIG. 13-88 Catalytic cracking unit. (New Horizons, *Lummus Co., New York, 1954.*)

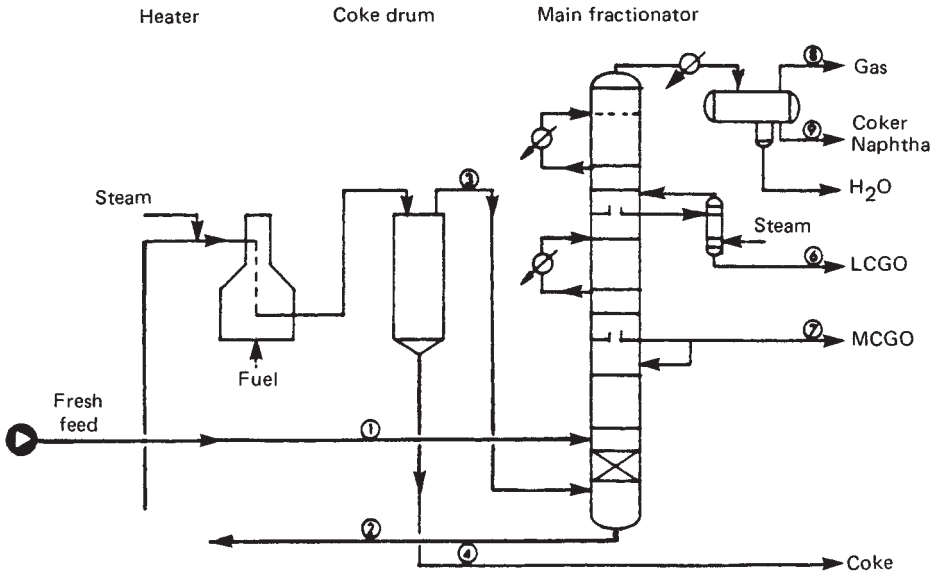

FIG. 13-89 Delayed-coking unit. (*Watkins,* Petroleum Refinery Distillation, *2nd ed., Gulf, Houston, 1979.*)

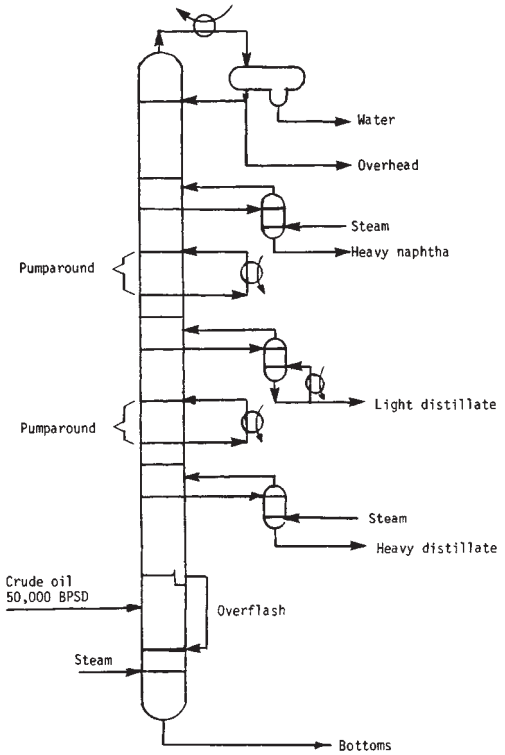

FIG. 13-90 Crude atmospheric tower.

TBP cut point between the heavy distillate and the bottoms = 650°F.
Percent overflash = 2 volume percent of feed.
Furnace outlet temperature = 343°C (650°F) maximum.
Overhead temperature in reflux drum = 49°C (120°F) minimum.

From the product specifications, distillate yields are computed as follows: From Fig. 13-86 and the ASTM D 86 50 percent temperatures, TBP 50 percent temperatures of the three intermediate cuts are obtained as 155, 236, and 316°C (311, 456, and 600°F) for the *HN*, *LD*, and *HD* respectively. The TBP cut points, corresponding volume fractions of crude oil, and flow rates of the four distillates are readily obtained by starting from the specified 343°C (650°F) cut point as follows, where *CP* is the cut point and *T* is the TBP temperature (°F):

$$CP_{HD,B} = 650°\text{F}$$

$$(CP_{HD,B} - T_{HD_{50}}) = 650 - 600 = 50°\text{F}$$

$$CP_{LD,HD} = T_{HD_{50}} - 50 = 600 - 50 = 550°\text{F}$$

$$(CP_{LD,HD} - T_{LD_{50}}) = 550 - 456 = 94°\text{F}$$

$$CP_{HN,LD} = T_{LD_{50}} - 94 = 456 - 94 = 362°\text{F}$$

$$(CP_{HN,LD} - T_{HN_{50}}) = 362 - 311 = 51°\text{F}$$

$$CP_{OV,HN} = T_{HN_{50}} - 51 = 311 - 51 = 260°\text{F}$$

These cut points are shown as vertical lines on the crude-oil TBP plot of Fig. 13-91, from which the following volume fractions and flow rates of product cuts are readily obtained:

Desired cut	Volume percent of crude oil	BPSD
Overhead (*OV*)	13.4	6,700
Heavy naphtha (*HN*)	10.3	5,150
Light distillate (*LD*)	17.4	8,700
Heavy distillate (*HD*)	10.0	5,000
Bottoms (*B*)	48.9	24,450
	100.0	50,000

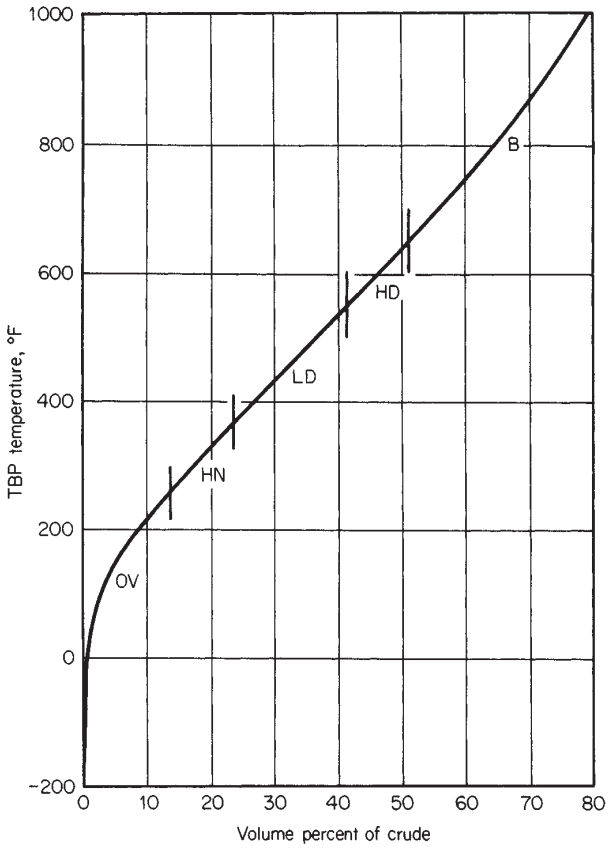

FIG. 13-91 Example of crude-oil TBP cut points.

As shown in Fig. 13-92, methods of providing column reflux include (*a*) conventional top-tray reflux, (*b*) pump-back reflux from side-cut strippers, and (*c*) pump-around reflux. The latter two methods essentially function as intercondenser schemes that reduce the top-tray-reflux requirement. As shown in Fig. 13-93 for the example being considered, the internal-reflux flow rate decreases rapidly from the top tray to the feed-flash zone for case *a*. The other two cases, particularly case *c*, result in better balancing of the column-reflux traffic. Because of this and the opportunity provided to recover energy at a moderate- to high-temperature level, pump-around reflux is the most commonly used technique. However, not indicated in Fig. 13-93 is the fact that in cases *b* and *c* the smaller quantity of reflux present in the upper portion of the column increases the tray requirements. Furthermore, the pump-around circuits, which extend over three trays each, are believed to be equivalent for mass-transfer purposes to only one tray each. Representative tray requirements for the three cases are included in Fig. 13-92. In case *c* heat-transfer rates associated with the two pump-around circuits account for approximately 40 percent of the total heat removed in the overhead condenser and from the two pump-around circuits combined.

Bottoms and three side-cut strippers remove light ends from products and may utilize steam or reboilers. In Fig. 13-92 a reboiled stripper is utilized on the light distillate, which is the largest side cut withdrawn. Steam-stripping rates in side-cut strippers and at the bottom of the atmospheric column may vary from 0.45 to 4.5 kg (1 to 10 lb) of steam per barrel of stripped liquid, depending on the fraction of stripper feed liquid that is vaporized.

Column pressure at the reflux drum is established so as to condense totally the overhead vapor or some fraction thereof. Flash-zone pressure is approximately 69 kPa (10 psia) higher. Crude-oil feed temper-

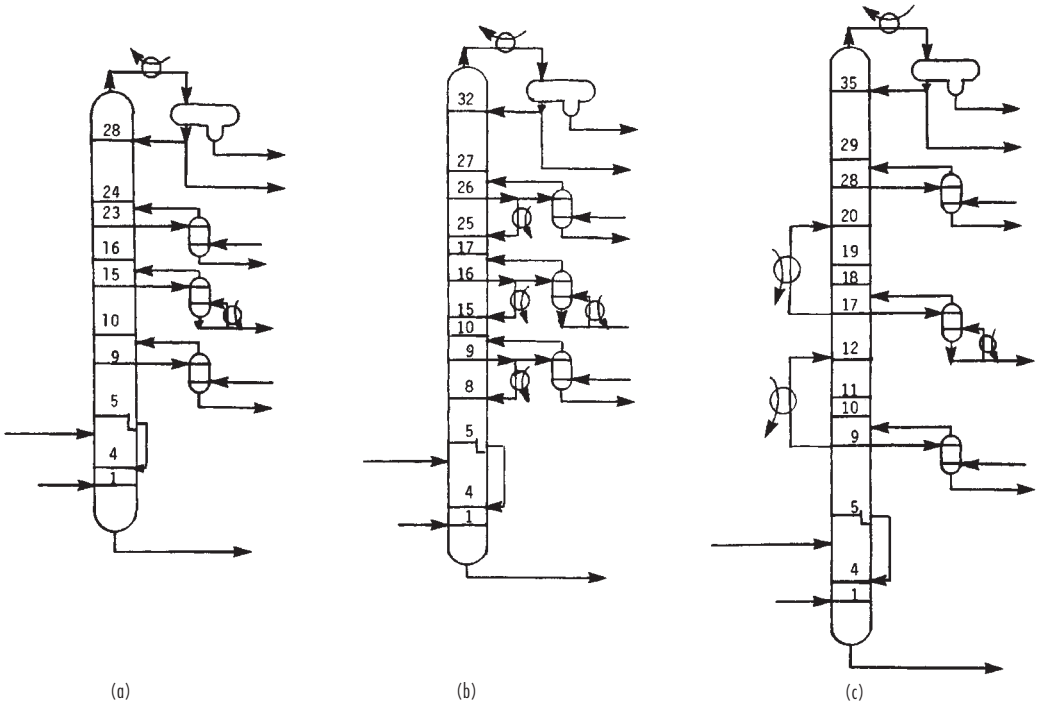

FIG. 13-92 Methods of providing reflux to crude units. (*a*) Top reflux. (*b*) Pump-back reflux. (*c*) Pump-around reflux.

ature at flash-zone pressure must be sufficient to vaporize the total distillates plus the overflash, which is necessary to provide reflux between the lowest sidestream-product draw-off tray and the flash zone. Calculations are made by using the crude-oil EFV curve corrected for pressure. For the example being considered, percent vaporized at the flash zone must be 53.1 percent of the feed.

Tray requirements depend on internal-reflux ratios and ASTM 5-95 gaps or overlaps, and may be estimated by the correlation of Packie (op. cit.) for crude units and the correlation of Houghland, Lemieux, and Schreiner (op. cit.) for main fractionators.

Example 9: Simulation Calculation of an Atmospheric Tower The ability of a rigorous calculation procedure to simulate operation of an atmospheric tower with its accompanying side-cut strippers may be illustrated by comparing commercial-test data from an actual operation with results computed with the REFINE program of ChemShare Corporation, Houston, Texas. The tower configuration and plant-operating conditions are shown in Fig. 13-94. Light-component analysis and the TBP and API gravity for the feed are given in Table 13-27. Representation of this feed by pseudocomponents is given in Table 13-28 based on 16.7°C (30°F) cuts from 82 to 366°C (180°F to 690°F), followed by 41.7°C (75°F) and then 55.6°C (100°F) cuts. Actual tray numbers are shown in Fig. 13-94. Corresponding theoretical-stage numbers, which were determined by trial and error to obtain a reasonable match of computed- and measured-product TBP distillation curves, are shown in parentheses. Overall tray efficiency appears to be approximately 70 percent for the tower and 25 to 50 percent for the side-cut strippers.

Results of rigorous calculations and comparison to plant data, when possible, are shown in Figs. 13-95, 13-96, and 13-97. Plant temperatures are in good

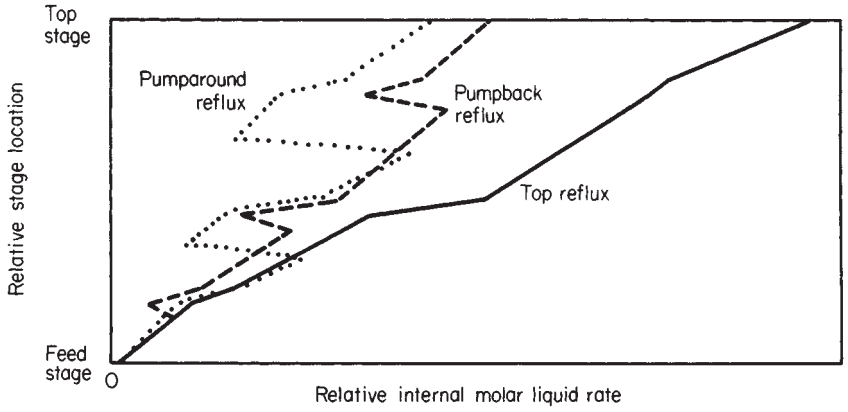

FIG. 13-93 Comparison of internal-reflux rates for three methods of providing reflux.

TABLE 13-27 Light-Component Analysis and TBP Distillation of Feed for the Atmospheric Crude Tower of Fig. 13-94

Light-component analysis	
Component	Volume percent
Methane	0.073
Ethane	0.388
Propane	0.618
n-Butane	0.817
n-Pentane	2.05

TBP distillation of feed		
API gravity	TBP, °F	Volume percent
80	−160.	0.1
70	155.	5.
57.5	242.	10.
45.	377.	20.
36.	499.	30.
29.	609.	40.
26.5	707.	50.
23.	805.	60.
20.5	907.	70.
17.	1054.	80.
10.	1210.	90.
−4.	1303.	95.
−22.	1467	100.

NOTE: To convert degrees Fahrenheit to degrees Celsius, °C = (°F − 32)/1.8.

TABLE 13-28 Pseudo-Component Representation of Feed for the Atmospheric Crude Tower of Fig. 13-94

No.	Component name	Molecular weight	Specific gravity	API gravity	(lb·mol)/h
1	Water	18.02	1.0000	10.0	.00
2	Methane	16.04	.3005	339.5	7.30
3	Ethane	30.07	.3561	265.8	24.54
4	Propane	44.09	.5072	147.5	37.97
5	*n*-Butane	58.12	.5840	110.8	43.84
6	*n*-Pentane	72.15	.6308	92.8	95.72
7	131 ABP	83.70	.6906	73.4	74.31
8	180 ABP	95.03	.7152	66.3	66.99
9	210 ABP	102.23	.7309	62.1	65.83
10	240 ABP	109.78	.7479	57.7	70.59
11	270 ABP	118.52	.7591	54.9	76.02
12	300 ABP	127.69	.7706	52.1	71.62
13	330 ABP	137.30	.7824	49.4	67.63
14	360 ABP	147.33	.7946	46.6	64.01
15	390 ABP	157.97	.8061	44.0	66.58
16	420 ABP	169.37	.8164	41.8	63.30
17	450 ABP	181.24	.8269	39.6	59.92
18	480 ABP	193.59	.8378	37.4	56.84
19	510 ABP	206.52	.8483	35.3	59.05
20	540 ABP	220.18	.8581	33.4	56.77
21	570 ABP	234.31	.8682	31.5	53.97
22	600 ABP	248.30	.8804	29.2	52.91
23	630 ABP	265.43	.8846	28.5	54.49
24	660 ABP	283.37	.8888	27.7	51.28
25	690 ABP	302.14	.8931	26.9	48.33
26	742 ABP	335.94	.9028	25.2	109.84
27	817 ABP	387.54	.9177	22.7	94.26
28	892 ABP	446.02	.9288	20.8	74.10
29	967 ABP	509.43	.9398	19.1	50.27
30	1055 ABP	588.46	.9531	17.0	57.12
31	1155 ABP	665.13	.9829	12.5	50.59
32	1255 ABP	668.15	1.0658	1.3	45.85
33	1355 ABP	643.79	1.1618	−9.7	29.39
34	1436 ABP	597.05	1.2533	−18.6	21.19
		246.90	.8887	27.7	1922.43

NOTE: To convert (lb·mol)/h to (kg·mol)/h, multiply by 0.454.

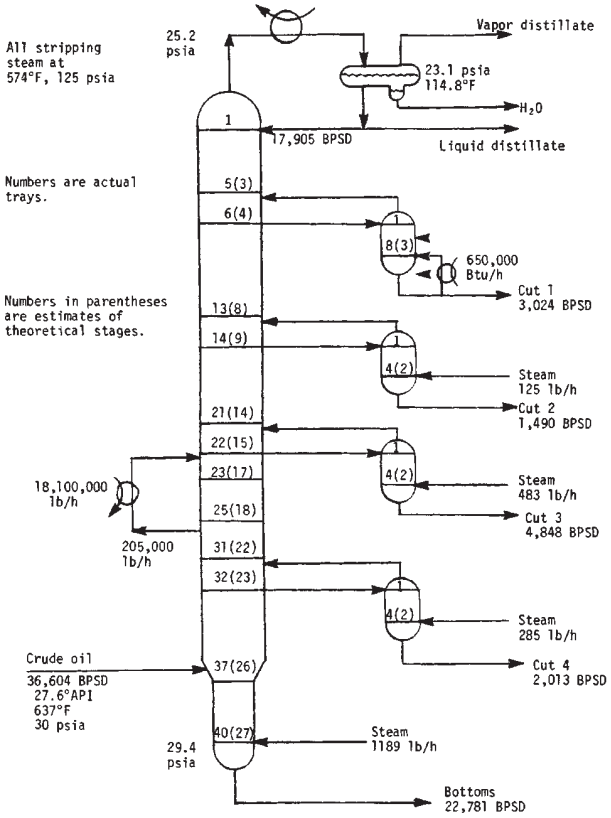

FIG. 13-94 Configuration and conditions for the simulation of the atmospheric tower of crude unit.

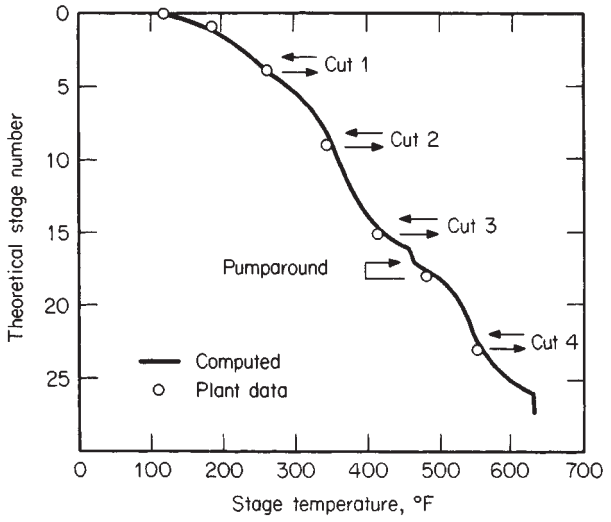

FIG. 13-95 Comparison of computed stage temperatures with plant data for the example of Fig. 13-94.

agreement with computed values in Fig. 13-95. Computed sidestream-product TBP distillation curves are in reasonably good agreement with values converted from plant ASTM distillations as shown in Fig. 13-96. Exceptions are the initial points of all four cuts and the higher-boiling end of the heavy-distillate curve. This would seem to indicate that more theoretical stripping stages should be added and that either the percent vaporization of the tower feed in the simulation is too high or the internal-reflux rate at the lower draw-off tray is too low. The liquid-rate profile in the tower is shown in Fig. 13-97. The use of two or three pump-around circuits instead of one would result in a better traffic pattern than that shown.

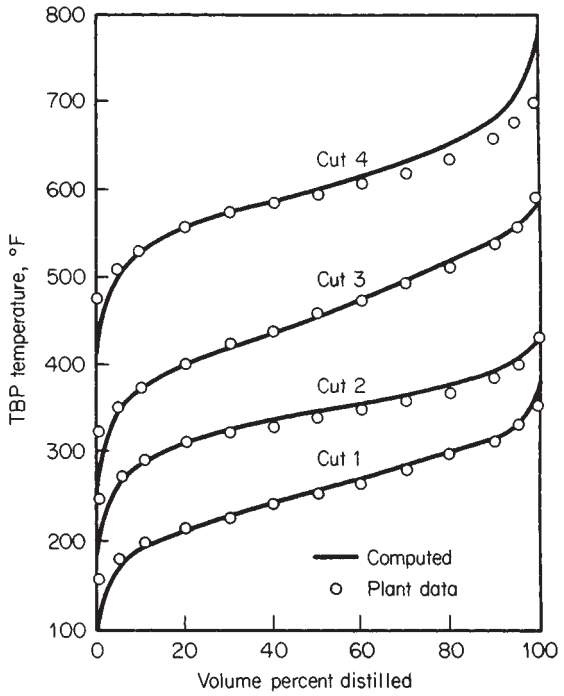

FIG. 13-96 Comparison of computed TBP curves with plant data for the example of Fig. 13-94.

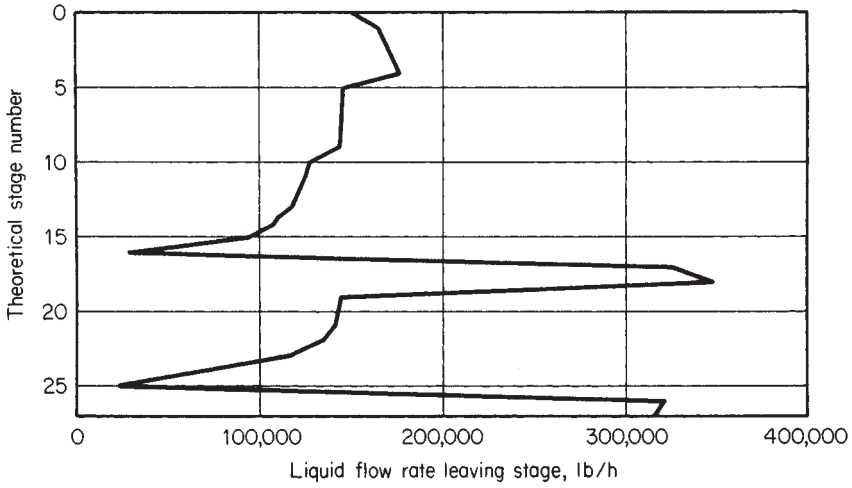

FIG. 13-97 Liquid-rate profile for the example of Fig. 13-94.

BATCH DISTILLATION

Batch distillation, which is the process of separating a specific quantity (the charge) of a liquid mixture into products, is used extensively in the laboratory and in small production units that may have to serve for many mixtures. When there are N components in the feed, one batch column will suffice where $N - 1$ simple continuous-distillation columns would be required.

Many larger installations also feature a batch still. Material to be separated may be high in solids content, or it might contain tars or resins that would plug or foul a continuous unit. Use of a batch unit can keep solids separated and permit convenient removal at the termination of the process.

SIMPLE BATCH DISTILLATION

The simplest form of batch still consists of a heated vessel (pot or boiler), a condenser, and one or more receiving tanks. No trays or packing are provided. Feed is charged into the vessel and brought to boiling. Vapors are condensed and collected in a receiver. No reflux is returned. The rate of vaporization is sometimes controlled to prevent "bumping" the charge and to avoid overloading the condenser, but other controls are minimal. This process is often referred to as Rayleigh distillation.

If we represent the moles of vapor by V, moles of liquid in the pot by M, the mole fraction of the more volatile component in this liquid by x, and the mole fraction of the same component in the vapor by y, a material balance yields

$$-y dV = d(Mx) \tag{13-133}$$

Since $dV = -dM$, substitution and expansion give

$$y dM = M\,dx + x dM \tag{13-134}$$

Rearranging and integrating give

$$\ln \frac{M_i}{M_f} = \int_{x_f}^{x_i} \frac{dx}{y - x} \tag{13-135}$$

where subscript i represents the initial condition and f the final condition of the liquid in the still pot. Integration limits have been reversed to obtain a positive integral. If equilibrium is assumed between liquid and vapor, the right-hand side of Eq. (13-135) may be evaluated by plotting $1/(y - x)$ versus x and measuring the area under the curve between limits x_i and x_f. If the mixture is a binary system for which relative volatility α is constant or if an average value that will serve for the range considered can be found, then the relationship that defines relative volatility,

$$\alpha = \frac{y/x}{(1 - y)/(1 - x)} \tag{13-136}$$

can be substituted into Eq. (13-135) and a direct integration can be made:

$$\ln\left(\frac{M_f}{M_i}\right) = \frac{1}{\alpha - 1} \ln\left[\frac{x_f(1 - x_i)}{x_i(1 - x_f)}\right] + \ln\left[\frac{1 - x_i}{1 - x_f}\right] \tag{13-137}$$

For any two components A and B of a multicomponent mixture, if constant α values are assumed for all pairs of components, $-dM_A/-dM_B = y_A/y_B = \alpha_{A,B}(x_A/x_B)$. When this is integrated, we obtain

$$\ln\left(\frac{M_{A(f)}}{M_{A(i)}}\right) = \alpha_{A,B} \ln\left(\frac{M_{B(f)}}{M_{B(i)}}\right) \tag{13-138}$$

where $M_{A(i)}$ and $M_{A(f)}$ are the moles of component A in the pot before and after distillation and $M_{B(i)}$ and $M_{B(f)}$ are the corresponding moles of component B.

A typical application of a simple batch still might be distillation of an ethanol-water mixture at 101.3 kPa (1 atm). The initial charge is 100 mol of ethanol at 18 mole percent, and the mixture must be reduced to a maximum ethanol concentration in the still of 6 mole percent. By using equilibrium data interpolated from Table 13-1,

x	y	$y - x$	$1/(y - x)$
0.18	0.517	0.337	2.97
.16	.502	.342	2.91
.14	.485	.345	2.90
.12	.464	.344	2.90
.10	.438	.338	2.97
.08	.405	.325	3.08
.06	.353	.293	3.41

Plotting $1/(y - x)$ versus x and integrating graphically between the limits of 0.06 and 0.18 for x, the area under the curve is found to be 0.358. Then, $\ln (M_i/M_j) = 0.358$, from which $M_j = 100/1.43 = 70.0$ mol. The liquid remaining consists of $(70.0)(0.06) = 4.2$ mol of ethanol and 65.8 mol of water. By material balance, the total distillate must contain $(18.0 - 4.2) = 13.8$ mol of alcohol and $(82 - 65.8) = 16.2$ mol of water. Total distillate is 30 mol, and distillate composition is $13.8/30 = 0.46$ mole fraction ethanol.

The simple batch still provides only one theoretical plate of separation. Its use is usually restricted to preliminary work in which products will be held for additional separation at a later time, when most of the volatile component must be removed from the batch before it is processed further, or for similar noncritical separations.

BATCH DISTILLATION WITH RECTIFICATION

To obtain products with a narrow composition range, a rectifying batch still is used that consists of a pot (or reboiler), a rectifying column, a condenser, some means of splitting off a portion of the condensed vapor (distillate) as reflux, and one or more receivers. Temperature of the distillate is controlled in order to return the reflux at or near the column temperature to permit a true indication of reflux quantity and to improve column operation. A subcooling heat exchanger is then used for the remainder of the distillate, which is sent to an accumulator or receiver. The column may also operate at elevated pressure or vacuum, in which case appropriate devices must be included to obtain the desired pressure. Equipment-design methods for batch-still components, except for the pot, follow the same principles as those presented for continuous units, but the design should be checked for each mixture if several mixtures are to be processed. It should also be checked at more than one point of a mixture, since composition in the column changes as distillation proceeds. Pot design is based on batch size and required vaporization rate.

In operation, a batch of liquid is charged to the pot and the system is first brought to steady state under total reflux. A portion of the overhead condensate is then continuously withdrawn in accordance with the established reflux policy. Cuts are made by switching to alternate receivers, at which time operating conditions may be altered. The entire column operates as an enriching section. As time proceeds, composition of the material being distilled becomes less rich in the more volatile components, and distillation of a cut is stopped when accumulated distillate attains the desired average composition.

CONTROL

The progress of batch distillation can be controlled in several ways:

1. *Constant reflux, varying overhead composition.* Reflux is set at a predetermined value at which it is maintained for the run. Since pot liquid composition is changing, instantaneous composition of the distillate also changes. The progress of a binary separation is illustrated in Fig. 13-98. Variation with time of instantaneous distillate composition for a typical multicomponent batch distillation is shown in Fig. 13-99. The shapes of the curves are functions of volatility, reflux ratio, and number of theoretical plates. Distillation is continued until the average distillate composition is at the desired value. In the case of a binary, the overhead is then diverted to another receiver, and an intermediate cut is withdrawn until the remaining pot liquor meets the required specification. The intermediate cut is usually added to

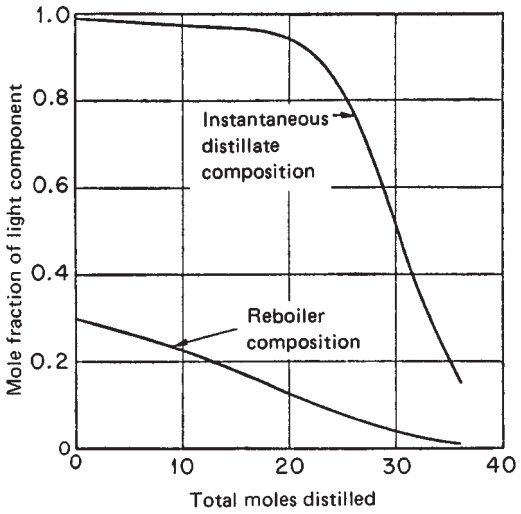

FIG. 13-98 Typical variation in distillate and reboiler compositions with amount distilled in binary batch distillation at a constant-reflux ratio.

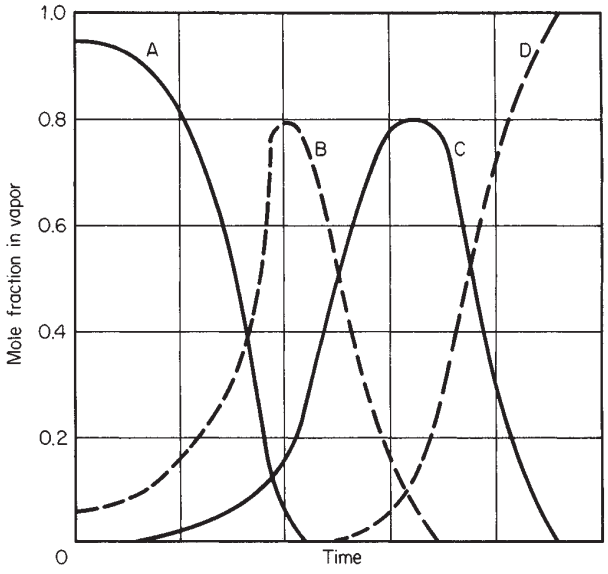

FIG. 13-99 Distillate composition profile for a batch distillation of a four-component mixture.

the next batch. For a multicomponent mixture, two or more intermediate cuts may be taken between product cuts.

2. *Constant overhead composition, varying reflux.* If it is desired to maintain a constant overhead composition in the case of a binary, the amount of reflux returned to the column must be constantly increased throughout the run. As time proceeds, the pot is gradually depleted of the lighter component. Finally, a point is reached at which the reflux ratio has attained a very high value. The receivers are then changed, the reflux is reduced, and an intermediate cut is taken as before. This technique can also be extended to a multicomponent mixture.

3. *Other control methods.* A cycling procedure can be used to set the pattern for column operation. The unit operates at total reflux until equilibrium is established. Distillate is then taken as total draw-off for a short period of time, after which the column is again returned to total-reflux operation. This cycle is repeated through the course of distillation. Another possibility is to optimize the reflux ratio in order to achieve the desired separation in a minimum of time. Complex operations may involve withdrawal of sidestreams, provision for intercondensers, addition of feeds to trays, and periodic charge addition to the pot.

APPROXIMATE CALCULATION PROCEDURES FOR BINARY MIXTURES

A useful method for a binary mixture employs an analysis based on the McCabe-Thiele graphical method. In addition to the usual assumptions of adiabatic column and equimolal overflow on the trays, the following procedure assumes negligible holdup of liquid on the trays, in the column, and in the condenser.

As a first step in the calculation, the minimum-reflux ratio should be determined. In Fig. 13-100, point D, representing the distillate, is on the diagonal since a total condenser is assumed and $x_D = y_D$. Point F represents the initial condition in the still pot with coordinates x_{pi}, y_{pi}. Minimum internal reflux is represented by the slope of the line DF,

$$(L/V)_{min} = (y_D - y_{pi})/(x_D - x_{pi}) \tag{13-139}$$

where L is the liquid flow rate and V is the vapor rate, both in moles per hour. Since $V = L + D$ (where D is distillate rate) and the external-reflux rate R is defined as $R = L/D$, then

$$L/V = R/(R + 1) \tag{13-140}$$

or

$$R_{min} = \frac{(L/V)_{min}}{1 - (L/V)_{min}} \tag{13-141}$$

The condition of minimum reflux for an equilibrium curve with an inflection point P is shown in Fig. 13-102. In this case the minimum internal reflux is

$$(L/V)_{min} = (y_D - y_P)/(x_D - x_P) \tag{13-142}$$

The operating reflux ratio is usually 1.5 to 10 times the minimum. By using the ethanol-water equilibrium curve for 101.3 kPa (1 atm) pressure shown in Fig. 13-101 but extending the line to a convenient point for readability, $(L/V)_{min} = (0.800 - 0.695)/(0.800 - 0.600) = 0.52$ and $R_{min} = 1.083$.

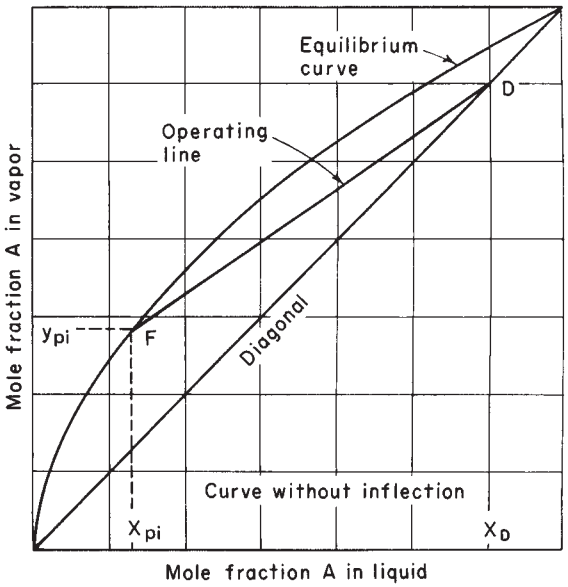

FIG. 13-100 Determination of minimum reflux for normal equilibrium curve.

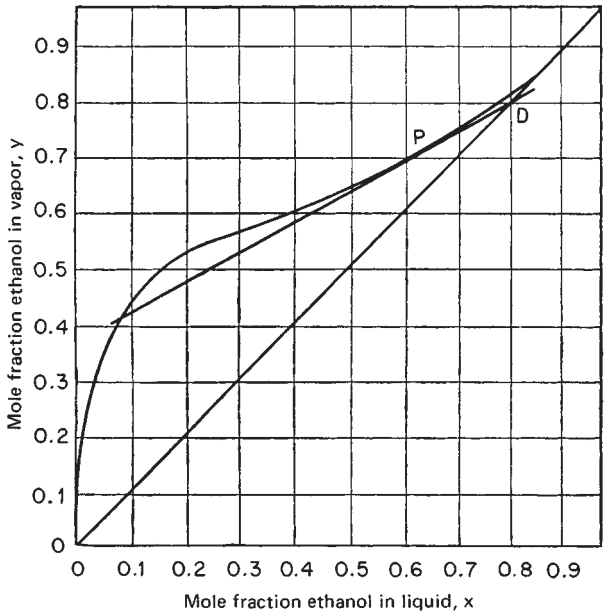

FIG. 13-101 Determination of minimum reflux for equilibrium curve with inflection.

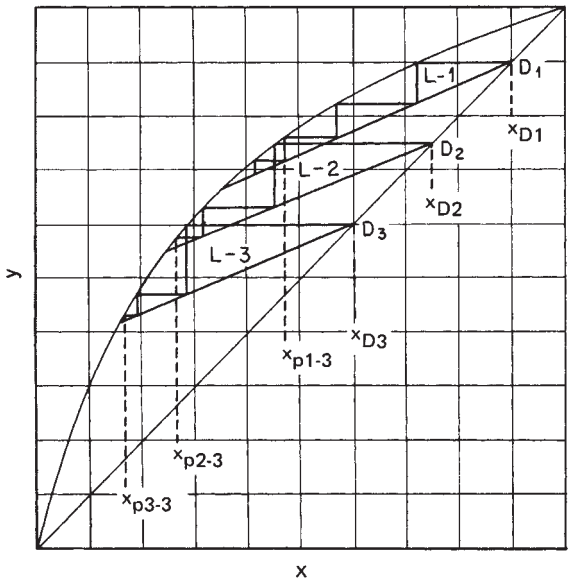

FIG. 13-102 Graphical method for constant-reflux operation.

OPERATING METHODS

Batch Rectification at Constant Reflux Using an analysis similar to the simple batch still, Smoker and Rose [*Trans. Am. Inst. Chem. Eng.*, **36,** 285 (1940)] developed the following equation:

$$\ln \frac{M_i}{M_f} = \int_{x_{pf}}^{x_{pi}} \frac{dx_p}{x_D - x_P} \tag{13-143}$$

An overall component balance gives the average or accumulated distillate composition $x_{D,\text{avg}}$

$$x_{D,\text{avg}} = \frac{M_i x_{pi} - M_f x_{pf}}{M_i - M_f} \tag{13-144}$$

If the integral on the right side of Eq. (13-143) is labeled Q, the time θ in hours for distillation can be found by

$$\theta = (R+1)\frac{M_i(e^Q - 1)}{Ve^Q} \tag{13-145}$$

An alternative equation is

$$\theta = \frac{R+1}{V}(M_i - M_f) \tag{13-146}$$

Development of these equations is given by Block [*Chem. Eng.*, **68,** 88 (Feb. 6, 1961)]. The calculation process is illustrated in Fig. 13-102. Operating lines are drawn with the same slope but intersecting the 45° line at different points. The number of theoretical plates under consideration is stepped off to find equilibrium bottoms composition. In the figure, operating line $L-1$ with slope L/V drawn from point D_1 where the distillate composition is x_{D1} has an equilibrium pot composition of $x_{p1\text{-}3}$ for three theoretical plates, x_{D2} has an equilibrium pot composition of $x_{p2\text{-}3}$, etc.; performing a graphical integration of the right side of Eq. (13-143) permits calculation of $x_{D,\text{avg}}$ from Eq. (13-144). An iterative calculation is required to find the M_f that corresponds to the specified $x_{D,\text{avg}}$.

To illustrate the use of these equations, consider a charge of 520 mol of an ethanol-water mixture containing 18 mole percent ethanol to be distilled at 101.3 kPa (1 atm). Vaporization rate is 75 mol/h, and the product specification is 80 mole percent ethanol. Let $L/V = 0.75$, corresponding to a reflux ratio $R = 3.0$. If the system has seven theoretical plates, with the pot considered as one of these plates, find how many moles of product will be obtained, what the composition of the residue will be, and the time that the distillation will take.

Using the vapor-liquid equilibrium data, plot a y-x diagram. Draw a number of operating lines at a slope of 0.75. Note the composition at the 45° intersection, and step off seven plates on each to find the equilibrium value of the bottoms. Some of the results are tabulated in the following table:

x_D	x_p	$x_D - x_p$	$1/(x_D - x_p)$
0.800	0.323	0.477	2.097
.795	.245	.550	1.820
.790	.210	.580	1.725
.785	.180	.605	1.654
.780	.107	.673	1.487
.775	.041	.734	1.362

Use a trial procedure by integrating between x_{pi} of 0.18 and various lower limits, and converge the procedure by graphing the results. It is found that $x_{D,\text{avg}} = 0.80$ when $x_{pf} = 0.04$, at which time the value of the integral = 0.205 = ln (M_i/M_f), so that $M_f = 424$ mol. Product = $M_i - M_f = 520 - 424 = 96$ mol. From Eq. (13-145),

$$\theta = \frac{(4)(520)(e^{0.205} - 1)}{(75)(e^{0.205})} = 5.2 \text{ h}$$

Batch Rectification at Constant Overhead Composition Bogart [*Trans. Am. Inst. Chem. Eng.*, **33,** 139 (1937)] developed the following equation for this situation with column holdup assumed to be negligible:

$$\theta = \frac{M_i(x_D - x_{pi})}{V}\int_{x_{pf}}^{x_{pi}} \frac{dx_p}{(1 - L/V)(x_D - x_p)^2} \tag{13-147}$$

where the terms are defined as before. The quantity distilled can then be found by

$$M_i - M_f = \frac{M_i(x_{pi} - x_{pf})}{x_D - x_{pf}} \tag{13-148}$$

The progress of a varying-reflux distillation is shown in Fig. 13-103. Distillate composition is held constant by increasing the reflux as pot composition becomes more dilute. Operating lines with varying slopes

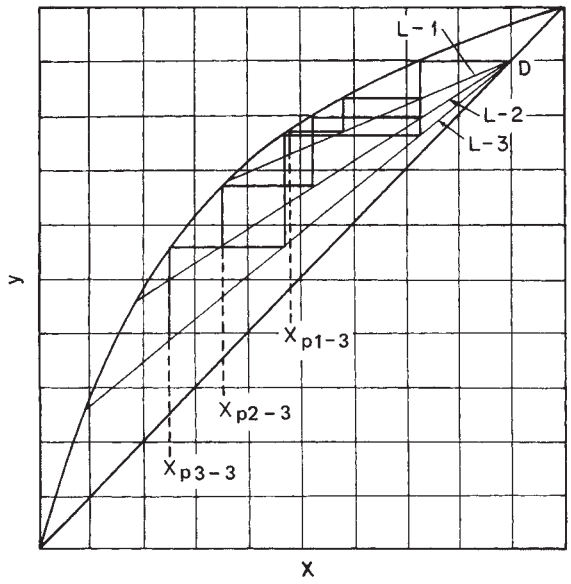

FIG. 13-103 Graphical method for constant-composition operation.

(= L/V) are drawn from the distillate composition, and the appropriate number of plates is stepped off to find the corresponding bottoms composition.

As an example, consider distilling at constant composition the same mixture that was used to illustrate constant reflux. The following table is compiled:

L/V	x_p	$x_D - x_p$	$1/(1 - L/V)(x_D - x_p)^2$
0.600	0.654	0.147	115.7
.700	.453	.348	27.5
.750	.318	.483	17.2
.800	.143	.658	11.5
.850	.054	.747	11.9
.900	.021	.780	16.4

If the right-hand side of Eq. (13-147) is integrated graphically by using a limit for x_{pf} of 0.04, the value of the integral is 1.615 and the time is

$$\theta = \frac{(520)(0.800 - 0.180)(1.615)}{75} = 7.0 \text{ h}$$

The quantity distilled can be found by Eq. (13-148):

$$M_i - M_f = \frac{(520)(0.180 - 0.040)}{0.800 - 0.040} = 96 \text{ mol}$$

Other Operating Methods A useful control method for difficult industrial or laboratory distillations is *cycling operation.* The most common form of cycling control is operating the column at total reflux until equilibrium is established, taking off the complete distillate for a short period of time, and then returning to total reflux. An alternative scheme is to interrupt vapor flow to the column periodically by the use of a solenoid-operated butterfly valve in the vapor line from the pot. In both cases, equations necessary to describe the system are very complex, as shown by Schrodt et al. [*Chem. Eng. Sci.*, **22,** 759 (1967)]. The most reliable method for establishing the cycle relationships is by experimental trial on an operating column. Several investigators have also proposed that batch distillation can be programmed to attain *time optimization* by proper variation of the reflux ratio. A comprehensive discussion is presented by Coward [*Chem. Eng. Sci.*, **22,** 503 (1967)].

The *choice of operating mode* depends upon characteristics of the specific system, the product specifications, and the engineer's preference in setting up a control sequence. Probably the most direct and most common method is *constant reflux.* Operation can be regulated by a timed reflux splitter, a ratio controller, or simply a pair of rotameters. Since composition is changing with time, some way must be found to estimate the average accumulated-distillate composition in order to define the end point. This is no problem when the specification is not critical or the change in distillate composition is sharply defined. When the composition of the distillate changes slowly with time, the cut point is more difficult to determine. Operating with *constant composition* (varying reflux), the specification is automatically achieved if control can be linked to concentration or some concentration-sensitive physical variable. The relative advantage, ratewise, of the two systems depends upon the materials being separated and upon the number of theoretical plates in the column. Results of a comparison of distillation rates by using the same initial and final pot composition for the system benzene-toluene are given in Fig. 13-104. Typical control instrumentation is presented in an article by Block [*Chem. Eng.*, **74,** 147 (Jan. 16, 1967)]. Control procedures for *reflux and vapor-cycling* operation and for the *time-optimal* process are largely a matter of empirical trial.

Effect of Column Holdup When the holdup of liquid on the trays and in the condenser is not negligible compared with the holdup in the pot, the distillate composition at constant-reflux ratio changes with time at a different rate than when the column holdup is negligible because of two separate effects. First, with an appreciable column holdup, composition of the charge to the pot will be higher in the light component than the pot composition at the start of the distillation; the reason for this is that before product takeoff begins, column holdup must be supplied, and its average composition is higher than that of the charge liquid from which it is supplied. Thus, when overhead takeoff begins, the pot composition is lower than it would be if there were no column holdup and separation is more difficult. The second effect of column holdup is to slow the rate of exchange of the components; the holdup exerts an inertia effect, which prevents compositions from changing as rapidly as they would otherwise, and the degree of separation is usually improved. As both these effects occur at the same time and change in importance during the course of distillation, it is difficult, without rigorous calculations, to predict whether the overall effect of holdup will be favorable or detrimental; it is equally difficult to estimate the magnitude of the holdup effect.

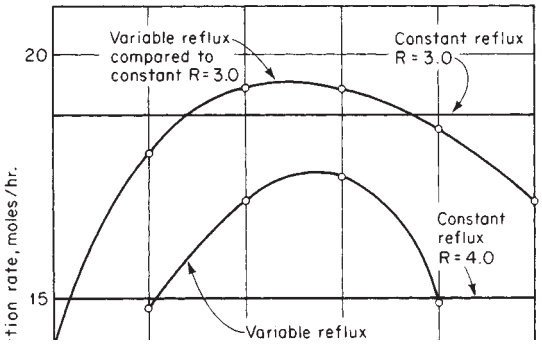

Although a number of studies were made and approximate methods developed for predicting the effect of liquid holdup in the period of the 1950s and 1960s, as summarized in the 6th edition of *Perry's Chemical Engineers' Handbook*, the complexity of the effect of liquid holdup is such that it is now best to use computer-based batch-distillation algorithms to determine the effect of holdup on a case-by-case basis.

SHORTCUT METHODS FOR MULTICOMPONENT BATCH RECTIFICATION

For preliminary studies of batch rectification of multicomponent mixtures, shortcut methods that assume constant molal overflow and negligible vapor and liquid holdup are useful. The method of Diwekar and Madhaven [*Ind. Eng. Chem. Res.*, **30,** 713 (1991)] can be used for constant reflux or constant overhead rate. The method of Sundaram and Evans [*Ind. Eng. Chem. Res.*, **32,** 511 (1993)] applies only to the case of constant reflux, but is easy to apply. Both methods employ the Fenske-Underwood-Gilliland (FUG) shortcut procedure at successive time steps. Thus, batch rectification is treated as a sequence of continuous, steady-state rectifications.

CALCULATIONAL METHODS

Rigorous Computer-Based Calculation Procedures It is obvious that a set of curves such as shown in Fig. 13-104 for a binary mixture is quite tedious to obtain by hand methods. The curves shown in Fig. 13-99 for a multicomponent batch distillation are extremely difficult to develop by hand methods. Therefore, since the early 1960s, when large digital computers became available, interest has been generated in developing rigorous calculation procedures for binary and multicomponent batch distillation. For binary mixtures of constant relative volatility, Huckaba and Danly [*Am. Inst. Chem. Eng. J.*, **6,** 335 (1960)] developed a computer program that assumed constant-mass tray holdups, adiabatic tray operation, and linear enthalpy relationships but did include energy balances around each tray and permitted use of nonequilibrium trays by means of specified tray efficiencies. Experimental data were provided to validate the simulation. Meadows [*Chem. Eng. Prog. Symp. Ser.* **46,** 59, 48 (1963)] presented a multicomponent-batch-distillation model that included equations for energy, material, and volume balances around theoretical trays. The only assumptions made were perfect mixing on each tray, negligible vapor holdup, adiabatic operation, and constant-volume tray holdup. Distefano [*Am. Inst. Chem. Eng. J.*, **14,** 190 (1968)] extended the model and developed a computer-based-solution procedure that was used to simulate successfully several commercial batch-distillation columns. Boston et al. [*Foundations of Computer-Aided Chemical Process Design*, vol. II, ed. by Mah and Seider, American Institute of Chemical Engineers, New York, 1981, p. 203) further extended the model, provided a variety of practical sets of specifications, and utilized modern numerical procedures and equation formulations to handle efficiently the nonlinear and often stiff nature of the multicomponent-batch-distillation problem. The simpler model of Distefano is used here to illustrate this nonlinear and stiff nature.

Consider the simple batch- or multicomponent-distillation operation in Fig. 13-105. The still consists of a pot or reboiler, a column with N theoretical trays or equivalent packing, and a condenser with an accompanying reflux drum. The mixture to be distilled is charged to the reboiler, to which heat is then supplied. Vapor leaving the top tray is totally condensed and drained into the reflux drum. Initially, no distillate is withdrawn from the system, but instead a total-reflux condition is established at a fixed overhead vapor rate. Then, starting at time $t = 0$, distillate is removed at a constant molal rate and sent to a receiver that is not shown in Fig. 13-105. Simultaneously, a fixed reflux ratio is established such that the overhead vapor rate is not changed from that at total reflux. Alternatively, heat input to the reboiler can be maintained constant and distillate rate allowed to vary accordingly. The equations of Distefano for a batch distillation operated in this manner are as follows (after minor rearrangement), where i,j refers to the ith of C components in the mixture and the fth of N theoretical plates.

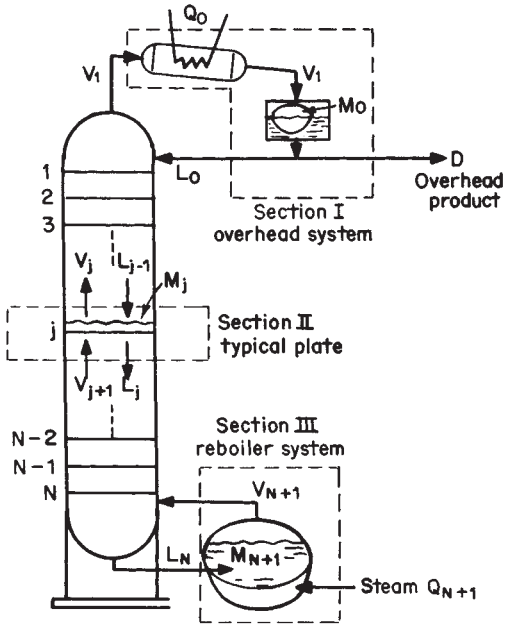

FIG. 13-105 Schematic of a batch-distillation column. [*Distefano,* Am. Inst. Chem. Eng. J., ***14,*** *190 (1963).*]

Component mole balances for total-condenser-reflux drum, trays, and reboiler, respectively:

$$\frac{dx_{i,0}}{dt} = -\left[\frac{L_0 + D + \dfrac{dM_0}{dt}}{M_0}\right] x_{i,0} + \left[\frac{V_1 K_{i,1}}{M_0}\right] x_{i,1} \qquad i = 1 \text{ to } C \quad (13\text{-}149)$$

$$\frac{dx_{i,j}}{dt} = \left(\frac{L_{j-1}}{M_j}\right) x_{i,j-1} - \left[\frac{L_j + K_{i,j}V_j + \dfrac{dM_j}{dt}}{M_j}\right] x_{i,j} + \left[\frac{K_{i,j+1}V_{j+1}}{M_j}\right] x_{i,j+1} \quad i = 1 \text{ to } C \quad j = 1 \text{ to } N \quad (13\text{-}150)$$

$$\frac{dx_{i,N+1}}{dt} = \left(\frac{L_N}{M_{N+1}}\right) x_{i,N} - \left[\frac{V_{N+1}K_{i,N+1} + \dfrac{dM_{N+1}}{dt}}{M_{N+1}}\right] x_{i,N+1} \qquad i = 1 \text{ to } C \quad (13\text{-}151)$$

where $L_0 = RD$.

Total mole balance for total-condenser-reflux drum and trays respectively:

$$V_1 = D(R+1) + \frac{dM_0}{dt} \quad (13\text{-}152)$$

$$L_j = V_{j+1} + L_{j-1} - V_j - \frac{dM_j}{dt} \qquad j = 1 \text{ to } N \quad (13\text{-}153)$$

Energy balance around jth tray:

$$V_{j+1} = \frac{1}{(H_{V_{j+1}} - H_{L_j})}\left[V_j(H_{V_j} - H_{L_j}) - L_{j-1}(H_{L_{j-1}} - H_{L_j}) + M_j\frac{dH_{L_j}}{dt}\right]$$

$$j = 2 \text{ to } N+1 \quad (13\text{-}154)$$

where H_V and H_L are molar vapor and liquid enthalpies respectively.

Phase equilibriums:

$$y_{i,j} = K_{i,j}x_{i,j} \qquad i = 1 \text{ to } C \qquad j = 1 \text{ to } N+1 \quad (13\text{-}155)$$

Mole-fraction sum:

$$\sum_i y_{i,j} = \sum_i K_{i,j}x_{i,j} = 1.0 \qquad j = 0 \text{ to } N+1 \quad (13\text{-}156)$$

Molar holdups in condenser-reflux drum, on trays, and in reboiler:

$$M_0 = G_0\rho_0 \quad (13\text{-}157)$$

$$M_j = G_j\rho_j \qquad j = 1 \text{ to } N$$

$$M_{N+1} = M^0_{N+1} - \sum_{j=0}^{N} M_j - \int_0^t D\,dt \quad (13\text{-}158)$$

where G is the constant-volume holdup, M^0_{N+1} is the initial molar charge to reboiler, and ρ is the liquid molar density.

Energy balances around condenser and reboiler respectively:

$$Q_0 = V_1(H_{V_1} - H_{L_0}) - M_0\frac{dH_{L_0}}{dt} \quad (13\text{-}159)$$

$$Q_{N+1} = V_{N+1}(H_{V_{N+1}} - H_{L_{N+1}}) - L_N(H_{L_N} - H_{L_{N+1}}) + M_{N+1}\left(\frac{dH_{L_{N+1}}}{dt}\right) \quad (13\text{-}160)$$

Equation (13-160) is replaced by the following overall energy-balance equation if Q_{N+1} is to be specified rather than D:

$$D = \frac{Q_{N+1} - H_{V_1}\left(\dfrac{dM_0}{dt}\right) - \displaystyle\sum_{j=1}^{N+1}\left(\frac{d(M_jH_{Lj})}{dt}\right)}{(R+1)H_{V_1} - RH_{L_0}} \quad (13\text{-}161)$$

With D and R specified, Eqs. (13-149) to (13-161) represent a coupled set of $(2CN + 3C + 4N + 7)$ equations constituting an initial-value problem in an equal number of time-dependent unknown variables, namely, $(CN + 2C)x_{i,j}$, $(CN + C)y_{i,j}$, $(N)L_j$, $(N + 1)V_j$, $(N + 2)T_j$, $(N + 2)M_j$, Q_0, and Q_{N+1}, where initial conditions at $t = 0$ for all unknown variables are obtained by determining the total-reflux steady-state condition for specifications on the number of theoretical stages, amount and composition of initial charge, volume holdups, and molar vapor rate leaving the top stage and entering the condenser.

Various procedures for solving Eqs. (13-149) to (13-161), ranging from a complete tearing method to solve the equations one at a time, as shown by Distefano, to a complete simultaneous method, have been studied. Regardless of the method used, the following considerations generally apply:

1. Derivatives or rates of change of tray and condenser-reflux drum liquid holdup with respect to time are sufficiently small compared with total flow rates that these derivatives can be approximated by incremental changes over the previous time step. Derivatives of liquid enthalpy with respect to time everywhere can be approximated in the same way. The derivative of the liquid holdup in the reboiler can likewise be approximated in the same way except when reflux ratios are low.

2. Ordinary differential Eqs. (13-149) to (13-151) for rates of change of liquid-phase mole fractions are nonlinear because the coefficients of $x_{i,j}$ change with time. Therefore, numerical methods of integration with respect to time must be employed. Furthermore, the equations may be difficult to integrate rapidly and accurately because they may constitute a so-called stiff system as considered by Gear (*Numerical Initial Value Problems in Ordinary Differential Equations,* Prentice Hall, Englewood Cliffs, N.J., 1971). The choice of time step for simple explicit numerical procedures (such as the Euler and Runge-Kutta methods) of integrating sets of ordinary differential equations in initial-value problems may be governed by either stability or truncation-error considerations. Truncation errors in the dependent variables may be scarcely noticeable and generally accumulate gradually with time. Instability generally causes sudden and severe errors that are very noticeable. When the equations are stiff, stability controls and extremely small time steps may be necessary to prevent instability. A common measure of the severity of stiffness is the stiffness ratio $|\lambda|_{max}/|\lambda|_{min}$, where λ is an eigenvalue for the jacobian matrix of the set of ordinary differential equations. For Eqs. (13-149) to (13-151), the jacobian matrix is tridiagonal if the equations and variables are arranged by stage (top down) for each component in order.

For a general jacobian matrix pertaining to C components and N theoretical trays, as shown by Distefano [*Am. Inst. Chem. Eng. J.,* **14,** 946 (1968)]. Gerschgorin's circle theorem (Varga, *Matrix Iterative Analysis,* Prentice Hall, Englewood Cliffs, N.J., 1962) may be employed to obtain bounds on the maximum and minimum absolute eigenvalues. Accordingly,

$$|\lambda|_{max} \le \max_{j=1,N}\left[\left(\frac{L_{j-1}}{M_j}\right) + \left(\frac{L_j + K_{i,j}V_j + \dfrac{dM_j}{dt}}{M_j}\right) + \left(\frac{K_{i,j+1}V_{j+1}}{M_j}\right)\right]$$

The maximum absolute eigenvalue corresponds to the component with the largest K value ($K_{L,j}$) and the tray with the smallest holdup. Therefore, if the derivative term and any variation in L_j, V_j, and $K_{i,j}$ are neglected,

$$|\lambda|_{max} \simeq 2\left[\frac{L_j + K_{i,j}V_j}{M_j}\right] \quad (13\text{-}162)$$

In a similar development, the minimum upper limit on the eigenvalue corresponds to the component with the largest K value and to the largest holdup, which occurs in the reboiler. Thus

$$|\lambda|_{min} = \left[\frac{L_N + K_{L,N}V_N}{M_{N+1}}\right] \quad (13\text{-}163)$$

Therefore, the lower bound on the stiffness ratio at the beginning of batch distillation is given approximately by

$$\frac{|\lambda|_{max}}{|\lambda|_{min}} = 2\left(\frac{M^0_{N+1}}{M_N}\right)$$

where M_{N+1} and M_N are the molar holdups in the reboiler initially and on the bottom tray respectively. In the sample problem presented by Distefano (ibid.) for the smallest charge, the approximate initial-stiffness ratio is of the order of 250, which is not considered to be a particularly large value. Using an explicit integration method, almost 600 time increments, which were controlled by stability criteria, were required to distill 98 percent of the charge.

At the other extreme of Distefano's sample problems, for the largest initial charge, the maximum-stiffness ratio is of the order of 1500, which is considered to be a relatively large value. In this case, more than 10,000 time steps are required to distill 90 percent of the initial change, and the problem is better handled by a stiff integrator.

In Distefano's method, Eqs. (13-149) to (13-161) are solved with an initial condition of total reflux at L_0 equal to $D(R + 1)$ from the specifications. At $t = 0$, L_0 is reduced so as to begin distillate withdrawal. The computational procedure is then as follows:

1. Replace L^0_j by $L^0_j - D$, but retain V^0_j and all other initial values from the total-reflux calculation.

2. Replace the holdup derivatives in Eqs. (13-149) to (13-151) by total-stage material-balance equations (e.g., $dM_j/dt = V_{j+1} + L_{j-1} - V_j - L_j$) and solve the resulting equations one at a time by the predictor step of an explicit integration method for a time increment that is determined by stability and truncation considerations. If the mole fractions for a particular stage do not sum to 1, normalize them.

3. Compute a new set of stage temperatures from Eq. (13-156). Calculate a corresponding set of vapor-phase mole fractions from Eq. (13-155).

4. Calculate liquid densities, molar tray and condenser-reflux drum holdups, and liquor and vapor enthalpies. Determine holdup and enthalpy derivatives with respect to time by forward difference approximations.
5. From Eqs. (13-152) to (13-154) compute a new set of values of liquid and vapor molar flow rates.
6. Compute the reboiler molar holdup from Eq. (13-158).
7. Repeat steps 2 through 6 with a corrector step for the same time increment. Repeat again for any further predictor and/or predictor-corrector steps that may be advisable. Distefano (ibid.) discusses and compares a number of suitable explicit methods.
8. Compute condenser and reboiler heat-transfer rates from Eqs. (13-159) and (13-160).
9. Repeat steps 2 through 8 for subsequent time increments until the desired amount of distillate has been withdrawn.

More flexible and efficient methods that can cope with stiffness in batch-distillation calculations utilize stable implicit integration procedures such as the method of Gear (op. cit.). Boston et al. (op. cit.) discuss such a method that also utilizes a two-tier equation-solving technique, referred to as the "inside-out" algorithm, that can handle both wide-boiling and narrow-boiling charges even when very nonideal mixtures are formed. In addition to the features of the Distefano model, the Boston et al. model permits multiple feeds, sidestream withdrawals, tray heat transfer, and vapor distillate and divides the batch-distillation process into a sequence of operation steps. At the beginning of each step, the reboiler may receive an additional charge, distillate or sidestream receivers may be dumped, and a feed reservoir may be refilled. Specifications for an operation step include feed, sidestream withdrawal, and tray heat-transfer rates. In addition, any two of the following five variables must be specified: reflux ratio, distillate rate, boil-up rate, condenser duty, and reboiler duty. An operation step is terminated when a specified criterion, selected from the following list, is reached: a time duration; a component purity in the reboiler, distillate, or distillate accumulator; an amount of material in the reboiler or distillate accumulator; or a reboiler or condenser temperature. The purity is specified to be met as the purity is increasing or decreasing. Finally, column configuration and operating conditions (number of stages, holdups, tray pressures, and feed, sidestream, and tray heat-transfer rates) can be changed at the beginning of each operation step. In addition, physical properties may be computed from a wide variety of correlations, including equation-of-state and activity-coefficient models.

Example 10: Calculation of Multicomponent Batch Distillation A charge of 45.4 kg · mol (100 lb·mol) of 25 mole percent benzene, 50 mole percent monochlorobenzene (MCB), and 25 mole percent orthodichlorobenzene (DCB) is to be distilled in a batch still consisting of a reboiler, a column containing 10 theoretical stages, a total condenser, a reflux drum, and a distillate accumulator. Condenser-reflux drum and tray holdups are 0.0056 and 0.00056 m^3 (0.2 and 0.02 ft^3) respectively. Pressures are 101.3, 107.6, 117.2, and 120.7 kPa (14.696, 15.6, 17, and 17.5 psia) at the condenser outlet, top stage, bottom stage, and reboiler respectively. Initially, the still is to be brought to total-reflux conditions at a boil-up rate of 45.4 (kg·mol)/h [100 (lb·mol)/h] leaving the reboiler. Then, at $t = 0$, the boil-up rate is to be increased to 90.8 (kg·mol)/h [200 (lb·mol)/h], and the reflux ratio is to be set at 3. The batch is then distilled in three steps. The first step, which is designed to obtain a benzene-rich product, is terminated when the mole fraction of benzene in the distillate being sent to the accumulator has dropped to 0.100 or when 2 h have elapsed. The purpose of the second operation step is to recover an MCB-rich product until the mole fraction of MCB in the distillate drops to 0.400 or 2 h have elapsed since the start of this step. The third step is to be terminated when the mole fraction of DCB in the reboiler reaches 0.98 or 2 h have elapsed since the start of this step. Ideal solutions and an ideal gas are assumed such that Raoult's law can be used to obtain K values. Calculations are made by the method of Boston et al. (op. cit.).

First, the total-reflux condition is computed by making several sets of stage-to-stage calculations from the reboiler to the condenser. For the first set, the reboiler composition is assumed to be that of the initial charge. This composition is adjusted by material balance to initiate each subsequent set of calculations until convergence is achieved. Results are shown in Table 13-29. From these data, the initial-stiffness ratio is approximately [2(99.74)/0.01218] = 16,400. Thus the equations are quite stiff, and an implicit integration method is preferred. Detailed calculated conditions at the end of the first operation step are given in Table 13-30. A short summary of computed conditions for each of the three operation steps is given in Table 13-31.

From Table 13-31, a total of 394 time increments were necessary to distill all but 22.08 lb·mol of the initial charge of 99.74 lb·mol following the establishment of total-reflux conditions. If this problem had to be solved by an explicit integrator, approximately 25,000 time increments would have been necessary.

Instantaneous distillate (or reflux) composition as a function of total accumulated distillate for all three operation steps is plotted in Fig. 13-106. From these results, an alternative schedule of operation steps can be derived to obtain three relatively rich cuts and two intermediate cuts for recycle to the next batch. One example is as follows:

		Composition, mole fractions		
Cut	Amount, lb·mol	Benzene	MCB	DCB
Benzene-rich	17.750	0.99553	0.00447	0.00000
Recycle 1	15.630	0.44120	0.55880	0.00000
MCB-rich	37.195	0.01164	0.98821	0.00015
Recycle 2	7.155	0.00000	0.55430	0.44570
DCB-rich	22.078	0.00000	0.02000	0.98000
Residual holdup	0.192	0.00000	0.11980	0.88020
Total	100.00	0.25000	0.50000	0.25000

NOTE: To convert pound·moles to kilogram·moles, multiply by 0.454.

From these results, 22.98 lb·mol, or almost 23 percent of the charge, would be recycled for redistillation. All three products are at least 98 mole percent pure.

TABLE 13-29 Total-Reflux Conditions

				x		
Stage	T, °F	L, (lb·mol)/h	M, lb·mol	Benzene	MCB	DCB
Condenser	175.94	116.4	0.1307	1.000	0.525×10^{-7}	0.635×10^{-15}
1	179.46	117.4	0.01304	1.000	0.266×10^{-6}	0.164×10^{-13}
2	180.05	117.5	0.01303	1.000	0.135×10^{-5}	0.424×10^{-12}
3	180.64	117.5	0.01303	1.000	0.683×10^{-5}	0.109×10^{-10}
4	181.22	117.6	0.01302	1.000	0.344×10^{-4}	0.279×10^{-9}
5	181.80	117.7	0.01302	1.000	0.173×10^{-3}	0.711×10^{-8}
6	182.41	117.7	0.01301	0.999	0.871×10^{-3}	0.180×10^{-6}
7	183.14	117.5	0.01300	0.996	0.435×10^{-2}	0.454×10^{-5}
8	184.54	116.4	0.01295	0.979	0.209×10^{-1}	0.112×10^{-3}
9	189.08	111.8	0.01278	0.901	0.965×10^{-1}	0.250×10^{-2}
10	205.91	100.0	0.01218	0.642	0.319	0.389×10^{-1}
Reboiler	250.96	0.0	99.74	0.248	0.501	0.251

NOTE: Reboiler duty = 1,549,000 Btu/h. To convert degrees Fahrenheit to degrees Celsius, °C = (°F − 32)/1.8; to convert pound-moles per hour to kilogram-moles per hour, multiply by 0.454; and to convert pound-moles to kilogram-moles, multiply by 0.454.

TABLE 13-30 Conditions at the End of the First Operation Step

Time = 0.5963 h

Stage	T, °F	(lb·mol)/h V	(lb·mol)/h L	M, lb·mol	y Benzene	y MCB	y DCB	x Benzene	x MCB	x DCB
Condenser	251.58	0	154.6	0.1113				0.100	0.900	0.292×10^{-5}
1	267.69	206.1	157.5	0.01992	0.0994	0.901	0.293×10^{-5}	0.276×10^{-1}	0.972	0.124×10^{-4}
2	271.21	209.0	158.0	0.01088	0.0449	0.955	0.101×10^{-4}	0.121×10^{-1}	0.988	0.405×10^{-4}
3	272.48	209.5	158.1	0.01087	0.0331	0.967	0.312×10^{-4}	0.884×10^{-2}	0.991	0.124×10^{-3}
4	273.28	209.6	158.2	0.01086	0.0306	0.969	0.943×10^{-4}	0.818×10^{-2}	0.991	0.373×10^{-3}
5	273.99	209.7	158.2	0.01085	0.0301	0.970	0.282×10^{-3}	0.806×10^{-2}	0.991	0.111×10^{-2}
6	274.75	209.7	158.1	0.01084	0.0300	0.969	0.839×10^{-3}	0.803×10^{-2}	0.989	0.329×10^{-2}
7	275.72	209.6	157.7	0.01083	0.0300	0.967	0.249×10^{-2}	0.801×10^{-2}	0.982	0.969×10^{-2}
8	277.29	209.2	156.6	0.01080	0.0300	0.963	0.731×10^{-2}	0.794×10^{-2}	0.964	0.280×10^{-1}
9	280.50	208.1	154.0	0.01073	0.0301	0.949	0.211×10^{-1}	0.772×10^{-2}	0.915	0.770×10^{-1}
10	287.47	205.4	148.5	0.01057	0.0302	0.912	0.577×10^{-1}	0.720×10^{-2}	0.803	0.189
Reboiler	301.67	200.0	0	66.40	0.0304	0.829	0.141	0.634×10^{-2}	0.617	0.376

NOTE: To convert pound-moles per hour to kilogram-moles per hour, multiply by 0.454; to convert pound-moles to kilogram-moles, multiply by 0.454.

TABLE 13-31 Calculated Conditions for each Operation Step

	Operation step 1	Operation step 2	Operation step 3
Time of operation step, h	0.5963	0.7944	0.04828
Number of time increments	201	154	39
Accumulated distillate			
Total lb·mol	33.38	41.99	2.361
Mole fractions			
Benzene	0.7360	0.0103	0.74×10^{-10}
MCB	0.2640	0.9537	0.2872
DCB	0.45×10^{-6}	0.036	0.7128
Reboiler holdup			
Total lb·mol	66.40	24.43	22.08
Mole fractions			
Benzene	0.0063	0.63×10^{-11}	0.20×10^{-12}
MCB	0.6172	0.0448	0.0200
DCB	0.3765	0.9552	0.9800
Temperatures, °F			
Condenser outlet	251.58	308.60	330.17
Reboiler outlet	301.67	362.63	366.39
Heat duties, million Btu/h			
Condenser	3.313	3.472	3.456
Reboiler	3.295	3.469	3.433

NOTE: To convert degrees Fahrenheit to degrees Celsius, °C = (°F − 32)/1.8; to convert pound-moles to kilogram-moles, multiply by 0.454; and to convert British thermal units per hour to kilo-joules per hour, multiply by 1.055.

RAPID SOLUTION METHOD

The quasi-steady-state method of Galindez and Fredenslund [*Comput. Chem. Engng.*, **12,** 281 (1988)] is a rapid alternative to the rigorous integration of the stiff differential equations. In their method, which is implemented in the CHEMCAD III process simulator of Chemstations, Inc., Houston, Texas, the transient conditions are simulated, without having to treat stiffness, by a succession of a finite number of continuous steady states of generally a few minutes of batch time each in duration. The calculations are started from an initialization at total-reflux conditions, taking into account holdup. Generally, computed results compare well with rigorous integration methods.

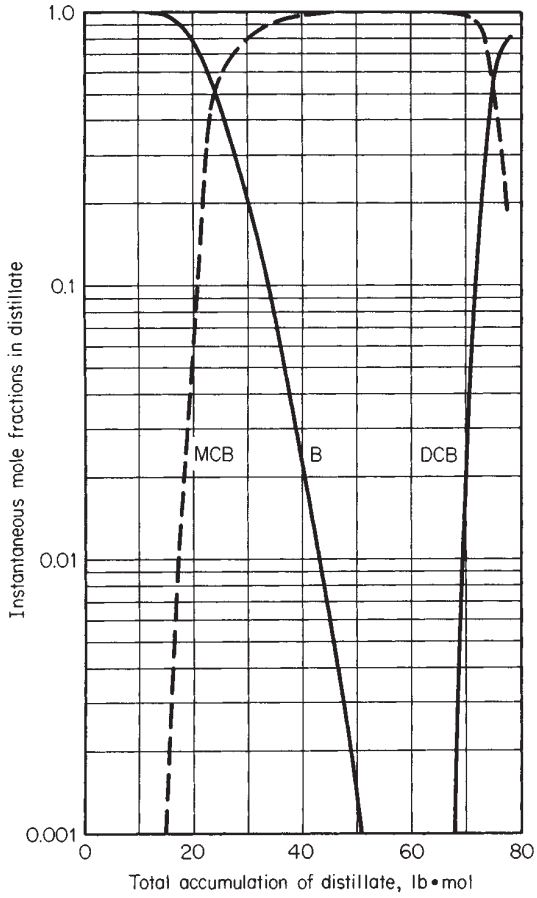

FIG. 13-106 Distillate-composition profile for the multicomponent-batch-distillation example.

DYNAMIC DISTILLATION

INTRODUCTION

As discussed in detail by Archer and Rothfus [*Chem. Eng. Prog. Symp. Series, No. 36,* **57,** 2 (1961)], dynamic or transient behavior of a continuous-distillation operation is important in determining (1) startup and shutdown procedures, (2) transition path between steady states, (3) effect of upsets and fluctuations on controllability, (4) residence times and mass-transfer rates, and (5) operating strategies that may involve deliberate imposition of controlled cyclic fluctuations or oscillations, as summarized by Schrodt [*Ind. Eng. Chem.*, **59**(6), 58 (1967)]. Dynamic behavior may be studied with no controllers in the system to obtain a so-called open-loop response. Alternatively, controllers may be added for certain variables that are to be controlled by manipulating other variables to obtain a so-called closed-loop response. For this latter case, controllers of various levels of complexity [e.g., on-off, proportional (P), proportional with integral action (PI), and proportional with integral and derivative action (PID)] can be considered for various values of tuning parameters, and specific valves of known characteristics may be incorporated if desired.

IDEAL BINARY DISTILLATION

Consider the closed-loop response during the dynamic distillation of an ideal binary mixture in the column shown in Fig. 13-107, under two assumptions of constant relative volatility at a value of 2.0 and constant molar vapor flow for a saturated liquid feed to tray N_s. Following the development by Luyben (op. cit.), it is not necessary to include energy-balance equations for each tray or to treat temperature and pressure as variables. Overhead vapor leaving top tray N_T is totally condensed for negligible liquid holdup with condensate flowing to a reflux drum having constant and perfectly mixed molar liquid holdup M_D. The reflux rate L_{N_T+1} is varied by a proportional-integral (PI) feedback controller to control distillate composition for a set point of 0.98 for the mole fraction x_D of the light component. Holdup of reflux in the line leading back to the top tray is neglected. Under dynamic conditions, y_{N_T} may not equal x_D.

At the bottom of the column, a liquid sump of constant and perfectly mixed molar liquid holdup M_B is provided. A portion of the liquid flowing from this sump passes to a thermosiphon reboiler, with the

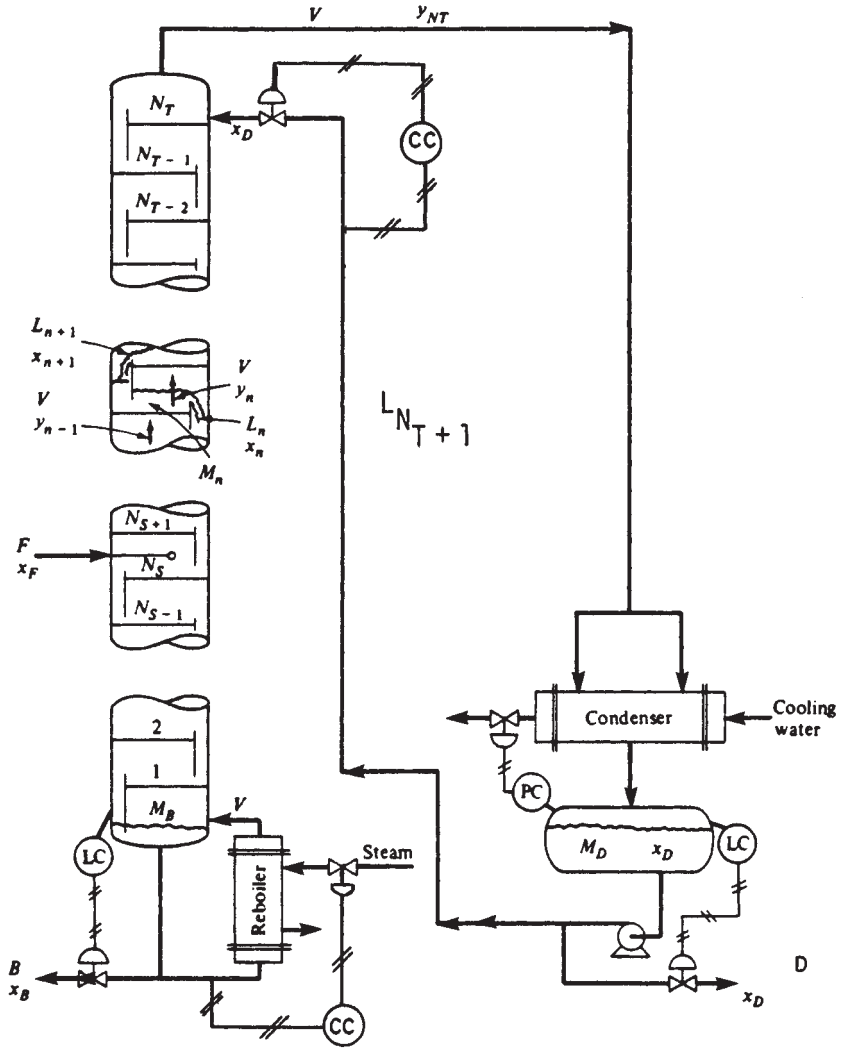

FIG. 13-107 Binary distillation column; dynamic distillation of ideal binary mixture.

remainder taken as bottoms product at a molar flow rate B. Vapor boil-up generated in the reboiler is varied by a PI feedback controller to control bottoms' composition with a set point of 0.02 for the mole fraction x_B of the light component. Liquid holdups in the reboiler and lines leading from the sump are assumed to be negligible. The composition of the boil-up y_B is assumed to be in equilibrium with x_B.

The liquid holdup M_n on each of the N_T equilibrium trays is assumed to be perfectly mixed but will vary as liquid rates leaving the trays vary. Vapor holdup is assumed to be negligible everywhere. Tray molar vapor rates V vary with time but at any instant in time are everywhere equal.

The dynamic material-balance and phase equilibrium equations corresponding to this description are as follows:

All trays, n:

$$dM_n/dt = F_n + L_{n+1} - L_n \tag{13-164}$$

$$\frac{d}{dt}(M_n x_n) = F_n x_{F_n} + L_{n+1}x_{n+1} + Vy_{n-1} - L_n x_n - Vy_n \tag{13-165}$$

$$L_n = \overline{L}_n + (M_n - \overline{M}_n)/\beta \tag{13-166}$$

$$y_n = \frac{\alpha x_n}{1 + (\alpha - 1)x_n} \tag{13-167}$$

Where F_n is nonzero only for tray N_s, y and x refer to the light component only such that the corresponding mole fractions for the heavy component are $(1 - y)$ and $(1 - x)$, $\overline{L}_n$ and $\overline{M}_n$ are the initial steady-state values, and β is a constant that depends on tray hydraulics.

For the condenser-reflux-drum combination:

$$D = V - L_{N_T+1} \tag{13-168}$$

$$M_D(dx_D/dt) = Vy_{NT} - Vx_D \tag{13-169}$$

For the reboiler:

$$B = L_1 - V \tag{13-170}$$

$$M_B(dx_B/dt) = L_1x_1 - Vy_B - Bx_B \tag{13-171}$$

$$y_B = \frac{\alpha x_B}{1 + (\alpha - 1)x_B} \tag{13-172}$$

The two PI-controller equations are

$$V = \overline{V} - K_{C_B}\left(E_B + \frac{1}{\tau_B}\int E_B\,dt\right) \tag{13-173}$$

$$L_{N_T+1} = \overline{L}_{N_T+1} + K_{C_D}\left(E_D + \frac{1}{\tau_D}\int E_D\,dt\right) \tag{13-174}$$

where $\overline{V}$ and $\overline{L}_{N_T+1}$ are initial values, K_C and τ are respectively feedback-controller gain and feedback-reset time for integral action, and E is the error or deviation from the set point as given by

$$E_B = x_B^{\text{set}} - x_B \tag{13-175}$$

$$E_D = x_D^{\text{set}} - x_D \tag{13-176}$$

These differential equations are readily solved, as shown by Luyben (op. cit.), by simple Euler numerical integration, starting from an initial steady state, as determined, e.g., by the McCabe-Thiele method, followed by some prescribed disturbance such as a step change in feed composition. Typical results for the initial steady-state conditions, fixed conditions, controller and hydraulic parameters, and disturbance given in Table 13-32 are listed in Table 13-33.

MULTICOMPONENT DISTILLATION

Open-loop behavior of multicomponent distillation may be studied by solving modifications of the multicomponent equations of Distefano [*Am. Inst. Chem. Eng. J.*, **14,** 190 (1968)] as presented in the subsection "Batch Distillation." One frequent modification is to include an equation, such as the Francis weir formula, to relate liquid holdup on a tray to liquid flow rate leaving the tray. Applications to azeotropic-distillation towers are particularly interesting because, as discussed by and illustrated in the following example from Prokopakis and Seider

TABLE 13-32 Initial and Fixed Conditions, Controller and Hydraulic Parameters, and Disturbance for Ideal Binary Dynamic-Distillation Example

Other initial conditions
$\overline{F} = 100$ (lb·mol)/min
$\overline{x}_F = 0.50$
$\overline{L}_{N_T+1} = 128.01$ (lb·mol)/min
$\overline{V} = 178.01$ (lb·mol)/min
$\overline{D} = 50$ (lb·mol)/min
$x_D^{\text{set}} = 0.98$
$\overline{B} = 50$ (lb·mol)/min
$x_B^{\text{set}} = 0.02$
$M_{n,n=1\text{ to }N_T} = 10$ lb·mol
Fixed conditions
$N_T = 20$
$N_S = 10$
$M_D = 100$ lb·mol
$M_B = 100$ lb·mol
Controller and hydraulic parameters
$K_{C_B} = K_{C_D} = 1000$ (lb·mol)/min
$\tau_B = 1.25$ min
$\tau_D = 5.0$ min
$\beta = 0.1$ min
Disturbance at $t = 0^+$
$x_F = 0.55$

Initial liquid-phase compositions	
Tray	x_n
Bottoms	0.02
1	0.035
2	0.05719
3	0.08885
4	0.1318
5	0.18622
6	0.24951
7	0.31618
8	0.37948
9	0.43391
10	0.47688
11	0.51526
12	0.56295
13	0.61896
14	0.68052
15	0.74345
16	0.80319
17	0.85603
18	0.89995
19	0.93458
20	0.96079
Distillate	0.98

NOTE: To convert pound-moles per minute to kilogram-moles per minute, multiply by 0.454; to convert pound-moles to kilogram-moles, multiply by 0.454.

[*Am. Inst. Chem. Eng. J.*, **29,** 1017 (1983)], the steep concentration and temperature fronts can be extremely sensitive to small changes in reflux ratio, boil-up rate, product recovery and purity, and feed rate and composition.

Consider azeotropic distillation to dehydrate ethanol with benzene. Initial steady-state conditions are as shown in Fig. 13-108. The overhead vapor is condensed and cooled to 298 K to form two liquid phases that are separated in the decanter. The organic-rich phase is returned to the top tray as reflux together with a portion of the water-rich phase and makeup benzene. The other portion of the water-rich phase is sent to a stripper to recover organic compounds. Ordinarily, vapor from that stripper is condensed and recycled to the decanter, but that coupling is ignored here.

Equations for the decanter are as follows if it is assumed that (1) there are constant holdups in the decanter of both phases in the same ratio as the ratio of the flow rates leaving the decanter, (2) there is a constant decanter temperature, and (3) the two liquid phases in the decanter are in physical equilibrium and each is perfectly mixed.

$$\frac{d}{dt}[M_d(x_i)_d] = V_N y_{i,N} - L_0(x_i)_0 - L_w(x_i)_w \tag{13-177}$$

$$dM_d/dt = V_N - L_0 - L_w \tag{13-178}$$

$$K_{d_i} = (x_i)_0/(x_i)_w = (\gamma_i)_w/(\gamma_i)_0 \tag{13-179}$$

where M_d is the total molar holdup of both phases in the decanter and the total composition in the decanter is

$$(x_i)_d = \frac{(x_i)_0 L_0 + (x_i)_w L_w}{L_0 + L_w} \tag{13-180}$$

Combination of Eqs. (13-177), (13-178), and (13-180) gives

$$\frac{d(x_i)_d}{dt} = \frac{V_N}{M_d}[y_{i,N} - (x_i)_d] \tag{13-181}$$

These equations, together with those for the tower, constitute a so-called stiff system. They were solved by Prokopakis and Seider (op. cit.), following a prescribed disturbance, using an adaptive semi-implicit Runge-Kutta integration technique by which V_N and the $y_{i,N}$ were obtained by integration of the equations for the tower. Then Eq. (13-181) was integrated to give $(x_i)_d$, which was used with Eqs.

TABLE 13-33 Results for Ideal Binary Dynamic-Distillation Example of Table 13-32*

	Mole fraction of light component in liquid					Flow rate, (lb·mol)/min	
Time, min	Bottoms	Stage 5	Stage 10	Stage 15	Distillate	Reflux	Boli-up
0.00	0.02000	0.18622	0.47688	0.74345	0.98000	128.01	178.01
.50	0.02014	0.19670	0.51310	0.74940	0.98000	128.01	178.16
1.00	0.02107	0.21174	0.52426	0.76049	0.98010	127.91	179.31
1.50	0.02217	0.22038	0.53026	0.76847	0.98034	127.64	181.06
2.00	0.02275	0.22209	0.53229	0.77217	0.98061	127.33	182.65
2.50	0.02268	0.21881	0.53141	0.77222	0.98076	127.11	183.69
3.00	0.02212	0.21287	0.52879	0.76993	0.98077	127.02	184.10
3.50	0.02132	0.20639	0.52560	0.76672	0.98065	127.07	183.99
4.00	0.02051	0.20104	0.52282	0.76381	0.98047	127.19	183.55
4.50	0.01987	0.19777	0.52109	0.76196	0.98030	127.32	182.98
5.00	0.01950	0.19679	0.52057	0.76142	0.98018	127.42	182.47
5.50	0.01939	0.19766	0.52106	0.76198	0.98014	127.45	182.14
6.00	0.01950	0.19956	0.52209	0.76315	0.98016	127.41	182.02
6.50	0.01972	0.20162	0.52320	0.76438	0.98022	127.33	182.08
7.00	0.01995	0.20314	0.52400	0.76525	0.98029	127.24	182.25
7.50	0.02012	0.20380	0.52434	0.76557	0.98034	127.15	182.43
8.00	0.02019	0.20362	0.52422	0.76537	0.98036	127.09	182.56
8.50	0.02016	0.20289	0.52381	0.76484	0.98035	127.07	182.61

*From Luyben, *Process Modeling, Simulation, and Control for Chemical Engineers*, McGraw-Hill, New York, 1973.
NOTE: To convert pound-moles per minute to kilogram-moles per minute, multiply by 0.454.

(13-179) and (13-180) to obtain the equilibrium compositions $(x_i)_0$ and $(x_i)_w$ leaving the decanter. The UNIQUAC equation was used with data from Gmehling and Onken (*Vapor-Liquid Equilibrium Data Collection*, DECHEMA Chemistry Data Ser., Vol. 1 (parts 1–10). Frankfurt, 1977) to obtain the activity coefficients needed in Eq. (13-179). Reboiler and decanter volumetric holdups were assumed constant at 1.0 m^3 (35.3 ft^3), and volumetric tray holdups were computed from

$$M_n = (\rho_L)_n A_n (h_{w_j} + h_{c_j}) \qquad (13\text{-}182)$$

where $(\rho_L)_n$ is the liquid density; A_n, the cross-sectional area of the active portion of the tray = 0.23 m^2 (2.48 ft^2); h_{w_j}, the weir height = 0.0254 m (0.0833 ft); and h_{c_j}, the weir crest, assumed to be constant at 0.00508 m (0.0167 ft). Accordingly, volumetric tray holdup was constant at 0.007 m^3 (0.247 ft^3).

Assume that at $t = 0^+$ the feed rate to tray 23 is disturbed by increasing it by 30 percent to 130 mol/min without a change in composition. The resulting ethanol liquid mole fraction on several trays is tracked in Fig. 13-109. Above tray 16, ethanol concentration remains very small. Below tray 9, ethanol concentration initially decreases fairly rapidly but

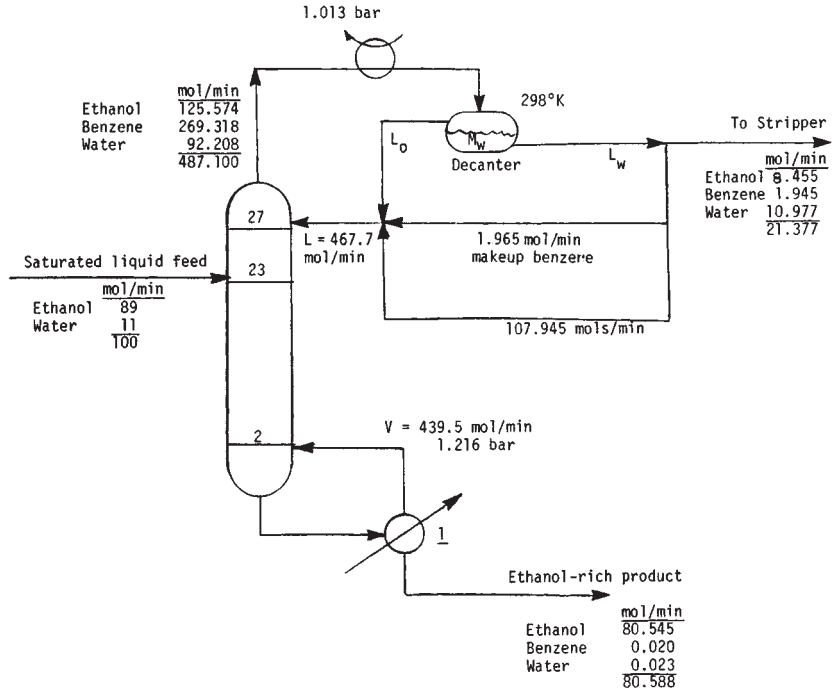

FIG. 13-108 Initial steady state for dynamic azeotropic distillation of ethanol-water with benzene.

then increases slowly and steadies out at significantly higher values than at the initial steady state. Tray 10 is one of the last trays to reach the new steady-state condition, which takes somewhat more than 200 min. This may be compared with initial residence times in the decanter and reboiler of approximately 50 and 250 min respectively. The movement through the column of concentration fronts for all three components is shown in Fig. 13-109. For the first 5 to 10 min, below tray 16, benzene and ethanol fronts shift downward. Then a reversal occurs, and the fronts shift upward until the new steady state is attained. The upward shift is expected because the increased feed rate increases the water-benzene entrainer ratio. The duration of the initial, temporary downward shift is highly dependent on tray holdup and is due to "wash-out" with the feed liquid. This phenomenon is also observed in the dynamic studies of Peiser and Grover [*Chem. Eng. Prog.*, **58**(9), 65 (1962)].

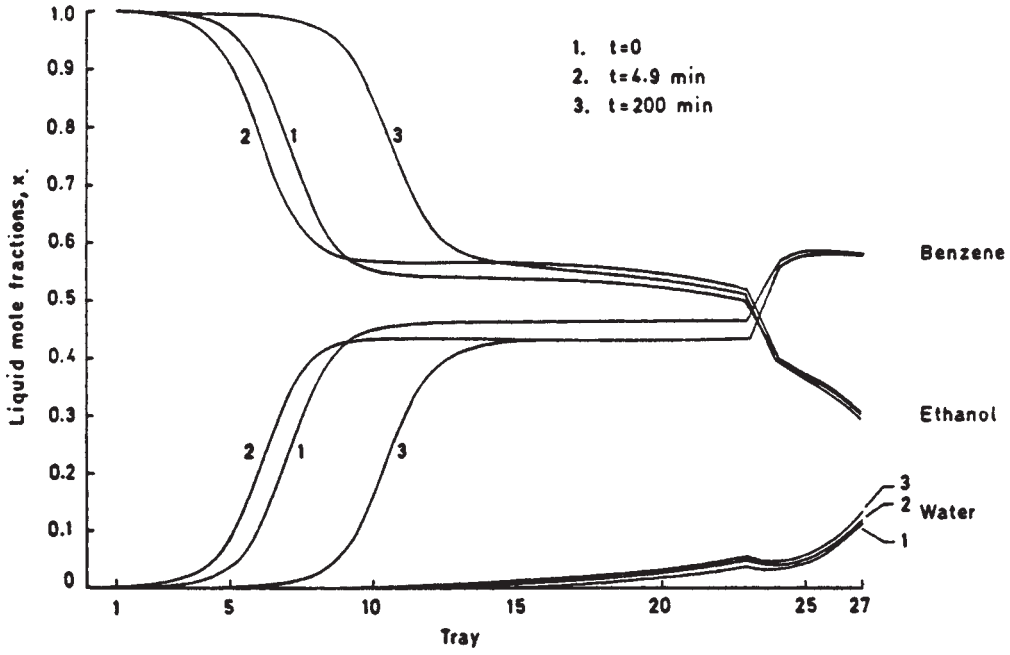

(a)

FIG. 13-109*a* Responses after a 30 percent increase in the feed flow rate for the multicomponent-dynamic-distillation example of Fig. 13-100. Profiles of liquid mole fractions at several times.

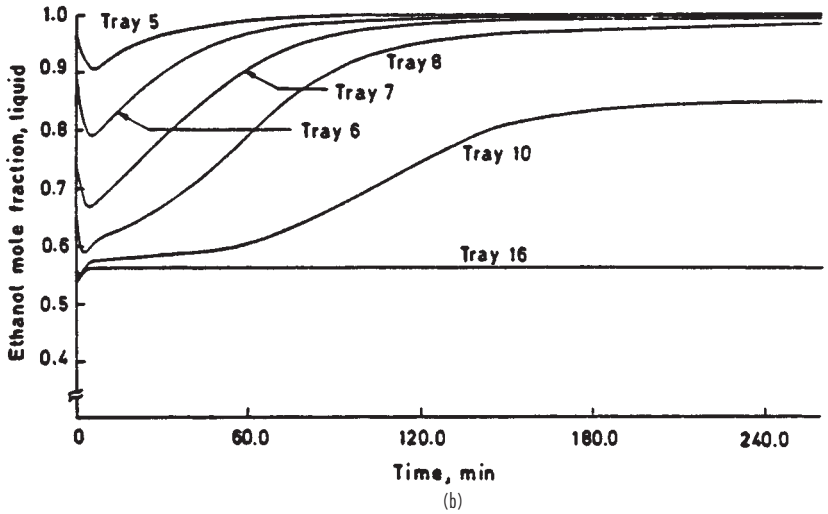

(b)

FIG. 13-109*b* Responses after a 30 percent increase in the feed flow rate for the multicomponent-dynamic-distillation example of Fig. 13-100. Alcohol mole fractions on several trays. (*Prokopakis and Seider,* Am. Inst, Chem. Eng. J., **29,** *1017 (1983).*]

If the feed rate is decreased, the trends of curves in Fig. 13-109 are reversed. The disturbance of other variables such as feed composition, boil-up ratio, and recycle of water-rich effluent from the decanter produces similar shifts in the steep concentration fronts, indicating that azeotropic towers are among the most sensitive separation operations, for which dynamic studies are essential if reliable process control is to be developed. Such studies indicate the importance of adjusting aqueous-phase recycle and reboiler duty to diminish the movement of steep concentration fronts and the possibility of multiple regimes of operation including unstable regimes, as shown by Magnussen et al. [*Inst. Chem. Eng. Symp. Ser.* **56** (1979)].

PACKED COLUMNS

Distillation-type separation operations may be conducted in packed rather than tray-type columns. In prior years, except for small columns, plate columns were heavily favored over packed columns. However, development of more efficient random or structured packing materials and the need to increase capacity, increase efficiency, or reduce pressure drop in many applications has resulted in more extensive use of packed columns in larger sizes in recent years. Both types of contacting devices are discussed extensively in Sec. 14 and by Billet (*Distillation Engineering*, Chemical Publishing, New York, 1979). Packed columns may employ dumped (random) packing, e.g., pall rings, or structured (ordered, arranged, or stacked) packing, e.g., knitted wire and corrugated and perforated sheets. Tray-type columns generally employ valve, sieve, or bubble-cap trays with downcomers. The choice between a packed column and a tray-type column is based mainly on economics when factors of contacting efficiency, loadability, and pressure drop must be considered.

Packed columns must be provided with good initial distribution of liquid across the column cross section and redistribution of liquid at various height intervals that decrease with increasing column diameter. A wide variety of distributors and redistributors are available. Packed columns should be considered when:

1. Temperature-sensitive mixtures are to be separated. To avoid decomposition and/or polymerization, vacuum operation may then be necessary. The smaller liquid holdup and pressure drop theoretical stage of a packed column may be particularly desirable.
2. Ceramic or plastic (e.g., propylene) is a desirable material of construction from a noncorrosion and liquid-wettability standpoint.
3. Refitting of a tray-type column is desired to increase loading, increase efficiency, and/or decrease pressure drop. Structured packing is particularly applicable in this case.
4. Liquid rates are very low and/or vapor rates are high, in which case structured packing may be particularly desirable.
5. The mixture to be separated is clear, nonfouling, and free of solids, and cleaning of column internals will not be necessary.
6. The mixture to be separated tends to form foam, which collapses more readily in a packed column.
7. High recovery of a volatile component by a batch operation is required. Liquid holdup is much lower in a packed column.

Packed columns are almost always used for column diameters less than 762 mm (30 in) but otherwise generally need not be considered when:

1. Multiple feeds, sidestreams, and/or intermediate condensers and/or intermediate reboilers are required or desirable.
2. A wide range of loadability (turndown ratio) is required. Valve trays are particularly desirable in this case.
3. Design data for separation of the particular or similar mixture in a packed column are not available. Design procedures are better established for tray-type columns than for packed columns. This is particularly so with respect to separation efficiency since tray efficiency can be estimated more accurately than packed height equivalent to a theoretical stage (HETP).